PREDICTION OF THE FLOW REGIME TRANSITIONS IN HIGH PRESSURE, LARGE DIAMETER, INCLINED MULTIPHASE PIPELINES

A Dissertation Presented to

The Faculty of the

Fritz J. and Dolores H. Russ

College of Engineering and Technology

Ohio University

In Partial Fulfillment

of the Requirement for the Degree

Doctor of Philosophy

by

Robert Joseph Wilkens

June, 1997

ACKNOWLEDGMENT

This author wishes to thank his parents, Paul and Joan Wilkens, for their unwavering support and encouragement through good times and bad. With personal and financial support, they have allowed my pursuits to be fully realized.

The author would also like to thank Professor W. Paul Jepson. He provided an opportunity to work closely with my desired field of fluid mechanics. His guidance, and the guidance and support of the NSF I/UCRC Corrosion in Multiphase Systems Center Advisory Board, allowed my goals to be achieved.

Along the way, guidance came from other sources which proved to be crucial in accomplishing this goal. Dr. Tony Green from BP co-advised me during my second year and Dr. Kevin Myers, who advised me during my master's thesis, provided continual support throughout my doctoral studies.

The assistance of others from this research center must also be appreciated. Dr. Madan Gopal provided career guidance. Jeff Maley, whose master's degree project of transitions, corrosion, and frequency, intermingled with my doctoral project, must be thanked for his experimental assistance. The equipment we used could not have been operated alone. Technical assistance was provided by Craig Lange and A. D. Pallini. Without them, the test apparatus may never have been commissioned. Janet Wintle provided support as a grammatical wizard.

The author would be remiss if he let the indescribable support of his fiancee Michelle go unacknowledged. Shellie, thank you for being there.

TABLE OF CONTENTS

LIST OF TABLES

LIST OF FIGURES

CHAPTER 1

INTRODUCTION

Multiphase flow pattern prediction has many design applications such as boiler tubes and oil and gas pipelines. Knowledge of the flow pattern is mandatory to define the underlying fluid mechanics in multiphase flow. An example of the need for this knowledge occurs in oil production from older sub-sea oil wells.

The oil that comes to the surface is accompanied by natural gas and later by formation water as well. The gas is always there, consisting of mostly methane. Other gases are also typically present such as carbon dioxide, hydrogen sulfide, and nitrogen. These are known as the acid gases because they potentially cause exceptionally corrosive environments. The gases may or may not be useful locally (*e.g.*, gas turbine power). As time passes and oil and gas are removed from the well, the reservoir pressure slowly drops. To boost the pressure, the petroleum engineers commonly inject any or all of the gases into the reservoir gas cap (the region above the oil) or into the water region (below the oil). The processing of the gas used to re-inject is typically only water removal. As the pressure drops further, this gas re-injection is not able to the maintain reservoir pressure. At this point an increasing amount of water seeps into the well from the surroundings to replace the exiting crude oil. Thus, as the wells age, the water cut (volumetric percent of the liquid which is water) increases. The carbon dioxide content at this stage has typically increased due to the re-injection, but the change is often negligible. Typical carbon dioxide levels are on the order of a few mol percent. Prudhoe Bay has 11 - 12 % (Green, 1997).

Gas gets into the production lines in other ways also. A well-established recovery technique is to inject gas into the well tubing part way down the pipeline. This acts to reduce the pressure required to lift the liquid solely by reducing the mixture density. The oil will absorb an exceptional amount of gas. This feature is highly pressure dependent. As the mixture loses pressure as it comes up from the reservoir, more gas evolves from the oil and some from the water. The gas pockets tend to coalesce. At production pressures (upwards of 2,000 psi), the gas density approaches on-half of the oil density. Thus, as the pressure reduces, typically from the several hundred meter climb from sub-sea, the gas pockets grow due to compressibility as the gas density decreases.

Figure 1.1 illustrates the typical flow patterns observed by Lee (1993) in horizontal oil/water/gas flow. At low liquid and gas velocities, the three phases flow in a smooth stratified pattern. The location of the fluids is solely based on density with the water flowing on the bottom, gas flowing along the top, and oil flowing in between the water and gas phases. As the gas flow rate is increased, the gas-oil interface becomes wavy while the three phases still remain stratified. The oil-water interface remains smooth. If the overall liquid flow rate were to be increased with low gas velocity, plug flow is reached. Three-phase plug flow is characterized by a wavy, yet mostly stratified, interface between the oil and water phases. The oil level in plug flow reaches the top of the pipe with regular, intermittent gas pockets passing which remove the oil from the top of the pipe. The gas seldom reaches down to the water film and there are few or no gas bubbles in the full pipe region.

If the gas flow rate is increased from the plug flow region, the slug flow region is reached. Characteristics of slug flow include the complete mixing of the oil and water layers, gas pockets of increased length, and bubble entrainment within the slug body (full pipe

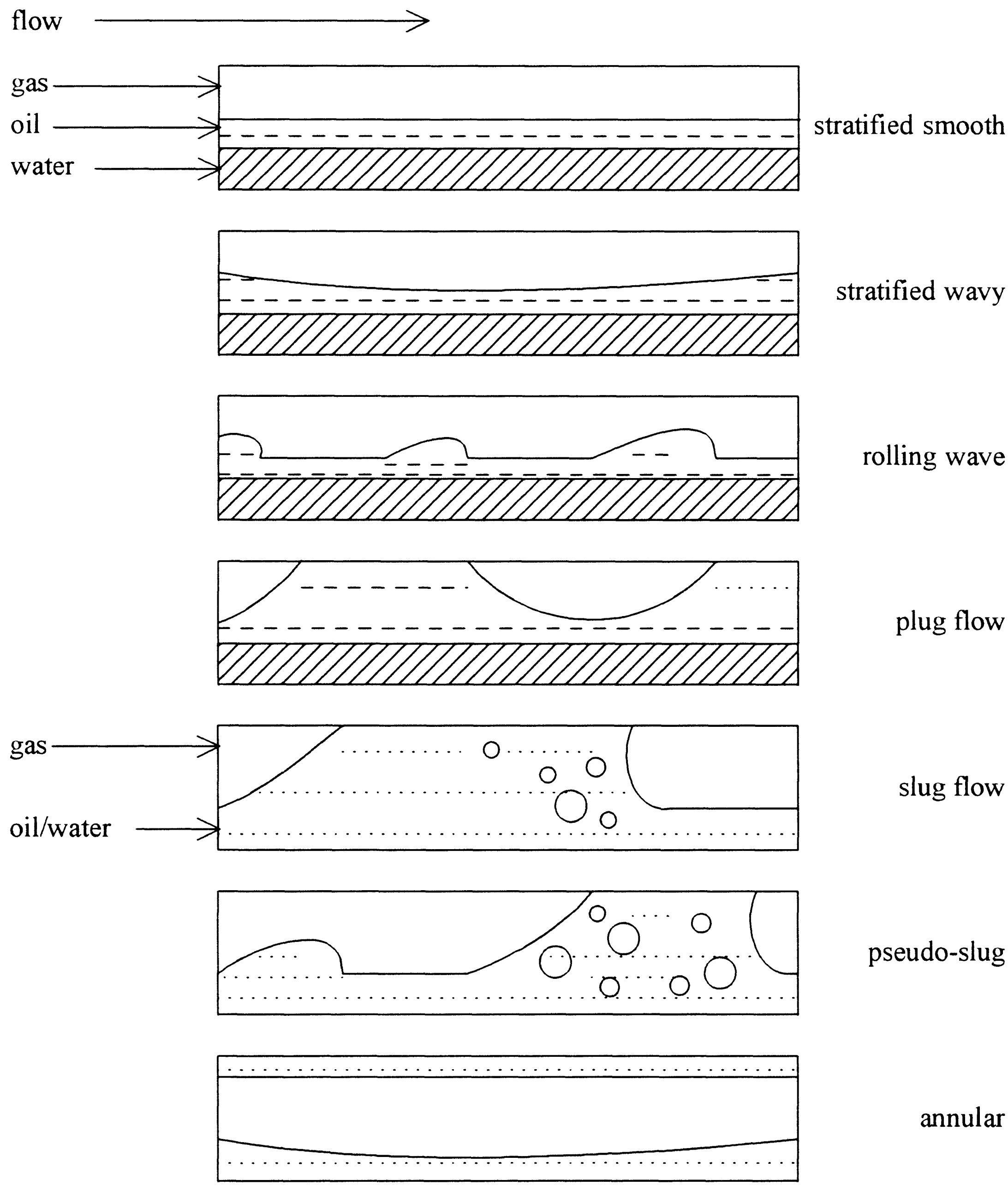

Figure 1.1: Flow patterns for oil/water/gas systems (Lee, 1993).

region). The front of the slug is highly turbulent with a high void fraction. The slug front has been shown to be the equivalent of a hydraulic jump by Jepson (1989). The slug front is slowed by the undercutting of the slow-moving film ahead of the slug. The undercutting of this film creates a large mixing eddy commonly referred to as the mixing zone. Fan *et al.* (1993) have shown that when this occurs, there is an irrecoverable pressure drop due to the deceleration of the slug that is several orders of magnitude greater than the frictional pressure drop. The velocity of the fast-moving slug front, the translational velocity, is also greater than that of the *in-situ* gas velocity. Thus, gas is entrained and passed back through the slug. The velocity of the liquid within the slug is less than the translational velocity. In vertical flow, the plug flow and slug flow regimes are identical.

At even higher gas flow rates a flow condition, often called pseudo-slug flow, will sometimes occur. Pseudo-slugs have characteristics similar to slugs with the exception that the liquid in the body region never fully bridges the full pipe diameter. In pseudo-slug flow the mixing region, which increases with increasing gas flow rate, has increased to the point where the mixing zone becomes larger than the slug body length. Thus, gas from behind the slug can now blow through the slug body. Pseudo-slugs can also be highly turbulent waves that do not have enough liquid to reach the top of the pipe. At still higher gas flow rates, annular flow occurs. Annular flow occurs when the less dense fluid (the gas) flows in a core along the center of the pipe while the more dense fluid (the oil/water mixture) flows as an annular ring around the pipe wall. A cross-sectional view would indicate that the liquid film thickness is not truly symmetrical. Rather, the top of the pipe has a film thickness of less than a millimeter.

The carbon dioxide, which has dissolved into the brine, forms a weak carbonic acid. This carbonic acid reacts with the iron of the typically carbon steel pipelines to form iron carbonate. This process is commonly referred to as sweet corrosion. Kaul (1996) noted that the corrosion rate is accelerated when the flow pattern is slug flow. It is thought that the iron carbonate film which is left behind from the reaction is immediately torn away by the highly-turbulent slugs. Thus, the corrosion rate is no longer mass transfer limited at the wall. Kaul's work primarily focused on the use of corrosion inhibitors in slug flow. Although these inhibitors reduced the corrosion rate substantially, they still left an unacceptable corrosion rate (on the order of millimeters per year). To compound the problem, economics currently force this corrosive mixture to be transported many miles from the well head to central collection stations before it can be separated. During this transport, the multiphase mixture travels through numerous changes in inclination which affect the flow pattern and flow characteristics. This can further enhance the corrosion. With the depletion of many of the larger oil reservoirs, oil companies have been forced to begin extraction of oil from these older wells.

Since the highest corrosion rate occurs in slug flow, the ability to predict this flow regime becomes of great importance. Additionally, avoiding this flow regime greatly reduces pumping costs.

The consequences of a major oil line break are severe. The current solution of the oil industry is to use corrosion inhibitors or to reduce the production rate. Corrosion inhibitors work by either adsorbing to the metal pipe surface or by reacting with corrosion products to form a protective layer. Kaul (1996) has shown that currently, corrosion inhibitors are not working well under slug flow conditions. Kaul has also shown that the corrosion rate is dependent upon the flow conditions and that commonly-used predictions such as De Waard *et al.*, (1993), which are based upon tests in beakers, are ineffective in describing pipeline corrosion. The first step in determining the predominant corrosion mechanisms is to understand the nature of the flow. With this information, new pipelines and separators can be properly sized.

A great deal of work has been carried out for two phase flows in small diameter pipes. This is not scalable to larger pipes. At smaller diameters (< 5-cm) slug characteristics and mechanisms differ from those found in larger diameter pipes. This is due in part to the scale of turbulence and gas bubbles being on the same order of size as the diameter. As will be explained in Chapter 2, some smaller diameter slug flow analyses make claims such as the slug rides on top of a film with no interaction with the film (Korbydan, 1961) or that waves which grow on a stratified film will grow to the top of the pipe (Taitel and Dukler, 1976). Jepson and Taylor (1993) claim that the pipe should be above 7.5-cm to mimic the mechanisms observed in large diameter pipelines. Further, little research has been done on three phase flow.

This work will provide the data necessary in large diameter three phase flow to include the effects of inclination and pressure.

CHAPTER 2

LITERATURE REVIEW

A thorough review of flow pattern modeling, existing flow pattern data, and slug flow characteristics follows.

2.1 Modeling of Flow Regime Transitions

Given an exact set of conditions with fully-developed flow and no terrain-induced flow effects, a particular flow pattern will occur. Many researchers have attempted to produce a way to report all of the necessary information to correlate the flow transitions. Baker (1954) produced what is thought to be the first flow regime map. He created a plot of the transition from one flow pattern to another with easily selected design conditions. Knowing the mass velocities of the liquid and the gas phases, along with the fluid properties, the flow pattern would be predicted by his flow pattern region plot. This was limited to two phase flow and did not include the effects of pressure, diameter, or inclination.

Mandhane *et al.* (1974) created a two-phase flow map based on the superficial gas and superficial liquid velocities. These are defined as the flow rate divided by the cross-sectional area of the pipe. With a map such as this, there should only be one for a given pipe diameter, inclination, gas, liquid, temperature, and pressure. The temperature and pressure mostly affect the fluid properties. Thus fluid properties, diameter, and inclination specify the flow map which applies. The Mandhane plots have since become a standard format for publishing flow regime data in multiphase flow.

Due to the numerous combinations of defining parameters, it would be impractical to create a flow map for every possible combination. Rather, a way of modeling based upon mechanistic criteria which compares well with existing data would better serve the needs of industry. The first realistic two-phase flow regime transition model with mechanistic criteria was produced by Taitel and Dukler (1976). This method is still used as a basis of comparison of all subsequent models. Figure 2.1 is a Mandhane plot of the transitions between the five major flow regimes (stratified, stratified wavy, intermittent, dispersed bubble, and annular) as specified by the Taitel and Dukler criteria. Their model combines plug, slug, and pseudo-slug flow together as intermittent flow. They also include one additional flow regime from those highlighted by Lee (1993): dispersed bubble.

Dispersed bubble flow occurs at high liquid and low gas flow rates. This is best characterized as full pipe liquid flow with small bubbles dispersed throughout the liquid in such a way that it is homogenous. The transition to this regime from intermittent flow is defined by Taitel and Dukler to be at the point where the turbulent flow forces overcome the buoyant forces of the gas bubbles.

The criteria for transition from stratified to stratified wavy flow is based upon wave generation. For this, Taitel and Dukler used the velocity criteria of Jeffreys (1925) and Benjamin (1959). These transitions are not of interest here since the primary flow regime transitions of interest to the oil and gas industry are the transition from stratified to slug flow and the transition from slug to annular flow.

For the transition from stratified to intermittent or annular flow using the Taitel and Dukler model, the simultaneous solution of two relations is required. The first is the conservation of momentum for the stratified film. Figure 2.2 depicts two phase stratified flow. The direction of the interfacial shear stress term is dictated by the *in-situ* velocity of

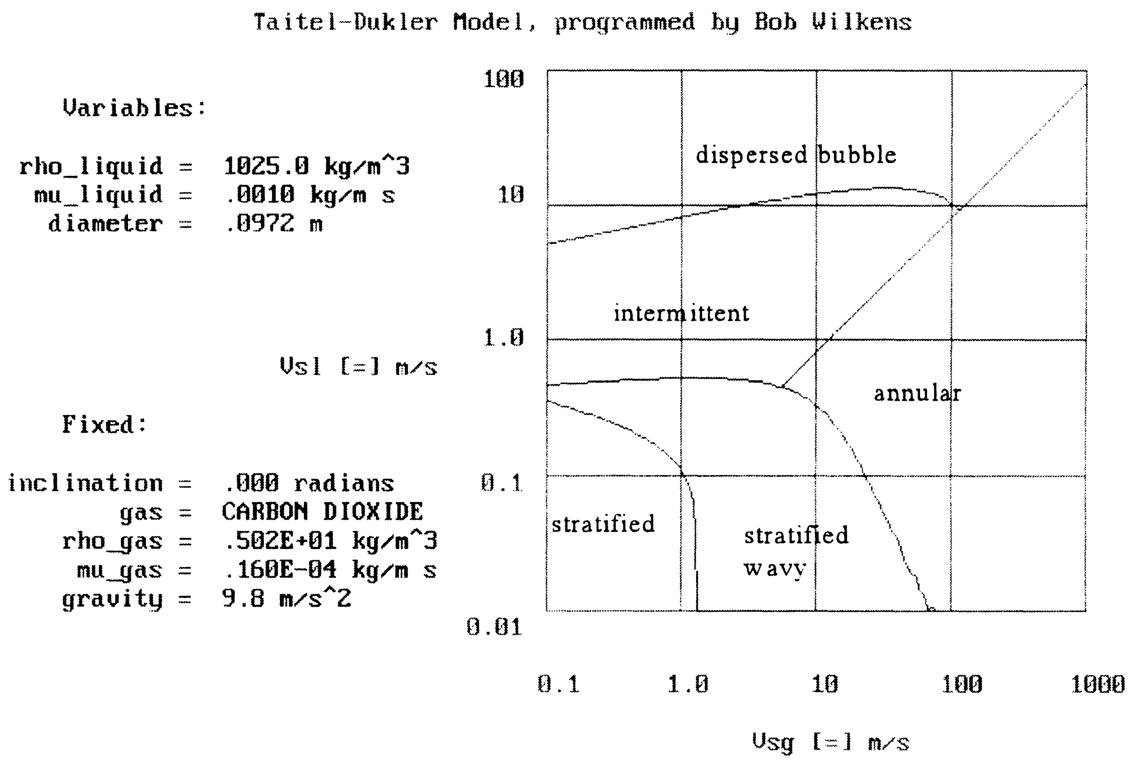

Figure 2.1: Flow regime transition map using Taitel and Dukler (1976) criteria.

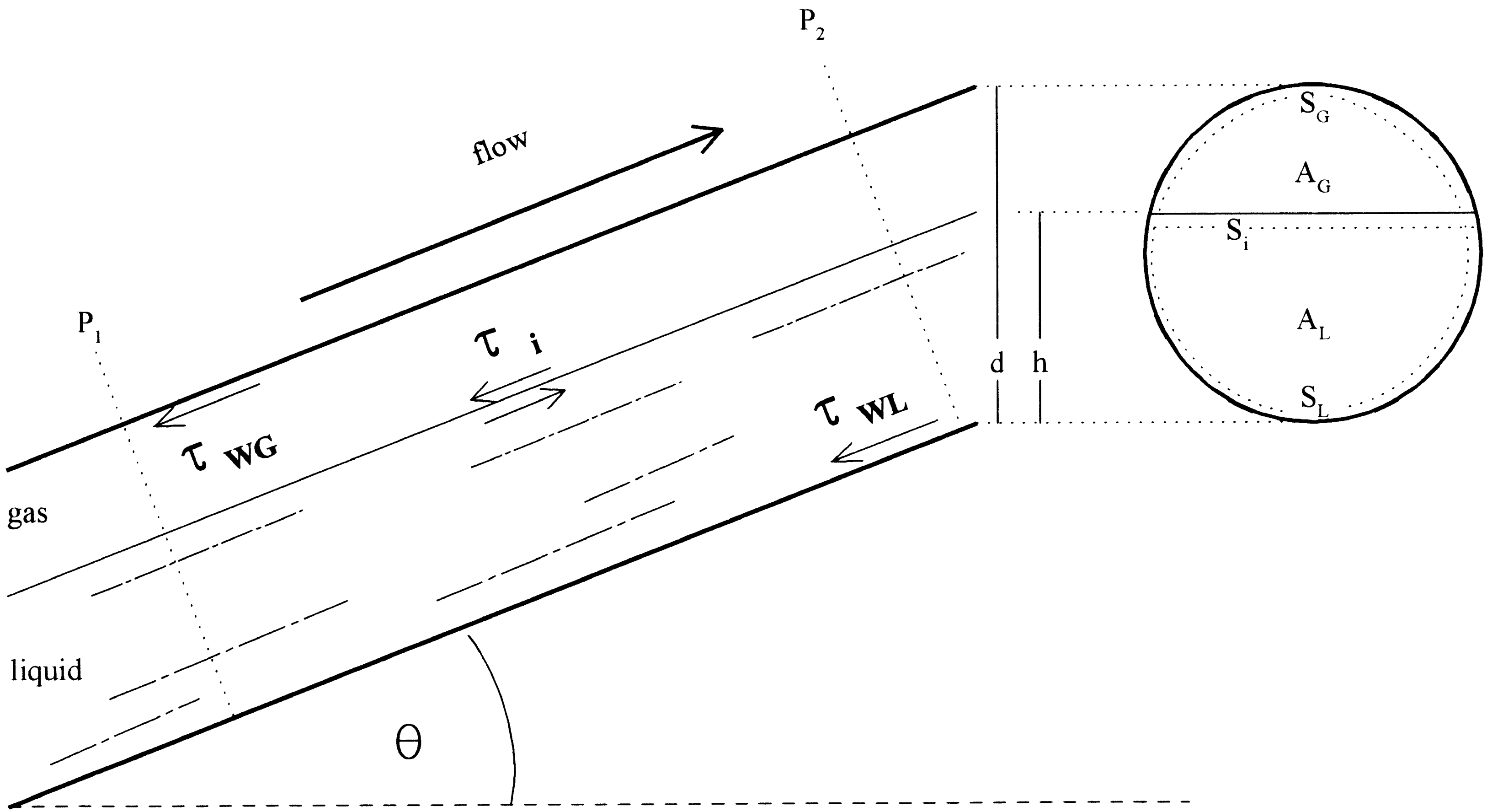

Figure 2.2: Shear stress diagram.

the gas phase exceeding the *in-situ* velocity of the liquid phase. The momentum conservation equation is generated by eliminating the pressure gradient from the momentum conservation for each individual phase.

$$\tau_{WL}\cdot\frac{S_L}{A_L} - \tau_{WG}\cdot\left(\frac{S_G}{A_G} + \frac{S_i}{A_G} + \frac{S_i}{A_L}\right) + (\rho_L - \rho_G)\cdot g\cdot\sin\theta = 0 \tag{2.1}$$

As will be seen later in Chapter 5, due to geometry the only unknowns in this equation are gas flow rate, liquid flow rate, and film thickness.

The second relation required for determining this transition involves the Kelvin-Helmholtz theory on wave stability. Taitel and Dukler noted that blockages (plugs, slugs, pseudo-slugs, annular flow) occurred if there was wave growth in the stratified film from a finite amplitude wave. Their criterion for transition thus states that when the conditions are sufficient for a wave to grow, intermittent or annular flow ensues. The wave growth condition is predicted from the Kelvin-Helmholtz stability criteria. This theory is based on the thought that as gas flows over a wave flowing between plates, it is forced to accelerate. This acceleration causes the pressure to decrease due to the Bernoulli effect. To compensate, the liquid level in the wave increases, opposing gravity. Taitel and Dukler apply this to the case of pipe flow with a small, but finite wave. Thus, the appropriate *in-situ* gas velocity required to exceed the gravitational force is determined.

$$u_G > \left(1 - \frac{h}{d}\right)\cdot\left[\frac{(\rho_L - \rho_G)\cdot A_G\cdot g\cdot\cos\theta}{\rho_G\cdot S_i\cdot d}\right]^{1/2} \tag{2.2}$$

At this point it should be specified that when Taitel and Dukler combined their equations in dimensionless form, there was a typographical error (Taitel and Dukler Equation 25). A quick substitution of the preliminary equations demonstrate that their dimensionless velocity term should be squared. For verification, the crude oil test case (Taitel and Dukler Figure 7) was solved both ways. It was clear that the proper solution was obtained with the squared term. Leaving this change out causes the transition to occur at a slightly higher liquid flow rate. This is mentioned because the Taitel and Dukler model plotted in most papers and dissertations for comparison is actually produced from the errant form of the equation.

The determination of whether this non-stratified flow is annular or intermittent must now be specified. Taitel and Dukler simply suggest that a stable slug can only form when the supply of liquid in the stratified liquid film is sufficient to maintain slug flow. If it is not sufficient, annular flow ensues. This matches the observations of Butterworth (1972). In their model, Taitel and Dukler propose that the minimum liquid required is a stratified film height of one-half of the pipe diameter.

This model has been verified (Barnea *et al.*, 1980, *etc.*) for small-diameter, low pressure, two phase systems at horizontal to near-horizontal pipe flow. The model has also been shown to not work well if the diameter is large (Jepson and Taylor, 1993) or with the presence of a third phase (Lee, 1993). Later researchers mostly revised the coefficients of the relations in the Taitel and Dukler model. Andritsos (1986) observed that Jeffreys waves do not occur for high viscosity liquids. Others have claimed that the minimum film height for slug flow should be changed to around 0.35 times the pipe diameter, while others have suggested that the film height requirement varies with slug length, film length, or liquid velocity.

In the solution of the momentum balance, the equation was transformed to dimensionless variables for ease of solution by incorporating the Lockhart-Matinelli parameter. To do this, the friction factor of the gas-liquid interface was estimated to be equivalent to the friction factor of the gas flowing against the wall. Andritsos and Hanratty (1987) demonstrated that this does not hold true at higher gas velocities and proposed a correction factor. This factor reduced the error in the momentum equation to within 10% of the experimental values, as measured by pressure drop, while the prediction from Taitel and Dukler was on the order of 50%. They proposed that if the superficial gas velocity was below a transitional superficial gas velocity, the interfacial friction factor was equivalent to the friction factor between the wall and the gas. Above the transitional superficial gas velocity, the interfacial friction factor could be estimated by:

$$f_i = f_G \cdot \left[1 + 15 \cdot \left(\frac{h}{d} \right)^{1/2} \cdot \left(\frac{V_{SG}}{V_{SG,t}} - 1 \right) \right] \qquad (2.3)$$

where the transitional superficial gas velocity is estimated by:

$$V_{SG,t} = \left(\frac{\rho_{Go}}{\rho_G} \right)^{1/2} \cdot 5\,\mathrm{m/s} \qquad (2.4)$$

and ρ_{Go} is the gas density at atmospheric conditions. The magnitude of this density ratio effect at higher pressures has not been reported.

Another improvement which has been presented is the three-phase momentum balance of Neogi *et al.* (1994). This is a modification of the film momentum balance of Taitel and Dukler (1976). This model differs by including an additional liquid phase and the shear stresses associated with it. Additionally, the model includes the gas-liquid interfacial friction factor modification of Andritsos and Hanratty (1987). This new model is then compared to experimental data to show close agreement to measured film heights in stratified flow.

For our concerns, we need a robust model which works well for large-diameter, three-phase, inclinable pipelines operating at high pressures such that the flow patterns can be predicted for typical transportation pipelines of the oil and gas production industry.

Jepson (1989) proposed new transition criteria for slug flow. Rather than wave growth to reach slug flow from stratified flow, Jepson postulated that a slug was a hydraulic jump which was propagating down the pipe. A hydraulic jump occurs when there is a change from subcritical to supercritical flow. Figure 2.3 illustrates the hydraulic jump in an open channel as devised by Chow (1959). A common measure of the turbulence of the hydraulic jump is the Froude number. The Froude number is less than unity for subcritical flow and greater than unity for supercritical flow. There are many forms of the Froude number which may be used in describing flow. In this treatment the film Froude number will be used. This is the ratio of the velocity difference between the film and the jump to the square root of the film height times the gravity.

$$Fr_f = \frac{V_t - V_f}{\left(g \cdot h_{eff}\right)^{1/2}} \tag{2.5}$$

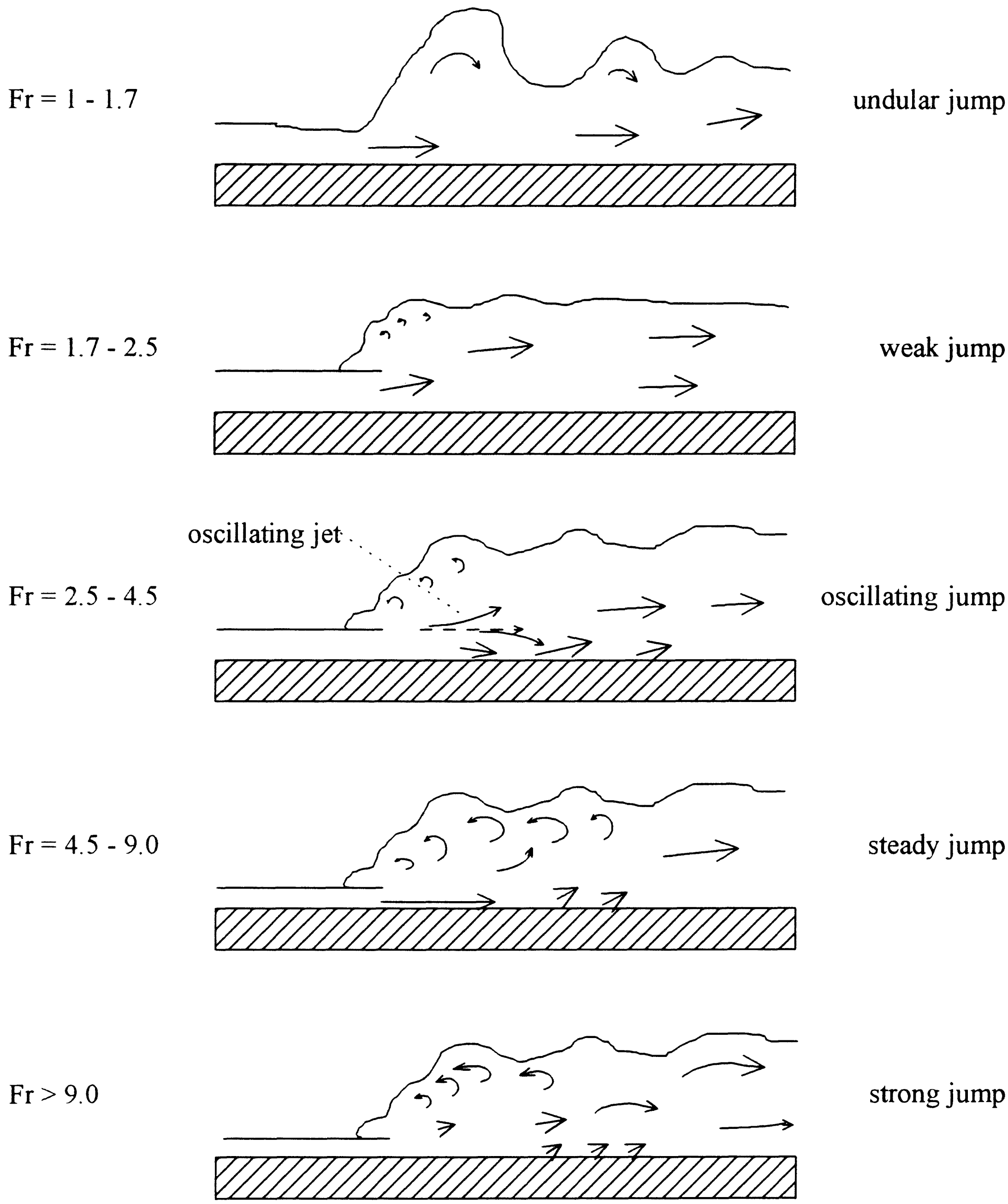

Figure 2.3: Characterization of the hydraulic jump by film Froude number (Chow, 1959).

For a pipe, the effective height is:

$$h_{eff} = \frac{A_L}{S_i} \tag{2.6}$$

As the film Froude number increases above unity in an open channel, stationary waves form. This is referred to in Figure 2.3 as an undular jump. For a film Froude number from about 1.7 to 2.5, a weak hydraulic jump is formed. This is characterized by a small area of recirculation (the beginnings of a mixing zone) as the high speed liquid film cuts into the slower, thicker jump. The high speed film holds back the thicker jump in what appears to defy physical laws. In fact, the height differential is maintained because the film is moving at a supercritical velocity, thus pressure cannot be transferred back into the film across the discontinuity in film height at the jump.

At a film Froude number of 2.5 to 4.5, the jump oscillates. That is, an oscillating jet enters the bottom of the jump and back again with an irregular period. A steady jump is formed from a film Froude of 4.5 to 9.0. In the steady jump, the end of the mixing zone marks both the end of the rolling wave and the point where the high velocity film slows to the liquid velocity in the jump. At a film Froude number greater than 9.0, a strong jump occurs. In a strong jump, the energy dissipation may reach as high as 85% (Chow, 1959).

The link between a slug and a hydraulic jump was first proposed by Kalinske and Robertson (1943). Their work used hydraulic jumps to remove air pockets from water pipes. Kouba and Jepson (1990) noted the similarity of the regions of Figure 2.3 to slug flow at similar film Froude numbers. Their ranges were 1.7 to 2.0, 2 to 5, 5 to 10, and over 10, for a weak slug, bubble pulsations, frothy roller, and very strong slugs, respectively.

With the hydraulic jump comes a separate conservation of momentum around the jump, as proposed by Stoker (1957), due to the discontinuity between the subcritical and supercritical flow regions. The Jepson (1989) model also uses a conservation of momentum for the liquid film region as proposed in the model of Taitel and Dukler (1976).

For closure, Jepson uses a conservation of mass around the slug body. Figure 2.4 represents a slug body with a coordinate system moving at the velocity of the liquid in the slug body. Dukler and Hubbard (1975) demonstrate that for a slug to be stable, the rate of liquid pick up at the front of the slug must be equal to the rate of liquid shedding at the rear of the slug. The rate of pickup at the front of the slug is well known. At the rear of the slug, Jepson proposes from observations that the shedding mimics that of a breaking dam. At the original site of a breaking dam, the height remains constant at four-ninths of the original height (Stoker, 1957). Also, the liquid velocity at a breaking dam is well known.

$$u = -\frac{2}{3}\cdot\sqrt{g\cdot h} \tag{2.7}$$

Transferred to a moving coordinate system and pipe flow, the liquid phase conservation of mass about a stable slug becomes

$$\rho_L\cdot\left[\left(u_L - V_S\right)\cdot\frac{A_L}{A} + \left(V_t - V_S\right)\cdot\frac{A_L}{A} + \left(V_t - V_G\right)\cdot\left(1 - \alpha_S\right)\right] = \rho_L\cdot\frac{2}{3}\cdot\sqrt{\frac{g\cdot d\cdot h}{4}\cdot\frac{A_{L_2}}{A}}\cdot\left(1 - \alpha_2\right) \tag{2.8}$$

For a pipe:

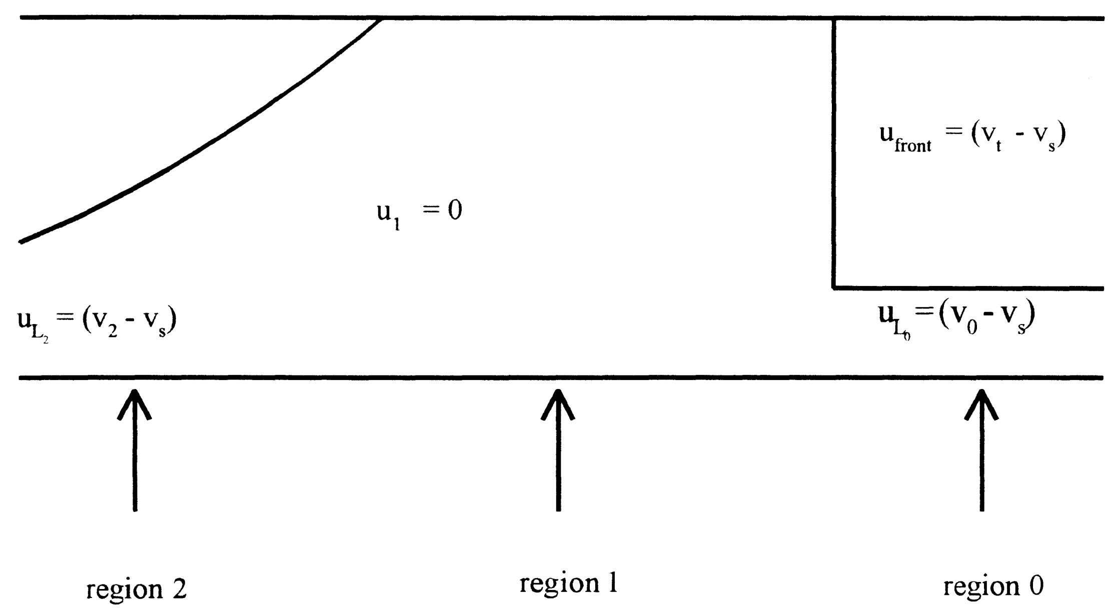

Figure 2.4: The three regions of the slug.

$$\frac{A_{L_2}}{A} \doteq \mathbf{0.442} \tag{2.9}$$

For the void fraction in the tail, α_2, no reported values have been found. Jepson (1989) specifies this value to be zero or equivalent to the average void fraction of the slug. Consider the void fraction distribution in Figure 2.5 for a fully developed slug as presented by Andreussi *et al.* (1993). The void fraction at the front of the slug is much high than it is in the body. The void fraction starts high at the front of the slug, then decreases rapidly through the mixing zone where it reaches a steady value through to the tail of the slug. Using a tail void of zero would clearly be too low, while using a tail void equal to the average void for the whole slug would be too high. It does appear, however, that the tail void would be well represented by the void fraction at the end of the mixing zone.

Jepson goes on to specify that at transition, as just one slug forms in the pipe, the superficial velocities in the film region match the input superficial velocities. Also, as the slug just touches the top of the pipe, the pressure exerted on the upper wall of the pipe in the slug region equals the pressure of the gas phase. This model is limited to atmospheric pressure and horizontal flow due to assumptions made in the equation development.

Thus, the goal of this work is to produce viable models to predict the transition between stratified and slug flow and the transition from slug to annular flow.

2.2 Flow Regime Transition Data

To create a successful flow regime transition model, data is necessary for comparison. There are many sources of flow regime transition data. As mentioned previously, the key

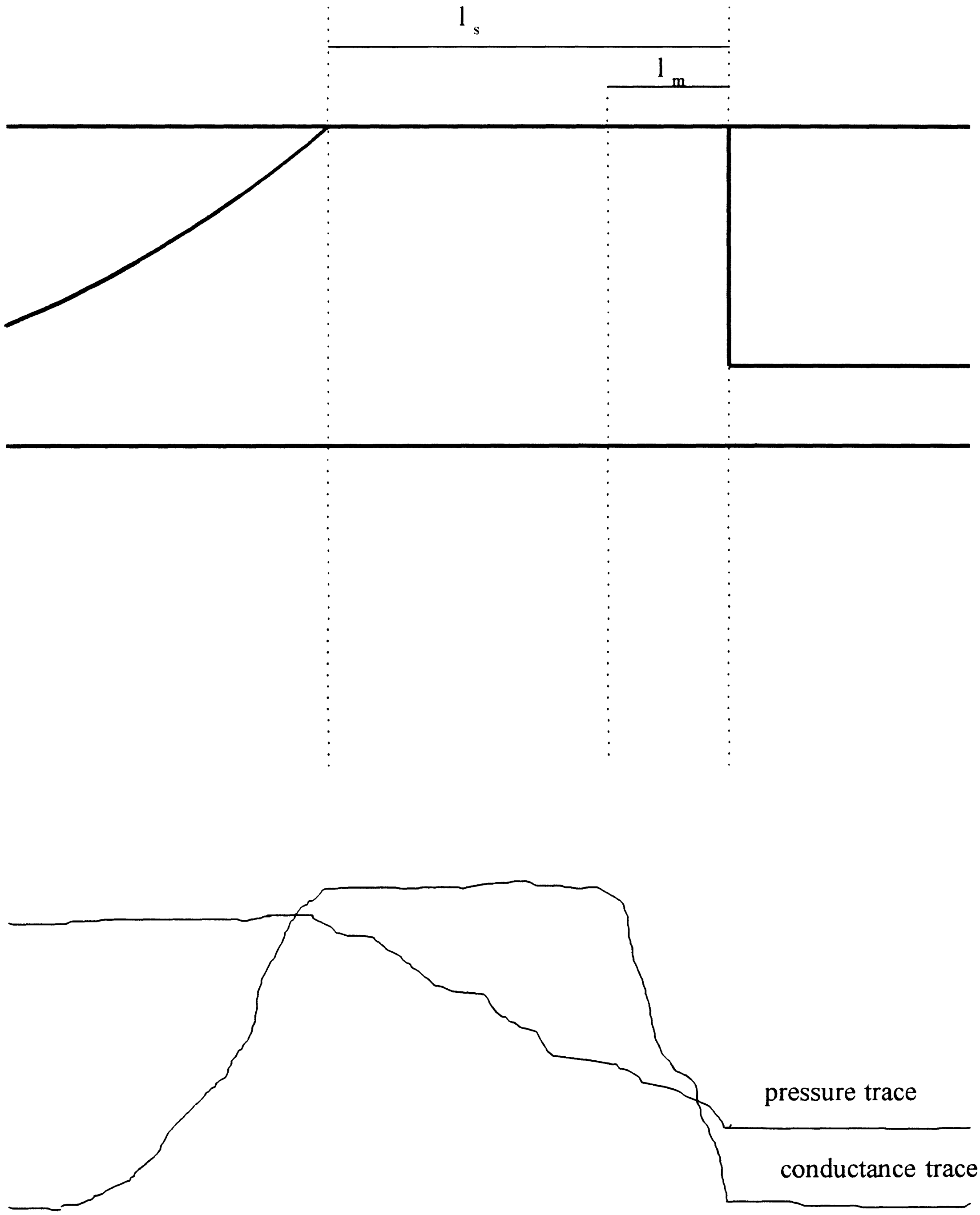

Figure 2.5: Liquid holdup along the slug body (Andreussi et al., 1993).

parameters to observe are fluid properties, inclination, and pipe diameter. The fluid properties are not as simple as they sound as temperatures and pressures affect many of the properties. Many of the flow regime transition maps which have been published are for air-water systems. Rarely are temperatures and pressures in the test section monitored and reported. Also, the water used is often tap water with no special treatment. The surface tension of inconsistent water supplies can vary by as much as 35%.

Baker (1954), as mentioned previously, produced the first flow regime map. He created the map with 2.54, 5.12, and 10.16-cm data then compared oil and gas field data from large diameter pipes with the intent of validating the model for prediction. As a result, little actual data is reported. Mandhane *et al.* (1974) compiled an extensive set of experimental flow regime transition maps comprising nearly 6,000 visual observations from various researchers. Although some of the data was for large pipe diameters, better than seventy percent of the observations were from pipe diameters less than two inches. They even note that their all encompassing map only works for smaller diameter pipes for this reason. The individual flow maps were also not included in the report.

Lin (1985) reported large and small diameter flow regime maps for horizontal air-water flow. Similarly, Jepson and Taylor (1993) and Wallis and Dobson (1973) reported large diameter flow regime maps, but they were also for horizontal air-water systems. Lee (1993) reported the flow regime transitions for a large diameter pipe with horizontal three phase flow. This data was for carbon dioxide gas, water, and a light-oil which is commercially available.

Limited flow map data exists for inclined pipelines. Gould *et al.* (1974) introduced

+45° and +90° flow pattern maps. Govier and Aziz (1972) presented a commonly used method of establishing flow patterns for inclined flow. Knowing the superficial velocities, densities, and interfacial tension, the system can be normalized to an air-water system. Then, specific ranges were correlated to occur for slug, bubble, froth, and annular flow. Barnea *et al.* (1985) proposed a model predicting transitions in inclined pipelines. Stanislav *et al.* (1986) reported inclined flow pattern data. Kokal and Stanislav (1986) characterized, extensively, the upflow and downflow patterns. The models and data compared well, however all of these studies involved two-phase flow. Additionally, flow in large-diameter pipes and at high-pressure have not been reported in inclined pipelines.

One intermediate step in this work is to create more flow regime data which includes the effects of inclination and pressure in a large diameter pipeline with oil-water-gas flow.

2.3 Slug Property Data and Modeling

Often in the slug transition model development, specific slug properties are necessary. These properties are also necessary for other design procedures. One of the earliest studies of slug mechanisms was by Korbydan (1961). The validity of this work is weak as it was based on studies in a tube which was one centimeter in diameter and less than two meters long. He proposed that the slug slipped along the top of the film with no interaction.

Dukler and Hubbard (1975) provided the first believable insight into mechanisms of the slug. The velocity of the slug was specified to be:

$$V_S = V_{SL} + V_{SG} \tag{2.10}$$

This has also been shown by Jepson (1989). A fundamental conclusion for Dukler and Hubbard was that for a slug to be stable, the rate of liquid pickup at the front must equal the rate of liquid shedding at the tail of the slug. The pickup at the front being well known, the rate of shedding was taken to be the liquid which, using the universal velocity profile, was flowing slower than the slug average velocity. From this, they were able to predict the translational velocity. Jepson showed that the translational velocity was better represented by:

$$V_t = \frac{V_S \cdot (1 - \alpha_S) - V_{SL}}{(1 - \alpha_S) - \dfrac{A_L}{A}} \tag{2.11}$$

This gives a better relation to what is found experimentally. A common way to consider the translational velocity is as a ratio with the superficial mixture velocity. At low gas flow rates, this ratio is about two (Kouba and Jepson, 1990; Jepson and Taylor, 1993). At higher gas flow rates, this ratio drops to a steady value of around 1.2 to 1.3. Gregory and Scott (1969) found this value to be around 1.35 in two centimeter diameter tubes. Dukler and Hubbard reported it to be 1.25 to 1.3. Kouba and Jepson specified 1.25 for superficial mixture velocities above 3 m/s. Jepson and Taylor showed the ratio tapering to 1.25 as the gas flow rate was increased.

Knowing the translational velocity, Dukler and Hubbard showed that the pressure drop across the slug could then be determined. Lin and Hanratty (1987) also reviewed the equations necessary for determining the pressure drop across a slug. Jepson and Taylor (1993) presented data on pressure drop in large diameter pipes.

A model for the length of a slug unit, the film region, and the slug was created by Dukler and Hubbard.

$$l_u = l_S + l_f \tag{2.12}$$

where:

$$l_u = \frac{V_t}{f_S} \tag{2.13}$$

These both match what was found by Andreussi *et al.* (1993). The slug length has never been well modeled. Jepson and Taylor present slug length data in large diameter pipes and show how it compares to what was found at other diameters. It is best to assume the slug length to be in the range of 15 to 22 times the pipe diameter (Andreussi, *etc.*)

A model for the length of the mixing zone was also established. For the diameter which it was developed (3.81-cm), their model has been found to largely over predict the mixing zone length. Since their model has no diameter correction, it largely under predicts the mixing zone length in large diameter pipes. Andreussi proposes that:

$$l_m \approx 30 \cdot \alpha_S \cdot d \tag{2.14}$$

The value of thirty was a correlation from data that they note might be fluid-dependent. Maley (1997b) presented the length of the mixing zone to be:

$$l_m = 0.061 \cdot Fr_f + 0.067 \tag{2.15}$$

This value was verified in this lab in 10-cm diameter pipes. It is well known that the mixing zone length scales with pipe diameter. At equal Froude number in this lab, the mixing zone length in a 10-cm pipe was found to one-third the length of the mixing zone in a 30-cm pipe. This matches the diameter effect found by Andreussi. It is suggested that the Maley prediction for the mixing zone length be converted for diameter. Since the diameter of her experiments was 10-cm, simply divide the diameter of the pipe of interest by 10-cm and then multiply by the mixing zone length from Equation 2.15.

Kouba and Jepson (1990) and Jepson and Taylor (1993) provided data on slug body void fraction. They found that in larger diameter pipes, the void fraction was higher than observed in smaller diameter pipes. Gregory *et al.* (1978) presented a commonly used method for determining void fraction based upon the superficial mixture velocity.

$$\alpha_S = 1 - \frac{1}{1 + \left(\frac{V_M}{8.66\,\mathrm{m/s}}\right)^{1.39}} \tag{2.16}$$

Barnea and Brauner (1985) presented a mechanistic slug body void fraction model comparing breakage forces and coalescing forces, but this model is only valid at low gas velocities. Andreussi *et al.* (1993) detailed the distribution of void within the slug and film including the effect on pressure and conductance traces. This was shown in Figure 2.5. Gopal (1994) studied void fraction as a function of distance in moving slugs, correlating it to the Froude number and fluid properties using a second order process model. This matched the Froude number dependence of void fraction demonstrated by Jepson and Taylor. This model is limited in that slugs were only studied at a film Froude number of up to 4. Maley

(1997b) studied the void fraction distribution in a stationary slug with various liquids and gases also correlating it to the Froude number with a lead-lag process model. This lead-lag model produces the void fraction at any location within the mixing zone.

$$\alpha_S(x) = \frac{X_{lg} - X_{ld}}{X_{lg}} \cdot e^{\left(-\frac{x}{X_{lg}}\right)} \tag{2.17}$$

Thus, the average void fraction within the mixing zone can be established by a simple integration.

$$<\alpha_{S,MZ}> = \frac{X_{lg} - X_{ld}}{l_m} \cdot \left[e^{\left(-\frac{x}{l_m}\right)} - 1 \right] \tag{2.18}$$

For a carbon dioxide water system:

$$\begin{aligned} X_{ld} &= 0.057 \cdot Fr_f - 0.25 \\ X_{lg} &= 0.16 \cdot Fr_f - 0.63 \end{aligned} \tag{2.19}$$

For a carbon dioxide light oil system:

$$\begin{aligned} X_{ld} &= 0.062 \cdot Fr_f - 0.057 \\ X_{lg} &= 0.18 \cdot Fr_f - 0.16 \end{aligned} \tag{2.20}$$

After the mixing zone, the lead-lag model no longer applies. Here the void fraction becomes constant at the end of the mixing zone until the end of the slug. This constant value can then be determined by evaluating the original model at the end of the mixing zone. Thus the average can be taken as:

$$<\alpha_S> = \frac{<\alpha_{S,MZ}>\cdot l_m + \alpha(x = l_m)\cdot(l_S - l_m)}{l_S} \tag{2.21}$$

Due to the lack of a better relation, the slug length should be taken to be fifteen pipe diameters.

Hubbard (1965) presented slug frequency data for a 3.7-cm tube. Jepson and Taylor provided data on slug frequency for a large diameter, horizontal pipe. Taitel and Dukler (1977) presented an exceptionally detailed slug frequency model that has gained little acceptance due to the rigorous calculations involved for the accuracy achieved. Gregory and Scott (1969) presented a commonly used slug frequency model based upon the slug Froude number. They solve this relation in two ways (one applies if the translational velocity is known, the other if only the superficial mixture velocity is known). If the translational velocity is known:

$$f_S = 0.0157\cdot\left[\frac{V_{SL}}{g\cdot d}\left(\frac{36\,\mathrm{m^2/s^2}}{V_t} + V_t\right)\right]^{1.2} \quad [=]\ s^{-1} \tag{2.22}$$

If the translational velocity is not known, they simply substitute with 1.35 times the mixture velocity and simplify. The value of 36 comes from their observation that the frequency tended to decrease until a translational velocity of 6 m/s, then it increased.

Hill and Wood (1990) also created a commonly used slug frequency model. Their model was based upon the equilibrium film height.

$$f_S = 0.275 \cdot \frac{V_M}{d} \cdot 10^{\left(2.68 \cdot \frac{h}{d}\right)} \; [=] \; hr^{-1} \tag{2.22}$$

Both of these models claim equal correlation to the data.

Although the data presented is mostly for low pressure, small-diameter, two-phase, horizontal pipelines, it does illustrate the interrelationship of these properties. Whatever slug property data can be collected while creating the flow regime maps will be reported such that it is available for high pressure, large diameter, inclined, multiphase slug flow.

CHAPTER 3

EXPERIMENTAL SETUP AND PROCEDURE

Due to the lack of available data on flow regimes and the effects of inclination, pressure, and water cut, experiments were carried out to investigate these parameters. A description of the experiments follows.

3.1 Description

An 18-m long, 9.72-cm inner diameter, high-pressure (13 MPa), high temperature (90°C), inclinable 316 stainless steel flow loop has been commissioned for the study of multiphase flow and its subsequent effects upon corrosion. Figure 3.1 is a process flowsheet of the system. A predetermined oil and water mixture is stored within a 1.4 m^3 mixing tank. The liquid is moved through the system by a centrifugal pump powered by a 3 - 15 kW variable speed Baldor motor. The liquid flow is then controlled within a range of zero to 100 m^3/hr with a combination of the variable speed pump and a recycle stream. Flow rate of this stream is maintained by the manipulation of gate valves labeled A and B. This recycle stream also serves to agitate the mixing tank to ensure well-mixed flow. The flow rate is determined in one of two liquid flow metering sections. For lower superficial liquid velocities (0.1 to 0.5 m/s) the liquid passes through a 2.43-cm inner diameter flow metering section. At higher superficial liquid velocities (0.5 to 1.5 m/s) the liquid passes through a 7.37-cm inner diameter flow metering section. In both cases, the flow rate was determined with a TMTR 510 frequency analyzer which was calibrated to a GH Flow Automation model number 6531 in-line turbine flow meter.

A 2-MPa feed line supplies carbon dioxide gas from a 20,000 kg receiver. After

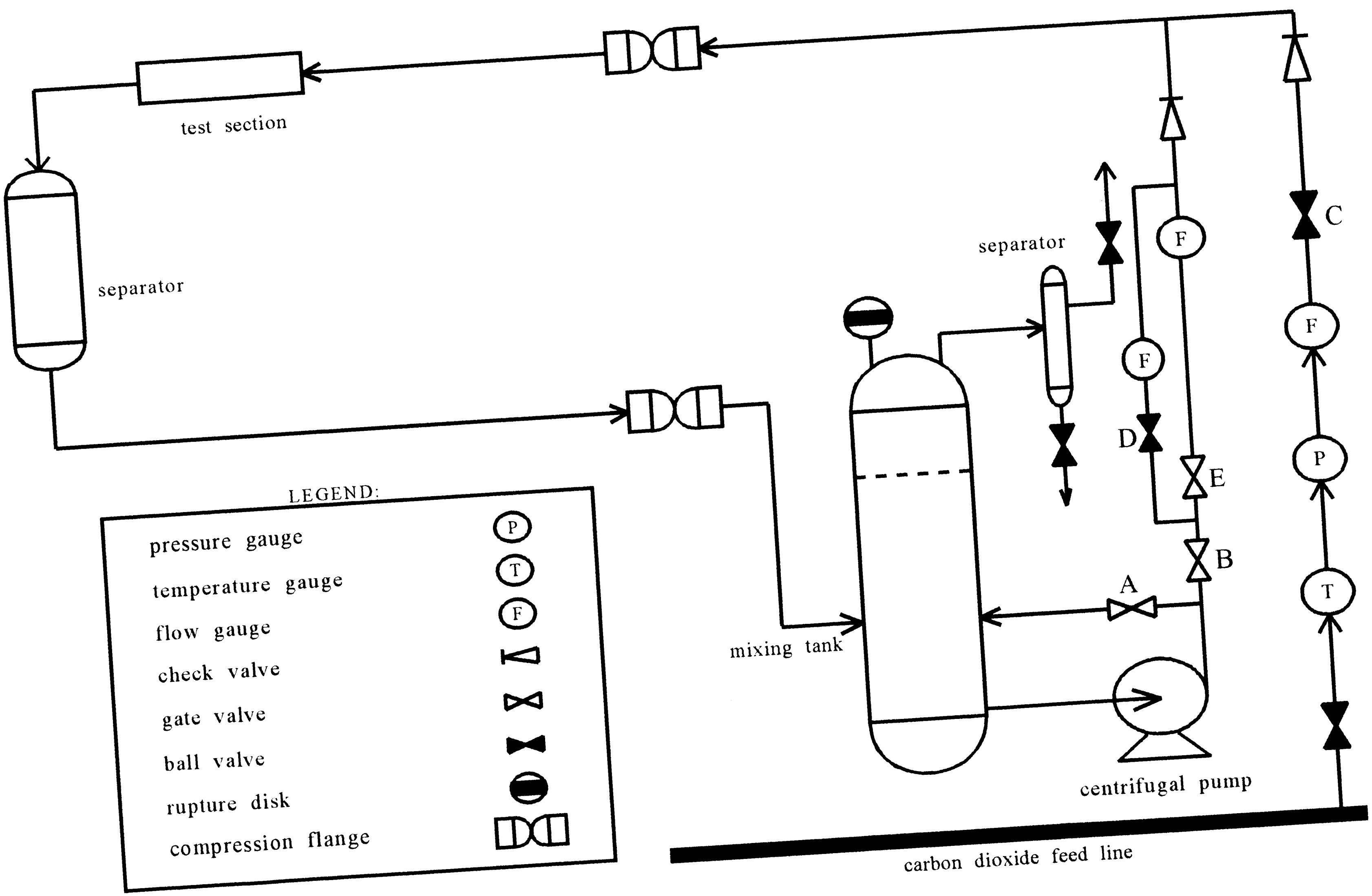

Figure 3.1: High-pressure, inclinable flow loop orientation.

passing through a pressure regulator, the gas flow rate is set by adjusting ball valve C. A Hedland variable area flow meter, with a range of 3 to 30 standard cubic meters per minute, is located between the ball valve and the pressure regulator to determine the gas flow rate. The gas temperature and pressure are monitored between the flow meter and the pressure regulator. The temperature is measured with a Noshok -75 to +75°C temperature gauge while the pressure is measured with a Noshok 0 to 2.8 MPa pressure gauge. The gas flow rate is corrected accordingly. The gas then passes through a check valve, to avoid possible liquid backflow, and into the liquid flow.

The combined flow enters the test loop through a compression flange, allowing the inclination to be set at any angle. Upon entering the inclined portion of the test loop, the multiphase mixture travels 18 meters before reaching the test section.

Figure 3.2 illustrates the test section with the instrument port locations. Port A is a fluid sampling port used primarily when preparing for corrosion experiments. Through this port, the iron and oxygen content can be monitored. System temperature is measured through port B with a type-K thermocouple connected to an OMEGA DP3200-TC electronic analyzer with display.

Any of the ports labeled C can be coupled and used to measure differential pressure. In these experiments, the differential pressures are measured between the two sets of taps placed 10 and 132-cm apart. The selection of these ports will be described later. The measurements are made with 0 to 35 kPa OMEGA PX-750 heavy duty differential pressure transducers. When activated with a +24 VDC signal, the transducers produce a current signal of 4 - 20 mA, corresponding to the differential pressure. This signal is sent through

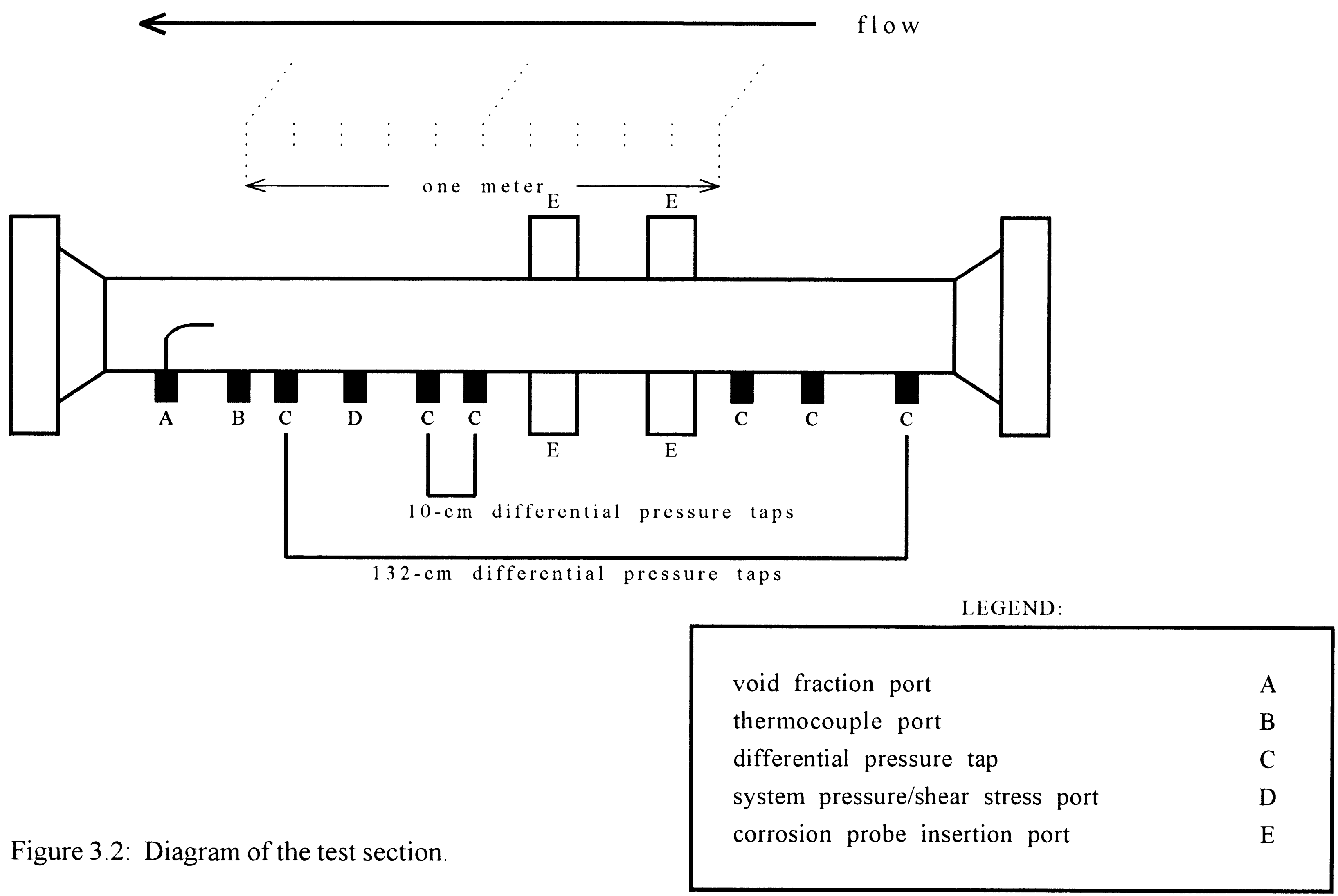

Figure 3.2: Diagram of the test section.

a second-order low-pass filter designed to eliminate frequencies greater than 10 kHz. This filter is necessary due to the high-frequency noise produced when using variable speed pumps. The signal is then shunted with a 500-ohm resistor across a Keithley-Metrabyte DAS 16-Jr. data acquisition board thus giving a signal of 2 to 10 volts. A 75 MHz Pentium PC has been programmed through QuickBASIC to average 100 data values before recording it to the hard disk. This occurs at a rate of 60 values for each channel per second for an overall sampling rate of 12 kHz. Prior to recording the data, a digital oscilloscope is used to ensure an absence of noise.

Port D is used to monitor the test section pressure. This pressure is measured with a 0 to 2.8 MPa Noshok pressure gauge. The ports marked E can be used to insert corrosion probes if necessary.

Additional data can be taken using two upflow and two downflow acoustic sensors provided by BP Research. These sensors are mounted on top of the pipe in the test section and at an equal distance of 18-m down the return leg of the flow loop. The signals from these sensors are also conditioned with a low-pass filter. These signals are recorded similarly to those for differential pressure. A separate program averages 75 data values before recording it to the hard disk. This occurs at a rate of 60 values per second for an overall sampling rate of 18 kHz.

Upon leaving the test section, the multiphase flow passes through a separator to prevent siphoning due to the declined angle of flow return and to destroy the flow pattern. The mixture passes back through another compression flange and then re-enters the mixing tank. The gas passes through a de-entrainment plate through a back-pressure regulating control valve, through a separator, and is vented to the atmosphere. The liquid from the separator is collected to be re-injected into the system.

3.2 Test Matrix

For this study, it was desired to have three phase (liquid-liquid-gas) flow data in a large diameter, inclinable pipeline which included the effects of pressure. The following fluids were selected. For the gas phase, carbon dioxide was used. For one liquid phase, a light oil, with the trade name LVT 200, from Conoco was selected. For the other liquid phase, the saltwater was used. The saltwater was made by adding a salt mixture to deionized water. The mixture used was Substitute Ocean Water ASTM D1141-52. Table 3.1 lists the properties of the fluids used in these experiments along with other properties of interest.

Table 3.1: Properties for fluids tested and other fluids of interest at 20° C.

fluid	density (kg/m^3)	viscosity (Pa•s)	surface tension (N/m)
saltwater	1025	0.001	0.07
light oil	810	0.003	0.03
CO_2 (0.10 MPa)	1.84	0.000016	---
CO_2 (0.14 MPa)	2.47	0.000016	---
CO_2 (0.27 MPa)	5.02	0.000016	---
CO_2 (0.45 MPa)	8.25	0.000016	---
CO_2 (0.79 MPa)	14.9	0.000016	---
CO_2 (1.48 MPa)	29.1	0.000016	---

For carbon dioxide, the density was predicted using the Redlich-Kwong equation with standard parameters as expressed by Reid *et al.* (1987). The gas viscosity was predicted using the Chung equation as expressed by Reid *et al.* (1987). The system temperature was maintained at 20°C. The matrix studied is listed in Table 3.2. Note that water cut is the volume percent of the liquid which is water.

Table 3.2: Experimental test matrix for flow regime and flow property determination.

property	range
water cut	40, 80, 100%
pressure	0.27, 0.45, 0.79 MPa
inclination	horizontal, ± 2°, ± 5°
temperature	20 °C
diameter	0.0972 m
superficial gas velocity	0 - 13 m/s
superficial liquid velocity	0.1, 0.5, 1.0, 1.5 m/s
gas	carbon dioxide
water	saltwater
oil	light oil

3.3 Nonvisual Flow Technique

Due to the high pressure operation of the system, and to prevent corrosion, the flow loop was constructed from 316 stainless steel. Thus, a nonvisual method of flow pattern determination and slug property measurement had to be established and validated. The following technique was established, is explained in detail in Wilkens and Jepson (1996), and is at the present time in the application process for a U.S. Patent.

Lin and Hanratty (1987) demonstrated that slugs could be detected, and their frequencies determined, by measuring single point pressure fluctuations. This was accomplished through a cross-correlation function of two single point pressures. When the time difference of the pressure fluctuations between the taps was appropriate for the superficial gas velocity and the distance between the sensors, the flow was slug. When it took too long, it was pseudo-slug flow. Andreussi *et al.* (1993) observed similar fluctuations in single point pressure measurements for slug flow. Recall that Figure 2.4 illustrates the pressure as a function of distance into the slug. Fan *et al.* (1993) demonstrated that as the slug passes a point in the pipeline wall the pressure increases suddenly due to the acceleration of the film, continues to rise in the slug body due to frictional losses, then rises further into the gas pocket which is forcing the slug down the pipe. Thus, the front of a slug can be identified from pressure measurements while the tail of the slug cannot.

Spedding and Spence (1993) identified waves and liquid films visually, and reported the corresponding pressure fluctuations. Although not noted by the authors, these fluctuations appear to have a characteristic shape and magnitude. Thus, it was decided that a technique using pressure fluctuations should be the answer for establishing flow patterns due to its nonintrusive nature.

For the conditions that would be used, a single point pressure transducer was impractical. The range necessary would be on the order of megapascals while the sensitivity would be on the order of a hundred pascals. Due to this, a technique was established using differential pressure transducers. The differential pressure method was validated by direct comparison with visual observations.

In a low pressure acrylic flow loop the differential pressure was recorded between two taps 149-cm apart. Simultaneously, a Super VHS recording of the flow was made. Figures 3.3 - 3.8 are the differential pressure traces for full pipe flow, stratified wavy flow, plug flow, slug flow, pseudo-slug flow, and annular flow, respectively. The full pipe and stratified wavy traces show little fluctuation as shown in Figures 3.3 and 3.4. Observations of the plug flow trace indicated the appearance of a low-frequency sinuous type wave with high frequency fluctuations superimposed on it. One of the key indications of plug flow is the magnitude of the differential pressure change (approximately 500 Pa). This corresponds to the hydrostatic difference in liquid height between a partially-full pipe, corresponding to the film region, and a full pipe, corresponding to the body of the plug. The visual frequency of the plugs also matched the low frequency of the sinuous wave observed in Figure 3.5.

Figure 3.6 shows the results for slug flow. The pressure fluctuations are now much greater with values of at least 1,500 Pa. The fluctuations are very different from those of plug flow. Characteristics include sharp changes in differential pressure with slug passage followed by periods which correspond to the film region. The frequency of the fluctuations matched visual observations.

At higher gas flow rates, pseudo-slug flow occurs. Here the magnitude of the differential pressure change also exceeds 1,500 Pa as seen in Figure 3.7. The frequency of this differential pressure trace was 52 per minute. Visually, only 23 slugs and pseudo-slugs were observed per minute. Careful frame-wise analysis indicated that the pressure fluctuations had reached the full magnitude even for small and medium sized waves. The

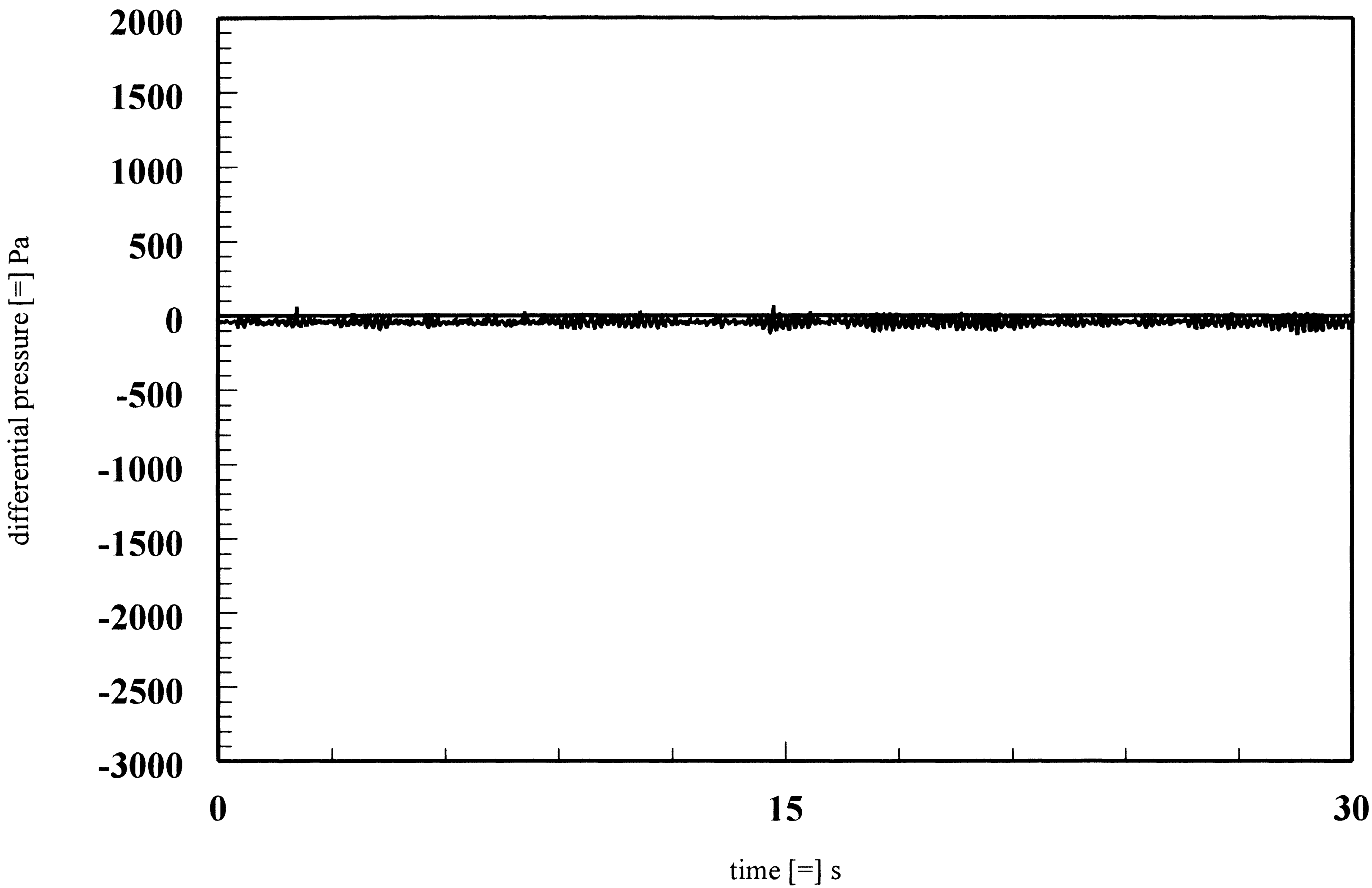

Figure 3.3: Differential pressure trace for full pipe flow.

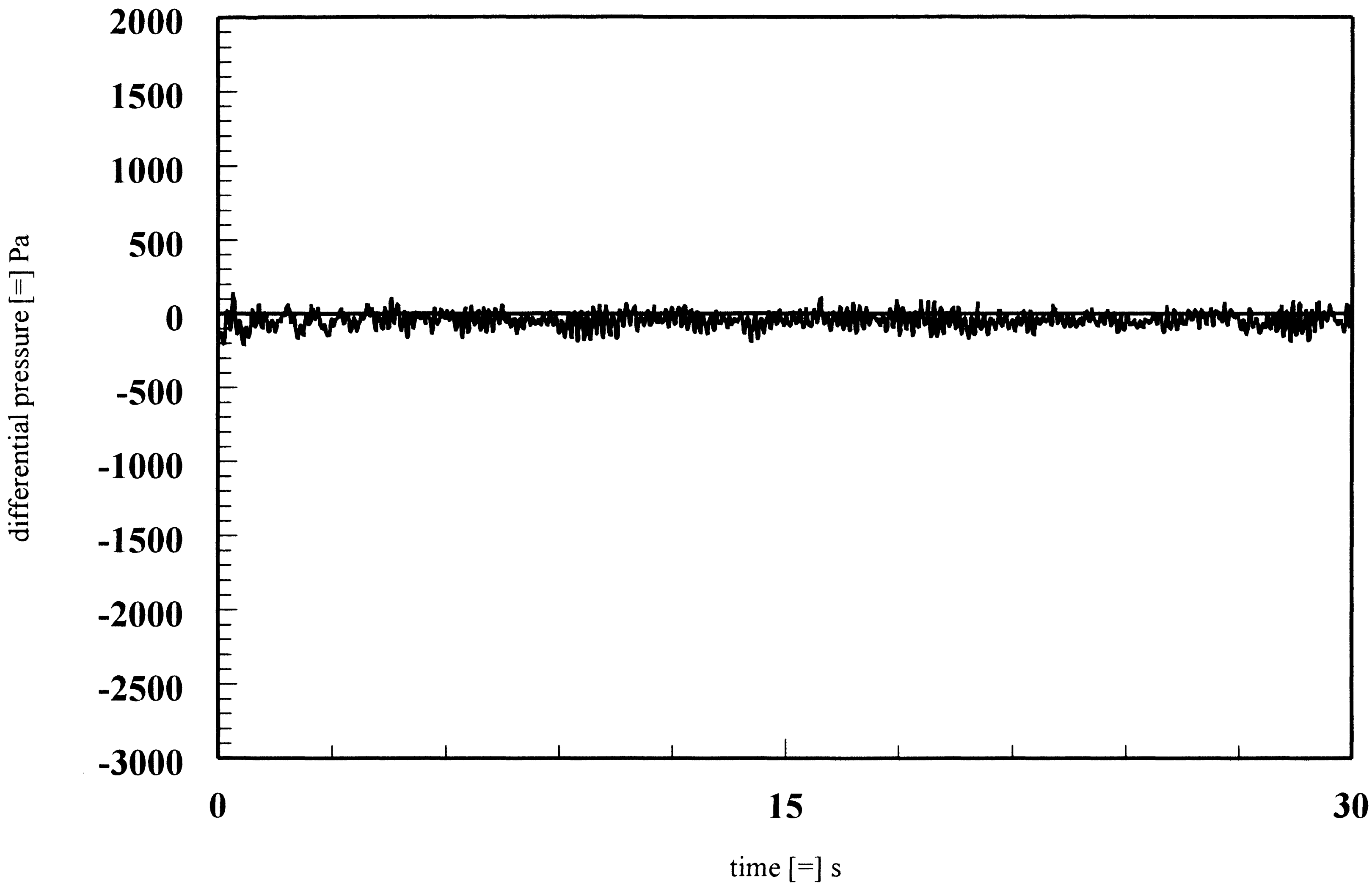

Figure 3.4: Differential pressure trace for stratified wavy flow.

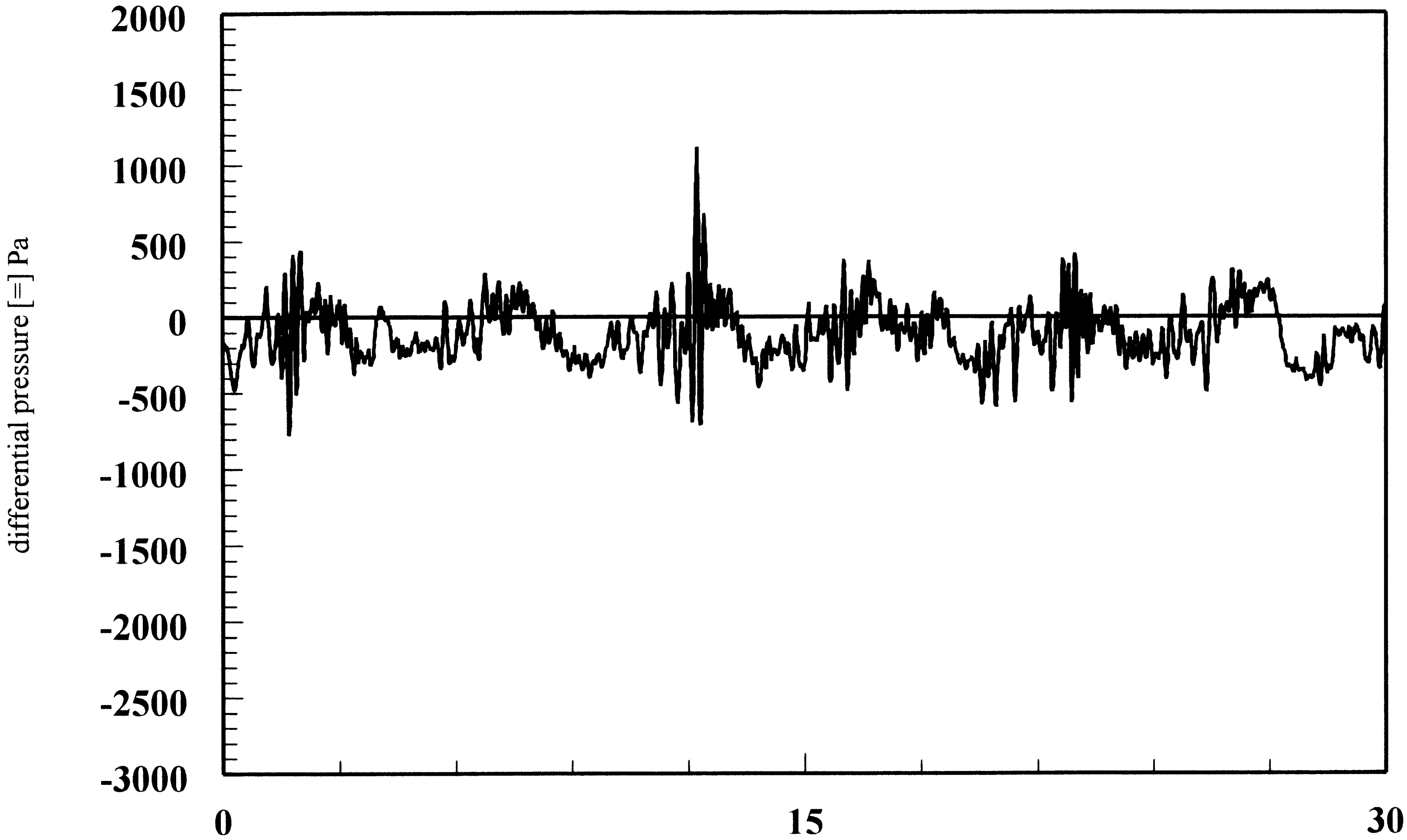

Figure 3.5: Differential pressure trace for plug flow.

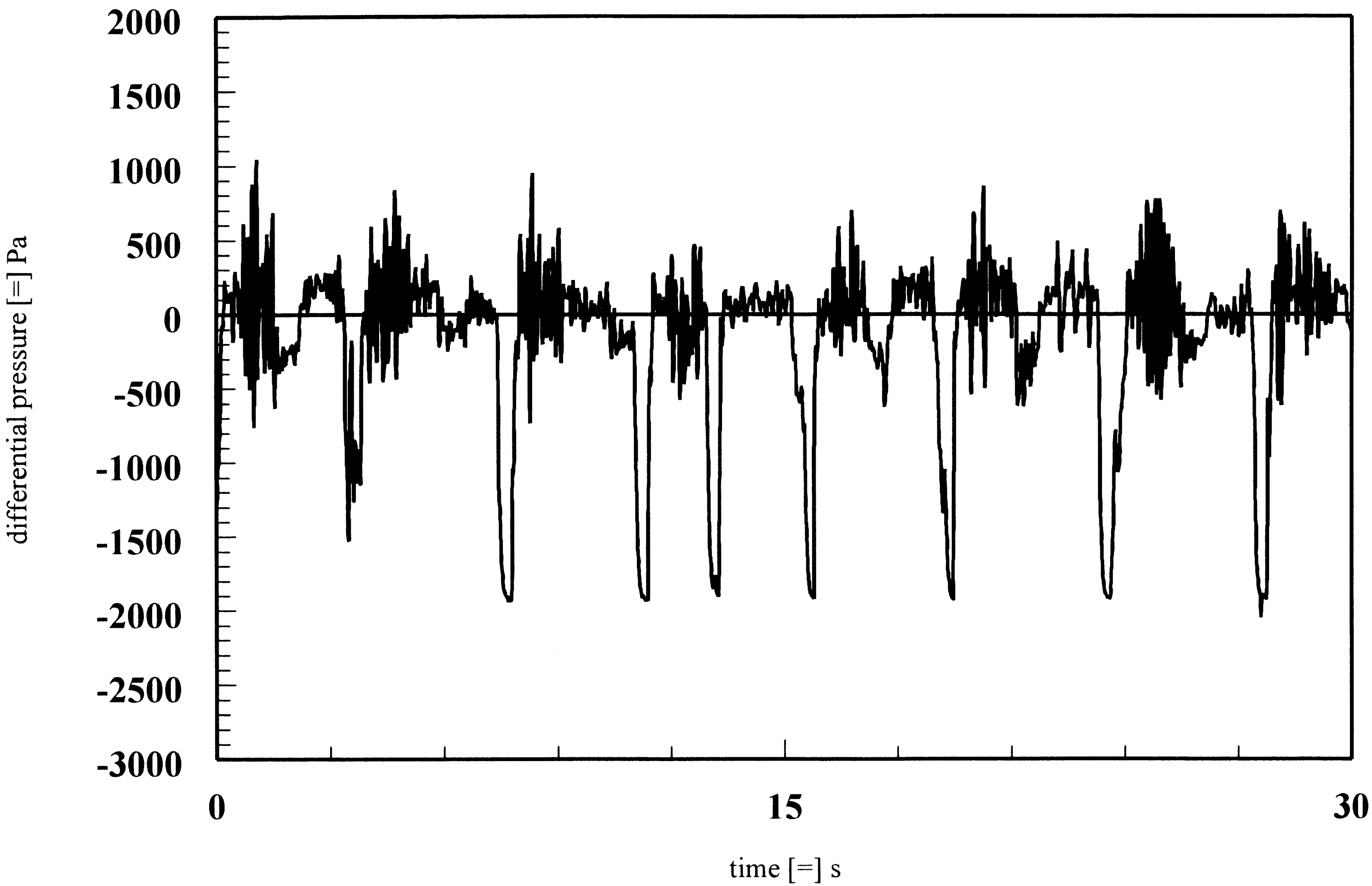

Figure 3.6: Differential pressure trace for slug flow.

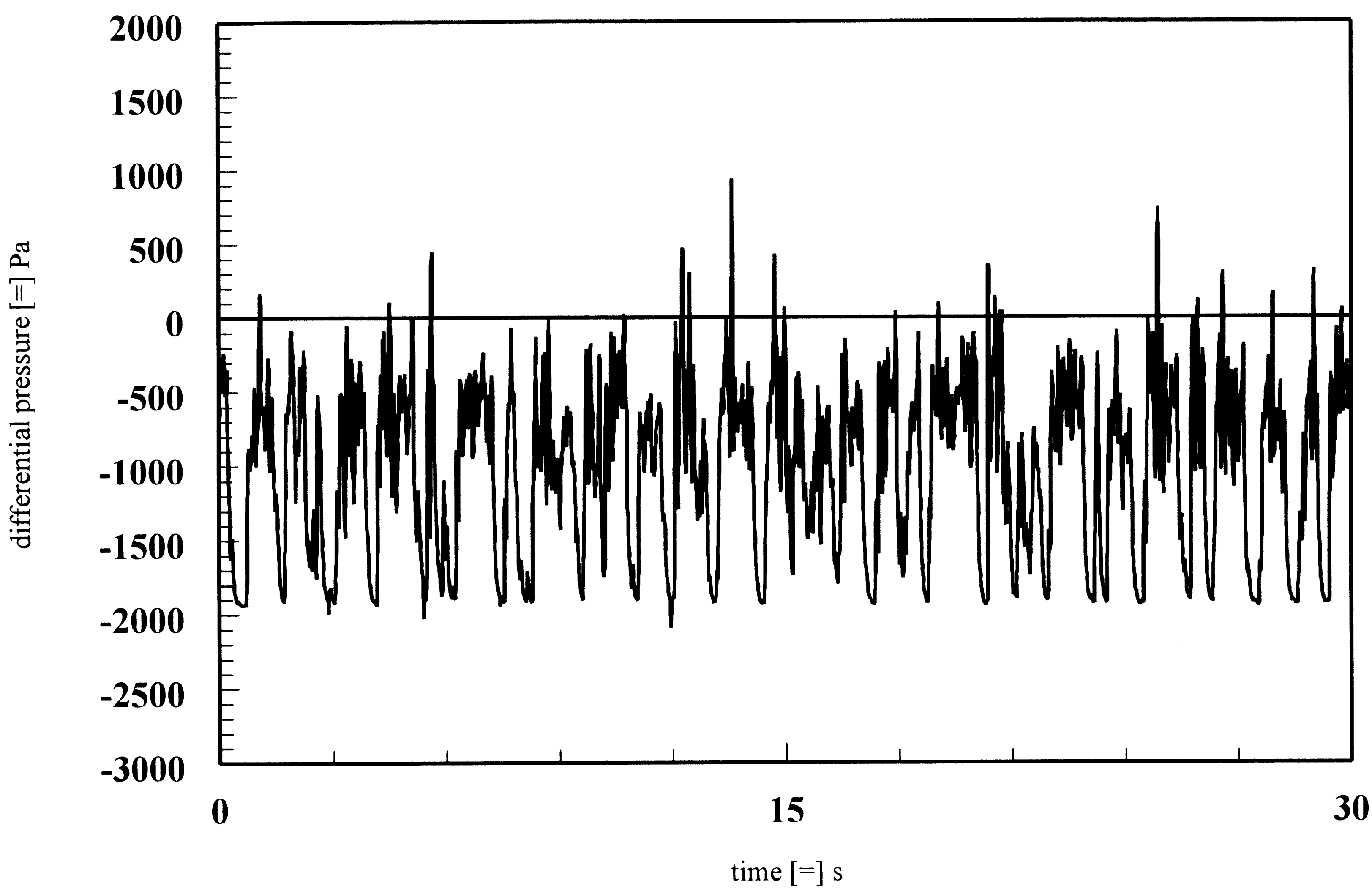

Figure 3.7: Differential pressure trace for pseudo-slug flow.

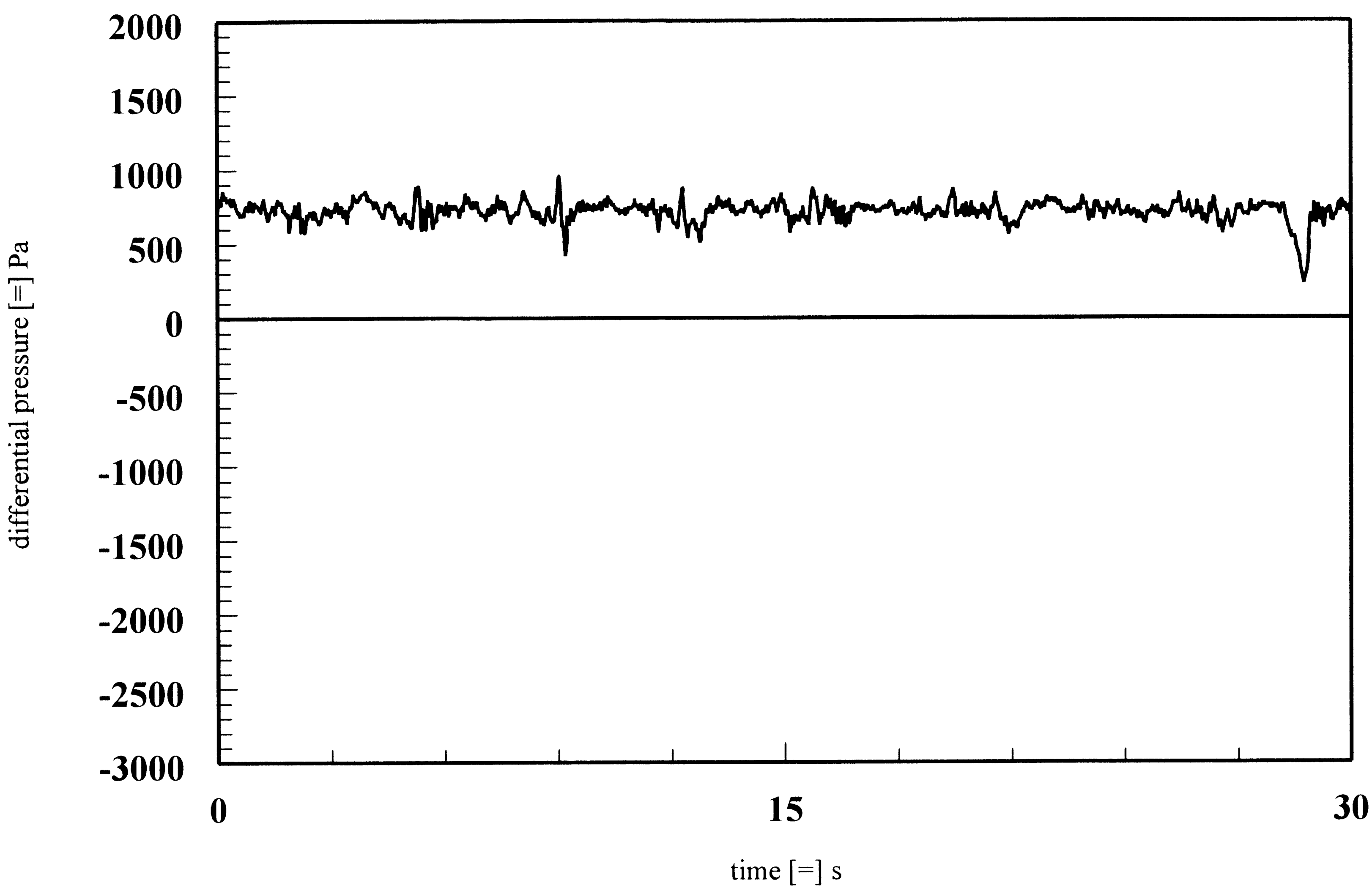

Figure 3.8: Differential pressure trace for annular flow.

frequency from Figure 3.7 was found to match the visually-observed frequency of intermittency, including small waves. Visual analysis also indicated that the velocity of these transients had been reduced in comparison to those of slug flow. The translational velocity of fully-aerated slugs was about 10% less while being about 50% less for waves. This matches those observed by Lin and Hanratty (1987).

Figure 3.8 shows the results for annular flow. Similar to full pipe and stratified flow, the differential pressure fluctuations are small. These fluctuations are typically less than 200 Pa.

From the pseudo-slug observations it was decided that two sets of differential pressure measurements can be used to identify flow patterns. The first set was between taps 132-cm apart with the second set of taps 10-cm apart. This short distance was selected such that no two slugs could simultaneously be between the taps. With two sets of differential pressure traces, a method of identifying the same slug on each trace is necessary. The location of each set of taps now becomes important. First, having both of the downstream taps from the same port was tried. With this arrangement, the two sets of differential pressure traces have fluctuations which end at the same time. It was found through experiment that sharing a tap caused too much interaction in the transducers. The pressure pulses were passing through the transducers and reflecting.

Therefore the best location of the second set of taps was completely between the first set of taps. Thus, the fluctuation from the second set of taps would be wholly inside the fluctuation of the first set of taps. This identification technique allows for easier correlation and the following criteria can then be used to establish flow pattern.

Stratified flow can be easily identified by both sets of differential pressure traces being relatively smooth (fluctuations smaller than 200 Pa). The same is true for annular and full pipe flow. The operator should know when full pipe flow is the case. Before each set of tests, a full pipe flow run should be used to verify that no external noise accompanies the data. It should be noted that the difference between annular and stratified flow cannot be isolated. With knowledge of when flow patterns occur, the annular flow regime can be specified for certain only when the gas flow rate is higher than that of a known slug or pseudo-slug case.

Plug flow is identified when there are regular differential pressure fluctuations of less than 1,500 Pa between the set of taps located 132-cm apart. It is also common in plug flow that the frequency decreases with an increase in gas flow rate. The velocity of the plug between the set of taps is usually about twice the superficial mixture velocity (the sum of the superficial gas and liquid velocities). This is noted from experiment and in the literature, as highlighted in Section 2.3.

The differential pressure fluctuation alone is not enough to identify slug flow. The characteristic translational velocity is also needed. The frequency at which the differential pressure fluctuations exceed 1,500 Pa for the 132-cm taps is recorded as F_{S1}. At the slug front, the pressure change is scalable to length. Through experiments of comparing with a known, it was verified that a differential pressure fluctuation of about 150 Pa for the taps separated by 10-cm was appropriate for slug flow. The frequency at which this occurred was marked as F_{S2}. To be a slug, it also must be moving at a characteristic velocity. Various researchers seem to agree that about 1.2 to 1.3 times the superficial liquid velocity is a good estimate of the translational velocity (see Section 2.3).

The translational velocity was determined using a distance to time ratio. The distance between the upstream taps for the two transducers was about 91-cm. Figure 3.9 is a differential pressure trace for a slug. The conditions were a superficial gas velocity of 9.3 m/s and a superficial liquid velocity of 1.0 m/s. The characteristic translational velocity should be about 12.4 m/s for this to be slug flow. This corresponds to a time delay between the two sets of pressure fluctuations of about 0.074 seconds. A set of parallel lines have been drawn in Figure 3.9 which are 0.074 seconds apart. The time delay matches what is expected. The frequency at which this occurs is reported as F_V.

It should be noted that early data did not have an upper limit for the translational velocity. The requirement was to reach at least 1.2 times the superficial mixture velocity. A better criterion is if the translational velocity is 1.2 to 1.4 times the superficial mixture velocity to be slug flow. Thus there are instances where there is an F_V for plug flow.

Pseudo-slug flow is marked when F_V is less than 50% of F_{S1} and F_{S2}. In pseudo-slug flow, the average translational velocity is about 0.5 to 1.2 times the superficial mixture velocity. Typically, slugs continue to occur in pseudo-slug flow. This is why the average translational velocity can be close to 1.2 times the superficial mixture velocity. Figures 3.9 and 3.10 represent such an instance. A set of parallel lines has been created for both figures which are exactly the time required for an appropriate translational velocity of a slug. Figure 3.9 shows that it meets the velocity criterion while Figure 3.10 shows that it does not. Thus, for the same conditions, at different moments in time, both flow patterns were present.

This technique is exceptionally tedious compared to the older visual methods, but it

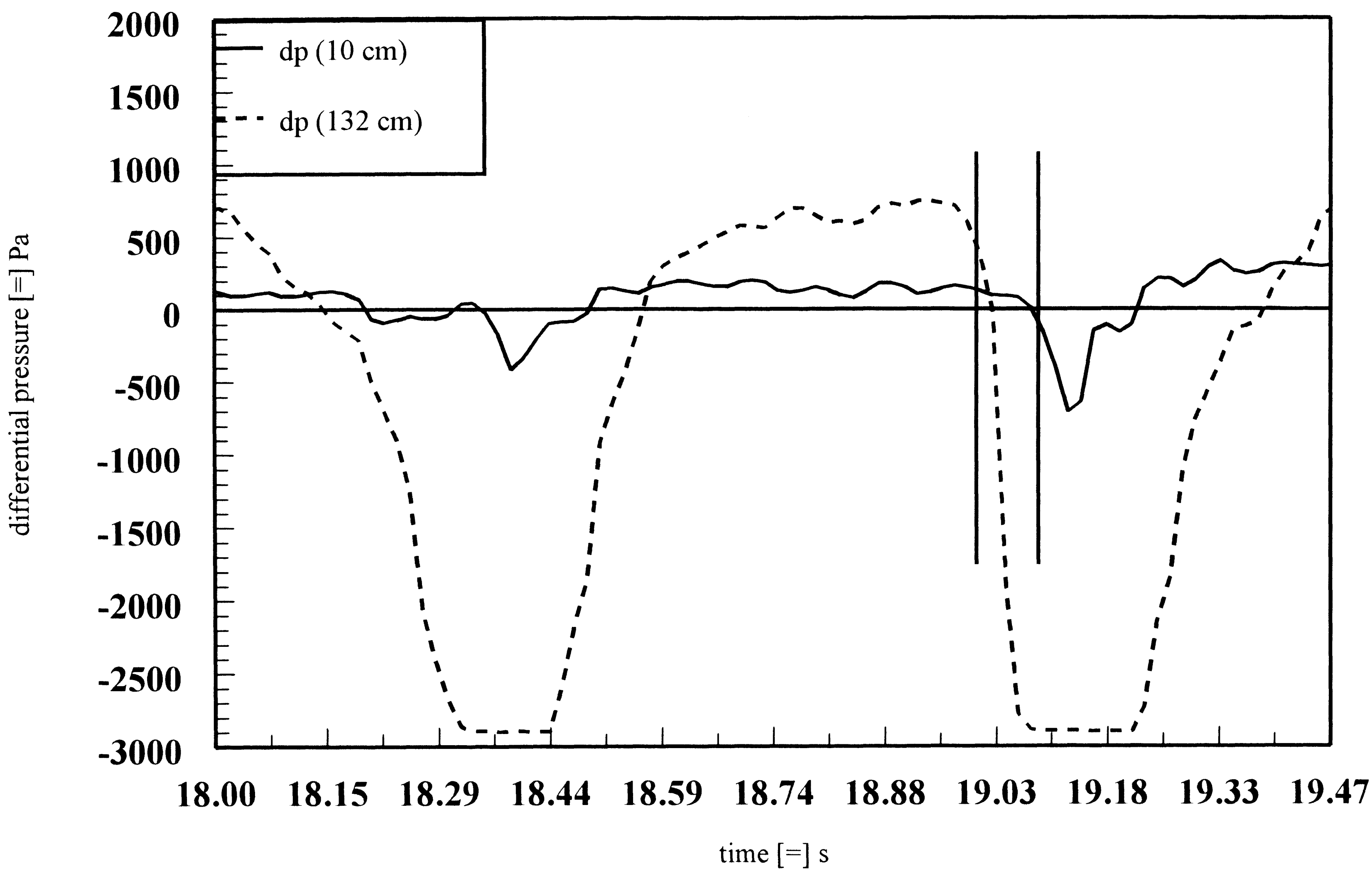

Figure 3.9: Differential pressure trace for V_t experimental = V_t predicted.

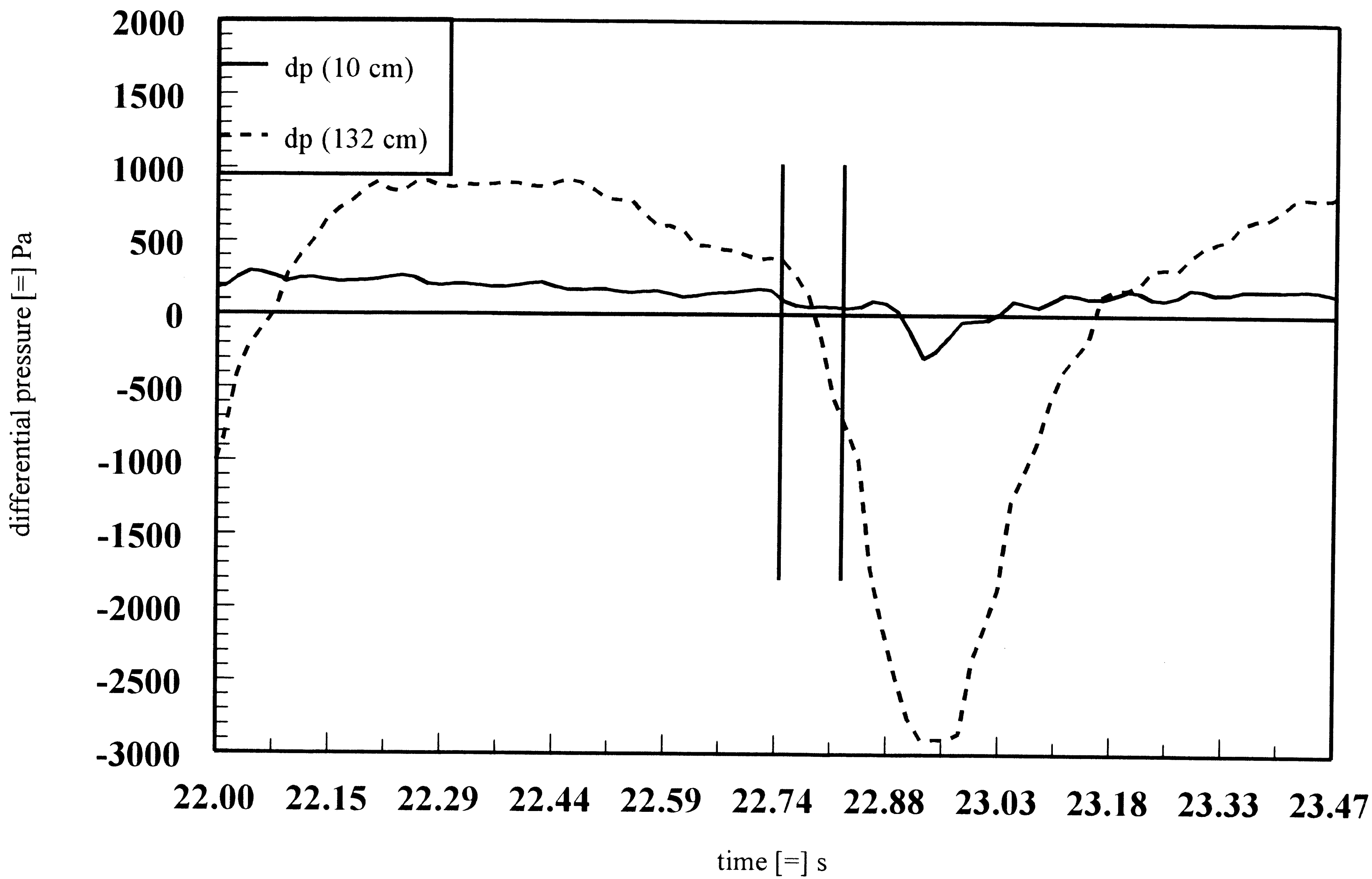

Figure 3.10: Differential Pressure trace for V_t experimental << V_t predicted.

has been proven to be valid.

3.4 Acoustic Technique

It was decided to collect downflow and upflow data simultaneously. To provide a non-intrusive method of flow regime determination, an acoustical method was adopted based on a technique suggested by BP. They noted in the field that they could detect slugs using these acoustical sensors. The idea of using two sensors at each location was spawned from what was found while creating the differential pressure method.

To establish criteria, an acoustic sensor was placed at the upstream tap for each differential pressure transducer. It was found through experiment that the eight-channel signal conditioner, designed especially for slug flow detection, amplified each channel differently. Additionally, each sensor had a slightly different sensitivity when plugged into the same channel. Four sensors were found to be reliable. These sensors were also found to be highly sensitive to how they were mounted.

The best response was found by mounting the sensors on the top of the pipe with a layer of silicone between the sensor and the pipe. It was then held fast with electrical tape wrapped around the sensor and the pipe. The chosen locations were the two upflow sensors, as noted before, and two downflow sensors an equal distance down the return flow. The downflow sensors were separated by the same distance (about 91-cm).

A sensor/channel combination of similar response was set for upflow and downflow. A more-sensitive set was placed as the upstream sensor and the less-sensitive set was placed downstream. The magnitude of fluctuation for slug flow was not as exact as it was for the pressure transducers. This was due to the differing amplifications and the dependence of the sensitivity on mounting. It was found through comparison with known flow patterns that a fluctuation of about 0.25 V was a good criterion for identifying a slug flow

Figure 3.11 is an acoustical trace for stratified flow. The fluctuations are small, typically less than about 0.02V. The same is observed for full pipe flow. Plug flow is not observed to occur in downflow. Figure 3.12 is an acoustical trace for slug flow. Because the fluctuations are quite dramatic, and since the sensitivity of the sensors vary, the front of the slug is difficult to isolate. It was found that the best way to determine the translational velocity was to divide the distance between the sensors by the time difference between the peaks of the acoustical fluctuations of the two traces. It was later determined that this matched what BP had found in the field. This method can thus establish whether the flow is stratified, slug, or annular.

3.5 Procedure

The experimental procedure for determining the flow regime follows. The mixing tank is filled with a predetermined volume of saltwater and oil. The valves controlling the recycle stream (A and B) are fully opened. The valve to the appropriate liquid flow rate metering line is opened while the other is closed. The pump motor is then activated and allowed to ramp to a set number of rotations per minute. When the set liquid flow rate is reached, the desired temperature must be reached. This is done by activating the heating system and setting the thermostat to the desired temperature.

Gas is allowed to pressurize the system by opening valve C of Figure 3.1 and setting the inlet pressure regulator at the desired operating pressure. The exhaust valve is left shut.

Now a baseline sample of data from the acoustic and differential pressure transducers

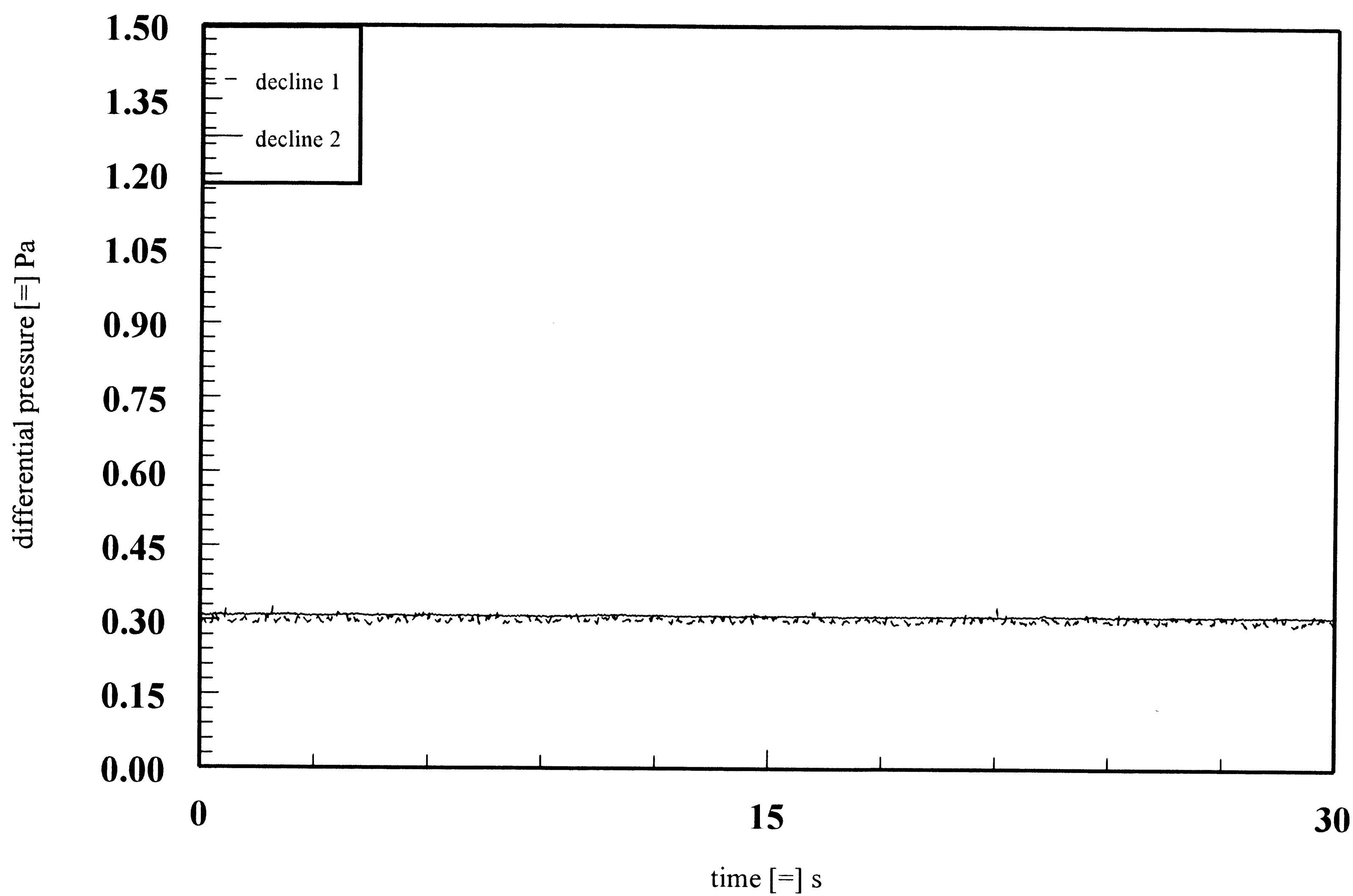

Figure 3.11: Acoustic trace for stratified flow.

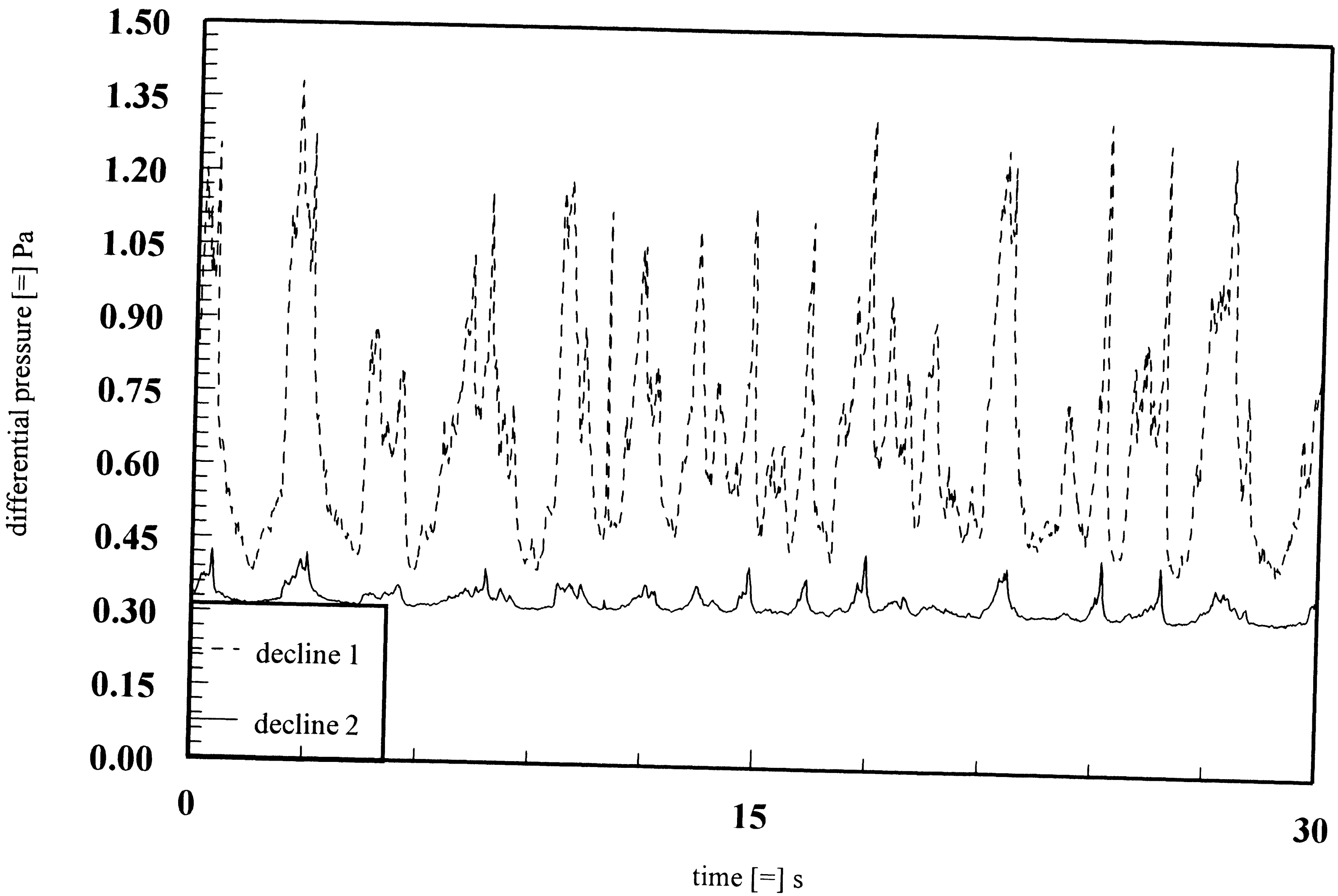

Figure 3.12: Acoustic trace for slug flow.

is taken. This is to verify that for full pipe flow, no fluctuations are found. The gas flow rate is now set. As gas is allowed to enter, it must also be exhausted. This can be done with a back pressure regulator. The gas flow rate is determined by reading the variable area flow meter. The flow meter is calibrated for carbon dioxide at 0.79 MPa and 20°C and must be corrected for temperature and pressure. The gas flow meter reading is recorded along with the gas metering line pressure and temperature. Next the differential pressure and acoustic data are taken. When the data acquisition is finished, all flow measurements are double checked.

The gas velocity is then increased and the procedure is repeated. The gas flow rate is continually increased until the maximum is reached. Sometimes this point is dictated by oil swelling and carryover into the separator (common with an 80% water cut at low pressures). Other times, the gas cannot exhaust as fast as it is entering and the pressure begins to rise (typically at lower pressures). And, there are times when the source pressure keeps depleting (typically at higher pressures). At times this upper limit can be as low as a V_{SG} of 5 m/s, while occasionally reaching 13 m/s.

Once the gas flow rate upper limit has been reached, the gas inlet is shut followed by the closing of the gas outlet. The next desired liquid flow rate is set (again by adjusting the rotations per minute on the pump motor). If necessary, the recycle stream valve is closed partially to increase the flow rate through the flow loop. Once the liquid flow rate is set, the entire process is repeated. When all of the desired conditions have been tested, the gas is shut off as before. Next, the heaters are turned off. Finally, the pump motor is allowed to ramp to a stop. Leaving the system pressurized allows for simpler setup for corrosion experiments as the system is then completely devoid of oxygen (less than a few ppb). If it is not anticipated that the fluids will be used for corrosion experiments, the exhaust gas is never closed when the feed gas is shut off. If the liquid has not carried over too much into the separator, the next water cut can be set by decanting the water and adding more oil.

CHAPTER 4

RESULTS & DISCUSSION

The results from the analysis of the differential pressure and acoustic measurements are presented. These include data on the frequency, translational velocity, and the length of a slug unit. Included in these tables are the frequencies predicted by Gregory and Scott (1969) and Hill and Wood (1990). Due to the extensive amount of data produced, these tables, along with the associated uncertainties, are located in Appendix A as Tables A.1 - A.137. For the downflow data, just the frequencies and predicted frequencies are reported. The flow regime maps which were created from this data are located in Appendix B as Figures B.1 - B.35.

While much data exists for this area, this is the first reported data in a large diameter multiphase inclined pipeline which includes the variation of pressure. Thus, the data will not be able to be directly compared to the literature. However, the trends observed in the literature (such as increasing diameter or inclination) should also be observed here.

4.1 Slug Translational Velocity

The slug translational velocity was measured as illustrated in Section 3.3. A value was recorded for each transient for a given set of conditions. These values were then averaged. Where indicated, the translational velocity was estimated and the value reported. The estimations were based upon what was found experimentally at similar conditions and what is reported in the literature as indicated in Section 2.3. In all cases, the value was reported as a ratio of the translational velocity to the superficial mixture velocity. This is for ease of comparison to the literature.

For the range of conditions tested, this velocity ratio was not largely affected by inclination, pressure, water cut, or superficial liquid velocity for a given flow pattern. Above a superficial gas velocity of about 2.5 m/s in slug flow, it was also independent of superficial gas velocity.

Figure 4.1 is a plot of the ratio of the translational velocity to the superficial mixture velocity for 100% saltwater at 0.45 MPa and +2° inclination. Above a superficial gas velocity of 2.5 m/s in slug flow, the velocity ratio was steady at about 1.2. At a superficial gas velocity of around 1 m/s in slug flow (superficial liquid velocity of 0.1 and 0.5 m/s) the velocity ratio was slightly higher at around 1.4. If the flow was plug flow (superficial liquid velocity of 1.0 and 1.5 m/s) the velocity ratio was close to 2.1. When annular flow was reached at a superficial liquid velocity of 0.1 m/s and a superficial gas velocity of about 9 m/s, the velocity ratio dropped to around 0.5.

The same trends are observed at higher pressures. Figure 4.2 is a plot of the translational velocity ratio for 100% saltwater at 0.79 MPa and +2° inclination. The velocity ratio remains around 1.2 for slug flow at a superficial gas velocity over 2.5 m/s. At a superficial gas velocity of about 1 m/s in slug flow (superficial liquid velocity = 0.1 m/s) the ratio is closer to 1.5. At the same gas flow rate in plug flow (superficial liquid velocity = 0.5, 1.0, 1.5 m/s) the velocity ratio is about 2.0. At a superficial liquid velocity of 0.1 m/s, it is seen that in pseudo-slug flow (superficial gas velocity of 5 m/s) and in annular flow (superficial gas velocity of 6 and 7 m/s) the velocity ratio drops to 1.1 and about 0.5, respectively.

A change in inclination was also not seen to have an effect on the velocity ratio.

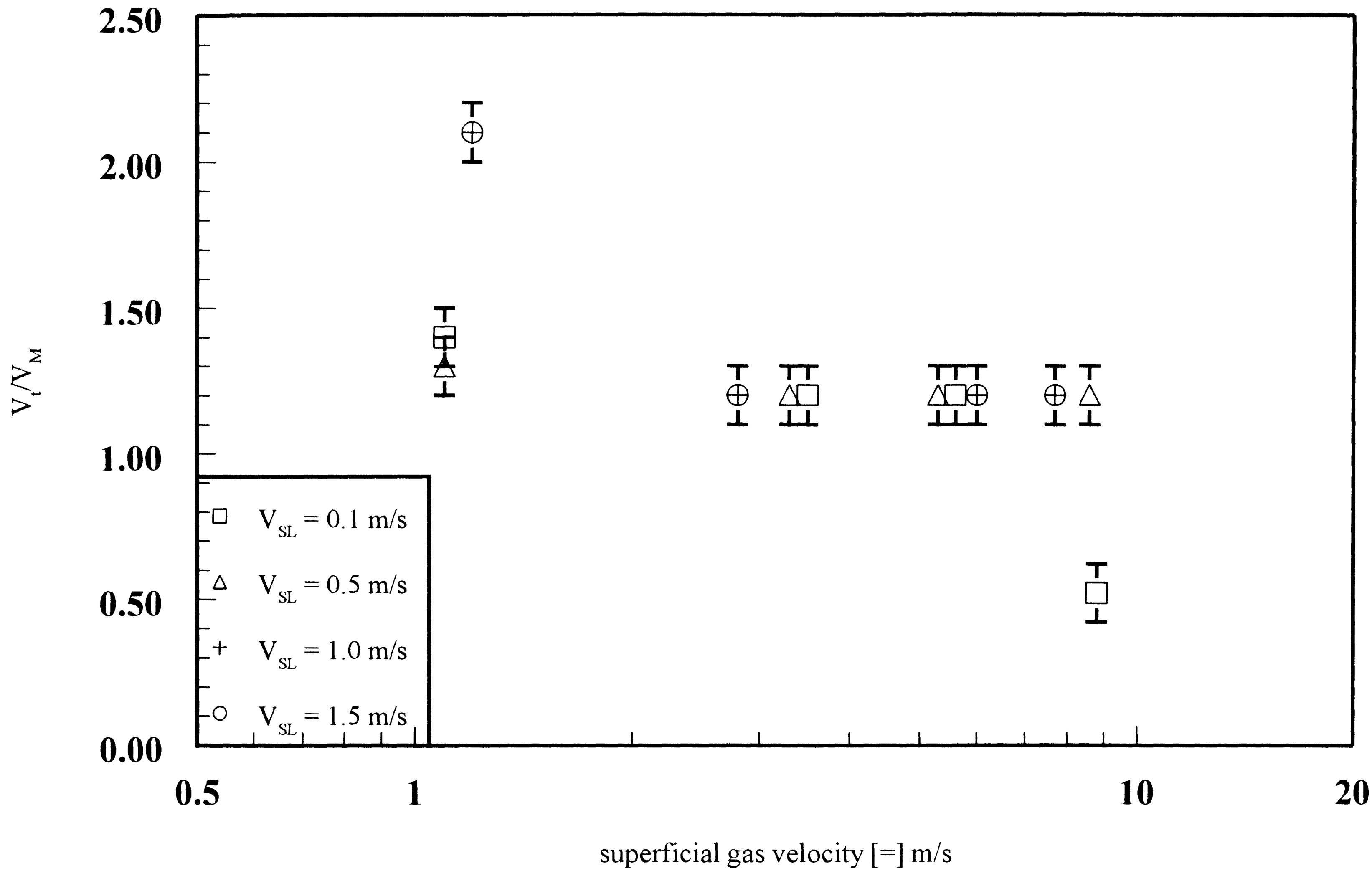

Figure 4.1: Translational velocity for 100% saltwater at 0.45 MPa and +2° inclination.

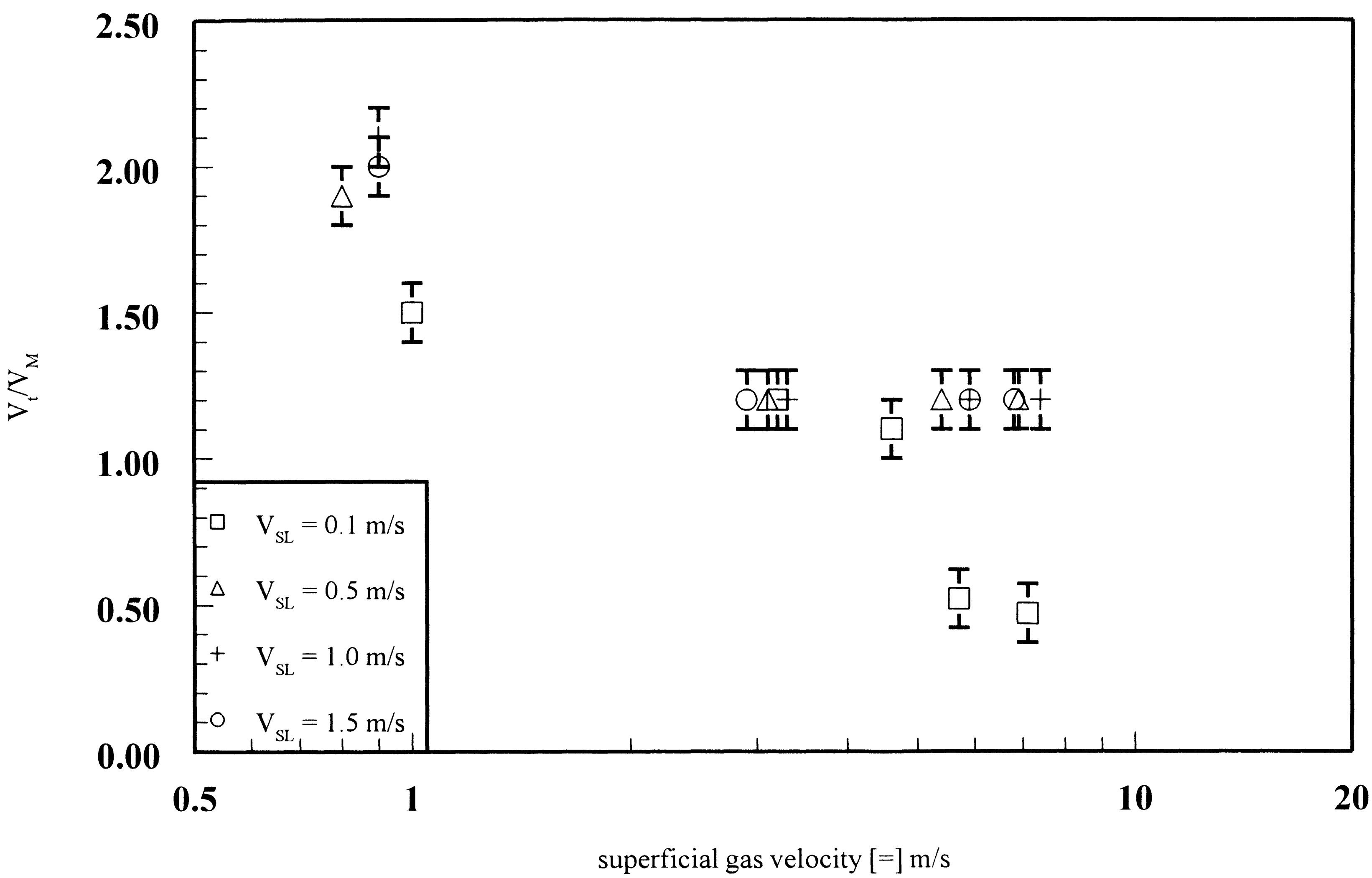

Figure 4.2: Translational velocity for 100% saltwater at 0.79 MPa and +2° inclination.

Figure 4.3 is a plot of the translational velocity ratio for 100% saltwater at 0.45 MPa and +5° inclination. Again it is seen that the ratio is about 2 in plug flow and is 1.2 in slug flow above a superficial gas velocity of 2.5 m/s. When pseudo-slug flow is reached, the average translational velocity ratio decreases to about 1.1. It then decreases further to about 0.5 when annular flow is reached.

A change in the water cut was also not observed to have a great effect on the velocity ratio. Figure 4.4 is a plot of the velocity ratio for 40% water cut at 0.45 MPa and +2° inclination. In plug flow, the velocity ratio is about 2.0. In slug flow, the velocity ratio decreases from about 1.3 at low superficial gas velocities to 1.2 at a superficial gas velocity of 2.5 m/s. When pseudo-slug flow is reached, the velocity ratio drops to about 1.1, dropping further to about 0.5 when annular flow is reached.

This large region of conditions for which the ratio was 1.2 for slug flow matches exceptionally well with the values (1.2 - 1.3) reported in the literature for slug flow in large diameter pipes as discussed in Section 2.3. For pseudo-slug flow, this average ratio was found to be in the range of 1.0 to 1.2 depending upon how many slugs were occurring simultaneously.

As the superficial gas velocity is increased to annular flow, the average translational velocity ratio drops to around 0.5. When this decrease occurs, typically all three reported frequencies are at zero.

As mentioned in Section 2.3, Jepson and Taylor (1993) found that the ratio in slug flow decreases from a value of around 1.6 at low gas flow rates to a value of 1.25 by a superficial mixture velocity of 3 m/s. They also indicated that in plug flow, the ratio was 2.0.

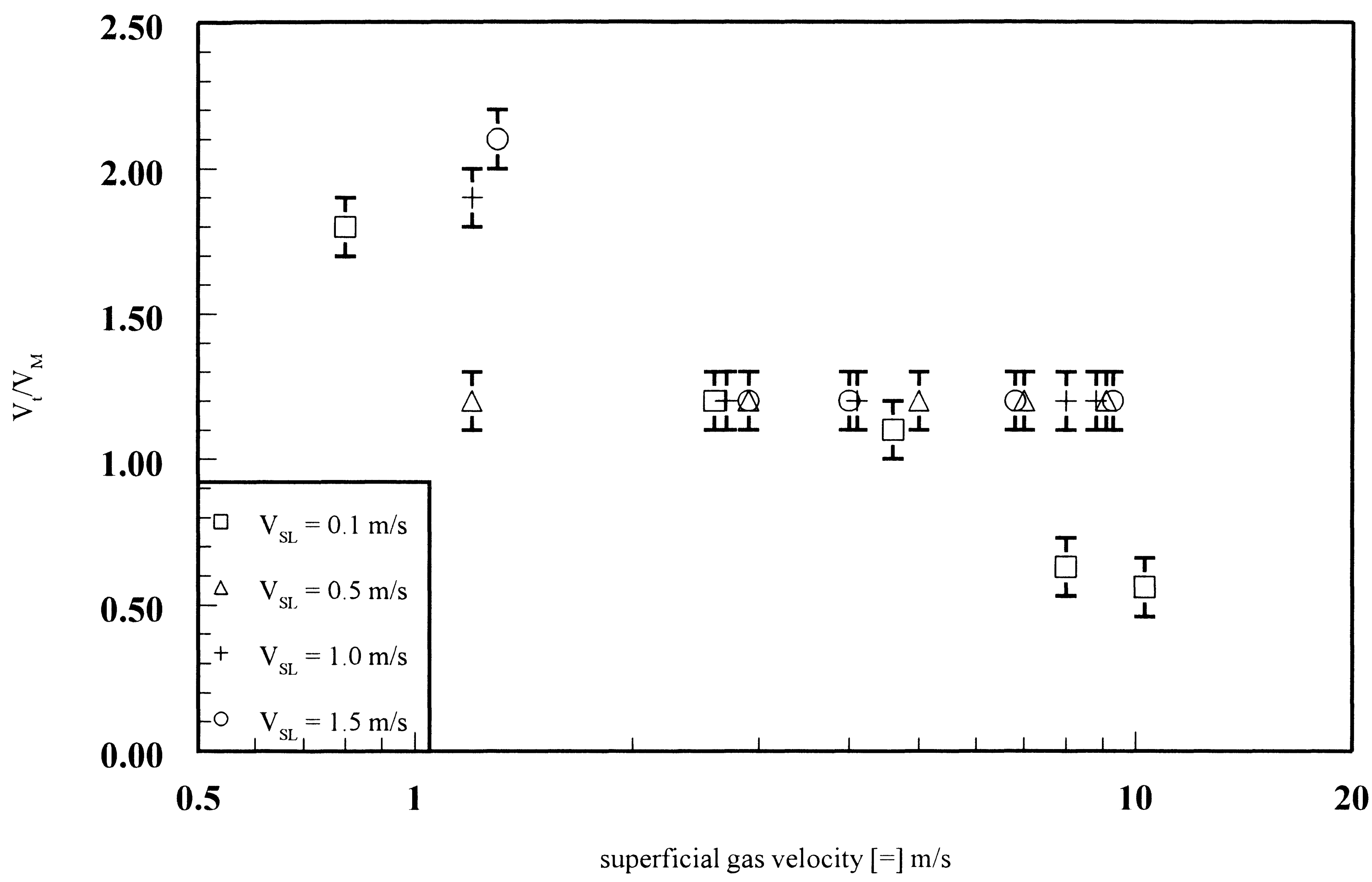

Figure 4.3: Translational velocity for 100% saltwater at 0.45 MPa and +5° inclination.

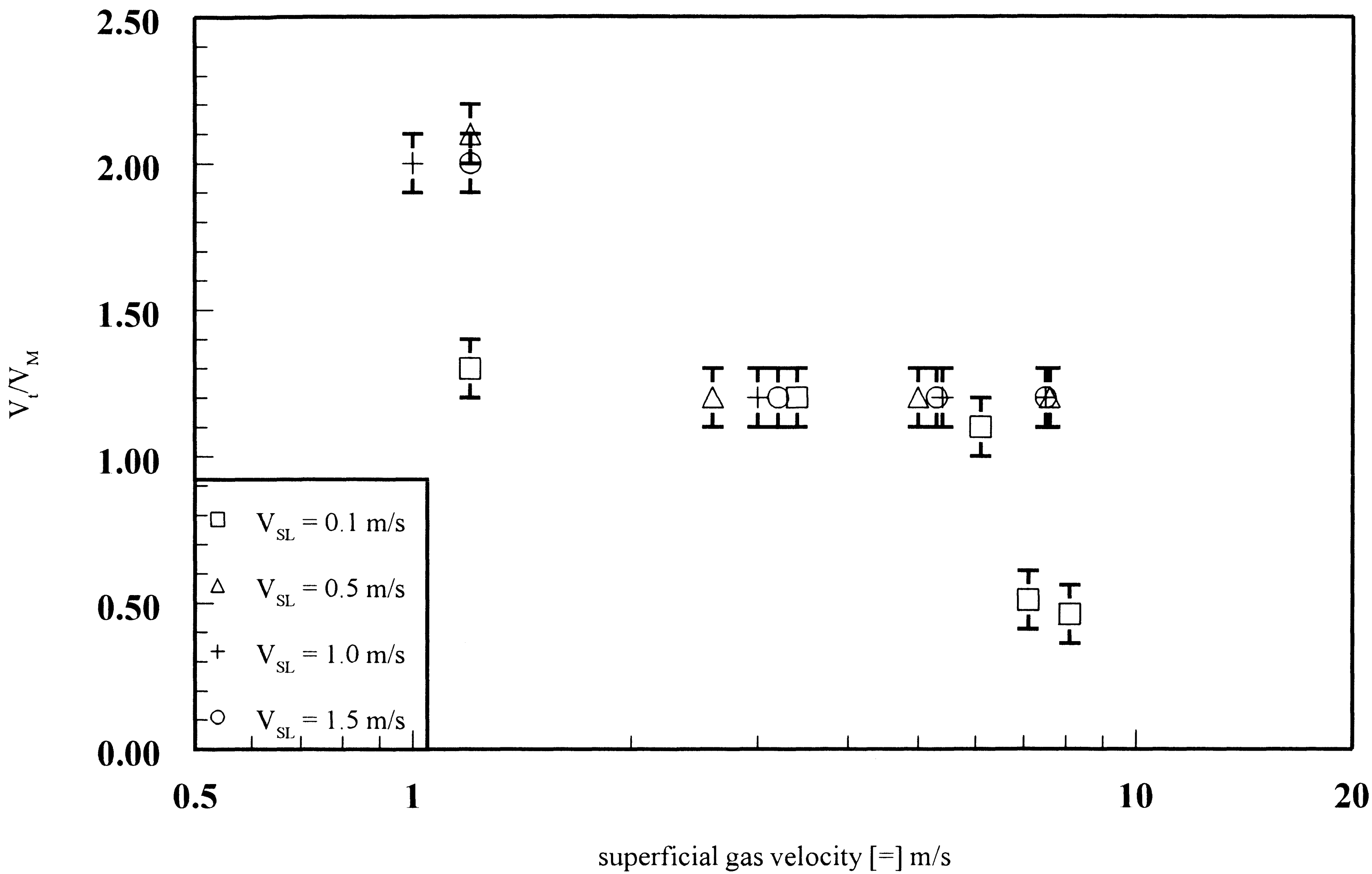

Figure 4.4: Translational velocity for 40% water cut at 0.45 MPa and +2° inclination.

From this, it can be said that the relation proposed by Jepson (1989) for the translational velocity prediction best relates the translational velocity. Also, it can be concluded that this ratio should be below a value of 1.3 at a superficial gas velocity above 2.5 m/s at all liquid flow rates, inclinations, pressures in this range, and water cuts in 10-cm diameter pipes. As pseudo-slug flow approaches, the ratio drops by about 10%, dropping to 50% at the transition to annular flow.

4.2 Estimated Film Froude Number

The film height and film velocity could not be determined experimentally for this stainless steel system. Due to this, they had to be estimated to calculate the film Froude number. The method used for this film Froude estimation was that established by Gopal (1994). He found:

$$Fr_f \approx \frac{V_t - V_{SL}}{\sqrt{g \cdot h_{eff}}} \tag{4.1}$$

The effective film height was then predicted using the three-phase stratified film height model of Neogi *et al.* (1994) to obtain the area of the liquid in the film and the length of the gas liquid interface. The limits to this are that in inclined flow at low superficial liquid velocities, the film velocity is known to reverse in direction. This has a larger effect at low gas flow rates than at higher flow rates. This also will over predict the film height in the stratified region because some liquid has gone to the slug body. Due to the square-root, this has little effect but it does lower the Froude number. The effect will be the same for all values reported. Finally, at higher gas flow rates, the film spreads up the walls of the pipe.

Thus the effective film height is over predicted again.

For modeling concerns this estimated film Froude number will be fine since it will be compared to the observations which will use the same estimations.

This estimated film Froude number had the tendency to increase with increasing gas flow rate. Figure 4.5 is a plot of the estimated film Froude number for slug flow in 100% saltwater at 0.45 MPa and +2° inclination. As the superficial gas velocity is increased from about 3 to 8 m/s, the Froude number increases from about 4 to 18. This is due to the effect of the superficial gas velocity on the translational velocity being of much greater magnitude than its effect than on the film height. An increase in the liquid flow rate is shown to slightly decrease the estimated film Froude number for the same flow pattern. But as the figure indicates, the error bars exceed this change. This slight decrease is due to the fact that increasing the superficial liquid velocity has nearly the same effect on both terms in the numerator of the Froude calculation, canceling itself out, while causing a slight increase in the film height. Thus, the Froude number should decrease slightly with increasing liquid flow rate at equal gas flow rate and flow pattern. These effects are also seen at other inclinations, water cuts, and pressures.

Increasing the pressure causes a slight increase in the estimated film Froude number. Figure 4.6 is a plot of the film Froude number for 100% saltwater at +2° inclination and pressures of 0.27 and 0.45 MPa. At a superficial gas velocity of 7.7 m/s and a superficial liquid velocity of 1.0 m/s, the Froude number for 0.27 and 0.45 MPa is 16.3 and 18.3, respectively. Again, these slight changes are still smaller than the error bars of the data. This slight increase is due to the fact that at higher pressures, the gas occupies more area in the

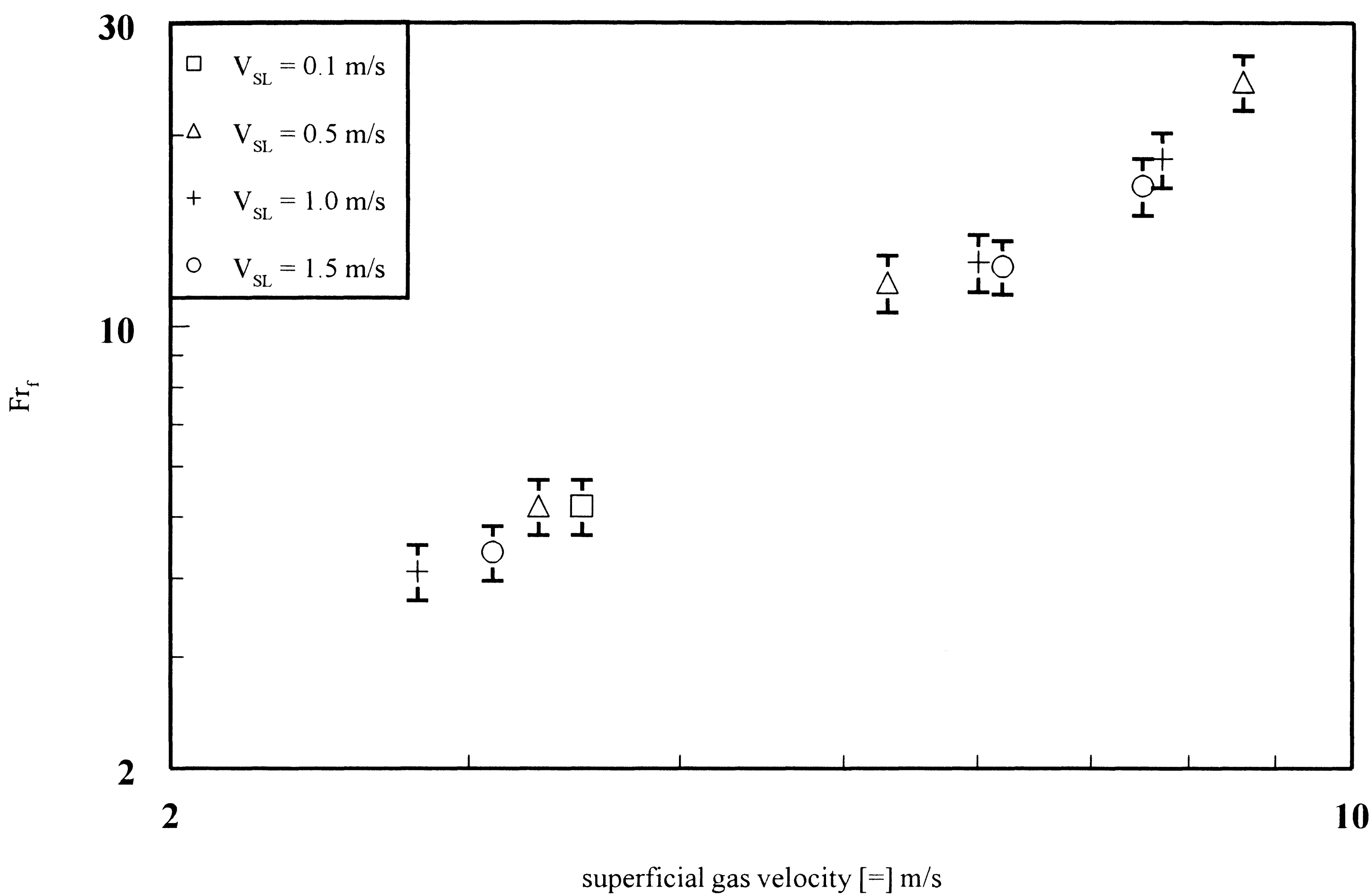

Figure 4.5: Slug flow estimated film Froude number for 100% saltwater at 0.45 MPa and +2° inclination.

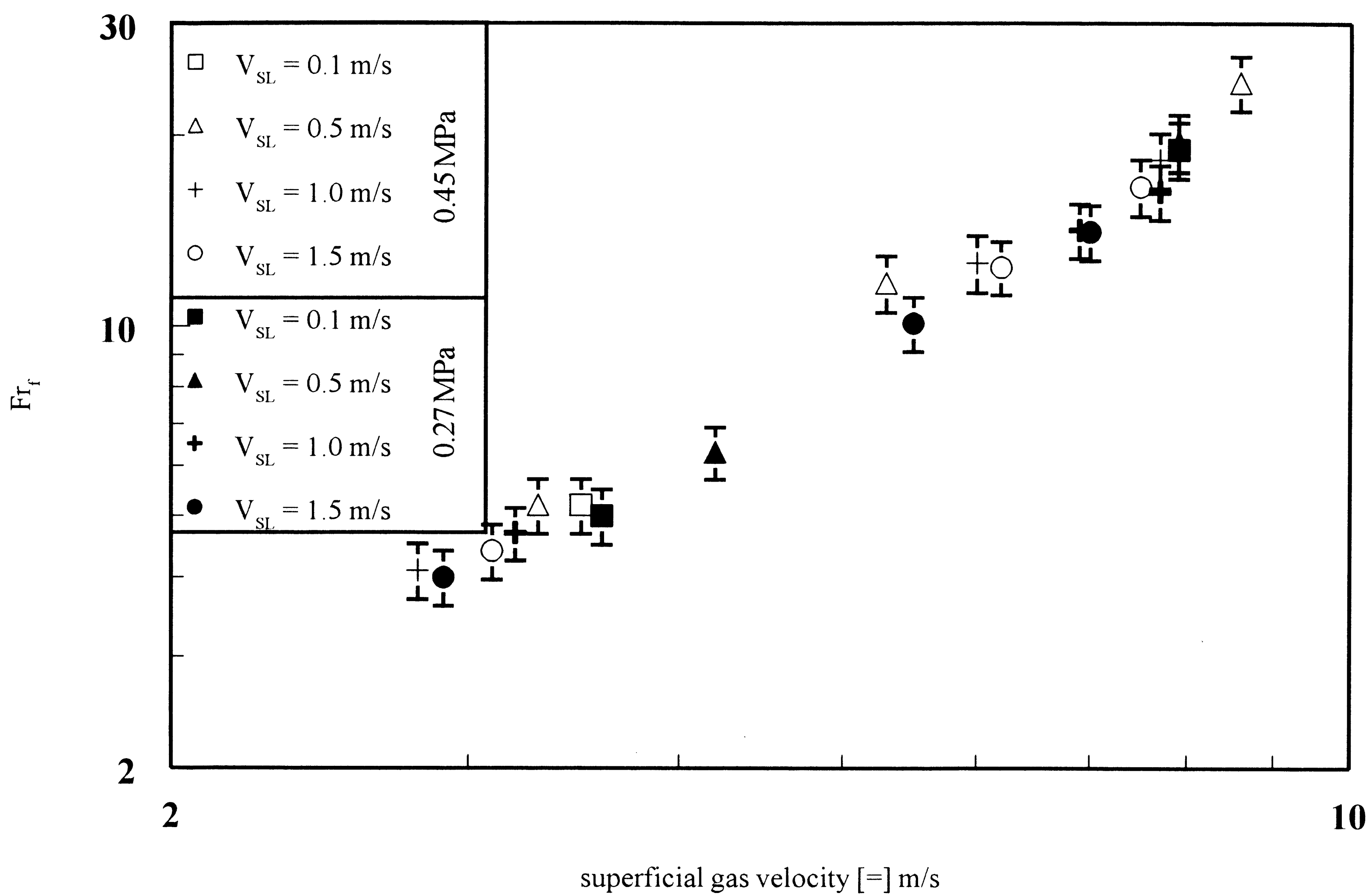

Figure 4.6: Slug flow estimated film Froude number for 100% saltwater at +2° inclination.

film region, thus lowering the effective film height and increasing the Froude number. The effect is observed at other water cuts and inclinations.

The effect of inclination was varying on the estimated film Froude number. Figure 4.7 is a plot of the film Froude number for 100% saltwater and 0.45 MPa at inclinations of -2 and +2°. At lower gas flow rates the Froude number is higher in downflow than in upflow while the opposite is true at the higher gas flow rates. This is due in part to the fact that, as mentioned previously, the film velocity is not adjusted for the change in direction of the flow in upflow. In upflow, the film is generally thicker and slower while in downflow the film is generally thinner and faster. This then has a varying effect on the Froude number which is affected both by film velocity and by film height.

Increasing the water cut had little effect on the estimated film Froude number. Figure 4.8 is a plot of the film Froude number at 0.45 MPa and +2° for 40 and 100% water cut. The slight variances in Froude number are both up and down and are much less than the error bars. Thus it is reasoned that there is little or no effect of water cut on the estimated film Froude number for the same flow pattern.

It was noted that the increase of the Froude number stopped above certain gas flow rates. This was due to the decrease in the translational velocity measured experimentally. The first decrease was due to the change from slug flow to pseudo-slug flow. As mentioned in Section 4.1, the average translational velocity typically drops from about 1.2 to about 1.1 times the superficial mixture velocity when pseudo-slugs and slugs coexist. Thus, the Froude number is reduced slightly when pseudo-slugs begin to be produced. If 1.2 times the mixture velocity is retained, it was noticed that this transition repeatedly occurred at estimated film

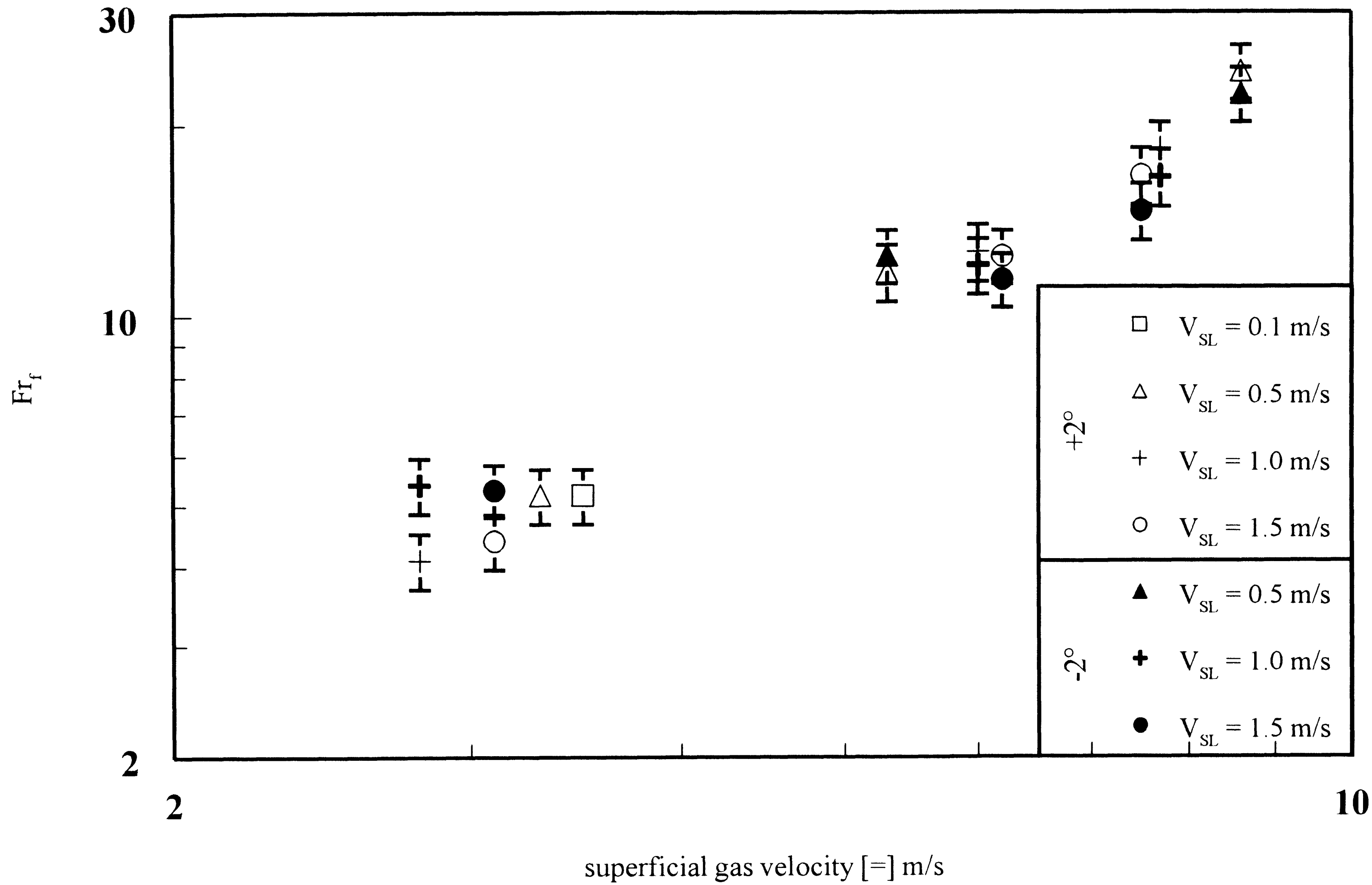

Figure 4.7: Slug flow estimated film Froude number for 100% saltwater at 0.45 MPa.

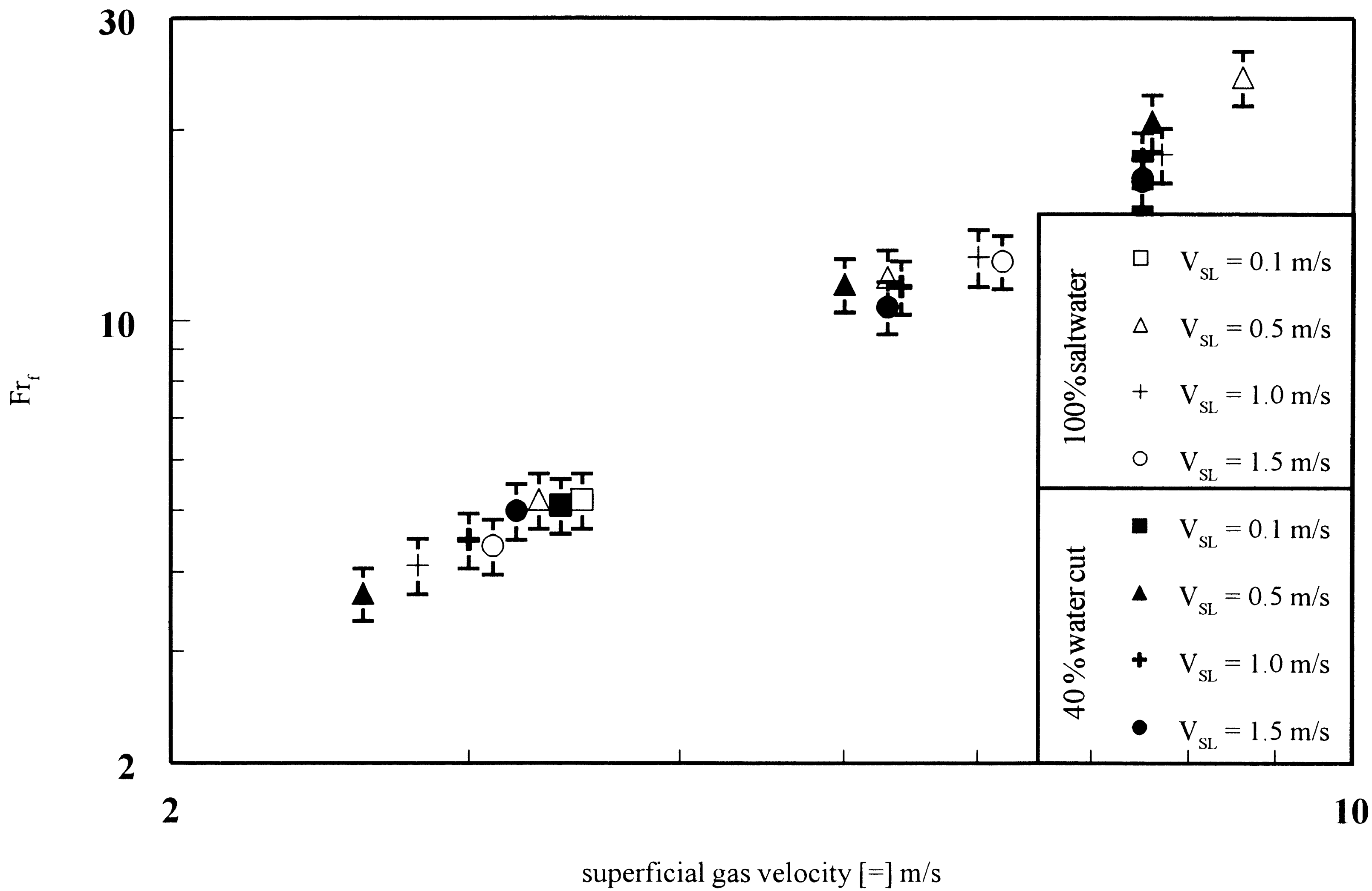

Figure 4.8: Slug flow estimated film Froude number at 0.45 MPa and +2°.

Froude numbers of 16 to 19. Tables 4.1, 4.2, and 4.3 indicate that for fixed pressure, water cut, and inclination, the pseudo-slug flow begins at estimated film Froude numbers of 17.8, 19.1, and 15.9, respectively.

Table 4.1: Froude number for 100% saltwater, 0.45 MPa, horizontal, $V_{SL} = 0.5$ m/s.

superficial gas velocity (m/s)	estimated film Froude number
1.4	2.1
3.3	5.7
5.1	9.5
7.5	17.8
10.3	19.6
13.6	31.3

Table 4.2: Froude number for 100% saltwater, 0.45 MPa, horizontal, $V_{SL} = 1.0$ m/s.

superficial gas velocity (m/s)	estimated film Froude number
1.3	2.1
3.4	5.3
4.9	8.0
7.8	16.1
9.3	19.1
12.2	25.5

Table 4.3: Froude number for 100% saltwater, 0.45 MPa, horizontal, V_{SL} = 1.5 m/s.

superficial gas velocity (m/s)	estimated film Froude number
1.7	2.8
3.4	5.1
5.6	9.3
8.1	15.9
9.1	18.6
0.3	20.1

It was also noted that when annular flow was reached, the estimated film Froude was again around 16 when using the measured translational velocity of the waves (approximately 0.5 times the superficial mixture velocity), but was in the range of 35 to 40 when using 1.2 times the superficial mixture velocity for the translational velocity. If the annular data point in Table 4.4 (superficial gas velocity of 9.4 m/s) is recalculated using 1.2 as a translational velocity ratio instead of 0.52, the estimated film Froude increases from 17.1 to 40. Similarly, if the annular data point from Table 4.5 (superficial gas velocity of 8.8 m/s) is recalculated using the ratio of 1.2 rather than 0.52, the estimated film Froude increases from 15.9 to 37.

4.3 Slug Frequency

As mentioned previously, in the data collection process three frequencies are obtained and reported. The first frequency is the frequency at which the differential pressure change between the pressure taps separated by 132-cm exceeds 1,500 Pa. This value is reported as F_{S1}. The second frequency reported is the frequency at which the differential pressure change between the pressure taps separated by 10-cm exceeds 150 Pa. This value is reported as F_{S2}.

Table 4.4: Froude number for 100% saltwater, 0.27 MPa, inclined +2°, V_{SL} = 0.1 m/s.

superficial gas velocity (m/s)	estimated film Froude number
1.4	1.9
3.6	5.0
7.9	19.0
9.4	17.1

Table 4.5: Froude number for 100% saltwater, 0.45 MPa, inclined +2°, V_{SL} = 0.1 m/s.

superficial gas velocity (m/s)	estimated film Froude number
1.1	4.4
3.5	5.2
5.6	17.7
8.8	15.9

The third frequency reported is the frequency at which the translational velocity is characteristic for the velocity of a slug. The frequency at which this occurs is reported as F_V. It is proposed that this is the true slug frequency and it will be the concentration of this discussion. The other frequencies will be referenced to validate flow regime (Section 4.5) and for comparison with what other researchers have found. For downflow measurements, the frequency is reported from the acoustic sensors as F_A. For all cases, commonly used frequency correlations are included. The slug frequency predicted by Gregory and Scott (1969) is reported as F_{GS} and the slug frequency predicted by Hill and Wood (1990) is reported as F_{HW}. It should be noted that when the horizontal data was recorded, plugs were included in the frequency as described in Section 3.4.

All frequencies were found to increase with increasing liquid flow rate for all conditions tested. This has been found by many researchers to hold true (Taitel and Dukler, 1977; Jepson and Taylor, 1993; Hubbard, 1965, *etc.*). Tables 4.6 - 4.8 contain the frequency data for horizontal flow with 100% saltwater and a system pressure of 0.79 MPa. They indicate that at a superficial gas velocity of about 1.2 m/s, the slug frequency increases from 16 to 20 to 26/min as the superficial liquid velocity is increased from 0.5 to 1.0 to 1.5 m/s, respectively. This is also seen with F_{S1} and F_{S2}. Both of the predictive models matched this increase. Hill and Wood increased from 3.5 to 9.1 to 15.7/min, respectively, while Gregory and Scott increased from 9.0 to 19.8 to 32.0/min, respectively. The Hill and Wood correlation consistently under predicted the frequency. The Gregory and Scott correlation was more reasonable, but over predicted the frequency.

This increase in frequency with liquid flow rate was also observed in upflow and in downflow. Both correlations do not predict the frequencies well in upflow or downflow primarily because they were developed from horizontal flow data. It was also observed that this increase with increasing liquid flow rate occurred at the other water cuts and pressures as well.

Table 4.6: Frequency data for 100% saltwater, horizontal, 0.79 MPa, V_{SL} = 0.5 m/s.

V_{SG} (m/s)	F_{S1} (min^{-1})	F_{S2} (min^{-1})	F_V (min^{-1})	F_{HW} (min^{-1})	F_{GS} (min^{-1})
1.3	14	18	16	5.0	13.7
3.3	14	8	8	3.5	9.0
5.6	6	6	6	2.2	8.8
7.6	12	10	2	1.4	8.8
8.3	20	14	0	1.3	9.1

Table 4.7: Frequency data for 100% saltwater, horizontal, 0.79 MPa, V_{SL} = 1.0 m/s.

V_{SG} (m/s)	F_{S1} (min^{-1})	F_{S2} (min^{-1})	F_V (min^{-1})	F_{HW} (min^{-1})	F_{GS} (min^{-1})
1.2	20	20	20	12.6	25
3.5	26	26	14	9.1	20.
5.1	30	34	12	7.2	20.
7.4	50	48	10	3.1	23

Table 4.8: Frequency data for 100% saltwater, horizontal, 0.79 MPa, V_{SL} = 1.5 m/s.

V_{SG} (m/s)	F_{S1} (min^{-1})	F_{S2} (min^{-1})	F_V (min^{-1})	F_{HW} (min^{-1})	F_{GS} (min^{-1})
1.2	34	26	26	20.	38
3.4	52	60	14	15.7	32
5.3	78	66	10	10.9	34

Increasing the gas flow rate generates interesting results. Various researchers disagree about whether the frequency increases or decreases with increasing gas flow rate. The truth is that they are both correct. Maybe it was best modeled by Gregory and Scott as they noted that the frequency decreased with an increasing superficial gas velocity below a translational velocity of about 6 m/s then it increased with an increasing superficial gas velocity. Thus at higher liquid flow rates, the change in direction occurs at lower superficial gas velocities. From what has been observed in the collection of this data, most researchers are observing the transition from high frequency plug flow to lower frequency slug flow. If just slugs are isolated, then the frequency only decreases with increasing gas flow rate at low liquid flow rates while always increasing with increasing gas flow rate at the higher liquid flow rates. As pseudo-slug flow ensues, this frequency again decreases.

At lower superficial liquid velocities, the frequency only decreases with increasing superficial gas velocity. Consider the slug frequency of 100% saltwater flow with a superficial liquid velocity of 0.1 m/s at +5° inclination and 0.79 MPa as presented in Table 4.9. F_{S1} decreases from 10 to 0/min, F_{S2} decreases from 10 to 0/min, and F_V decreases from 6 to 0/min as the superficial gas velocity is increased from 2.6 to 10.3 m/s.

For these cases, Gregory and Scott severely under predict the frequency while the Hill and Wood relation is more reasonable. At the lower gas velocity, Hill and Wood predict 12.0/min while Gregory and Scot predict 1.5/min. Both decrease to a value of about 1/min at the higher gas flow rate.

Table 4.9: Frequency data for 100% saltwater, +5° inclined, 0.45 MPa, V_{SL} = 0.1 m/s.

V_{SG} (m/s)	F_{S1} (min^{-1})	F_{S2} (min^{-1})	F_V (min^{-1})	F_{HW} (min^{-1})	F_{GS} (min^{-1})
0.8	14	12	0	10.4	2.9
2.6	10	10	6	12.0	1.5
4.6	4	4	4	15.0	1.3
8.0	2	0	0	0.8	1.3
10.3	0	0	0	0.7	1.2

At moderate liquid flow rates, the frequency can often become independent of the gas flow rate. Table 4.10 presents the frequency data for 100% saltwater flow at a pressure of 0.45 MPa, inclined +5°, and with a superficial liquid velocity of about 0.5 m/s. All three experimental frequencies remain at about 22/min, regardless of the gas velocity. For this case, the Hill and Wood correlation begins around 20/min at the lower gas flow rates, then suddenly decreasing to 1 - 3/min at higher gas flow rates. The Gregory and Scott relation again under predicts the frequency, but does remain constant at about 10/min. These trends occur for all inclinations, pressures, and water cuts.

Pressure and water cut were found to have little effect on the frequency. Inclination was found to have a large impact on the slug frequency. This was found for all pressures and water cuts. Tables 4.7 and 4.11 report the frequency data for 100% saltwater at a pressure of 0.79 MPa and inclinations of 0 and +5°, respectively. At a superficial gas velocity of around 5.1 m/s, the horizontal F_{S1}, F_{S2} and F_V are 30, 34, and 12/min, respectively. For +5° inclined flow, the respective frequencies increase to 48, 48, and 46/min. The predictive models will not be compared for this as they do not incorporate inclination.

Table 4.10: Frequency data for 100% saltwater, +5° inclined, 0.45 MPa, V_{SL} = 0.5 m/s.

V_{SG} (m/s)	F_{S1} (min^{-1})	F_{S2} (min^{-1})	F_V (min^{-1})	F_{HW} (min^{-1})	F_{GS} (min^{-1})
1.2	22	18	10	18.6	15.1
2.9	28	24	22	19.4	9.4
5.0	22	22	20	2.7	8.6
7.0	20	20	18	1.6	9.4
9.1	18	18	16	1.1	10.7

Table 4.11: Frequency data for 100% saltwater, +5° inclined, 0.79 MPa, V_{SL} = 1.0 m/s.

V_{SG} (m/s)	F_{S1} (min^{-1})	F_{S2} (min^{-1})	F_V (min^{-1})	F_{HW} (min^{-1})	F_{GS} (min^{-1})
0.9	0	0	0	22	22
2.0	38	36	32	22	23
3.0	44	42	40	18.5	20.
5.2	48	48	46	3.1	20.
6.7	64	60	56	3.0	22

In downflow, the frequency is observed to decrease slightly with steeper decent. Tables 4.12 and 4.13 report frequency data for 40% water cut at 0.79 MPa and inclinations of -2° and -5°, respectively. At a superficial gas velocity of around 6.3 m/s, the measured frequency decreases from 64 to 48/min by decreasing the angle of flow.

Table 4.12: Frequency data for 40% water cut, -2° inclined, 0.79 MPa, V_{SL} = 1.5 m/s.

V_{SG} (m/s)	F_A (min^{-1})	F_{HW} (min^{-1})	F_{GS} (min^{-1})
0.9	0	6.4	---
3.4	52	7.9	32
5.4	54	7.1	37
6.3	64	5.7	40.

Table 4.13: Frequency data for 40% water cut, -5° inclined, 0.79 MPa, V_{SL} = 1.5 m/s.

V_{SG} (m/s)	F_A (min^{-1})	F_{HW} (min^{-1})	F_{GS} (min^{-1})
1.0	0	1.9	---
2.7	0	3.1	---
3.8	40	3.7	32
5.1	50	4.2	36
6.4	48	3.9	41

4.4 Slug Unit Length

The length of the slug unit was determined as suggested by Dukler and Hubbard (1975) and by Andreussi *et al.* (1993).

$$l_u = \frac{V_t}{f_S} \tag{4.2}$$

For horizontal and upflow, the frequency used was F_V while in downflow F_A was used.

In all cases, the unit length was found to decrease with increasing liquid flow rate. Table 4.14 reports the slug unit length for 40% water cut at 0.79 MPa inclined +5°. At a superficial gas velocity of about 5.0 m/s, the slug unit length decreases from 94 to 16.9, 9.3, and 7.5 m as the superficial liquid velocity is increased from 0.1 to 0.5, 1.0, and 1.5 m/s. Table 4.15 reports the slug unit length for 80% water cut at 0.27 MPa inclined -2°. At a superficial gas velocity of about 6.0 m/s, the length decreases from infinite to 27, 15.3, and 12.4 m as the superficial liquid velocity increased from 0.1 to 0.5, 1.0, and 1.5 m/s.

Table 4.14: Slug unit length for 40% water cut, +5° inclined, 0.79 MPa.

V_{SG} (m/s)	l_u (m)	V_{SL} (m/s)
5.1	94	0.1
4.7	16.9	0.5
5.0	9.3	1.0
5.1	7.5	1.5

Table 4.15: Slug unit length for 80% water cut, -2° inclined, 0.79 MPa.

V_{SG} (m/s)	l_u (m)	V_{SL} (m/s)
6.3	---	0.1
6.3	27	0.5
5.8	15.3	1.0
6.1	12.4	1.5

This is expected for increasing liquid flow rate. Consider the notion that the actual slug length remains relatively constant, as highlighted in Section 2.3, at about 15 to 20 times the pipe diameter. Within a slug unit length, mass is conserved from the input superficial velocities. If the liquid flow rate is increased at a constant gas flow rate, the ratio of liquid to gas in the slug unit must also be increased. The ratio of liquid to gas is higher in the slug than it is in the film region. Since the slug length remains relatively constant, a decrease in the overall slug unit length corresponds to a higher ratio of liquid to gas.

The slug unit length was found to both increase and decrease with increasing gas flow rate depending upon the liquid flow rate. At lower liquid flow rates, the unit length increases greatly with increasing gas flow rate. At moderate liquid flow rates, the length increases slightly to a maximum with increasing gas flow rate. At higher liquid flow rates, the length increases slightly to a maximum then decreases slightly with increasing gas flow rate. Table 4.16 reports the slug unit length for 40% water cut at a 0.27 MPa and inclined +5°. At a superficial liquid velocity of 0.1 m/s, the length increases from 19 to 32, 63, and 141 m as the superficial gas velocity was increased from 1.3 to 3.5, 7.0, and 8.1 m/s. At a superficial liquid velocity of 0.5 m/s, the length increases from 5.7 to 10.2, 17.5, and 22 m as the superficial gas velocity is increased from 1.3 to 3.0, 5.4, and 7.4 m/s. At a superficial liquid velocity of 1.0 m/s, the length increases from 6.2 to 10.8, 12.3, and 12.8 m as the superficial gas velocity is increased from 1.8 to 4.3, 5.6, and 7.4 m/s. At a superficial liquid velocity of 1.5 m/s, the length increases from 6.3 to 8.4 m then decreases to 7.6 m as the superficial gas velocity is increased from 3.1 to 5.2 to 7.0 m/s.

Table 4.16: Slug unit length for 40% water cut, +5° inclined, 0.27 MPa.

V_{SG} (m/s)	l_u (m)	V_{SL} (m/s)
1.3	19.0	0.1
3.5	32	0.1
7.0	63	0.1
8.1	140	0.1
1.3	5.7	0.5
3.0	10.2	0.5
5.4	17.5	0.5
7.4	22	0.5
1.8	6.2	1.0
4.3	10.8	1.0
5.6	12.3	1.0
7.4	12.8	1.0
1.4	---	1.5
3.1	6.3	1.5
5.2	8.4	1.5
7.0	7.6	1.5

This result is expected. Similar to the liquid flow rate, as the gas flow rate is increased at a constant liquid flow rate, the ratio of gas to liquid in the slug unit also increases. Like for the liquid flow, a higher ratio of gas to liquid corresponds to a larger slug unit for a constant slug length. Thus as the gas flow rate was increased, the unit length increased. The reason this began to taper was the greater void fraction in the slug at the higher gas and liquid flow rates.

Inclination has a slight effect on the slug unit length. As the flow is inclined upwards, the slug unit length is decreased. As the flow is inclined downwards, the slug unit length is increased. This is due in part to the fact that the slugs are known to be shorter and more frequent in inclined flow. With a shorter slug, a mass conservation requires a shorter film region. Magnifying this is the counter effects of having a thinner, faster film region in downflow and a thicker, slower region in upflow. Table 4.17 reports the slug unit length for 80% water cut and 0.45 MPa flow at inclinations of +5, +2, -2, and -5°. As the angle lowered from upflow to downflow at a superficial gas velocity of 3.5 m/s, the slug unit length increases, slightly, from 5.7 to 6.3, 8.6, and 11.2 m, respectively. This effect was seen at other water cuts and pressures.

Table 4.17: Slug unit length for 80% water cut, V_{SG} = 3.5 m/s, 0.45 MPa.

inclination (degrees)	l_u (m)	V_{SL} (m/s)
+5	5.7	1.5
+2	6.3	1.5
-2	8.6	1.5
-5	11.2	1.5

As with the frequency and translational velocity, the slug unit length was found to have little effect from water cut and pressure in the range studied.

4.5 Flow Regimes

The flow regimes were determined from the criteria established in Sections 3.3 and 3.4. The data necessary for testing the criteria has been presented in Section 4.3 and is listed in Appendix A as Tables A.1 - A.137. As mentioned previously, the flow regime data has been plotted into flow regime maps which are located in Appendix B as Figures B.1 - B.35.

The flow regimes identified were plug flow, stratified flow, slug flow, pseudo-slug flow, and annular flow. Plug flow, slug flow, and pseudo-slug flow will often be collectively termed slug flow. Plug flow is actually of little interest and is not known to occur in downflow. Slug flow was found to dominate the flow regime map as the inclination was increased to as little as +2°. This is expected as it has been found by many researchers (Kokal and Stanislav, 1989, *etc.*). It is often considered in the field that if the outlet is higher than the inlet, stratified flow will not occur (Green, 1997). Figure 4.9 is a flow regime map for 100% saltwater, horizontal, 0.45 MPa flow. At superficial liquid velocities of up to 0.3 m/s, stratified flow is observed to occur while slug flow was observed to occur at a superficial liquid velocity of 0.4 m/s. Pseudo-slug and annular flow occurred at the higher gas flow rates while plug flow occurred at the lower gas flow rates.

Figure 4.10 represents the flow regime map for 100% saltwater, +2° inclined, 0.45 MPa flow. No stratified flow was observed to occur. In its place at equal flow rates is slug flow. At a superficial liquid velocity as low as 0.1 m/s, slug flow is still observed to occur, allowing slug flow to dominate the flow regime map. At a superficial liquid velocity as low as 0.1 m/s, slug flow is still observed to occur. This effect is seen at other pressures and water cuts as well.

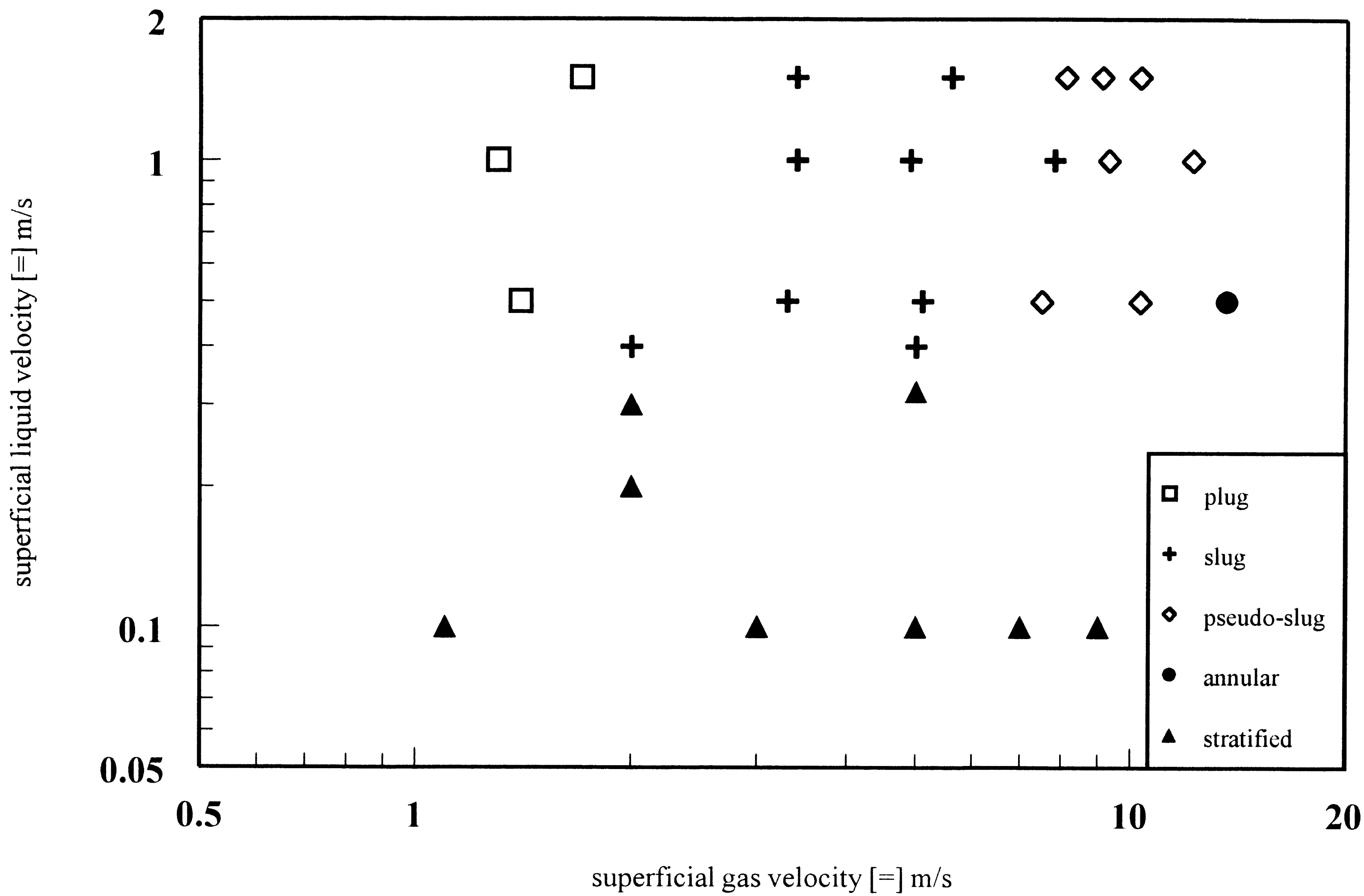

Figure 4.9: Flow regime map for 100% saltwater at 0.45 MPa and horizontal.

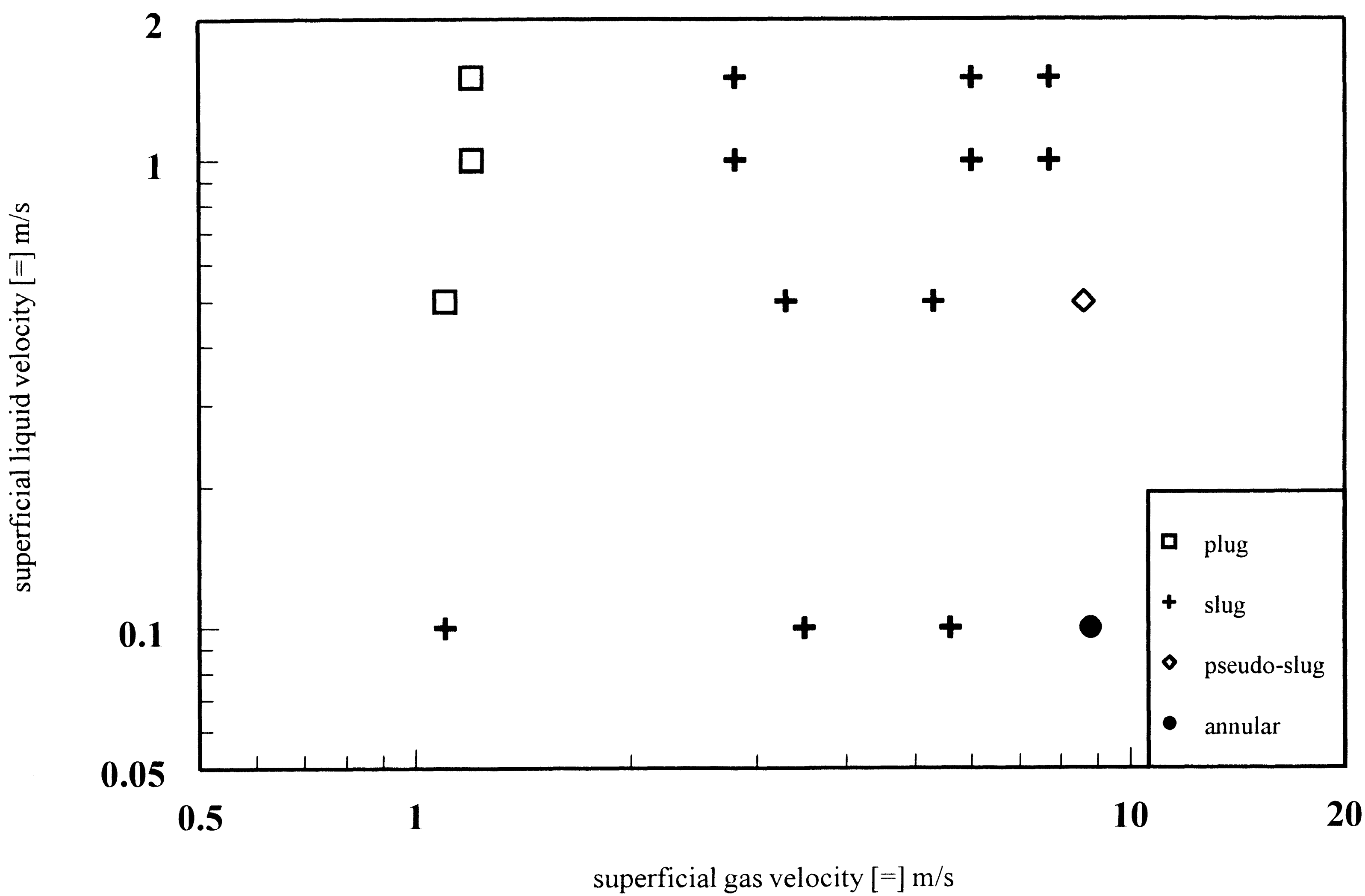

Figure 4.10: Flow regime map for 100% saltwater at 0.45 MPa and +2° inclination.

In downward flow, stratified flow dominates the flow regime map. The transition from stratified to slug flow becomes much more dependent upon the superficial gas velocity. Recall that in Figure 4.9, the transition from stratified to slug flow on the axes given was relatively horizontal (*i.e.*, occurring at a similar superficial liquid velocity for all superficial gas velocities studied). Figure 4.11 shows that if the pipe inclination is set to -2°, the transition becomes much more dependent upon the gas flow rate. At a superficial gas velocity of about 1 m/s, only stratified flow is observed at superficial liquid velocities as high as 1.5 m/s. At a superficial gas velocity of about 3 m/s, slug flow occurs at a superficial liquid velocity as low as 1 m/s while stratified flow occurs at a superficial liquid velocity of 0.5 m/s. At a superficial gas velocity of around 9 m/s, slug flow is observed to occur at a superficial liquid velocity as low as 0.5 m/s while stratified flow occurs at a superficial liquid velocity of 0.1 m/s. This trend is observed at other water cuts and at other pressures.

These stratified-slug transition results are expected and have been seen by other researchers (Kokal and Stanislav, 1989, *etc.*). In downflow, the liquid film is thinner and faster. At lower superficial gas velocities, more liquid is required to bridge across the pipe. At higher gas velocities, the film thickness is not much different from that in horizontal flow at high gas velocities, and the transition occurs near where it is expected to occur in horizontal flow.

Further downward inclination causes the transition from stratified to slug flow to occur at higher liquid flow rates. Figure 4.12 is a flow regime map for 80% water cut, 0.27 MPa, at -2° inclination. At a superficial gas velocity of about 6 m/s, slug flow is observed at a superficial liquid velocity of 0.5 m/s. Figure 4.13 is a flow regime map for the same

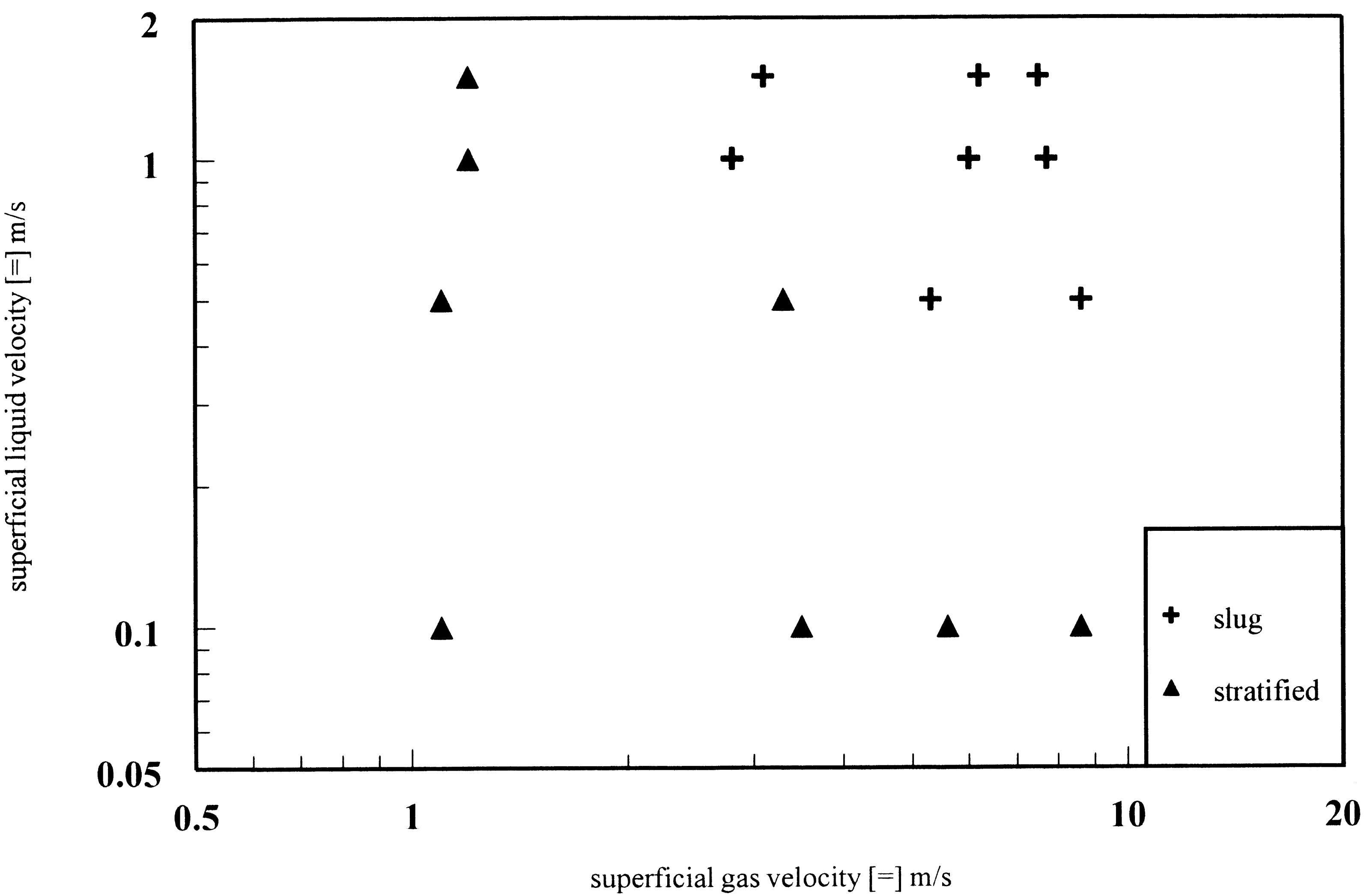

Figure 4.11: Flow regime map for 100% saltwater at 0.45 MPa and -2° inclination.

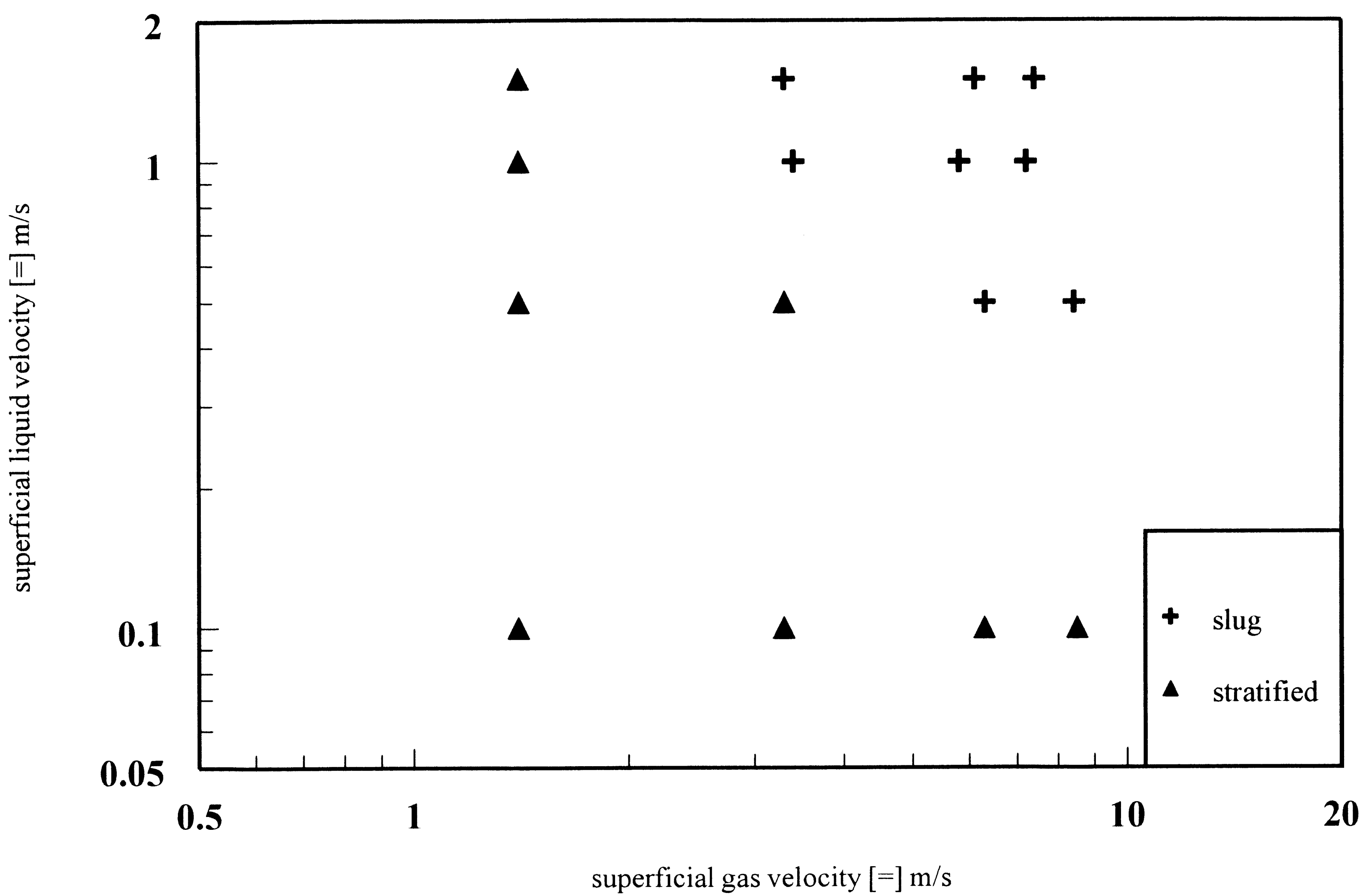

Figure 4.12: Flow regime map for 80% saltwater/20% light oil at 0.27 MPa and -2° inclination.

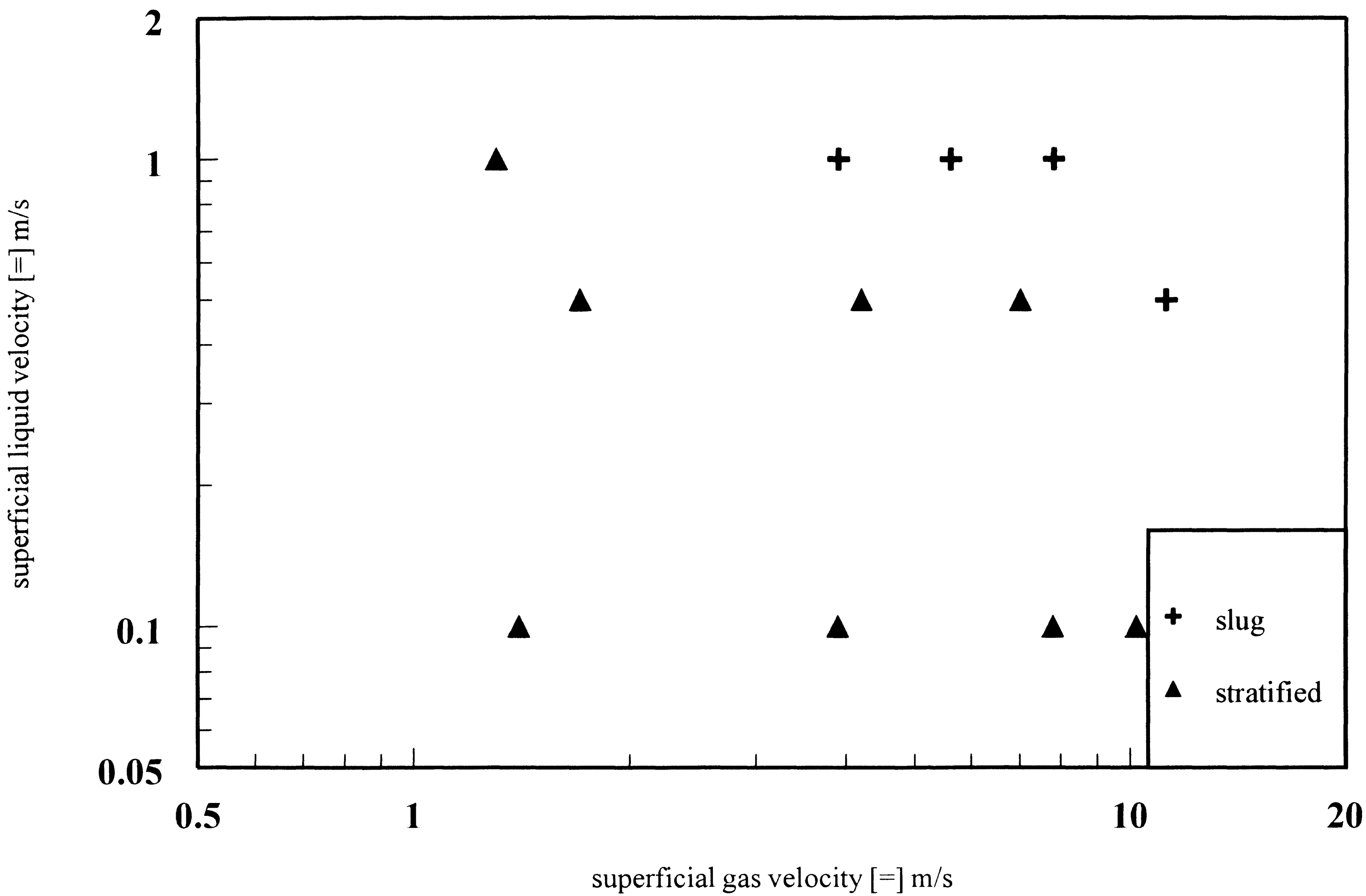

Figure 4.13: Flow regime map for 80% saltwater/20% light oil at 0.27 MPa and -5° inclination.

conditions at -5° inclination. At a superficial gas velocity of about 6 m/s, stratified flow occurs at a superficial liquid velocity of 0.5 m/s. This is observed at other pressures and at other water cuts. This is also expected as mentioned previously due to the thinner film in downflow. This further decrease was also observed by Kokal and Stanislav (1989).

Water cut was not observed to have an effect for the ranges tested. In horizontal flow, effect of pressure could not be discerned. It was observed, however, that the transition from stratified to slug flow in Figure 4.9 for 0.45 MPa was at a slightly higher liquid flow rate than it was at 0.13 MPa as reported by Lee (1993). Lee reported the transition to occur at a superficial liquid velocity of a little less than 0.3 m/s. Figure 4.9 indicates a transition at a superficial liquid velocity of about 0.35 m/s.

At moderate liquid flow rates in downflow, the transition to slug flow occurred at slightly higher gas flow rates with increasing pressure. Figures 4.13 and 4.14 represent the flow conditions at pressures of 0.27 and 0.45 MPa, respectively. At a pressure of 0.27 MPa and a superficial liquid velocity of 1 m/s, slug flow occurs at a superficial gas velocity of 4 m/s. At a pressure of 0.45 MPa and a superficial liquid velocity of 1 m/s, stratified flow still occurs at a superficial gas velocity of 5 m/s.

The transition to annular flow was found to occur in roughly the same location for all conditions tested at a superficial gas velocity around 10 m/s. The transition occurred at lower gas flow rate with low liquid flow rates and at a higher gas flow rate for the higher liquid flow rates. Figure 4.15 indicates that slug flow occurs at a superficial liquid velocity of 0.5 m/s and a superficial gas velocity of just less than 10 m/s, while at a superficial liquid velocity of around 0.1 m/s, annular flow was observed to occur at a superficial gas velocity

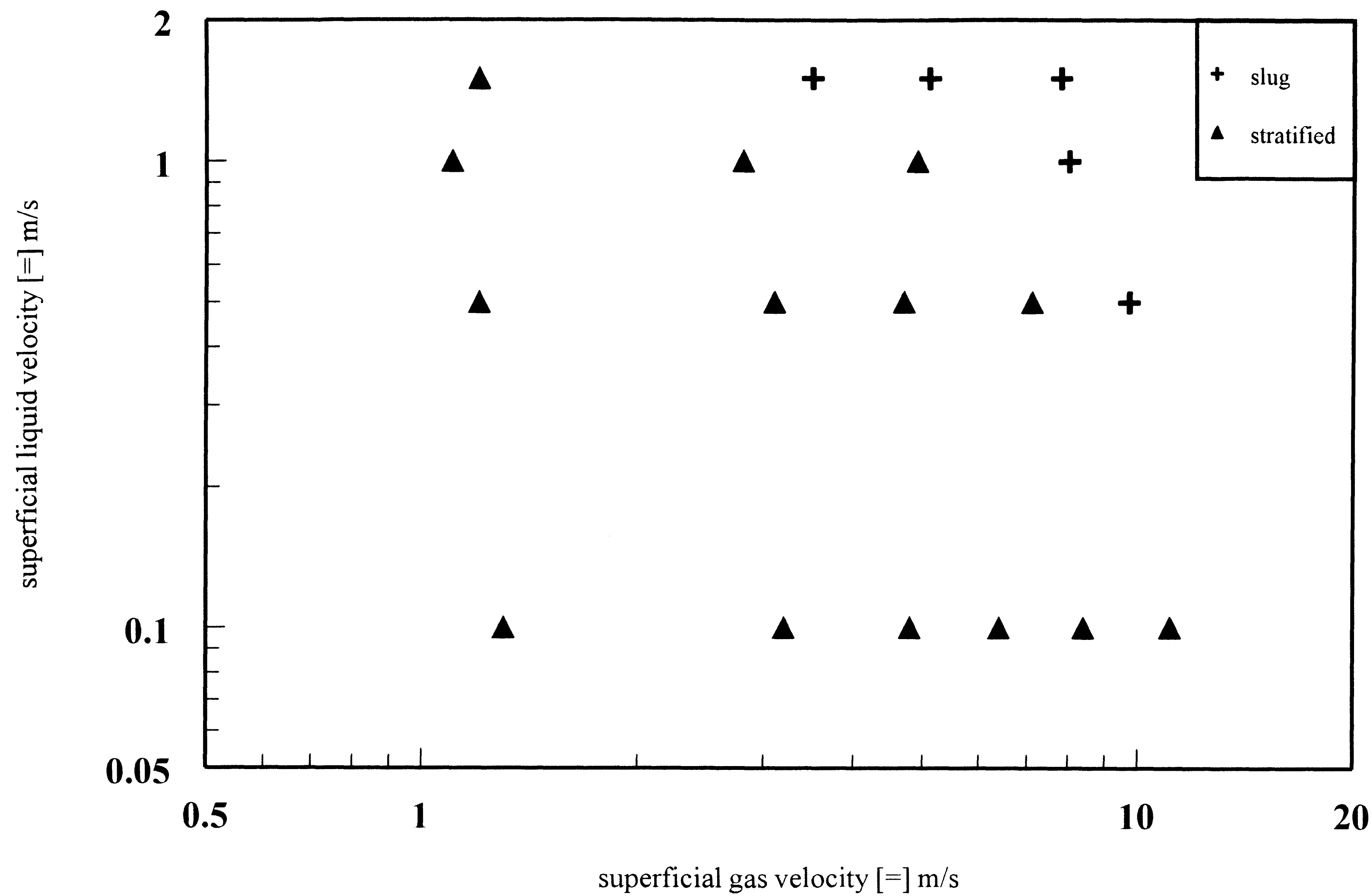

Figure 4.14: Flow regime map for 80% saltwater/20% light oil at 0.45 MPa and -5° inclination.

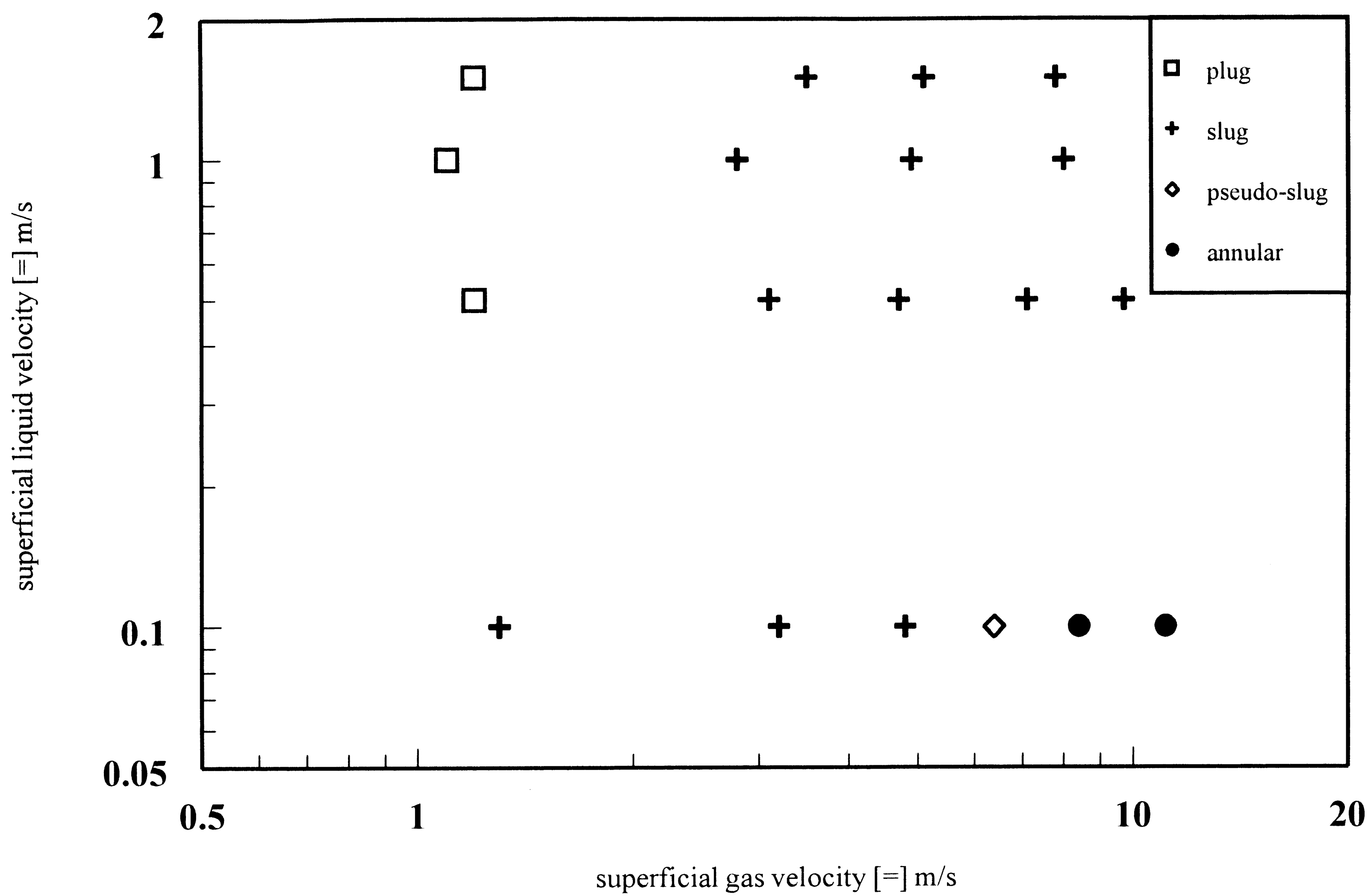

Figure 4.15: Flow regime map for 80% saltwater/20% light oil at 0.45 MPa and +5° inclination.

as low as just over 8 m/s. This was also observed by Kokal and Stanislav (1989). Inclination was found to have little effect on the transition in the range of conditions tested here. It appears that the gas flow rate required to reach annular flow is slightly lower in upflow and slightly higher in downflow. But nothing is observed which exceeds the uncertainties associated with the superficial gas velocity. Kokal and Stanislav also observed a slight decrease in gas required to reach annular flow with an increase in inclination, but it was on the order of their uncertainty. They concluded that this transition was relatively insensitive to inclination (-9° to +9°). Water cut was also found to have little observable effect on the transition to annular flow for the conditions tested.

Pressure was found to have a marked effect on the transition. As the pressure was increased, the transition to annular flow was observed to occur at lower superficial gas velocities. This effect has been observed in the field (Green, 1997) and is reasonable. Since annular flow is largely a density driven effect, it follows that the ratio of densities of the process fluids should affect this transition. In oil-water flows, when annular flow conditions occur, the less-dense and more viscous fluid (oil) flows in the core. In gas-liquid annular flow, the less-dense and less viscous fluid (gas) flows in the core. Since liquid-liquid annular flow occurs at a less-dense fluid superficial velocity of around 1 m/s for an oil with a specific gravity of near unity and around 5 m/s for an oil with a specific gravity of around 0.8 (Brauner and Maron, 1992), and since for gas-liquid annular flow occurs at a less-dense fluid superficial velocity of around 10 m/s, the closer the densities are, the lower the velocity requirement. Brauner and Maron demonstrated that as the oil specific gravity approached unity, the effect increased rapidly. As listed earlier, the gas density increases from 5.02 to

14.9 kg/m^3 as the pressure is increased from 0.27 to 0.79 MPa. Although this is a slight change with respect to the liquid density, there is a large effect on the ratio of the two.

Figures 4.16 and 4.17 represent the same flow conditions at pressures of 0.27 and 0.79 MPa, respectively. At 0.27 MPa and a superficial liquid velocity of 0.1 m/s, slug flow was observed to occur at a superficial gas velocity of about 8 m/s. At 0.79 MPa and a superficial liquid velocity of 0.1 m/s, annular flow was found to occur at a superficial gas velocity as low as 7 m/s. This effect can also be seen at other water cuts and at other inclinations.

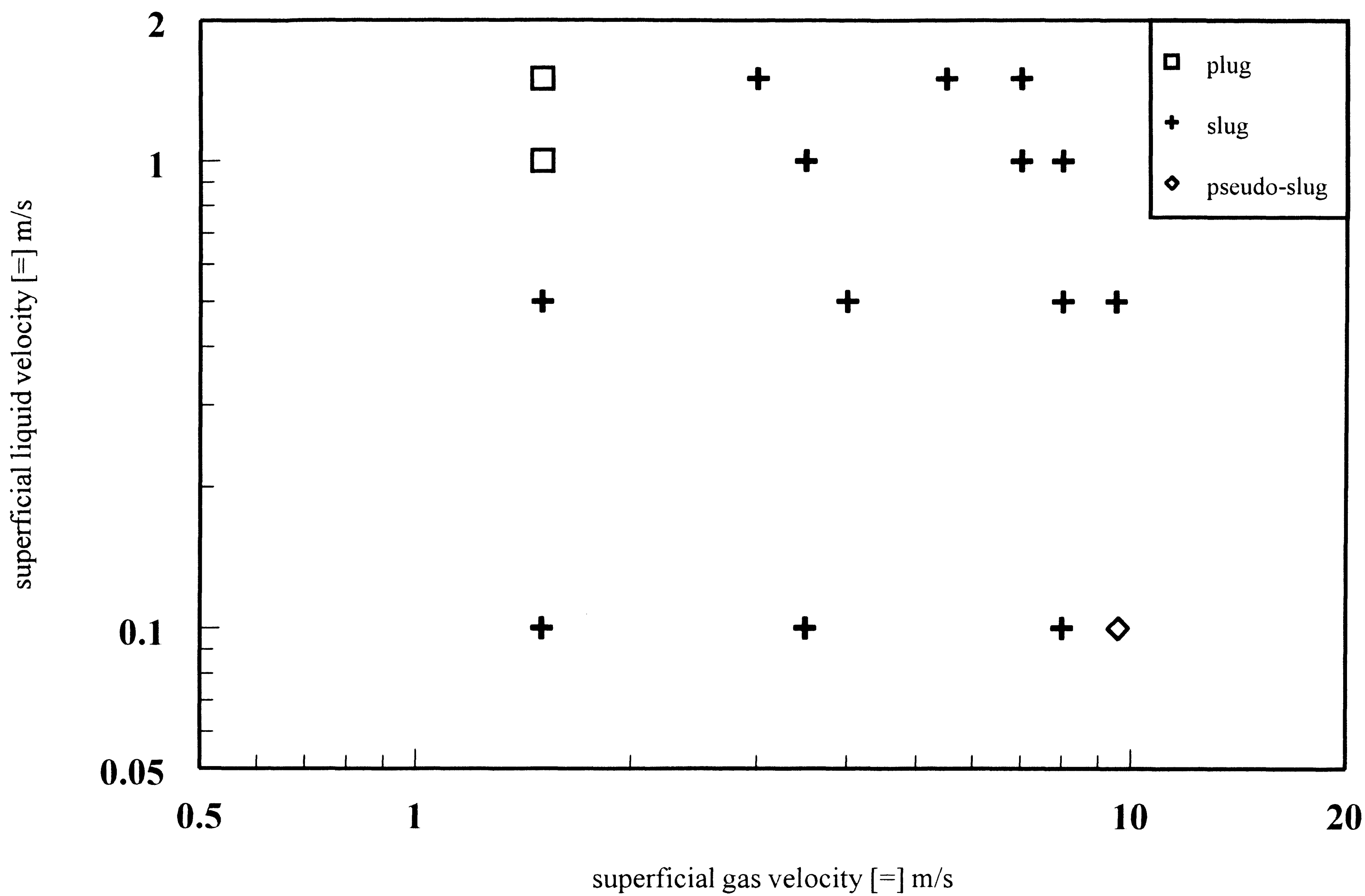

Figure 4.16: Flow regime map for 100% saltwater at 0.27 MPa and +5° inclination.

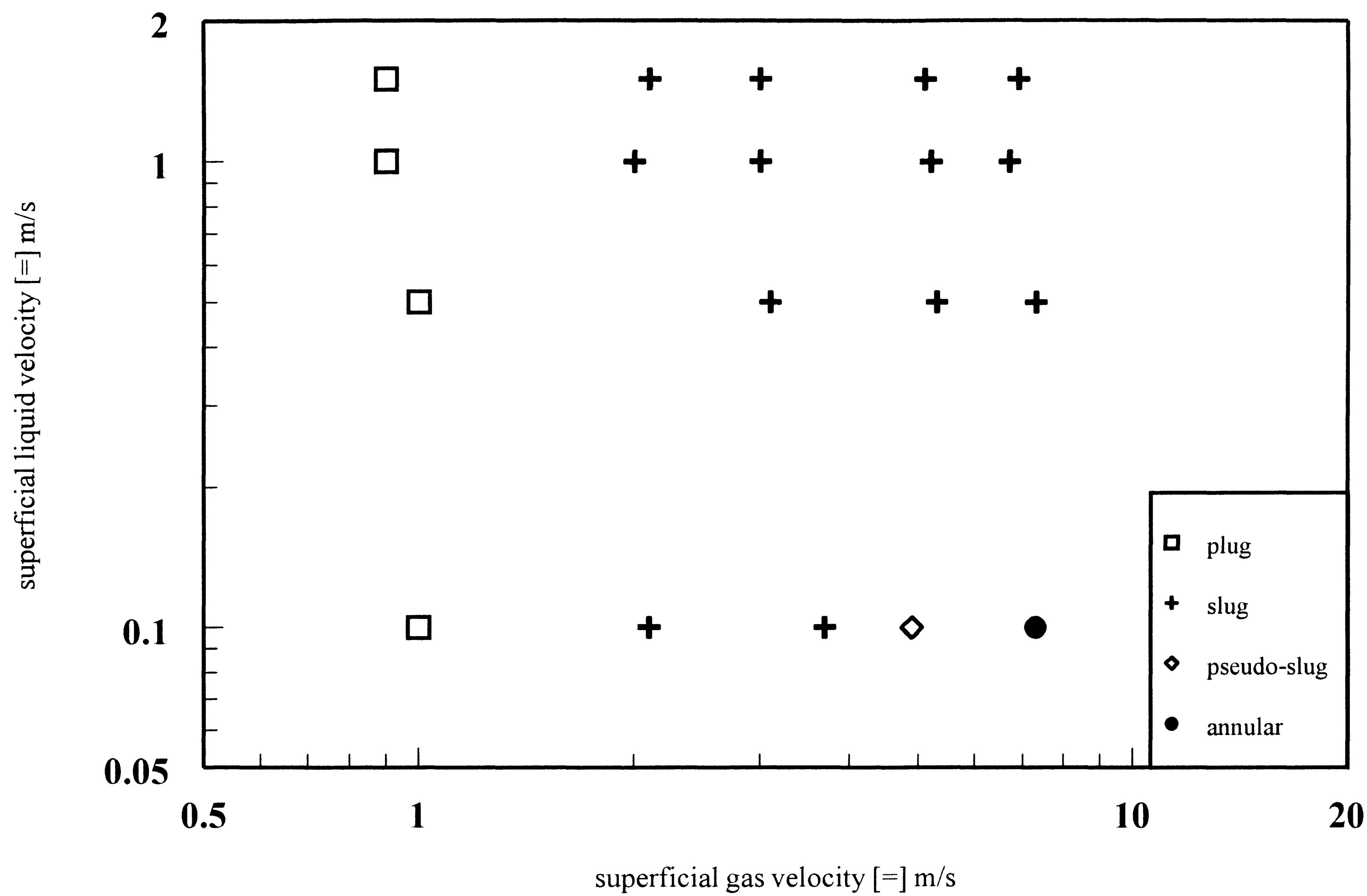

Figure 4.17: Flow regime map for 100% saltwater at 0.79 MPa and +5° inclination.

CHAPTER 5

STRATIFIED-SLUG TRANSITION MODEL DEVELOPMENT

A mechanistic model has been developed for predicting the transition from stratified to slug flow in three-phase, large-diameter pipelines which includes the effect of inclination and pressure. The basis for the stratified to slug transition model is the coexistence of stratified flow and slug flow. This approach stems from the ideas expressed by Jepson (1989). He noted that at transition from stratified to slug flow, there is only one slug in the pipe such that the contribution of the slug to the liquid flow is negligible. The stratified film between slugs can now be assumed to be equivalent to stratified flow. Lee (1993) found that in stratified flow of oil, water, and gas, all three fluids remained segregated. Based on this information, Neogi *et al.* (1993) proposed a three-phase film height model based on mass and momentum balances. This was later verified by Taitel *et al.* (1995). Figure 5.1 shows the shear stresses present in stratified flow of oil, water, and gas.

The conservation of momentum can be written for each phase. For the gas phase:

$$-A_G\left(\frac{dP}{dx}\right)_G - \tau_{WG}\cdot S_G - \tau_{iB}\cdot S_{iB} - \rho_G\cdot A_G\cdot g\cdot \sin(\theta) = 0 \tag{5.1}$$

Similarly, the conservation of momentum for the oil phase (liquid B) can be expressed:

$$-A_{LB}\left(\frac{dP}{dx}\right)_{LB} - \tau_{WLB}\cdot S_{LB} + \tau_{iB}\cdot S_{iB} - \tau_{iA}\cdot S_{iA} - \rho_{LB}\cdot A_{LB}\cdot g\cdot \sin(\theta) = 0 \tag{5.2}$$

For the water phase (liquid A):

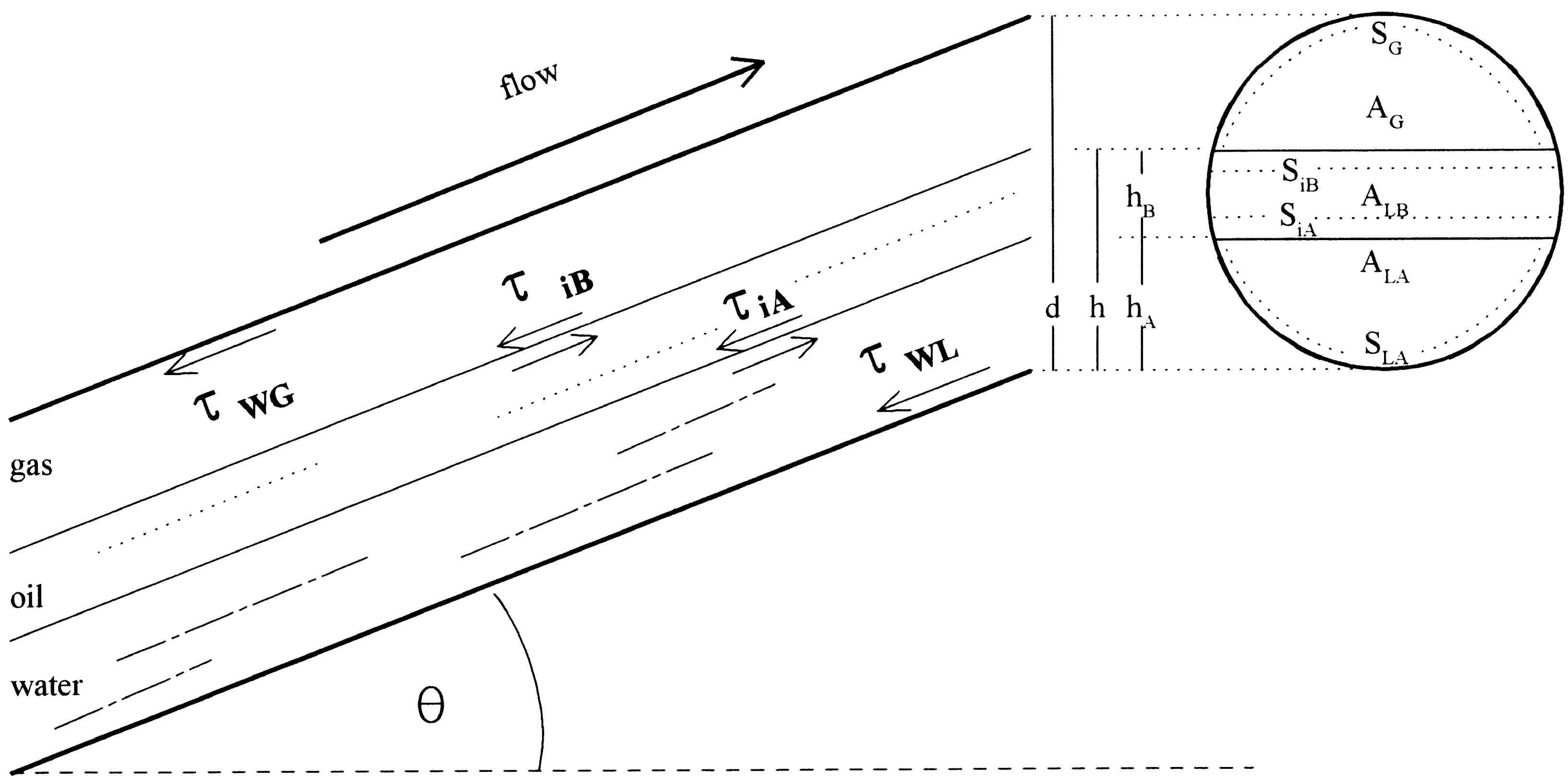

Figure 5.1: Three phase shear stress diagram.

$$-A_{LA}\left(\frac{dP}{dx}\right)_{LA} - \tau_{WLA}\cdot S_{LA} + \tau_{iA}\cdot S_{iA} - \rho_{LA}\cdot A_{LA}\cdot g\cdot \sin(\theta) = 0 \tag{5.3}$$

Assuming the pressure gradient in each phase to be equal, Equations 5.1 and 5.2 can be combined to eliminate the pressure gradient.

$$\frac{\tau_{WG}\cdot S_G}{A_G} - \frac{\tau_{WLB}\cdot S_{LB}}{A_{LB}} + \tau_{iB}\cdot S_{iB}\cdot\left(\frac{1}{A_G}+\frac{1}{A_{LB}}\right) - \frac{\tau_{iA}\cdot S_{iA}}{A_{LA}} + \left(\rho_G - \rho_{LB}\right)\cdot g\cdot \sin(\theta) = 0 \tag{5.4}$$

Similarly, Equations 5.2 and 5.3 can be combined to form:

$$\frac{\tau_{WLB}\cdot S_{LB}}{A_{LB}} - \frac{\tau_{WLA}\cdot S_{LA}}{A_{LA}} + \tau_{iA}\cdot S_{iA}\cdot\left(\frac{1}{A_{LB}}+\frac{1}{A_{LA}}\right) - \frac{\tau_{iB}\cdot S_{iB}}{A_{LB}} + \left(\rho_{LB} - \rho_{LA}\right)\cdot g\cdot \sin(\theta) = 0 \tag{5.5}$$

The fluid wall shear stress terms can be represented using a Blausius-type relation (Taitel and Dukler, 1976):

$$\tau_{WX} = \frac{\rho_X\cdot u_X^2\cdot C_X}{2}\cdot\left(\frac{D_X\cdot u_X}{\nu_X}\right)^{-n_X} \tag{5.6}$$

where the subscript X represents the phase of interest (G, LA, or LB). Neogi *et al.* (1993) allow the interfacial shear between the oil and water layers to be estimated by:

$$\tau_{iA} = \frac{\rho_{LB}\cdot C_{LB}}{8}\cdot\left(u_{LB} - u_{LA}\right)^2\cdot\left(\frac{D_{LB}\cdot u_{LB}}{\nu_{LB}}\right)^{-n_{LB}} \tag{5.7}$$

This assumes a smooth interface between the fluids.

The gas-liquid interfacial shear stress is often estimated to be equivalent to the gas wall shear stress (Gazley, 1949). This assumes that the liquid is moving sufficiently slow that the gas sees it as a wall. It also assumes the interface is smooth. This second assumption does not hold at higher gas flow rates. Andritsos and Hanratty (1987) found a way to take into account the waves that occur at the interface at higher gas velocities. They proposed that the interfacial friction factor is best approximated in two parts. At lower gas velocities, the interfacial friction factor is the same as the friction factor between the gas phase and the wall. Above some transitional superficial gas velocity, $V_{SG,t}$, the friction factor increases linearly with superficial gas velocity. Andritsos and Hanratty reported a friction factor modification which was calculated from experimental data. When they determined their friction factor modification, the interfacial velocity was taken to be zero. Thus the interfacial shear stress is calculated in a similar fashion as the gas wall shear stress. If $V_{SG} < V_{SG,t}$ then:

$$\tau_{iB} = \tau_{WG} = \frac{\rho_G \cdot C_G \cdot u_G^2}{2} \cdot \left(\frac{D_G \cdot u_G}{\nu_G} \right)^{-n_G} \tag{5.8}$$

If $V_{SG} > V_{SG,t}$ then:

$$\tau_{iB} = \tau_{WG} \cdot \left[1 + 15 \cdot \left(\frac{h}{d} \right)^{1/2} \cdot \left(\frac{V_{SG}}{V_{SG,t}} - 1 \right) \right] \tag{5.9}$$

where the transitional superficial gas velocity is estimated by:

$$V_{SG,t} = \left(\frac{\rho_{Go}}{\rho_G}\right)^{1/2} \cdot 5\,m/s \tag{5.10}$$

and ρ_{Go} is the gas density at atmospheric conditions. The magnitude of this density ratio effect at higher pressures has not been reported.

The friction correlation coefficients are dependent upon the phase Reynolds number. For example, if the gas phase is turbulent then $C_G = 0.046$ and $n_G = 0.2$. The friction factor is discontinuous in switching from laminar to turbulent flow. If the transition to turbulent flow is specified at $Re_G > 1500$, the Blausius-type relation for the shear stress becomes continuous for the correlation coefficients provided, allowing easier solution of the iterative equations. If it is not turbulent, then $C_G = 16$ and $n_G = 1$. The same coefficients are used for both liquid phases. The phase Reynolds number is calculated as:

$$Re_X = \left(\frac{D_X \cdot u_X}{\nu_X}\right) \tag{5.11}$$

The hydraulic diameter for liquid A is calculated by:

$$D_{LA} = \frac{4 \cdot A_{LA}}{S_{LA}} \tag{5.12}$$

for liquid B it is:

$$D_{LB} = \frac{4 \cdot A_{LB}}{S_{LB} + S_{iA}} \tag{5.13}$$

and the hydraulic diameter for the gas phase is calculated by:

$$D_G = \frac{4 \cdot A_G}{S_G + S_{iB}} \tag{5.14}$$

These are the relations used by Neogi *et al.* (1993) using the criteria of Agrawal (1975). Taitel *et al.* (1995) did not include S_{iA} in Equation 5.12. Since the Neogi results are compared to experimental data, and since this should have little affect due to the order of magnitude of this friction factor, the Neogi method will be used.

As the transition is made from stratified to slug flow, it is suggested that the superficial gas and liquid velocities in the film region are the same as the input superficial gas and liquid velocities. Thus, the *in-situ* fluid velocities can be determined from:

$$u_X = \frac{V_{SX} \cdot A}{A_X} \tag{5.15}$$

Taitel and Dukler (1976) showed that the geometric variables can all be related to the film height. The gas wetted perimeter is calculated by:

$$S_G = d \cdot \cos^{-1}\left(2 \cdot \frac{h}{d} - 1\right) \tag{5.16}$$

The gas-liquid interfacial surface is then calculated by:

$$S_{iB} = d \cdot \sin\left(\frac{S_G}{d}\right) \tag{5.17}$$

and the gas area is found to be:

$$A_G = \frac{d^2}{4} \cdot \left[\frac{S_G}{d} - \cos\left(\frac{S_G}{d} \right) \cdot \sin\left(\frac{S_G}{d} \right) \right] \tag{5.18}$$

The perimeter of liquid A is calculated by:

$$S_{LA} = \pi \cdot d - d \cdot \cos^{-1}\left(2 \cdot \frac{h_A}{d} - 1 \right) \tag{5.19}$$

The oil-water interfacial surface is then calculated by:

$$S_{iA} = d \cdot \sin\left(\frac{\pi \cdot d - S_{LA}}{d} \right) \tag{5.20}$$

The area of liquid A is then determined from:

$$A_{LA} = \frac{\pi \cdot d^2}{4} - \frac{d^2}{4} \cdot \left[\frac{\pi \cdot d - S_{LA}}{d} - \cos\left(\frac{\pi \cdot d - S_{LA}}{d} \right) \cdot \sin\left(\frac{\pi \cdot d - S_{LA}}{d} \right) \right] \tag{5.21}$$

The area of liquid B is now:

$$A_{LB} = \frac{\pi \cdot d^2}{4} - A_{LA} - A_{LB} \tag{5.22}$$

The wetted perimeter of liquid B is calculated as:

$$S_{LB} = \pi \cdot d - S_{LA} - S_G \tag{5.23}$$

There are now two equations with four unknowns: superficial gas velocity, superficial liquid velocity, water film height, oil film height. Dukler and Hubbard (1975) suggest that slug flow is not stable until the rate of liquid pickup at the front of the slug is equal to the rate of liquid shedding at the tail of the slug. Jepson (1989) suggests that the best way to determine the rate of shedding at the tail is to use a breaking dam analogy. He noticed that the shedding at the tail of the slug is much like the breaking of a dam. At the original site of a dam break, the liquid height remains at a constant four-ninths of its original height. Also at that site, it has been well established (Stoker, 1957) that the liquid velocity is:

$$u = -\frac{2}{3}\cdot\sqrt{g\cdot h} \tag{5.24}$$

Recall from Figure 1.1 that for slug flow Lee (1993) found the oil and water phases to be well mixed within the slug. Thus, one should consider the slug to be two phases: liquid and gas. Consider the liquid density and viscosity to be a weighted average of those for oil and water.

Recall that Figure 2.4 illustrates a slug with an axial coordinate system moving with the average slug velocity. Jepson (1989) produced a conservation of mass for this system in the liquid phase as:

$$\rho_L\cdot\left[\left(u_L - V_S\right)\cdot\frac{A_L}{A} + \left(V_t - V_S\right)\cdot\frac{A_L}{A} + \left(V_t - V_G\right)\cdot\left(1 - \alpha_S\right)\right] = \rho_L\cdot\frac{2}{3}\cdot\sqrt{\frac{g\cdot d\cdot\pi}{4}\cdot\frac{A_{L_2}}{A}}\cdot\left(1 - \alpha_2\right) \tag{5.25}$$

For a pipe Jepson shows that:

$$\frac{A_{L_2}}{A} \approx \mathbf{0.442} \tag{5.26}$$

For the void fraction in the tail, α_2, no reported values have been found. Jepson (1989) specifies this value to be either zero or equivalent to the average void fraction within the slug. Forcing the value to be zero would be too low, and allowing it to be the average void would be too high. Consider the plot of liquid holdup in Figure 2.5. The void fraction is much higher at the front of the slug than it is in the tail. The void fraction actually remains the same after the end of the mixing zone through to the tail of the slug. Thus, the tail void fraction is best approximated as the value at the end of the mixing zone:

$$\alpha_2 = \alpha(x = l_m) \tag{5.27}$$

Jepson (1989) further shows from a mass balance that at transition:

$$V_S = V_{SL} + V_{SG} \tag{5.28}$$

and:

$$V_t = \frac{V_S \cdot (1 - \alpha_S) - V_{SL}}{(1 - \alpha_S) - \overline{A_L}} \tag{5.29}$$

where:

$$\overline{A_L} = \frac{A_L}{A} \tag{5.30}$$

The *in-situ* gas velocity is calculated from:

$$u_G = \frac{\left(V_S - V_t\right)\cdot\alpha_S}{\left(1 - \overline{A_L}\right)} + V_t \tag{5.31}$$

The *in-situ* liquid velocity is calculated from Equation 5.15. Now Equation 5.25 can be rewritten in a quadratic of the liquid holdup as:

$$\begin{aligned}&\left(1 - \alpha_S\right)^2\cdot\left(V_S\cdot\overline{A_L} - V_{SL}\right)\\ &+ \left(1 - \alpha_S\right)\cdot\left[C_1 + \overline{A_L}\cdot\left(V_{SL} - C_1 - V_S\cdot\overline{A_L}\right)\right]\\ &+ \overline{A_L}\cdot\left[2\cdot\left(V_S\cdot\overline{A_L}^2 - V_{SL}\cdot\overline{A_L} - V_S\cdot\overline{A_L} + V_{SL}\right) + C_1\cdot\overline{A_L} - C_1\right] = 0\end{aligned} \tag{5.32}$$

where:

$$C_1 = \frac{2}{3}\cdot\frac{A_{L_2}}{A}\cdot\sqrt{\frac{g\cdot\pi\cdot d}{4}}\cdot\left(1 - \alpha_2\right) \tag{5.33}$$

Now a third relation has been specified which has six unknowns: superficial gas velocity, superficial liquid velocity, water film height, oil film height, average void fraction, void fraction at the end of the mixing zone. The first four are the same as in Equations 5.4 and 5.5. Information is now required for the void fraction in the slug mixing zone, body, and tail. These can be specified with the lead-lag model of Maley (1997b). Although several void fraction models work reasonably well, this is the correlation recommended since three phase flow can be incorporated.

Void fraction is not constant through the slug. The void fraction is highest at the front of the mixing zone and decreases until the end of the mixing zone is reached. Throughout the remainder of the slug body, the void fraction remains constant. The lead-lag model evaluates the void fraction at a given distance into the mixing zone.

$$\alpha(x) = \frac{X_{lg} - X_{ld}}{X_{lg}} \cdot e^{\left(-\frac{x}{X_{lg}}\right)} \tag{5.34}$$

Thus, the average slug void in the mixing zone can be determined by integrating Equation 5.34 across the mixing zone.

$$\langle \alpha_{MZ} \rangle = \frac{\int_{x=0}^{x=l_m} \alpha(x) dx}{l_m - 0} = \frac{X_{ld} - X_{lg}}{l_m} \cdot \left[e^{\left(-\frac{l_m}{X_{lg}}\right)} - 1 \right] \tag{5.35}$$

The void fraction in the slug body and slug tail is the same as the void fraction at the end of the mixing zone. This is determined by evaluating Equation 5.34 at $x = l_m$. Thus, the true average slug body void fraction might be estimated by a weighted-average of the mixing zone void and the body void.

$$\langle \alpha_S \rangle = \frac{\langle \alpha_{MZ} \rangle \cdot l_m + \alpha(x = l_m) \cdot (l_s - l_m)}{l_s} \tag{5.36}$$

The length of the slug is calculated as fifteen times the pipe diameter as suggested by Andreussi *et al.* (1993).

Three parameters must be determined to apply Equations 5.30 and 5.31: lead distance, lag distance, mixing zone length. Maley (1997b) has correlated each of these to the film Froude number. Although Maley is working on correlating the coefficients to fluid properties, much still needs to be verified. The original correlation coefficients are used here. These are presented in Section 2.3. For all cases, the length of the mixing zone is determined by:

$$l_m = 0.061 \cdot FR_f + 0.067 \tag{5.37}$$

It is suggested that in using this model, each of these parameters be corrected for diameter. This is accomplished by multiplying by the ratio of the desired diameter to the base diameter from which the Maley model was created (10-cm). This then gives the length of the mixing zone equal to the length of the slug (fifteen pipe diameters) at a film Froude number of 23. The film Froude number is determined by:

$$Fr_f = \frac{V_t - u_L}{\left(g \cdot h_{eff}\right)^{1/2}} \tag{5.38}$$

Chow (1959) defines the effective film height as the ratio of liquid area to gas-liquid interfacial distance.

$$h_{eff} = \frac{A_L}{S_{iB}} \tag{5.39}$$

Now, Equation 5.35 can be determined from the same three unknowns: superficial gas velocity, superficial liquid velocity, film height. Equations 5.4, 5.5, 5.32, 5.34, and 5.35

can now be combined to solve the six unknowns to determine the transition line. It should be noted that the Maley model is correlated to data at film Froude numbers of 4 to 18. It was shown to be inappropriate at Froude numbers below 6. It is expected that the model of Gopal (1994) would be appropriate for film Froude numbers up to this point, but the model needs to be modified to incorporate the offset at the front of the slug. The Gregory *et al.* (1978) model for void fraction has been shown to apply well for the low mixture velocities. This relation is:

$$\alpha_S = 1 - \frac{1}{1 + \left(\frac{V_{SL} + V_{SG}}{8.66\, m/s} \right)^{1.39}} \tag{5.40}$$

Thus, up to a film Froude number of 6, the Gregory correlation with a tail void of zero (Jepson, 1989) is applied along with Equations 5.4, 5.5, and 5.32. Figure 5.2 is a solution procedure flow chart. Starting with the fluid properties, pipe diameter, and inclination, the transition from stratified to slug flow is determined. For a given superficial gas velocity, the transition occurs at one superficial liquid velocity. The superficial gas velocity is then specified and varied through the range of interest and the superficial liquid velocity for transition is determined. First, the superficial liquid velocity is guessed. There is only one solution to Equations 5.4 and 5.5 for the film heights at a given superficial gas and superficial liquid velocity. The film heights cannot be determined explicitly from the equations. A two-function modified Newton-Raphson procedure is then used to determine the film heights and geometric variables. For the first pass, the Gregory correlation (Equation 5.40) is used to determine void fraction. If the Froude number is greater than 6,

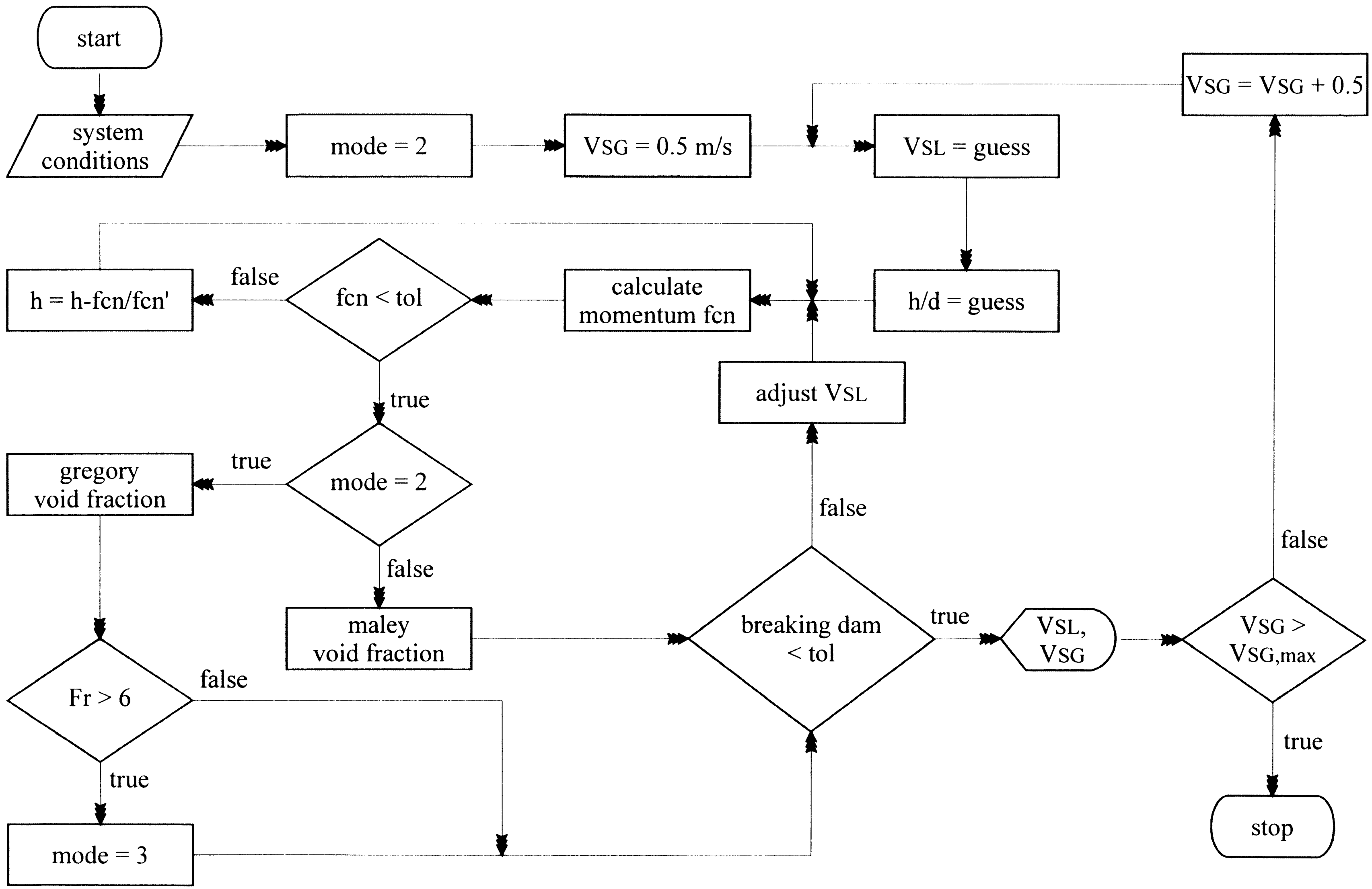

Figure 5.2: Stratified-slug solution procedure flow chart.

subsequent calculations are made using the Maley (1997b) relations (Equations 5.34 and 5.35). The void fraction is then compared with the value from the breaking dam conservation of mass (Equation 5.32). If the values do not match, a new guess for the superficial liquid velocity is made. Once the proper superficial liquid velocity is determined, the value is incremented. The next superficial gas velocity is then evaluated.

CHAPTER 6

SLUG-ANNULAR TRANSITION MODEL DEVELOPMENT

A mechanistic model has been developed for predicting the transition from slug to annular flow. Previous researchers have demonstrated the presence of secondary flows, wave spreading, droplet deposition, *etc.* in describing annular flow. The basis for this slug to annular transition model is the coexistence of annular flow and slug flow. The transition will also incorporate other criteria such as a maximum film Froude number, maximum slug body void fraction, and the liquid holdup in the slug becoming equal to the liquid area in the film region. To these criteria an additional mechanism has been specified: the minimization of pressure drop.

Lee (1993) noted that in both annular flow and in slug flow, the oil and water are completely mixed. For this reason, the equations are developed for the two-phase liquid-gas case. In annular flow, the film spreads along the circumference of the pipe wall. Investigators disagree as to when annular flow is reached from stratified flow. Lin (1985) suggested that annular flow is reached when the film has spread completely around the pipe as in Figure 6.1. In this case, the gas-liquid interface is quite rough, and the liquid has spread completely around the pipe, although only to the thickness of 1 to 2 mm at the top while remaining thicker at the bottom. Zabaras (1996) considers the spreading in Figure 6.2 to be sufficient enough to be termed annular flow.

For this model, the annular film will be considered to spread just enough that it meets at the top of the pipe. Figures 6.3a and 6.3b represent when the film has not quite and has just spread completely around the pipe, respectively. For wave spreading, previous

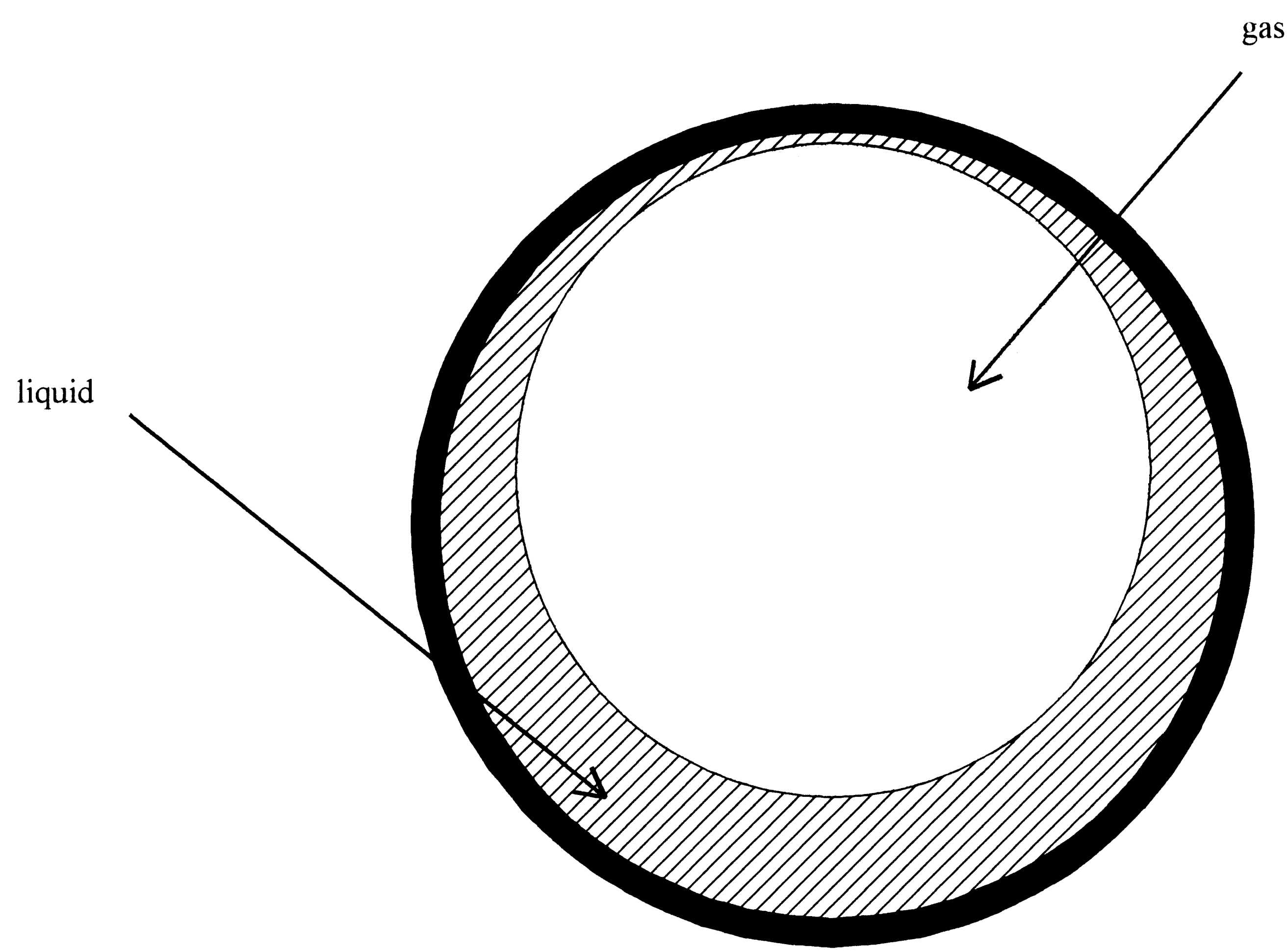

Figure 6.1: Annular flow with film encircling the pipe.

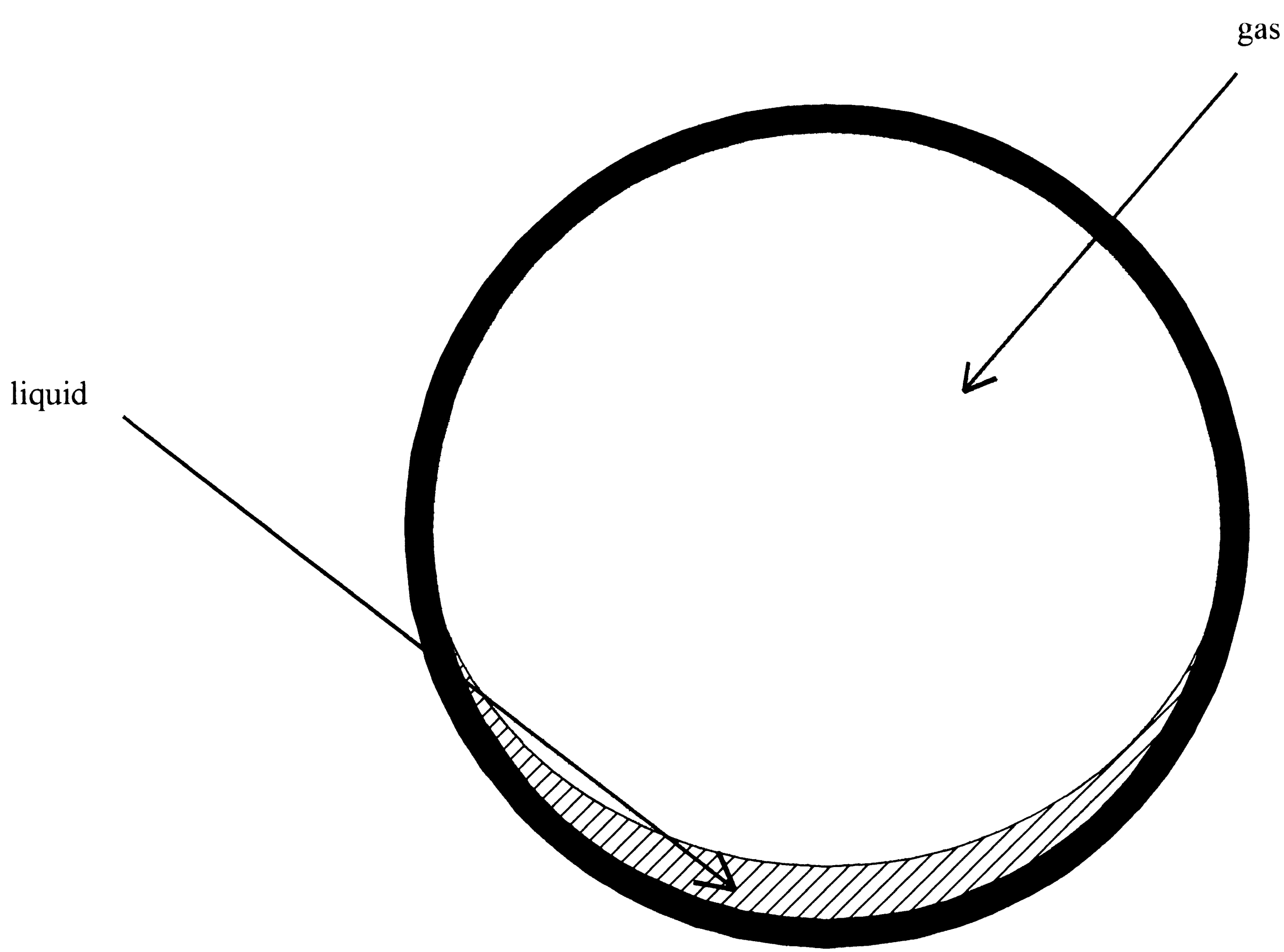

Figure 6.2: Annular flow with film starting to spread.

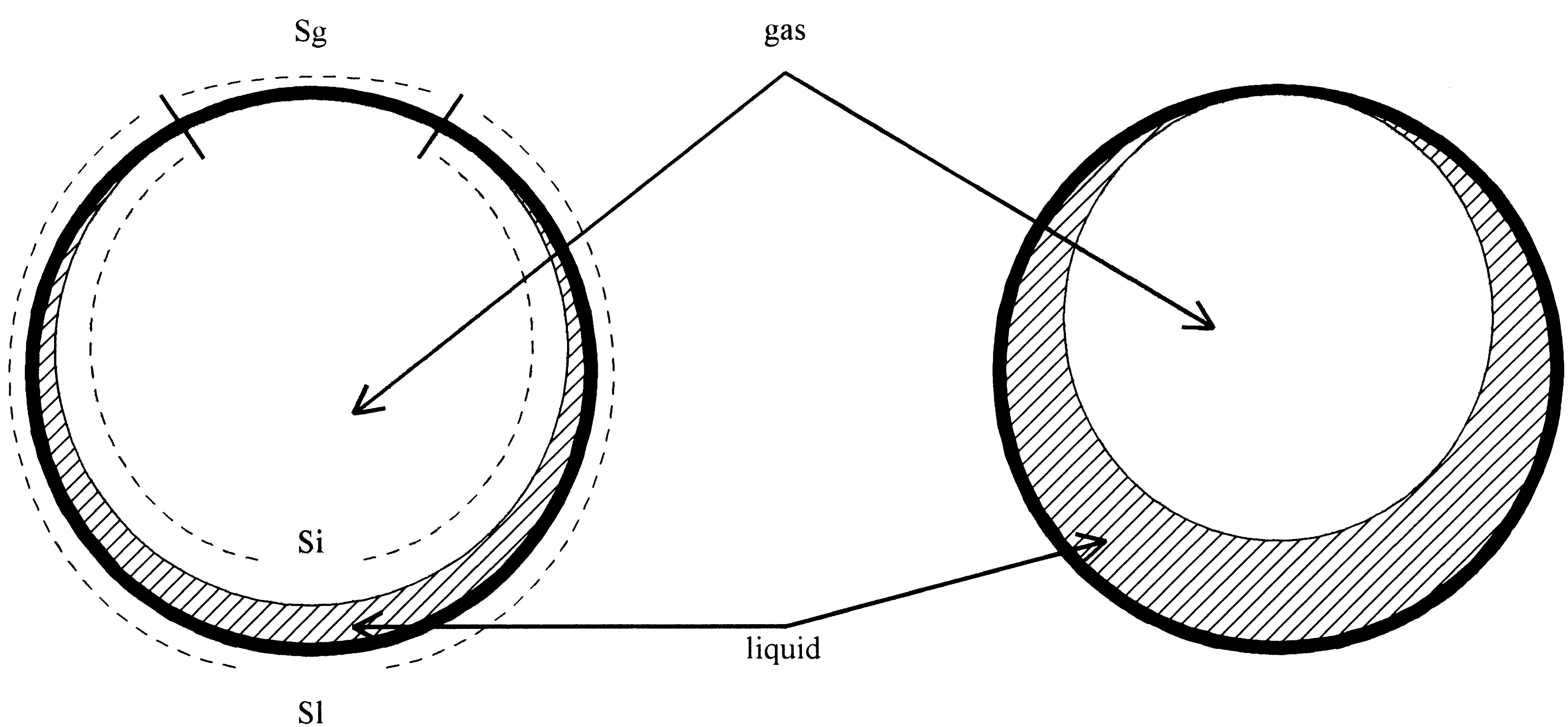

Figure 6.3a: Film not quite complete.

Figure 6.3b: Film completely spread.

geometric relations between arc lengths, areas, and heights no longer apply. It is extremely important that the geometric relations developed for the stratified to slug transition model not be used inadvertently in this model.

Figure 6.4 illustrates the shear stresses acting on the system. From this the annular flow conservation of momentum can be solved. For the gas phase:

$$-A_G\left(\frac{dP}{dx}\right)_G - \tau_{WG}\cdot S_G - \tau_i\cdot S_i - \rho_G\cdot A_G\cdot g\cdot \sin(\theta) = 0 \tag{6.1}$$

Similarly, the conservation of momentum for the liquid phase can be expressed:

$$-A_L\left(\frac{dP}{dx}\right)_L - \tau_{WL}\cdot S_L + \tau_i\cdot S_i - \rho_L\cdot A_L\cdot g\cdot \sin(\theta) = 0 \tag{6.2}$$

Assuming the pressure gradient in the gas phase to be equal to the pressure gradient in the liquid phase, Equations 6.1 and 6.2 can be added to eliminate the interfacial shear and give:

$$-(A_G + A_L)\cdot\left(\frac{dP}{dx}\right) - \tau_{WG}\cdot S_G - \tau_{WL}\cdot S_L - (\rho_L\cdot A_L + \rho_G\cdot A_G)\cdot g\cdot \sin(\theta) = 0 \tag{6.3}$$

The pressure drop can now be represented as:

$$\frac{dP}{dx} = -\frac{1}{A}\cdot\tau_{WG}\cdot S_G - \frac{1}{A}\cdot\tau_{WL}\cdot S_L - \frac{g\cdot\sin(\theta)}{A}\cdot(\rho_L\cdot A_L + \rho_G\cdot A_G) \tag{6.4}$$

In determining what would drive the fluids to prefer the state of Figure 6.3b to Figure 6.3a, it was speculated that it was the path of least resistance. If the spreading occurs so as

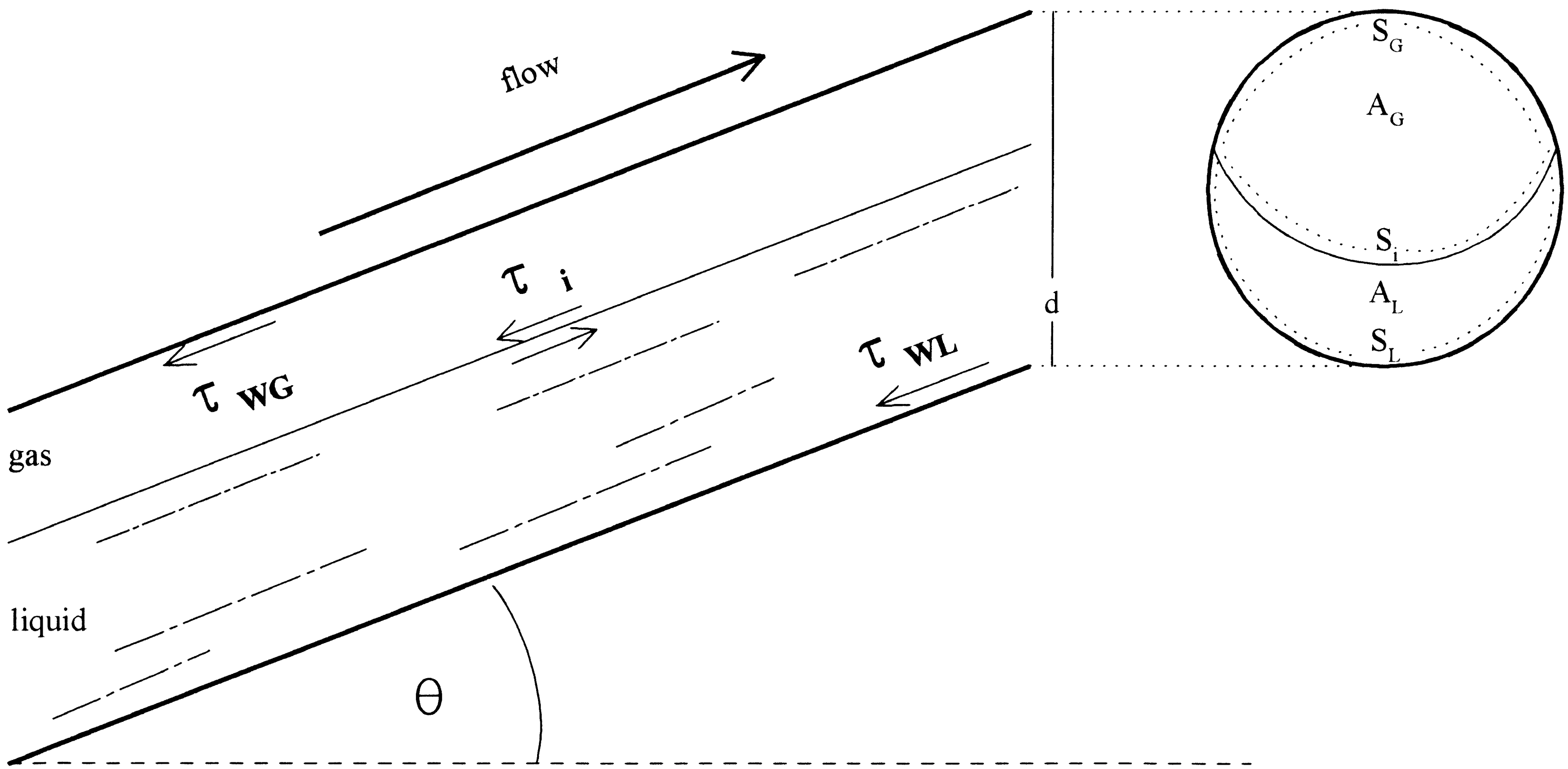

Figure 6.4: Shear stress diagram.

to take the path of least resistance, then it occurs to minimize the pressure drop. In physical terms, the shear at the wall of the gas is greater than that of the liquid for Figure 6.3a such that true pressure drop minimization occurs where the gas has no perimeter. Thus, the solution lies in the minimization of the pressure drop as given in Equation 6.4. This is obtained by setting the partial derivative of the pressure drop with respect to the gas perimeter equal to zero and evaluating where the gas perimeter equals zero.

$$\frac{\delta\left(\frac{dP}{dx}\right)}{\delta S_G} = -\frac{1}{A}\cdot\left[\frac{\delta(\tau_{WG}\cdot S_G)}{\delta S_G} + \frac{\delta(\tau_{WL}\cdot S_L)}{\delta S_G} + g\cdot\sin(\theta)\cdot\frac{\delta(\rho_L\cdot A_L + \rho_G\cdot A_G)}{\delta S_G}\right] = 0 \qquad (6.5)$$

Expanding the terms, gives the governing equation:

$$S_G\cdot\frac{\delta\tau_{WG}}{\delta S_G} + \tau_{WG} + S_L\cdot\frac{\delta\tau_{WL}}{\delta S_G} + \tau_{WL}\cdot\frac{\delta S_L}{\delta S_G} + g\cdot\sin(\theta)\cdot\left(\rho_G\cdot\frac{\delta A_G}{\delta S_G} + \rho_L\cdot\frac{\delta A_L}{\delta S_G}\right) = 0 \qquad (6.6)$$

Note that:

$$S_G + S_L = \pi\cdot d = constant \qquad (6.7)$$

Such that:

$$\frac{\delta S_G}{\delta S_G} + \frac{\delta S_L}{\delta S_G} = 0 \qquad (6.8)$$

which means that:

$$\frac{\delta S_L}{\delta S_G} = -1 \tag{6.9}$$

Also note that:

$$A_G + A_L = \frac{\pi \cdot d^2}{4} = constant \tag{6.10}$$

such that:

$$\frac{\delta A_G}{\delta S_G} = -\frac{\delta A_L}{\delta S_G} \tag{6.11}$$

The governing equation now becomes:

$$\tau_{WG} - \tau_{WL} + S_G \cdot \frac{\delta \tau_{WG}}{\delta S_G} + S_L \cdot \frac{\delta \tau_{WL}}{\delta S_G} + \left(\rho_L - \rho_G\right) g \cdot \sin(\theta) \frac{\delta A_L}{\delta S_G} = 0 \tag{6.12}$$

The liquid wetted perimeter becomes the pipe perimeter and the gas perimeter becomes zero in annular flow. Since the derivative of the gas wall shear stress is not infinite, the third term is eliminated. Now the derivative of the liquid wall shear stress is evaluated. First, the liquid wall shear stress is defined using a Blausius-type relation.

$$\tau_{WL} = \frac{\rho_L \cdot u_L^2 \cdot C_L}{2} \cdot \left(\frac{D_L \cdot u_L}{\nu_L} \right)^{-n} \tag{6.13}$$

such that the derivative is:

$$\frac{\delta\tau_{WL}}{\delta S_G} = \tau_{WL}\cdot\left[\frac{2}{u_L}\cdot\frac{\delta u_L}{\delta S_G} - n\cdot\left(\frac{D_L\cdot u_L}{\nu_L}\right)^{-1}\cdot\frac{1}{\nu_L}\cdot\frac{\delta(u_L\cdot D_L)}{\delta S_G}\right] \tag{6.14}$$

Recall that:

$$u_L = \frac{V_{SL}\cdot A}{A_L} \tag{6.15}$$

Therefore:

$$\frac{\delta u_L}{\delta S_G} = -\frac{V_{SL}\cdot A}{A_L^2}\cdot\frac{\delta A_L}{\delta S_G} = -\frac{u_L}{A_L}\cdot\frac{\delta A_L}{\delta S_G} \tag{6.16}$$

Note that:

$$u_L\cdot D_L = \frac{V_{SL}\cdot A}{A_L}\cdot\frac{4\cdot A_L}{S_L} = \frac{4\cdot A\cdot V_{SL}}{S_L} \tag{6.17}$$

Thus:

$$\frac{\delta(u_L\cdot D_L)}{\delta S_G} = -4\cdot A\cdot V_{SL}\cdot\frac{1}{S_L^2}\cdot\frac{\delta S_L}{\delta S_G} = \frac{4\cdot A\cdot V_{SL}}{S_L^2} \tag{6.18}$$

Substituting these relations into the shear stress derivative gives:

$$\frac{\delta\tau_{WL}}{\delta S_G} = \frac{\rho_L \cdot C_L}{2} \cdot \left(\frac{D_L \cdot u_L}{\nu_L}\right)^{-n} \left[-2 \cdot u_L \cdot \frac{u_L}{A_L} \cdot \frac{\delta A_L}{\delta S_G} - \frac{n \cdot u_L^2}{D_L \cdot u_L} \cdot \frac{4 \cdot A \cdot V_{SL}}{S_L^2}\right] \tag{6.19}$$

which simplifies to:

$$\frac{\delta\tau_{WL}}{\delta S_G} = \frac{\rho_L \cdot C_L}{2} \cdot \left(\frac{D_L \cdot u_L}{\nu_L}\right)^{-n} \left[-\frac{2 \cdot u_L^2}{A_L} \cdot \frac{\delta A_L}{\delta S_G} - \frac{n \cdot u_L^2}{S_L}\right] \tag{6.20}$$

Now Equation 6.12 has been reduced to one derivative. It is not expected that the liquid area changes much with respect to the gas perimeter. One possible solution follows. Figure 6.5 is the cross-sectional view of a film region with spreading. Let A_G' represent the area of the gas bound between the top of the pipe and the line S_i'. This is much like the area of the gas when no spreading occurs. Let A_{GS} represent the area of the gas that is due only to the spreading of the liquid (below the line S_i'). The area of the gas is now:

$$A_G = A_G' + A_{GS} \tag{6.21}$$

This leads to:

$$\frac{\delta A_G}{\delta S_G} = \frac{\delta A_G'}{\delta S_G} + \frac{\delta A_{GS}}{\delta S_G} \tag{6.22}$$

Recall the geometric relations from the case of no spreading:

$$\frac{S_G}{d} = \cos^{-1}\left(2 \cdot \frac{h}{d} - 1\right) \tag{6.23}$$

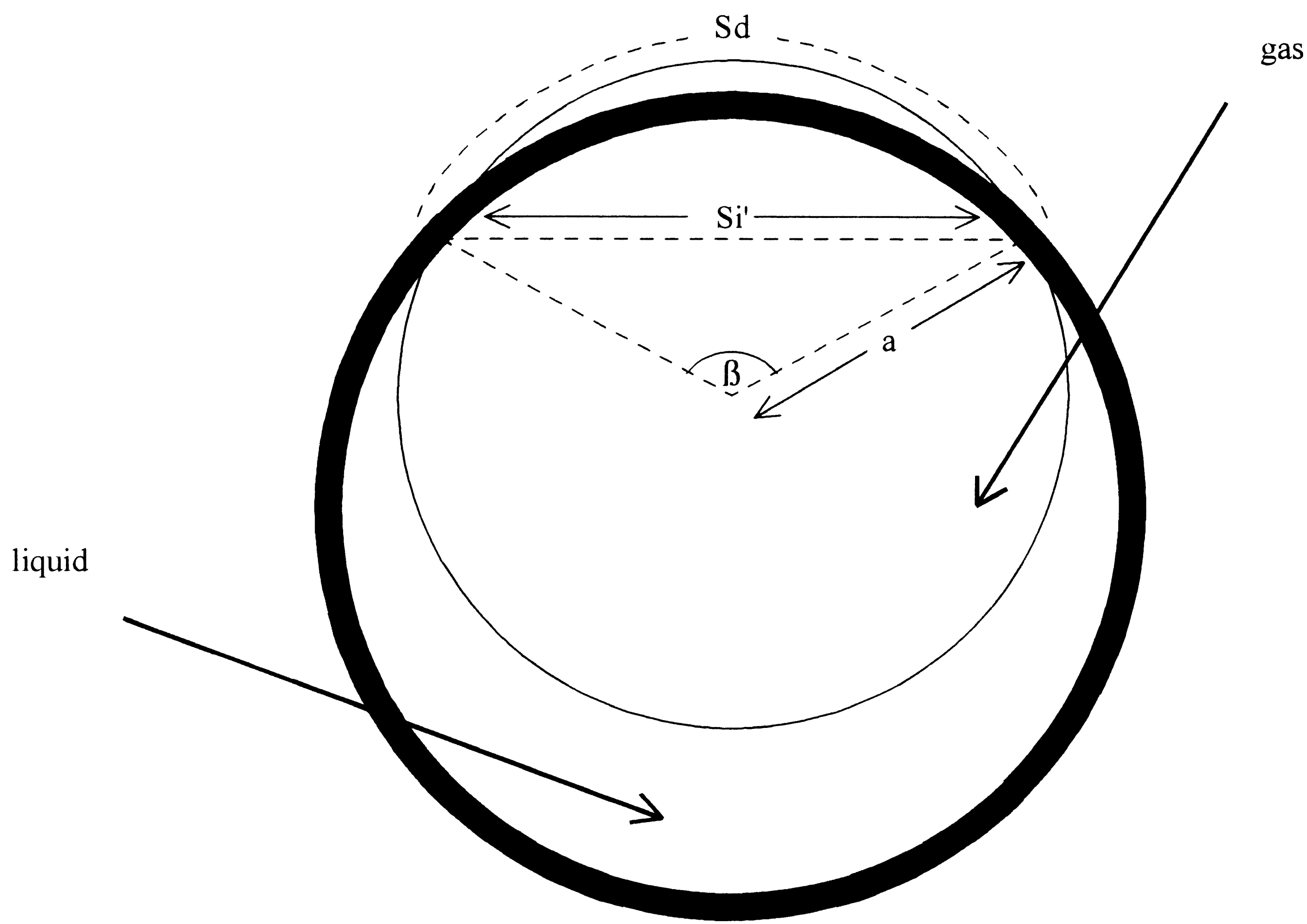

Figure 6.5: Film spreading variables.

which can be rearranged to be:

$$2\cdot\frac{h}{d} - 1 = \cos\left(\frac{S_G}{d}\right) \tag{6.24}$$

Also note that:

$$\frac{S_i'}{d} = \left(1 - \cos^2\left(\frac{S_G}{d}\right)\right)^{1/2} = \sin\left(\frac{S_G}{d}\right) \tag{6.25}$$

Thus:

$$A_G' = \frac{d^2}{4}\cdot\left[\frac{S_G}{d} - \cos\left(\frac{S_G}{d}\right)\cdot\sin\left(\frac{S_G}{d}\right)\right] \tag{6.26}$$

The derivative of which is:

$$\frac{\delta A_G'}{\delta S_G} = \frac{d^2}{4}\cdot\left[\frac{1}{d} - \left(\cos^2\left(\frac{S_G}{d}\right) - \sin^2\left(\frac{S_G}{d}\right)\right)\cdot\frac{1}{d}\right] = \frac{d}{2}\cdot\sin^2\left(\frac{S_G}{d}\right) \tag{6.27}$$

Since the gas perimeter is zero:

$$\frac{\delta A_G'}{\delta S_G} = 0 \tag{6.28}$$

Which simplifies Equation 6.22 and with Equation 6.11 gives:

$$\frac{\delta A_L}{\delta S_G} = -\frac{\delta A_{GS}}{\delta S_G} \tag{6.29}$$

Now the area of the gas that is due only to the spreading of the liquid is expressed:

$$A_{GS} = \pi \cdot a^2 - \frac{1}{2} \cdot a^2 (\beta - \sin(\beta)) = a^2 \left(\pi - \frac{\beta}{2} + \frac{\sin(\beta)}{2} \right) \tag{6.30}$$

The liquid area derivative can now be expressed as:

$$\frac{\delta A_L}{\delta S_G} = -2 \cdot a \cdot \left(\pi - \frac{\beta}{2} + \frac{\sin(\beta)}{2} \right) \cdot \frac{\delta a}{\delta S_G} - a^2 \cdot \left(-\frac{1}{2} + \frac{\cos(\beta)}{2} \right) \cdot \frac{\delta \beta}{\delta S_G} \tag{6.31}$$

From the law of sines:

$$\frac{\sin\left(\frac{180 - \beta}{2} \right)}{a} = \frac{\sin(\beta)}{S_i'} \tag{6.32}$$

From the half-angle formula and the addition formula we know that:

$$\sin\left(\frac{180 - \beta}{2} \right) = \left(\frac{1 + \cos(\beta)}{2} \right)^{1/2} \tag{6.33}$$

We also know that:

$$S_i = (2 \cdot \pi - \beta) \cdot a \tag{6.34}$$

Now Equation 6.32 can be rewritten substituting Equations 6.25, 6.33, and 6.34 to give:

$$S_i = \frac{d\cdot(2\cdot\pi - \beta)\cdot\sin\left(\frac{S_G}{d}\right)}{\sin(\beta)}\cdot\left(\frac{1+\cos(\beta)}{2}\right)^{1/2} \tag{6.35}$$

This enables the calculation of the derivative:

$$\frac{\delta S_i}{\delta S_G} = d\cdot\sin\left(\frac{S_G}{d}\right)\cdot\left[-\frac{(2\cdot\pi-\beta)}{2}\cdot\frac{1}{2}\cdot\left(\frac{1+\cos(\beta)}{2}\right)^{-1/2} - \left(\frac{(2\cdot\pi-\beta)}{\sin^2(\beta)}\cdot\cos(\beta) - \frac{1}{\sin(\beta)}\right)\cdot\left(\frac{1+\cos(\beta)}{2}\right)^{1/2}\right]\cdot\frac{\delta\beta}{\delta S_G} + \frac{(2\cdot\pi-\beta)}{\sin(\beta)}\cdot\left(\frac{1+\cos(\beta)}{2}\right)^{1/2}\cdot d\cdot\cos\left(\frac{S_G}{d}\right)\cdot\frac{1}{d} \tag{6.36}$$

This can then be simplified to:

$$\sin(\beta)\cdot\frac{\delta S_i}{\delta S_G} = -d\cdot\left[\frac{\pi}{2}\cdot\sin(\beta)\cdot\sin\left(\frac{S_G}{d}\right) + \frac{2\cdot\pi\cdot\sin\left(\frac{S_G}{d}\right)}{\sin(\beta)} + \sin\left(\frac{S_G}{d}\right)\right]\frac{\delta\beta}{\delta S_G} + 2\cdot\pi \tag{6.37}$$

Recall that in annular flow, $S_G = 0$ and $\beta = 0$. And, since the partial derivative of the gas-liquid interface is not infinite, Equation 6.37 reduces to:

$$0 = -\frac{2\cdot\pi\cdot d\cdot S_i}{2\cdot\pi\cdot d}\cdot\frac{\delta\beta}{\delta S_G} + 2\cdot\pi \tag{6.38}$$

Which allows the derivative to be solved.

$$\frac{\delta\beta}{\delta S_G} = \frac{2\cdot\pi}{S_i} \tag{6.39}$$

The liquid area derivative is now:

$$\frac{\delta A_L}{\delta S_G} = -2 \cdot \pi \cdot a \cdot \frac{\delta a}{\delta S_G} \tag{6.40}$$

Note from Figure 6.5 that:

$$S_D = a \cdot \beta \tag{6.41}$$

Using the product rule:

$$\frac{\delta S_D}{\delta S_i} = a \cdot \frac{\delta \beta}{\delta S_G} + \beta \cdot \frac{\delta a}{\delta S_G} \tag{6.42}$$

Near $S_G = 0$:

$$\frac{\delta S_D}{\delta S_G} \approx 1 \tag{6.43}$$

Now we can rearrange and solve:

$$\frac{\delta a}{\delta S_G} = \frac{1 - a \cdot \frac{\delta \beta}{\delta S_G}}{\beta} = \frac{1 - \frac{2 \cdot \pi \cdot a}{S_i}}{\beta} = \frac{0}{0} \tag{6.44}$$

Since the result is undefined, use L'Hôpital's Rule:

$$\frac{\delta a}{\delta S_G} = \frac{-2\cdot\pi\cdot\left[\frac{S_i - a\cdot\frac{\delta S_i}{\delta a}}{S_i^2}\right]}{\frac{\delta\beta}{\delta a}} \tag{6.45}$$

Taking the partial derivative of Equation 6.34 gives:

$$\frac{\delta S_i}{\delta a} = (2\cdot\pi - \beta) - a\cdot\frac{\delta\beta}{\delta a} \tag{6.46}$$

If this is substituted into Equation 6.45 and evaluated where $\beta = 0$, it can be simplified to:

$$\frac{\delta a}{\delta S_G} = -2\cdot\pi\cdot\left[\frac{\frac{1}{S_i} - \frac{2\cdot\pi\cdot a}{S_i^2}}{\frac{\delta\beta}{\delta a}} - \frac{a^2}{S_i^2}\right] \tag{6.47}$$

From geometry, we know that in annular flow:

$$S_i = 2\cdot\pi^{1/2}\cdot A_G^{1/2} \tag{6.48}$$

Since the remaining derivative is non-zero, substituting for S_i allows Equation 6.47 to be reduced to:

$$\frac{\delta a}{\delta S_G} = -\frac{1}{2\cdot\pi} \tag{6.49}$$

Now, the liquid area derivative can be determined.

$$\frac{\delta A_L}{\delta S_G} = a = \frac{S_i}{2 \cdot \pi} = \frac{A_G^{1/2}}{\pi^{1/2}} \tag{6.50}$$

As expected, the value of this derivative is quite small even using this method which over-predicts its value. Equation 6.12 can now be completely specified.

$$\tau_{WG} - \tau_{WL} \cdot \left[1 + \frac{2 \cdot d \cdot \pi^{1/2} \cdot A_G^{1/2}}{A_L} + n \right] + (\rho_L - \rho_G) g \cdot \sin(\theta) \cdot \frac{A_G^{1/2}}{\pi^{1/2}} = 0 \tag{6.51}$$

The liquid wall shear stress has been specified in Equation 6.13. The appropriate form for the gas wall shear stress is expressed in Equation 5.6 from the previous section. The *in-situ* liquid velocity is specified in Equation 6.15. The appropriate calculation of the *in-situ* gas velocity is written similarly, as seen in Equation 5.15. The liquid hydraulic diameter is seen in Equation 6.17. For the gas phase, the hydraulic diameter is determined by Equation 5.14.

In annular flow, both phases are turbulent. Thus, C_G and C_L are 0.046 while n and m are 0.2. Now we have one equation with three unknowns: superficial gas velocity, superficial liquid velocity, liquid area in the film region.

When slugs become highly aerated, they reach a point where they can hold no more gas. One more gas bubble and blow-through occurs. Thus, another mechanism specified is the maximum slug body void fraction. This maximum value is determined by interpolation of the chart from Jepson and Taylor (1993). Although this maximum is likely to also be fluid dependent, the diameter dependency is clearly established. For an air-water system in 2.58, 5.12, and 30.0-cm diameter pipes, Jepson and Taylor (1993) demonstrated that the maximum slug body void fraction reaches 0.45, 0.55, and 0.62, respectively.

Once this maximum slug body void fraction has been specified, a second equation can be specified. Although most models work reasonably well, the method recommended here is the lead-lag model of Maley (1997b). Recall that the void fraction is not constant through the slug. Figure 2.5 contains a conductance trace of a slug. Notice that the void fraction is highest at the front of the mixing zone and decreases until the end of the mixing zone is reached. Throughout the remainder of the slug body, the void fraction remains constant. The lead-lag model (Equation 5.34) evaluates the void fraction at a given distance into the mixing zone. Thus, the average slug void in the mixing zone can be determined by integrating this equation across the mixing zone (Equation 5.35).

After the mixing zone, the lead-lag model no longer applies. Near annular flow, however, the mixing zone encompasses the entire slug body. In fact, in pseudo-slug flow, the mixing zone length has just reached the length of the slug. Thus Equation 5.35 is sufficient for determining the average slug body void fraction. Three parameters must be determined to apply Equation 5.35: lead distance, lag distance, mixing zone length. Maley (1997b) has correlated each of these values to the film Froude number for several fluids. These are reported in Section 2.3.

This model has not yet been evaluated for effects of diameter, pressure, or inclination. Each of the parameters must be corrected for diameter as described earlier. For a given liquid, the void fraction is then solely dependent upon the film Froude number. This agrees with the result of Kouba and Jepson (1990). So, another criterion is included in that the maximum slug body void fraction occurs at a maximum film Froude number. At this point, specifying either a maximum film Froude number or a maximum slug void fraction has an equal result. Thus a second criterion, which was observed experimentally here, is met. Note that the film Froude number is determined by:

$$Fr_f = \frac{V_t - u_L}{\left(g \cdot h_{eff}\right)^{1/2}} \tag{6.52}$$

Near annular flow, the translational velocity has been experimentally observed to be approximately 1.2 times the superficial mixture velocity. This is similar to the value that has been observed in the literature (Section 2.3). Thus, we specify that:

$$V_t = 1.2 \cdot \left(V_{SG} + V_{SL}\right) \tag{6.53}$$

From experiments, it was found that pseudo-slug flow should occur at a Froude number of about 16 to 19. At this point, the average translational velocity began to decrease. With the decrease in translational velocity came a decrease in the film Froude number. The Froude number then increased again to a value of about 16, then annular flow ensued. When annular flow was reached, the average measured translational velocity ratio had become about 0.5. As discussed in Section 4.1, if the velocity ratio had remained at 1.2, the anticipated Froude number at the transition to annular flow is expected to be about 35. For this model, the ratio of translational velocity to the superficial mixture velocity is taken to be 1.2.

The effective film height is defined as the ratio of liquid area to gas-liquid interface. This is not well-defined for annular flow when the film completely spreads around the pipe.

In keeping with the intent of an effective film height, it was determined that the appropriate method is to keep the gas-liquid interfacial length as the denominator:

$$h_{eff} = \frac{A_L}{S_i} = \frac{A_L}{2 \cdot \pi^{1/2} \cdot A_G^{1/2}} \tag{6.54}$$

Now, Equation 5.35 can be determined from three unknowns: superficial gas velocity, superficial liquid velocity, liquid area in the film region. This, along with Equation 6.51, allows the transition to be determined. Figure 6.6 is a solution procedure flow chart.

Starting with the fluid properties, pipe diameter, and inclination, the transition from slug to annular flow is determined. The maximum void fraction is determined by linear interpolation of the data table of Jepson and Taylor (1993). Using the Maley (1997b) relation as expressed in Equation 5.35, the Froude number for this maximum void fraction and fluid properties is determined. The solution occurs at multiple liquid areas in the film region. The area is increased from a low value until it reaches the liquid holdup minimum (one minus the maximum slug void fraction). An initial guess is made for the superficial gas velocity. From Equation 6.53, the superficial liquid velocity is determined. Then the minimization of pressure drop is calculated (Equation 6.51). If the equation is not satisfied, the superficial gas velocity is adjusted. Once the pressure drop minimization is satisfied, the next liquid area is examined.

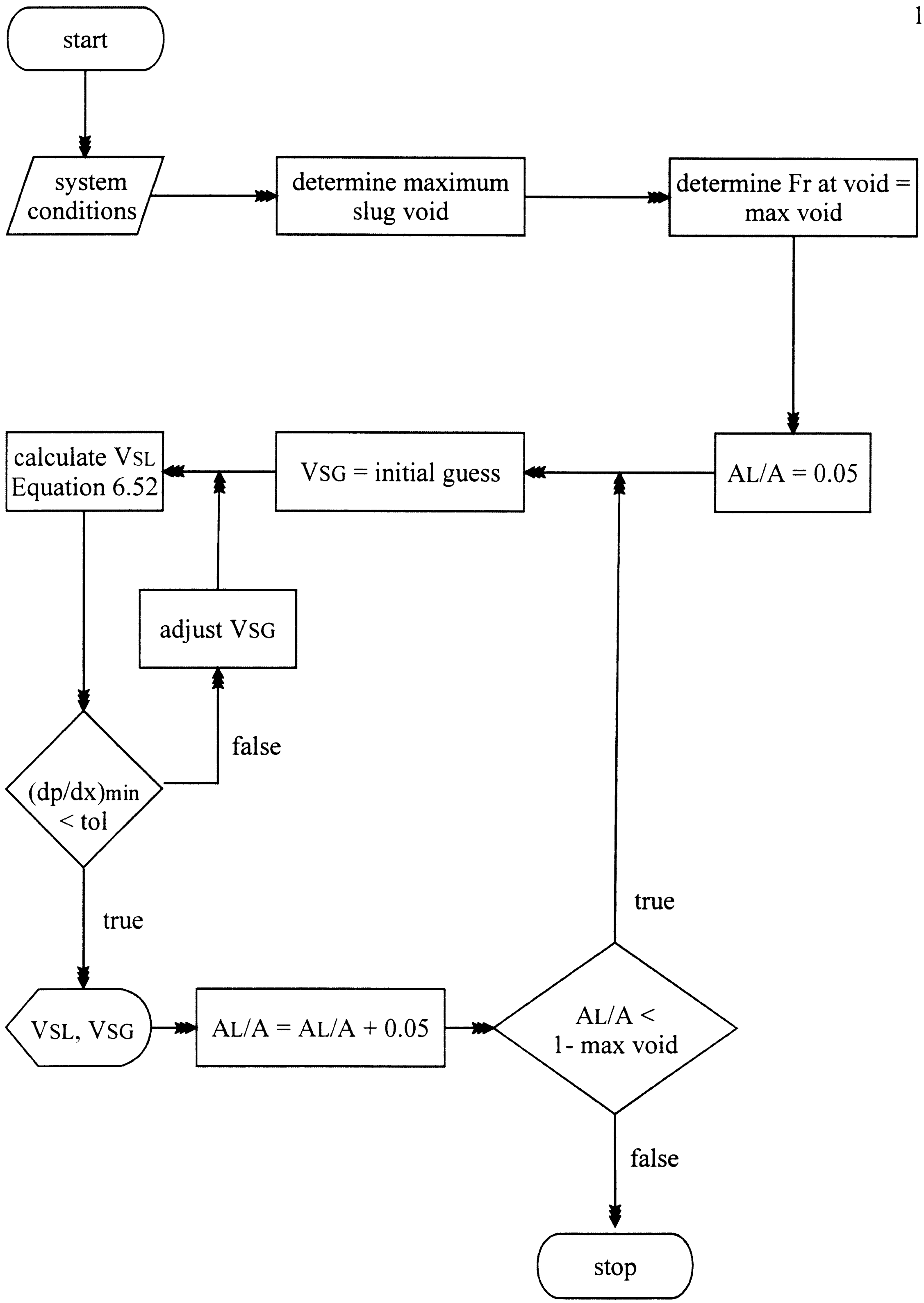

Figure 6.6: Slug-annular solution procedure flow chart.

CHAPTER 7

MODEL RESULTS AND DISCUSSION

Criteria and equations for both the stratified-slug transition model and the slug-annular transition model were used to create computer programs which can predict the transitions based on input fluid properties and geometry. The programs, titled "STRAT_SL.EXE" and "SL_AN.EXE", were written and compiled using Microsoft Fortran Powerstation v1.0. The source code for each program is included in Appendices C and D, respectively. The solution procedure used in each program follows that outlined at the end of Chapters 5 and 6.

7.1 Preliminaries

The first step in the slug-annular transition model solution is to determine the maximum void fraction for the slug. For the diameter of these experiments (9.72-cm), linear interpolation of the maximum slug void data of Jepson and Taylor (1993) indicates a maximum slug void of just over 56%. Applying the integrated Maley (1997b) void fraction (Equation 5.35) to the slug length indicates that for a carbon dioxide gas-water system, this corresponds to a film Froude number of 35. This matches the maximum Froude number for the transition to annular flow indicated in Section 4.2 if the pseudo-slugs were to remain slugs (35 - 40). For carbon dioxide with light oil, this void fraction corresponds to a film Froude number of approximately 28. It was noted experimentally that the upper value for the film Froude number was slightly lower with a decrease in water cut. For water cuts of 40, 80, and 100%, the maximum Froude number is then 31, 34, and 35, respectively.

For the transition from stratified to slug flow, the model produced a reasonable transition when compared with the experimental data. At higher gas pressures, the friction factor correction of Andritsos and Hanratty (1987) begins to dominate the momentum equation. This forced the transition at high pressures to occur at a higher superficial liquid velocity than was anticipated. As the pressure becomes substantial, the increased gas density forces the transitional superficial gas velocity, as determined by Equation 5.10, to become exceptionally low. The onset of waves are then predicted at a superficial gas velocity as low as 1 to 2 m/s. Additionally, the interfacial friction factor correlation (Equation 5.9) then allows the friction factor to become much exceptionally high at higher superficial gas velocities.

Calculations indicated that the friction factor at 0.79 MPa had become fifty times the value of the wall friction factor. Upon reviewing the development of the interfacial friction factor correlation, it became obvious that the correlation was designed so as to tend towards a limit of fifteen times the wall friction factor. A review of the data presented indicated that 15 was the highest ratio observed experimentally for the range of viscosities and diameters tested. This also matches the interfacial friction factor suggested for small amplitude waves of 0.0142 by Miya *et al.* (1971). The prediction of the wall friction factor used here (Equation 5.6) indicates a value of 0.002 and 0.003. From this, the interfacial friction factor was given the limit of 15 times the wall friction factor.

The models were plotted, along with the experimental data and the Taitel and Dukler (1976) model. The results follow.

7.2 Results

Figure 7.1 is a flow regime map for 100% water cut, horizontal flow at 0.45 MPa. Both the Taitel and Dukler (1976) model and the stratified-slug model give a reasonable prediction of the transition of stratified to slug flow at lower gas flow rates. The modeled transitions occur at slightly lower liquid flow rates than were found experimentally. At these flow rates, slug occurrence is on the order of one slug per hour and would not be observed with the procedure outlined here for flow regime identification. Clearly at low gas flow rates, near plug flow, the mechanism of wave growth (Taitel and Dukler) applies. As the gas flow rate is increased, however, the wave growth model falls apart. This begins to occur at a superficial gas velocity of about 3 m/s. Coincidentally, this is when the hydraulic jump mechanism becomes dominant. The stratified-slug transition model increases to a superficial liquid velocity of about 0.4 m/s.

The film actually begins to spread around the wall of the pipe at higher gas flow rates. To test the effect of this, the momentum equation was solved for the case of spreading using the equations developed for the annular flow model. At a superficial gas velocity of about 10 m/s, the transition occurred at a superficial liquid velocity of about 0.35 m/s. Since the degree of spreading, and when it will ensue, are difficult to predict, the model was developed only for the case of no spreading.

The Taitel and Dukler annular transition does not match the data. Slug flow and pseudo-slug flow occur on both sides of the modeled transition. At lower gas flow rates, the model begins to approach the plug flow regime as well. Modifications of this model, which to this point have been changing the minimum height requirement, simply create solutions

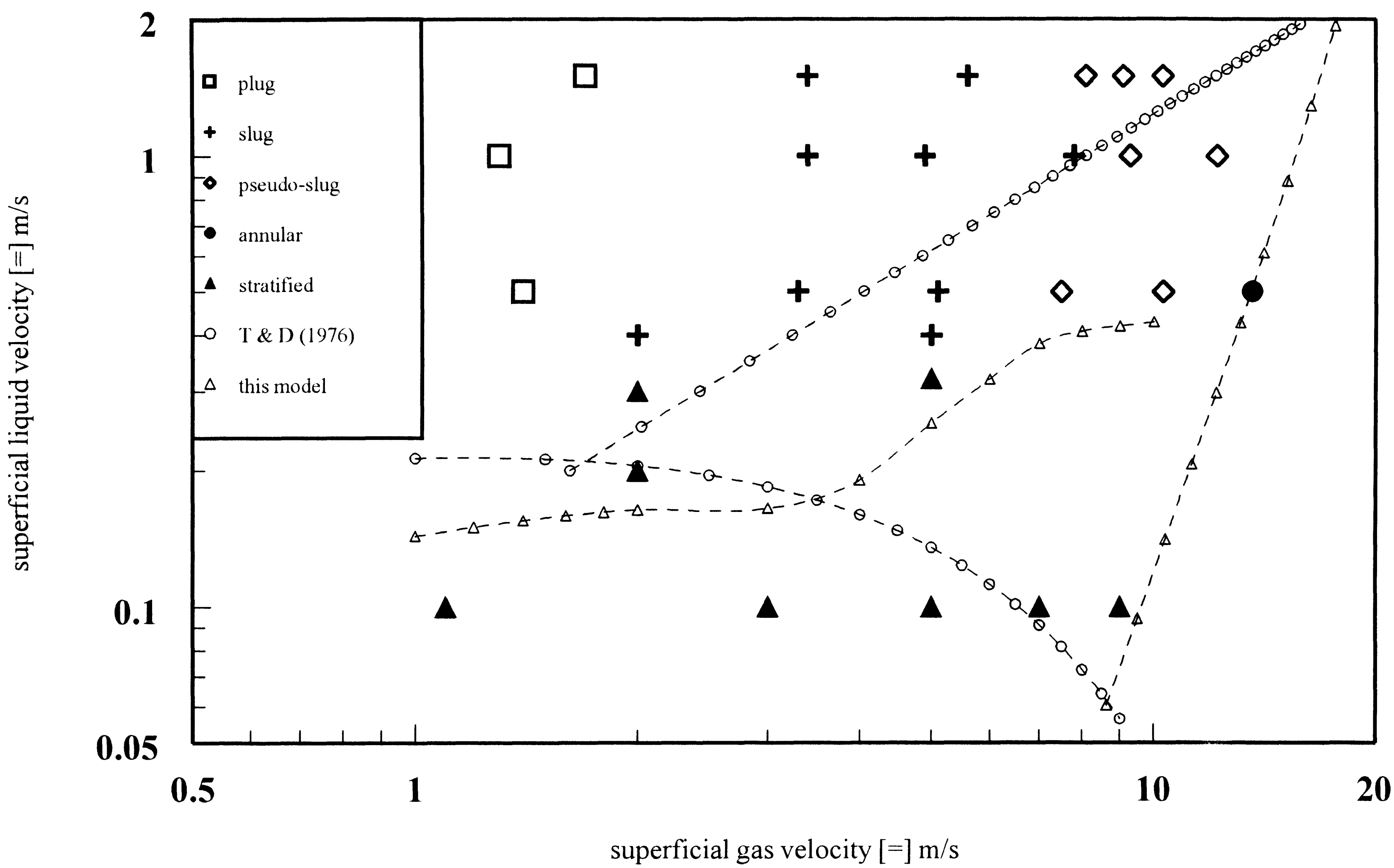

Figure 7.1: Flow regime map for 100% water cut, horizontal, 0.45 MPa.

which are parallel to this one. The slug-annular transition model gives a much better prediction of the location of this change in flow patterns. No slug flow or pseudo-slug flow was found to occur at gas flow rates above this model. The transition also pierces a data point that happened to be at the transition.

Both the stratified-slug and the slug-annular models can be validated by parametric variation. From this point, the models will be presented separately for clarity.

First consider the effects of changing inclination. Recall from Section 4.5 that increasing the inclination to +2 and +5° eliminated stratified flow for the conditions tested. The same was true in both the Taitel and Dukler model and the stratified-slug model. Neither model found stratified flow above an inclination of 0.25°.

Figure 7.2 illustrates the stratified to slug flow transition for 100% saltwater at 0.45 MPa flowing at an inclination of -2°. At low gas flow rates, both models predict the transition reasonably well. Above a superficial gas velocity of 5 m/s, the Taitel and Dukler model drops to predicting slug flow at a superficial liquid velocity as low as 0.1 m/s at a superficial gas velocity of around 9 m/s. Slug flow would clearly not occur at a lower liquid flow rate in down flow than it did in horizontal flow. The stratified-slug model stops decreasing at a superficial gas velocity of 5 m/s then rises slightly before stopping at a superficial liquid velocity of 0.45 m/s.

Figure 7.3 compares the transition from slug to annular flow for 40% water cut at 0.45 MPa and inclinations of +5 and -5°. Recall from Section 4.5 that the experimental data indicated little difference in the annular transition at different inclinations. At +5°, the Taitel and Dukler model gives a reasonable prediction of the transition to annular flow. The

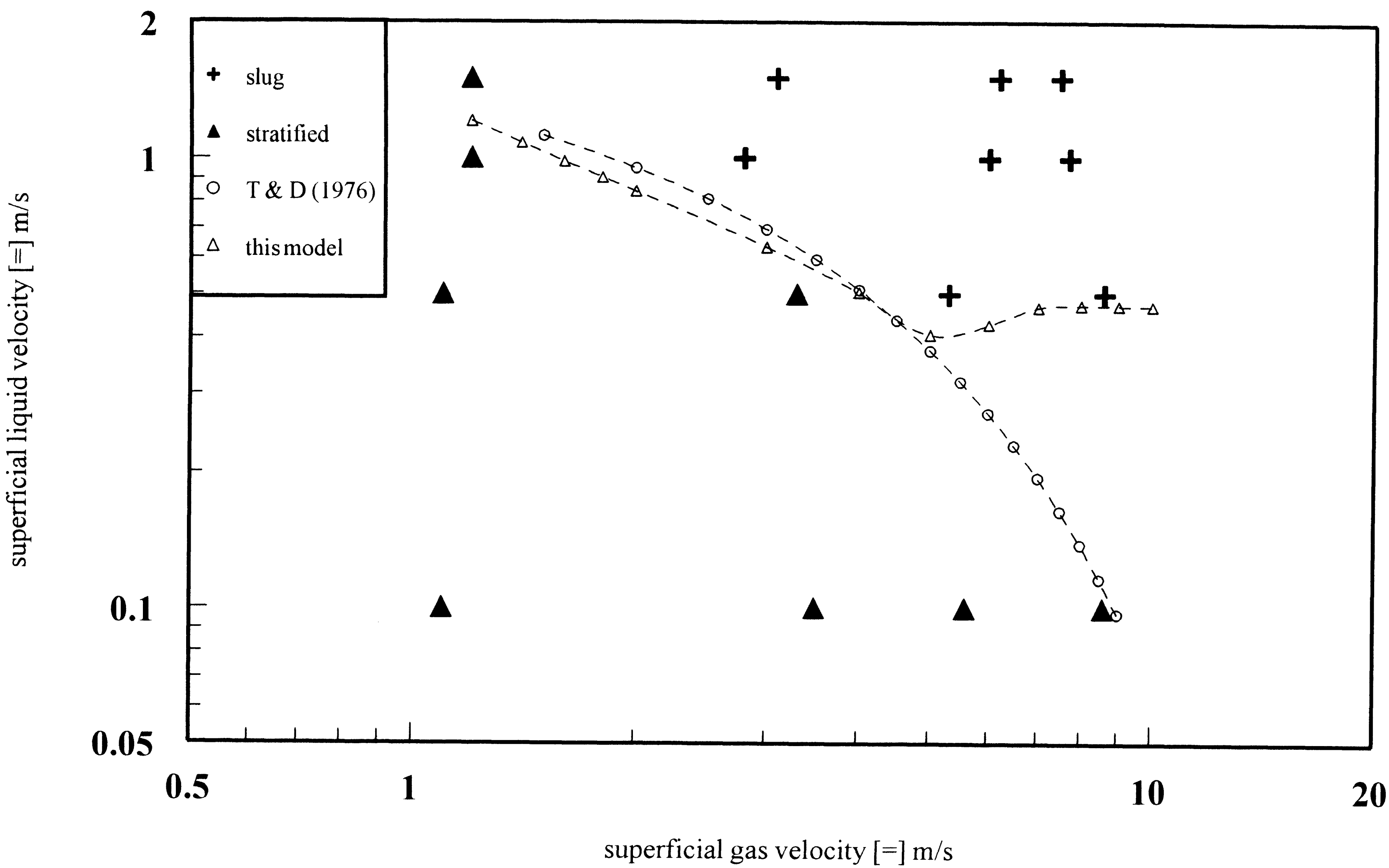

Figure 7.2: Stratified transition for 100% water cut, 0.45 MPa, -2°.

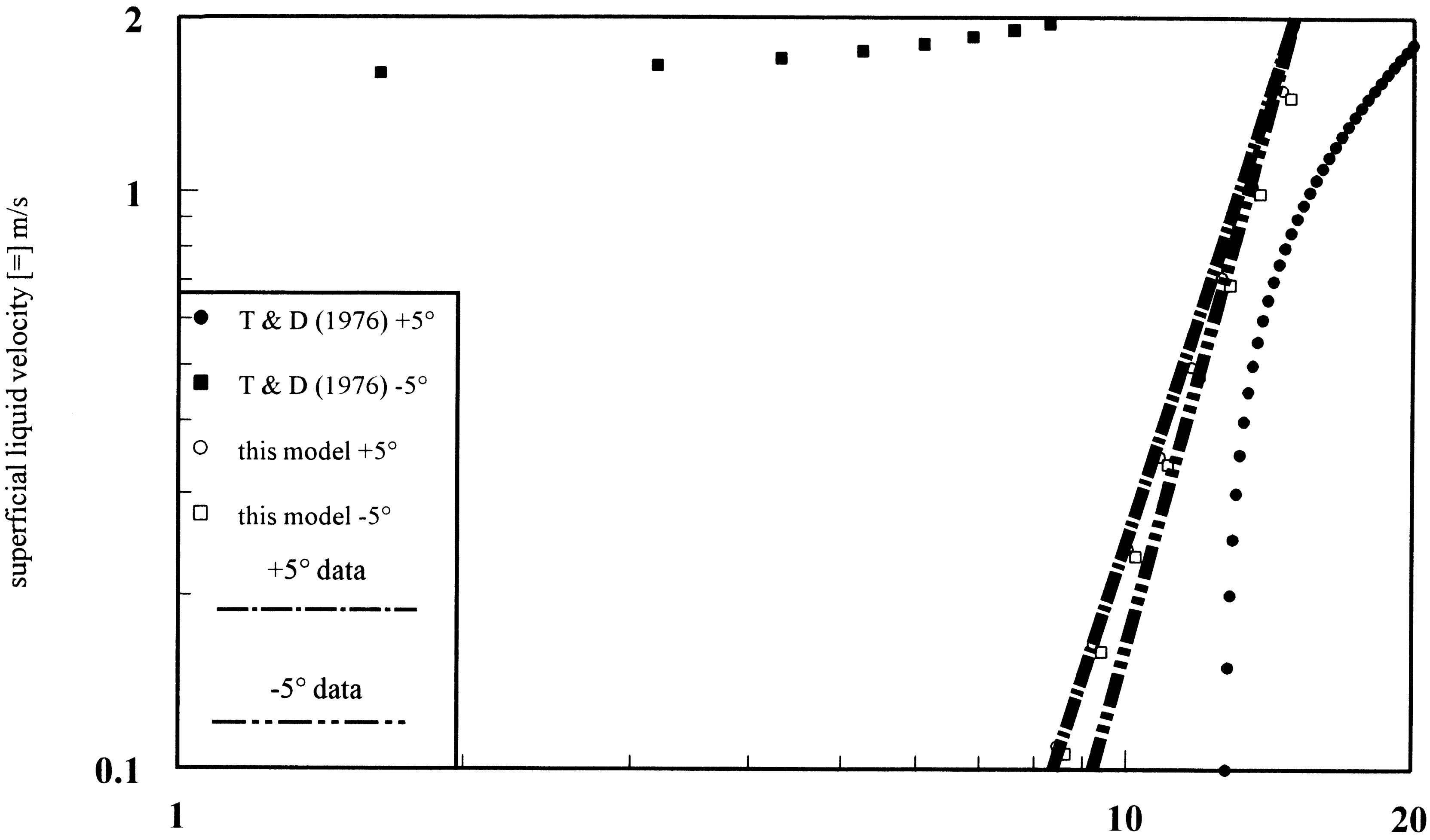

Figure 7.3: Annular transition for 40% water cut, 0.45 MPa.

transition consistently occurs at a higher superficial gas velocity than was found experimentally. At -5°, the Taitel and Dukler model shows no relation to what was found experimentally. The transition appears to occur at almost a constant superficial liquid velocity of 1.5 to 2 m/s. The slug-annular model predicted the transition exceptionally well, mostly overlapping the data. The model also indicated little effect of inclination.

Now, consider the effect of pressure on the transitions. Figure 7.4 indicates the transition from stratified to slug flow for an 80% water cut flowing at -5° inclination at pressures of 0.45 and 0.79 MPa. Recall from Section 4.5 that an increase in pressure caused a slight increase in the superficial liquid velocity required to reach slug flow. This trend is demonstrated in the experimental data presented. The Taitel and Dukler model again reasonably predicts the transition at the lower gas flow rates, but predicts the transition to occur at extremely low superficial liquid velocities at the higher gas flow rates. Further, the Taitel and Dukler model incorrectly predicts the effect of pressure. Their model indicates that increasing the pressure causes the superficial liquid velocity required for transition to be lowered. This cannot be true. Recall the momentum balance as presented in Section 2.1. At a higher pressure, the gas wall friction factor is increased. For the equation to remain true, the wall shear stress of the liquid phase must be raised. This is then done by increasing the liquid velocity.

The stratified-slug model also reasonably predicts the location of the transition. At low gas flow rates, no effect of pressure is observed. This is due to the fact that the Gregory relation used cannot account for the pressure. At the higher superficial gas velocities, the effect of pressure is observed.

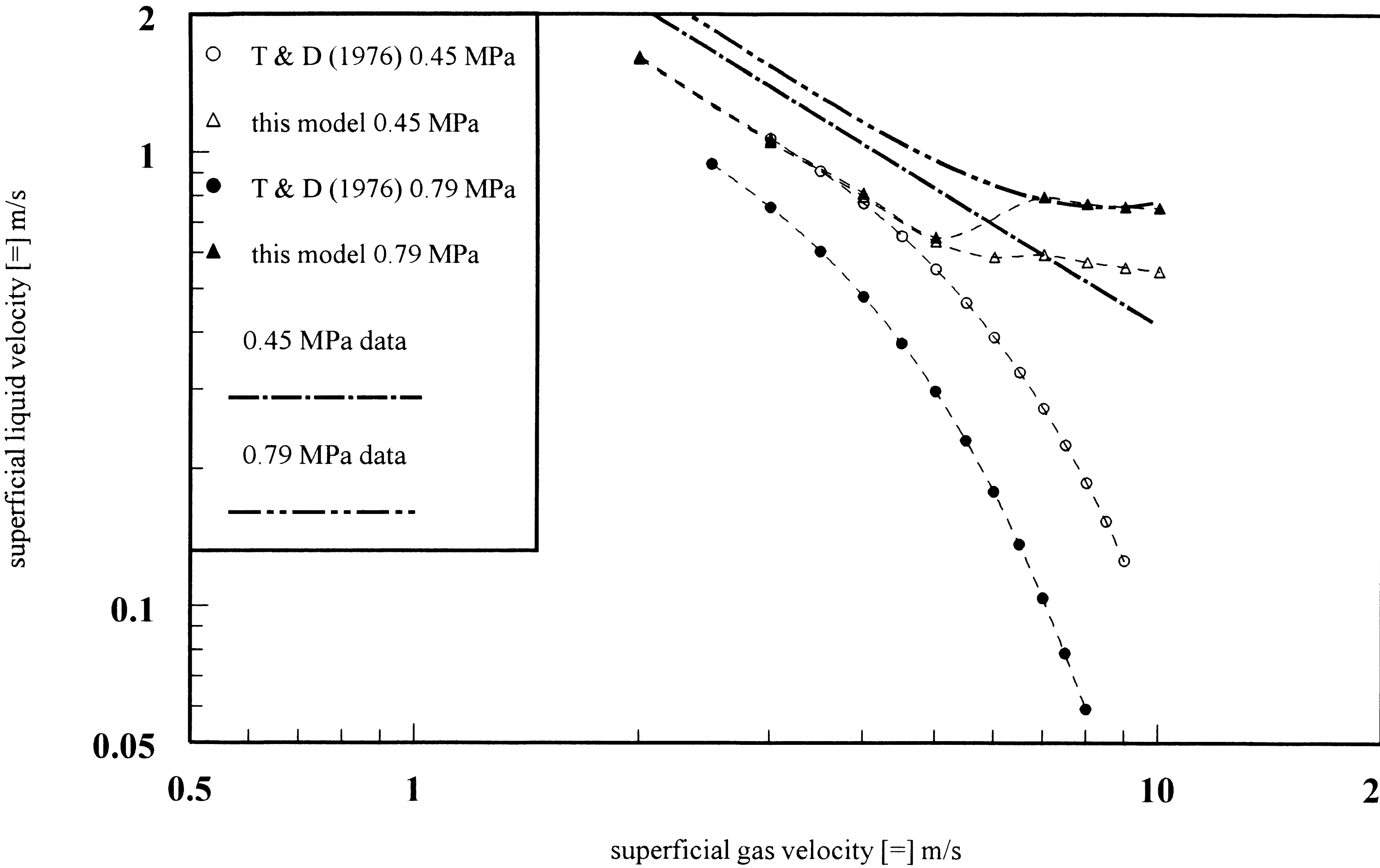

Figure 7.4: Stratified transition for 80% water cut, -5°.

Figure 7.5 illustrates the effect of pressure on the transition from slug to annular flow for 100% saltwater horizontal flow. As discussed in Section 4.5, an increase in pressure causes the transition to occur at a lower superficial gas velocity. The transitions, as isolated by Maley (1997a), have been included. The Taitel and Dukler model represents the change in superficial gas velocity required for an increase in pressure. However, the location of the transition does not match the data. The slug-annular model represents the location, and the effect of pressure, exceptionally well.

As reported in Section 4.5, water cut was found to have only a slight effect on the transitions. This was also seen in the models. To demonstrate the validity of the models at any water cut, the water cut was varied in Figures 7.1 - 7.5.

Since the diameter of the system was fixed, comparison for diameter effect must use transitions found in the literature. Figure 7.6 illustrates how the diameter affects the stratified to slug flow transition in horizontal, large diameter pipes. The transitions included are those of Lee (1993) for a 10-cm pipe with water and carbon dioxide, Lin (1985) for a 9.53-cm pipe with water and air, and Jepson and Taylor (1993) for a 30-cm pipe with water and air. All transitions begin at a relatively constant superficial liquid velocity with an occasional dip in liquid flow rate with increasing gas flow rate. At a superficial gas velocity of about 5 to 6 m/s, there is an abrupt rise in the required superficial liquid velocity.

At a diameter of about 10-cm, Lee and Lin have consistently different liquid flow rate requirements. This is highlighted to demonstrate how slight variances in fluid properties and geometry can have a dramatic effect on the transition. What has appeared to this point to be a large difference between model and experiment is not. It could be caused by an inclination

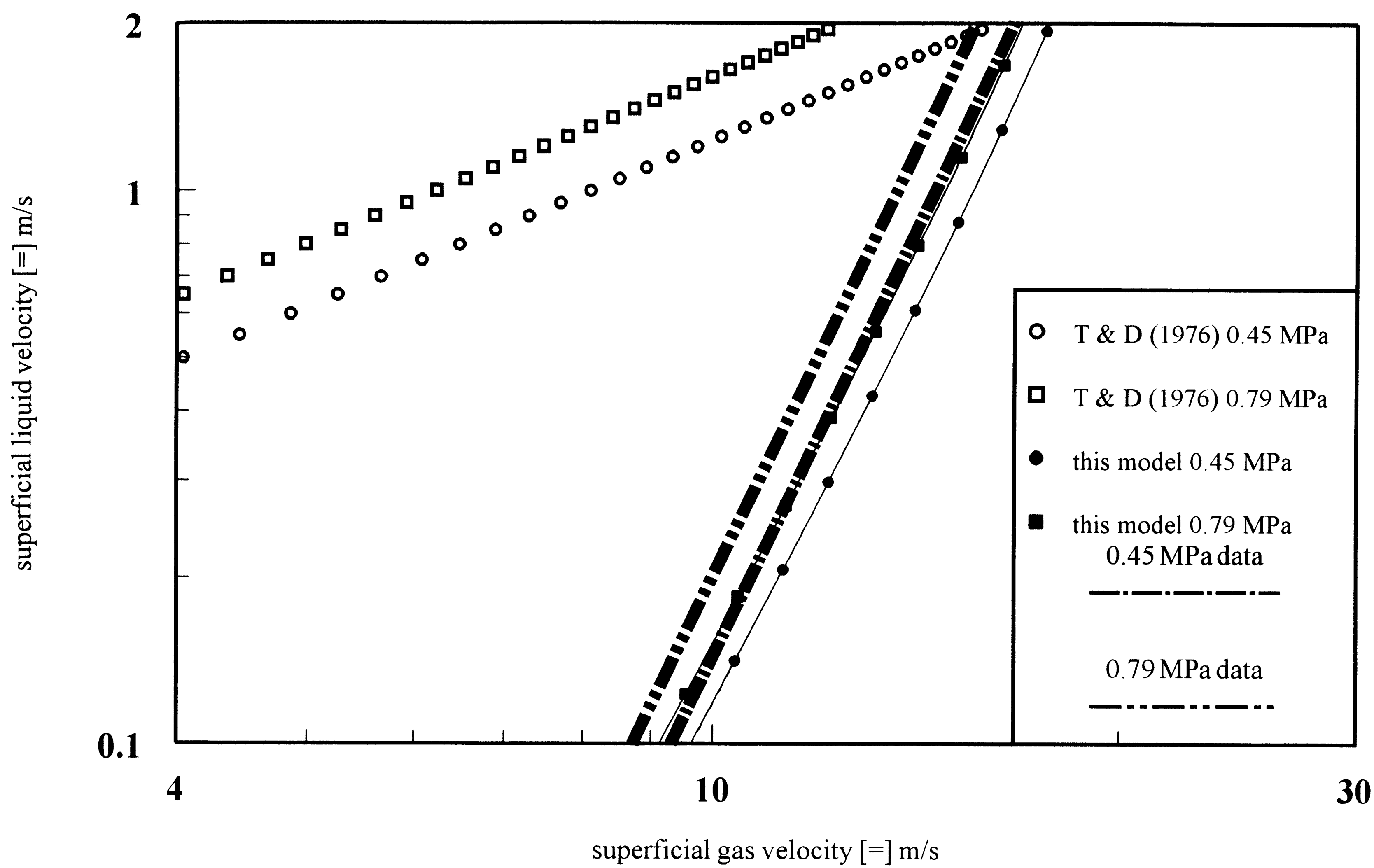

Figure 7.5: Annular transition for 100% water cut, horizontal.

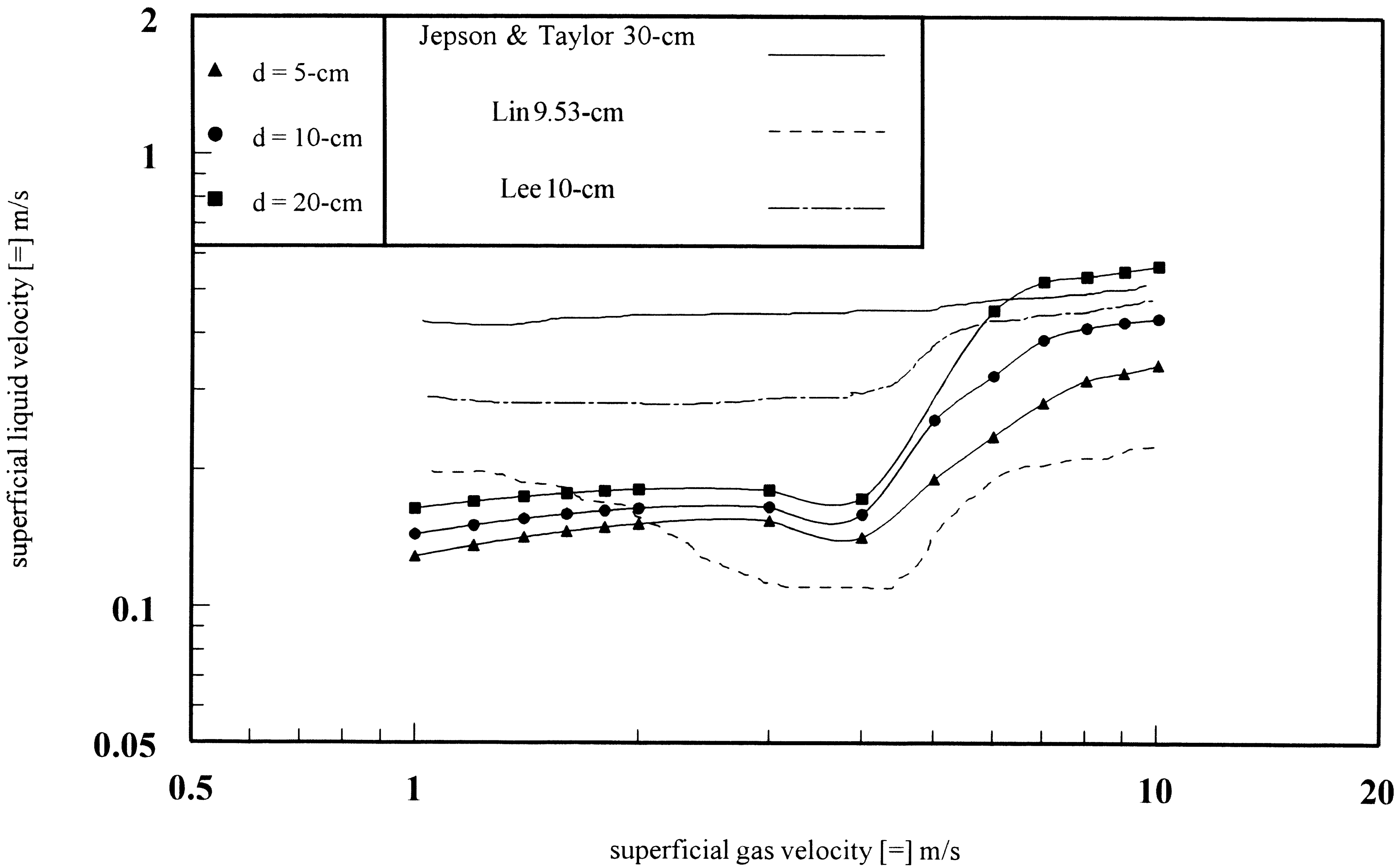

Figure 7.6: Stratified transition for 100% water cut, horizontal, 0.45 MPa.

error of a few-tenths of a degree). From this, it can be seen that increasing the diameter increases the superficial liquid velocity required for transition to slug flow.

The model has been solved for 0.45 MPa at diameters of 5, 10, and 20-cm. The model indicates an increase in superficial liquid velocity required for each increase in diameter. The modeled transition was of the same shape of the transitions reported in the literature. At lower gas velocities, the effect of diameter is not well-modeled. This is thought to be due to the lack of a diameter correction for the Gregory *et al.* (1978) void fraction correlation. At the higher gas flow rates, the effect of diameter is appropriate.

Figure 7.7 illustrates the effect of diameter on the transition from slug to annular flow. Comparing the transition to annular flow from different researchers becomes even more inexact. As mentioned in the Chapter 6, there are differing opinions about where annular flow occurs. This becomes especially pronounced when the apparatus allows inexact visual criteria. From this, it should be observed that in comparing trends, it is best to use a consistent source (same author) for annular flow. The transitions are reported from Lin (1985), at diameters of 2.54-cm and 9.53-cm, and from Lee (1993) at a diameter of 10-cm. Recall that the smaller diameter tubes mostly affect the slug transition mechanisms. Also, it is not expected that diameter change would have an opposite effect at smaller diameters than in larger diameter pipes. Finally, the model won't be used to predict Lin's data, rather it will be used to see what happens when the diameter is adjusted. Lin's requirements for annular flow were higher than most other data surveyed. If any waves were present, it was not considered annular flow. This flow was primarily annular mist. For the same reason, Lin's data will be used to compare the effects of diameter.

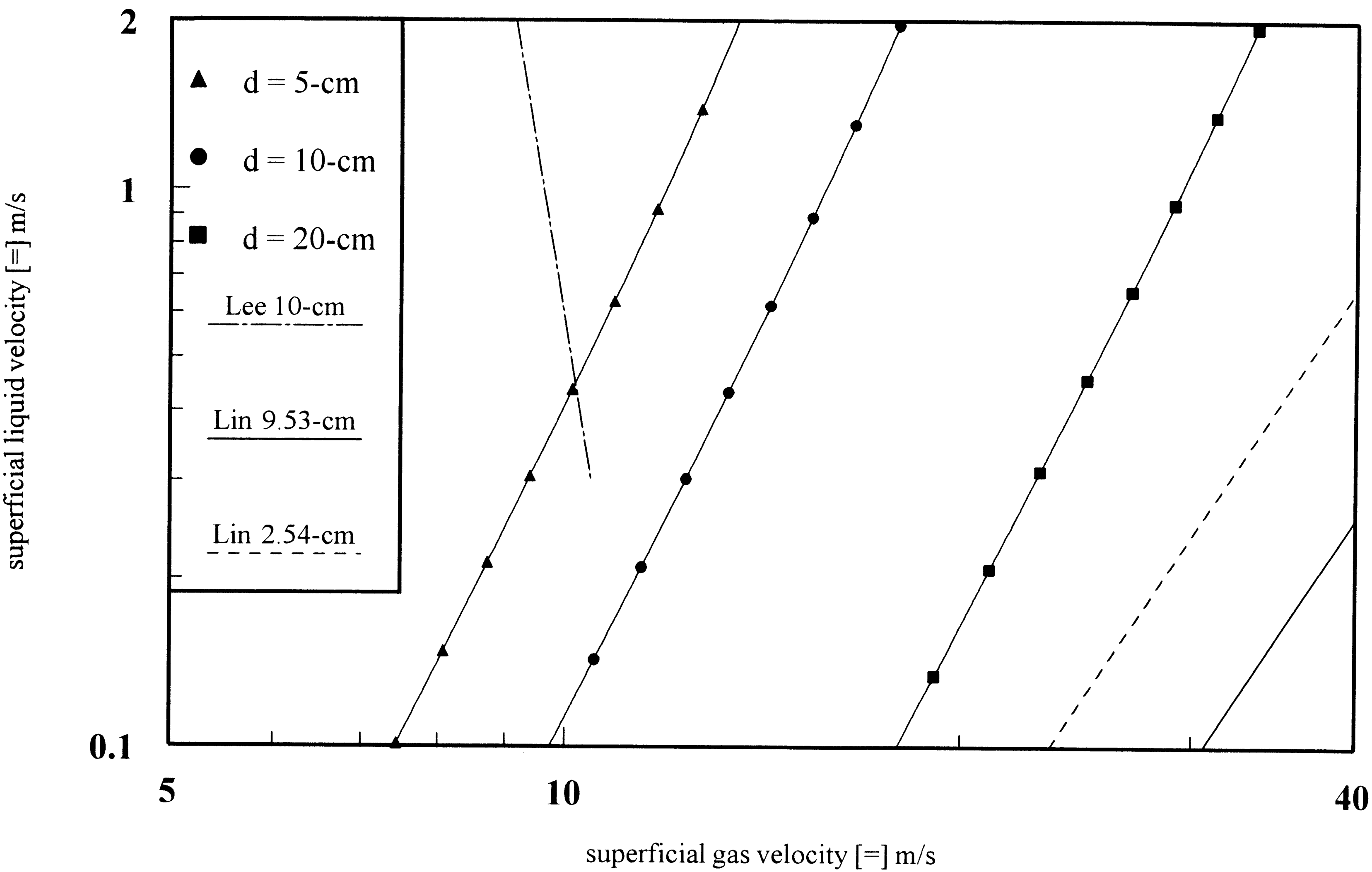

Figure 7.7: Annular transition for 100% water cut, horizontal, 0.45 MPa.

Lin shows that increasing the diameter has caused the annular transition to occur at a higher superficial gas velocity. The slug-annular model was evaluated for 100% saltwater horizontal flow at a pressure of 0.45 MPa, at diameters of 5, 10, and 20-cm. The transition was found to occur at higher superficial gas velocities with increasing pipe diameter. This matches what was observed by Lin. It should further be noted that field data indicates that in exceptionally large diameter pipes (greater than 60-cm) annular flow has never been observed to occur (Green, 1997).

CHAPTER 8

CONCLUSIONS

Based on the experimental results the following conclusions are made. The ratio of translational velocity to the superficial mixture velocity was not largely affected by inclination, pressure, water cut, liquid flow rate, or gas flow rate for the same flow pattern at the conditions tested. For plug flow, the ratio of translational velocity to superficial mixture velocity was around 2.0. As the gas flow rate was increased, the velocity ratio decreased to a value of about 1.2. This value was reached by a superficial gas velocity of 2.5 m/s. The average velocity ratio in pseudo-slug flow was 0.5 to 1.2.

Inclination and water cut were found to have little effect on the estimated film Froude number for the range of conditions tested. The Froude number was found to increase slightly with increasing pressure. The Froude number increased with increasing gas flow rate. The Froude number was found to reach a maximum of 16 to 19 when pseudo-slug flow was reached. The Froude number then dropped due to the decreased translational velocity. The Froude number then continued to increase with increasing gas flow rate to a value of about 16 before annular flow would ensue.

Pressure and water cut had little effect on the slug frequency for the range of conditions studied. Upflow caused an increase in slug frequency while downflow caused a slight decrease in slug frequency. Increasing the liquid flow rate increased the slug frequency. The frequency decreased with increasing gas flow rate in going from plug flow to slug flow. At low liquid flow rates the frequency continued to decrease with increasing gas flow rate while at high liquid flow rates the frequency increased with increasing gas flow rate.

Water cut and pressure had little effect on the slug unit length for the range of conditions studied. The slug unit length decreased with increasing liquid flow rate. The length increased with increasing gas flow rate, reaching a maximum at higher liquid flow rates. In upflow the unit length was smaller while in downflow the unit length was slightly larger.

Stratified flow was eliminated in upflow while slug flow was found to dominate. In downflow stratified flow was dominant while slug flow was reduced. In downflow, water cut was found to have little measurable effect on the transition from stratified to slug flow. Water cut was found to have little effect on the transition from slug to annular flow. Increasing pressure caused the stratified to slug transition to occur at slightly higher liquid flow rates. The transition from slug to annular flow was found to not be largely dependent on the inclination. Increasing pressure caused the annular transition to occur at lower gas flow rates.

Based on the modeled transitions, the following conclusions are made. The maximum slug void fraction of Jepson and Taylor (1993) correlated reasonably well with the maximum estimated film Froude number observed experimentally using the Maley (1997b) relation. Overall, the stratified-slug modeled transition was reasonably close to what was observed experimentally. In upflow, no stratified flow was found to occur. In downflow the liquid flow rate required for transition to slug flow was higher than in horizontal flow. The liquid flow rate required decreased with increasing gas flow rate. Also in downflow, the water cut was found to only have a slight effect on the transition. An increase in pressure caused a slight increase in the liquid flow rate required to reach transition. An increase in pipe diameter was found to require an increase in superficial liquid velocity to reach transition.

The slug-annular transition model matched exceptionally well with the data and the transitions established by Maley (1997a). The transition showed little change with inclination and only a slight change with water cut. The lower the water cut, the lower the gas velocity required for transition. This was similar to the effect of increasing pressure. An increase in pressure increases the gas density. The closer the gas and liquid density, the lower the gas flow rate requirement. This effect was slight in changing water cut because of only having a slight percentage difference in the ratio. The gas density had to nearly double to obtain a measurable effect.

CHAPTER 9

REFERENCES

Agrawal, S.S., G.A. Gregory, and G.W. Govier, "An Ananlysis of Horizontal Stratified Two-Phase Flow in Pipes," *Can. J. Chem. Engng.*, **51**, 280-286, 1973.

Andreussi, P., K.H. Bendiksen, and O.J. Nydal, "Void Distribution in Slug Flow," *Int. J. Multiphase Flow*, **19**, 817-828, 1993.

Andritsos, N., "Effect of Pipe Diameter and Liquid Viscosity on Horizontal Stratified Flow," Ph.D. Thesis, University of Illinois, Urbana-Champaign, 1986.

Andritsos, N. and T.J. Hanratty, "Influence of Interfacial Waves in Stratified Gas-Liquid Flows," *AIChE J.*, **33**, 444-454, 1987.

Baker, O., "Simultaneous Flow of Oil and Gas," *Oil and Gas J.*, **53**, 185-195, 1954.

Barnea, D., O. Shoham, and Y. Taitel, "Gas Liquid Flow in Inclined Tubes; Flow Patterns and Transitions in Upward Flow," *Chem. Eng. Sci.*, **40**, 131-136, 1985.

Barnea, D. and N. Brauner, "Holdup of the Liquid Slug in Two Phase Intermittent Flow," *Int. J. Multiphase Flow*, **11**, 43-, 1985.

Barnea, D., O. Shoham, Y. Taitel, and A.E. Dukler, "Flow Pattern Transitions for Gas-Liquid Flow in Horizontal and Inclined Pipes: Comparison of Experimental Data with Theory," *Int. J. Multiphase Flow*, **6**, 217-225, 1980.

Benjamin, B.T., "Shearing Flow over a Wavy Boundary," *J. Fluid Mech.*, **6**, 161-205, 1959.

Butterworth, D. "A Visual Study of Mechanism in Horizontal Air-Water Flow," AERE-M2556, UKAEA, Harwell, 1972.

Brauner, N. and D.M. Maron, "Flow Pattern Transitions in Two-Phase Liquid-Liquid Flow in Horizontal Tubes," *Int. J. Multiphase Flow*, **18**, 123-140, 1992.

Chow, V.T., *Open Channel Hydraulics*, McGraw-Hill, New York, 1959.

DeWaard, C., U. Lotz, and D.E. Milliams, "Prediction of CO_2 Corrosion of Carbon Steel," Corrosion/93, NACE, paper no. 69, 1-17, 1993

Dukler, A.E., and M.G. Hubbard, "A Model for Gas-Liquid Slug Flow in Horizontal and Near Horizontal Tubes," *Ind. Eng. Chem. Fund.*, **14**, 337-347, 1975.

Fan, Z., Z. Ruder and T.J. Hanratty, "Pressure Profiles for Slugs in Horizontal Pipelines," *Int. J. Multiphase Flow*, **19**, 421-437, 1993.

Gazley, C., "Interfacial Shear and Stability in Two-Phase Flow," Ph.D. Thesis, University of Deleware, Newark, 1949.

Gopal, M., "Visualization and Mathematical Modelling of Horizontal Multiphase Flow," Ph.D. Thesis, Ohio University, Athens, Ohio, 1994.

Govier, G.W. and K. Aziz, *The Flow of Complex Mixtures in Pipes*, Van Nostrand Reinhold, New York, 1972.

Gould, T.L., M. Tek, and D.L. Katz, "Two Phase Flow Through Vertical, Inclined, or Curved Pipes," *J. Petrol. Tech.*, **26**, 915-926, 1974

Green, A., BP Exploration, personal electronic communication, April, 1997.

Gregory, G.A. and D.S. Scott, "Correlation of Liquid Slug Velocity in Horizontal Cocurrent Gas-Liquid Slug Flow," *AIChE J.*, **15**, 933-935, 1969.

Gregory, G.A., M.K. Nicholson, and K. Aziz, "Correlation of the Liquid Volume Fraction in the Slug for Horizontal Gas-Liquid Flow," *Int. J. Multiphase Flow*, **4**, 33-39, 1978.

Hill, T.J. and D.G. Wood, "A New Approach to the Prediction of Slug Frequency," SPE Annual Technical Conf., 141-149, 1990.

Hubbard, A.E., "An Analysis of Horizontal Gas-Liquid Slug Flow," Ph.D. Thesis, University of Houston, 1965.

Jeffreys, H., "On the Formation of Water Waves by Wind," *Proc. R. Soc. London*, **A107**, 189-206, 1925.

Jepson, W.P., "Modelling the Transition to Slug Flow in Horizontal Conduit," *Can. J. Chem. Engng.*, **67**, 731-740, 1989.

Jepson, W.P. and R.E. Taylor, "Slug Flow and Its Transitions in Large-Diameter Horizontal Pipes," *Int. J. Multiphase Flow*, **19**, 411-420, 1993.

Kalinske, A.A. and Robertson, "Closed Conduit Flow," Air Entrainment Symposium, *Trans. ASCE*, **108**, 1435-1447, 1943.

Kaul, Ashwini, "Study of Slug Flow Characteristics and Performance of Corrosion Inhibitors, in Multiphase Flow, in Horizontal Oil and Gas Pipelines," M.S. Thesis, Ohio University, Athens, Ohio, 1996.

Kokal S.L. and J.F. Stanislav, "An Experimental Study of Two Phase Flow in Slightly Inclined Pipes-I. Flow Patterns," *Chemical Engineering Science*, **44**, 665-679, 1989.

Korbydan, E.S., "Flow Model for Two-Phase Slug Flow in Horizontal Tubes," *J. Bas. Engng.*, **83**, 613-618, 1961.

Kouba G.E. and W.P. Jepson, "The Flow of Slugs in Horizontal, Two Phase Pipelines," *Tran. ASME*, **112**, 10-24, 1990.

Lee, Ai Hsin, "A Study of Flow Regime Transitions for Oil-Water-Gas Mixtures in Large Diameter Horizontal Pipelines," M.S. Thesis, Ohio University, Athens, Ohio, 1993.

Lee, A-H, J-Y Sun, and W.P. Jepson, "Study of Flow Regime Transitions of Oil-Water-Gas Mixtures in Horizontal Pipelines," *Proc. 3rd Int. Offshore and Polar Engineering Conf.* (ISOPE-93), **2**, 159-164, 1993.

Lin, P.Y., "Flow Regime Transitions in Horizontal Gas-Liquid Flow," Ph.D. Thesis, University of Illinois, Urbana-Champaign, 1985.

Lin, P.Y. and T.J. Hanratty, "Detection of Slug Flow from Pressure Measurements," *Int. J. Multiphase Flow*, **13**, 13-21, 1987.

Maley, J., "Slug Flow Characteristics and Corrosion Rates in Inclined High Pressure Multiphase Flow Pipes," M.S. Thesis, Ohio University, Athens, Ohio, 1997.

Maley, L., "A Study of Slug Flow Charateristics in Large Diameter Horizontal Multiphase Pipelines," M.S. Thesis, Ohio University, Athens, Ohio, 1997.

Mandhane, J.M., G.A. Gregory, and K. Aziz, "A Flow Pattern Map for Gas-Liquid Flow in Horizontal Pipes: Predictive Models," *Int. J. Multiphase Flow*, **1**, 537-553, 1974.

Miya, M., D.E. Woodmansee, and T.J. Hanratty, "A Model for Roll Waves in Gas-Liquid Flow," *Chem. Engineering Sci.*, **26**, 1915-, 1971.

Neogi, S, A.H. Lee, and W.P. Jepson, "A Model for Multiphase (Gas-Water-Oil) Stratified Flow in Horizontal Pipelines," SPE Asia and Pacific Oil and Gas Conf., 553-561, 1994.

Reid, R.C., J.M. Prausnitz, and B.E. Poling, *The Properties of Liquids and Gases*, 4th ed., McGraw-Hill, New York, 1987.

Spedding, P.L. and D.R. Spence, "Flow Regimes in Two-Phase Gas-Liquid Flow," *Int. J. Multiphase Flow*, **19**, 245-280, 1993.

Stanislav, J.F., S. Kokal, and M.K. Nicholson, "Intermittent Gas-Liquid Flow in Upward Inclined Pipes," *Int. J. Multiphase Flow*, **12**, 325-335, 1986.

Stoker, J.J., *Water Waves*, Interscience Publishers, New York, 1957.

Taitel, Y., D. Barnea, and J.P. Brill, "Stratified Three Phase Flow in Pipes," *Int. J. Multiphase Flow*, **21**, 53-60, 1995.

Taitel, Y. and A.E. Dukler, "A Model for Predicting Flow Regime Transitions in Horizontal and Near Horizontal Gas-Liquid Flow," *AIChE J.*, **22**, 47-55, 1976.

Taitel, Y. and A.E. Dukler, "A Model for Slug Frequency During Gas-Liquid Flow in Horizontal and Near Horizontal Pipes," *Int. J. Multiphase Flow*, **3**, 585-596, 1977.

Wallis, G.B. and J.E. Dobson, "The Onset of Slugging in Horizontal Stratified Air-Water Flow," *Int. J. Multiphase Flow*, **1**, 173-193, 1973.

Wilkens, R., and W.P. Jepson, "Studies of Multiphase Flow in High Pressure Horizontal and +5 Degree Inclined Pipelines," *Proc. 6th Int. Offshore and Polar Engineering Conf.* (ISOPE-96), **2**, 139-145, 1996.

Zabaras, G.J., Shell Exploration and Production, personal communication, November, 1996.

CHAPTER 10

NOMENCLATURE

Variable	Definition
a	film spreading variable (radius), m
A	cross-sectional area, m^2
C	friction factor coefficient
C_l	flow rate in the tail, m^3/s
d	pipe inner diameter, m
D	hydraulic diameter, m
F_A	acoustically measured frequency, min^{-1}
Fr	Froude number
f	frequency, s^{-1}
F_{S1}	frequency measured between 132-cm pressure taps, min^{-1}
F_{S2}	frequency measured between 10-cm pressure taps, min^{-1}
F_V	slug frequency, min^{-1}
g	local gravity, m/s^2
h	film height, m
h_{eff}	effective film height, m
l	length, m
l_m	mixing zone length, m
l_u	slug unit length, m
m	friction factor exponent (gas)
n	friction factor exponent (liquid)
P	pressure, Pa
Re	Reynolds number
S	perimeter length, m
u	*in-situ* velocity, m/s
V	velocity, m/s
V_{SG}	superficial gas velocity, m/s
$V_{SG,t}$	transitional superficial gas velocity, m/s
V_{SL}	superficial liquid velocity, m/s
V_t	translational velocity, m/s
X	axial distance, m
X_{LD}	lead distance, m
X_{LG}	lag distance, m

GREEK:

α	void fraction
β	film spreading variable (angle), radians
μ	viscosity, Pa•s
ν	kinematic viscosity, m^2/s
π	ratio of circumference to diameter
ρ	density, kg/m^3
τ	shear stress,
θ	pipe inclination from horizontal, radians

SUBSCRIPTS:

2	referring to the slug tail region
D	film spreading variable (length)
f	in the film ahead of the slug
G	for the gas
G_O	for the gas at atmospheric pressure
GS	film spreading variable (gas from spread)
i	gas-liquid interface
iA	oil-water interface
iB	gas-oil interface
L	for the liquid
LA	liquid A (water)
LB	liquid B (oil)
L_2	for the liquid in the slug tail region
M	superficial mixture
MZ	in the mixing zone
S	for the slug
X	dummy variable
W	at the wall

OTHER

<>	average value
OVERBAR	non-dimensionalized value
‘	film spreading variable (alternative)

CHAPTER 11

APPENDIX A

All experimental frequencies are ± 4/min uncertainty. The accuracy of the superficial gas velocity is ± 0.4 m/s with a repeatability of ± 0.1 m/s. The linearity of the superficial liquid velocity is ± 0.01 m/s with a repeatability of ± 0.001 m/s. The uncertainty of the experimental V_t calculation is V_t^2*0.015 s/m (*e.g.*, V_t = 10 m/s ± 1.5 m/s). However, these values are averaged for all F_V, bringing the overall uncertainty for the experimentally determined V_t/V_m well below the predicted uncertainty of ± 0.2 (note the consistency of the reported values). Similarly, the uncertainty for l_u was calculated to be ± 14%. Note that for horizontal flow, data was taken at a superficial liquid velocity of 0.1 m/s also, but nothing is reported because it was stratified in all cases. Additionally, tests were run at zero gas flow rate for each liquid flow rate to verify the signals but are not included in the data tables. The system pressure was maintained within 0.007 MPa.

Table A.1: Flow property summary for 100% saltwater with carbon dioxide gas at a pressure of 0.45 MPa in a horizontal pipe at a superficial liquid velocity of 0.5 m/s.

V_{SG} (m/s)	V_t/V_m est.	Fr_f est.	F_{S1} (min^{-1})	F_{S2} (min^{-1})	F_V (min^{-1})	l_u (m)	F_{HW} (min^{-1})	F_{GS} (min^{-1})
1.4	1.2	2.1	22	20	16	8.6	6.6	14.0
3.3	1.2	5.7	18	10	10	27	4.8	9.0
5.1	1.2	9.5	26	20	8	50.	4.1	8.6
7.5	1.2	17.8	26	26	6	96	1.7	9.7
10.3	1.1	19.6	42	34	4	97	1.4	8.6
13.6	1.1	31.3	60	60	0	---	1.4	8.7

Table A.2: Flow property summary for 100% saltwater with carbon dioxide gas at a pressure of 0.45 MPa in a horizontal pipe at a superficial liquid velocity of 1.0 m/s.

V_{SG} (m/s)	V_t/V_m est.	Fr_f est.	F_{S1} (min^{-1})	F_{S2} (min^{-1})	F_V (min^{-1})	l_u (m)	F_{HW} (min^{-1})	F_{GS} (min^{-1})
1.3	1.2	2.1	42	34	42	3.9	15.1	25.8
3.4	1.2	5.3	24	22	18	17.6	12.1	19.9
4.9	1.2	8.0	30	20	20	21	11.1	20.0
7.8	1.2	16.1	80	54	54	11.7	3.7	23.6
9.3	1.1	19.1	76	60	18	20.	2.8	19.7
12.2	1.1	25.5	80	82	0	---	2.3	19.8

Table A.3: Flow property summary for 100% saltwater with carbon dioxide gas at a pressure of 0.45 MPa in a horizontal pipe at a superficial liquid velocity of 1.5 m/s.

V_{SG} (m/s)	V_t/V_m est.	Fr_f est.	F_{S1} (min^{-1})	F_{S2} (min^{-1})	F_V (min^{-1})	l_u (m)	F_{HW} (min^{-1})	F_{GS} (min^{-1})
1.7	1.2	2.8	50	60	62	4.0	22.5	34.7
3.4	1.2	5.1	50	46	34	10.4	19.6	32.0
5.6	1.2	9.3	68	58	52	9.8	12.3	34.4
8.1	1.2	15.9	94	94	40	17.3	5.6	40.4
9.1	1.2	18.6	98	92	28	27	4.9	43.7
10.3	1.1	20.1	110	120	18	24	4.0	32.6

Table A.4: Flow property summary for 100% saltwater with carbon dioxide gas at a pressure of 0.79 MPa in a horizontal pipe at a superficial liquid velocity of 0.5 m/s.

V_{SG} (m/s)	V_t/V_m est.	Fr_f est.	F_{S1} (min^{-1})	F_{S2} (min^{-1})	F_V (min^{-1})	l_u (m)	F_{HW} (min^{-1})	F_{GS} (min^{-1})
1.3	1.2	2.3	14	18	16	8.8	5.0	13.7
3.3	1.2	6.0	14	8	8	34	3.5	9.0
5.6	1.2	11.8	6	6	6	73	2.2	8.8
7.6	1.1	17.5	12	10	2	146	1.4	8.8
8.3	1.1	20.4	20	14	0	---	1.3	9.1

Table A.5: Flow property summary for 100% saltwater with carbon dioxide gas at a pressure of 0.79 MPa in a horizontal pipe at a superficial liquid velocity of 1.0 m/s.

V_{SG} (m/s)	V_t/V_m est.	Fr_f est.	F_{S1} (min^{-1})	F_{S2} (min^{-1})	F_V (min^{-1})	l_u (m)	F_{HW} (min^{-1})	F_{GS} (min^{-1})
1.2	1.2	2.0	20	20	20	7.9	12.6	25.3
3.5	1.2	5.7	26	26	14	23	9.1	19.8
5.1	1.2	8.9	30	34	12	37	7.2	20.2
7.4	1.2	15.8	50	48	10	60.	3.1	23.0

Table A.6: Flow property summary for 100% saltwater with carbon dioxide gas at a pressure of 0.79 MPa in a horizontal pipe at a superficial liquid velocity of 1.5 m/s.

V_{SG} (m/s)	V_t/V_m est.	Fr_f est.	F_{S1} (min^{-1})	F_{S2} (min^{-1})	F_V (min^{-1})	l_u (m)	F_{HW} (min^{-1})	F_{GS} (min^{-1})
1.2	1.2	2.1	34	26	26	7.5	20.3	37.8
3.4	1.2	5.3	52	60	14	25	15.7	32.0
5.3	1.2	9.0	78	66	16	31	10.9	33.9

Table A.7: Flow property summary for 100% saltwater with carbon dioxide gas at a pressure of 0.27 MPa in a +2° inclined pipe at a superficial liquid velocity of 0.1 m/s.

V_{SG} (m/s)	V_t/V_m	Fr_f est.	F_{S1} (min^{-1})	F_{S2} (min^{-1})	F_V (min^{-1})	l_u (m)	F_{HW} (min^{-1})	F_{GS} (min^{-1})
1.4	1.3	1.9	6	6	2	60	16.4	2.3
3.6	1.2	5.0	8	8	4	64	22.7	1.3
7.9	1.1	19.0	6	4	2	270	0.7	1.4
9.4	0.52	17.1	0	0	0	---	0.6	1.3

Table A.8: Flow property summary for 100% saltwater with carbon dioxide gas at a pressure of 0.27 MPa in a +2° inclined pipe at a superficial liquid velocity of 0.5 m/s.

V_{SG} (m/s)	V_t/V_m	Fr_f est.	F_{S1} (min^{-1})	F_{S2} (min^{-1})	F_V (min^{-1})	l_u (m)	F_{HW} (min^{-1})	F_{GS} (min^{-1})
1.4	1.3	2.1	24	22	8	18.8	20.8	12.9
4.2	1.2	6.3	26	24	22	15.3	23.3	8.6
7.9	1.2	19.5	34	32	28	21	2.3	10.0
9.2	1.2	23.7	32	34	28	24	2.0	10.8

Table A.9: Flow property summary for 100% saltwater with carbon dioxide gas at a pressure of 0.27 MPa in a +2° inclined pipe at a superficial liquid velocity of 1.0 m/s.

V_{SG} (m/s)	V_t/V_m	Fr_f est.	F_{S1} (min^{-1})	F_{S2} (min^{-1})	F_V (min^{-1})	l_u (m)	F_{HW} (min^{-1})	F_{GS} (min^{-1})
1.5	1.9	3.9	14	24	0	---	29.0	20.3
3.2	1.2	4.7	38	32	36	8.5	31.5	20.0
6.9	1.2	14.2	50	50	46	12.1	5.4	22.0
7.7	1.2	16.3	60	56	52	11.8	4.7	23.2

Table A.10: Flow property summary for 100% saltwater with carbon dioxide gas at a pressure of 0.27 MPa in a +2° inclined pipe at a superficial liquid velocity of 1.5 m/s.

V_{SG} (m/s)	V_t/V_m	Fr_f est.	F_{S1} (min^{-1})	F_{S2} (min^{-1})	F_V (min^{-1})	l_u (m)	F_{HW} (min^{-1})	F_{GS} (min^{-1})
1.4	2.1	4.5	14	16	0	---	35.6	32.0
2.9	1.2	4.0	52	48	48	6.4	37.6	32.6
5.5	1.2	10.1	68	60	60	8.3	11.2	34.1
7.0	1.2	14.1	80	76	74	8.4	7.9	37.9

Table A.11: Flow property summary for 100% saltwater with carbon dioxide gas at a pressure of 0.45 MPa in a +2° inclined pipe at a superficial liquid velocity of 0.1 m/s.

V_{SG} (m/s)	V_t/V_m	Fr_f est.	F_{S1} (min^{-1})	F_{S2} (min^{-1})	F_V (min^{-1})	l_u (m)	F_{HW} (min^{-1})	F_{GS} (min^{-1})
1.1	1.4	4.4	10	4	4	26	12.4	2.7
3.5	1.2	5.2	6	6	6	42	14.4	1.3
5.6	1.2	17.7	6	6	4	104	0.7	1.3
8.8	0.52	15.9	0	0	0	---	0.6	1.3

Table A.12: Flow property summary for 100% saltwater with carbon dioxide gas at a pressure of 0.45 MPa in a +2° inclined pipe at a superficial liquid velocity of 0.5 m/s.

V_{SG} (m/s)	V_t/V_m	Fr_f est.	F_{S1} (min^{-1})	F_{S2} (min^{-1})	F_V (min^{-1})	l_u (m)	F_{HW} (min^{-1})	F_{GS} (min^{-1})
1.1	1.3	1.7	12	10	4	32	17.5	15.1
3.3	1.2	5.2	24	22	18	15.7	18.9	8.9
5.3	1.2	11.7	24	24	20	20.	2.5	8.7
8.6	1.2	24.2	26	26	18	36	1.5	10.4

Table A.13: Flow property summary for 100% saltwater with carbon dioxide gas at a pressure of 0.45 MPa in a +2° inclined pipe at a superficial liquid velocity of 1.0 m/s.

V_{SG} (m/s)	V_t/V_m	Fr_f est.	F_{S1} (min^{-1})	F_{S2} (min^{-1})	F_V (min^{-1})	l_u (m)	F_{HW} (min^{-1})	F_{GS} (min^{-1})
1.2	2.1	3.7	12	16	0	---	24.1	20.5
2.8	1.2	4.1	40	38	34	7.9	24.9	20.7
6.0	1.2	12.6	52	48	42	11.7	4.1	20.9
7.7	1.2	18.3	70	66	60	10.5	3.2	23.6

Table A.14: Flow property summary for 100% saltwater with carbon dioxide gas at a pressure of 0.45 MPa in a +2° inclined pipe at a superficial liquid velocity of 1.5 m/s.

V_{SG} (m/s)	V_t/V_m	Fr_f est.	F_{S1} (min^{-1})	F_{S2} (min^{-1})	F_V (min^{-1})	l_u (m)	F_{HW} (min^{-1})	F_{GS} (min^{-1})
1.2	2.1	4.2	0	0	0	---	31.3	32.1
2.8	1.2	4.4	60	64	54	5.9	30.2	32.3
6.0	1.2	12.4	76	72	68	8.0	6.4	35.5
7.7	1.2	16.6	84	82	80	8.1	4.9	39.0

Table A.15: Flow property summary for 100% saltwater with carbon dioxide gas at a pressure of 0.79 MPa in a +2° inclined pipe at a superficial liquid velocity of 0.1 m/s.

V_{SG} (m/s)	V_t/V_m	Fr_f est.	F_{S1} (min^{-1})	F_{S2} (min^{-1})	F_V (min^{-1})	l_u (m)	F_{HW} (min^{-1})	F_{GS} (min^{-1})
1.0	1.5	1.7	12	10	6	16	10.0	2.9
3.2	1.2	5.4	10	8	6	41	9.8	1.4
4.6	1.1	7.9	2	2	2	162	7.5	1.3
5.7	0.52	8.5	0	0	0	---	0.5	1.6
7.1	0.47	11.6	0	0	0	---	0.5	1.5

Table A.16: Flow property summary for 100% saltwater with carbon dioxide gas at a pressure of 0.79 MPa in a +2° inclined pipe at a superficial liquid velocity of 0.5 m/s.

V_{SG} (m/s)	V_t/V_m	Fr_f est.	F_{S1} (min^{-1})	F_{S2} (min^{-1})	F_V (min^{-1})	l_u (m)	F_{HW} (min^{-1})	F_{GS} (min^{-1})
0.8	1.9	2.1	14	12	0	---	14.2	12.9
3.1	1.2	5.0	24	22	16	16.1	12.4	9.2
5.4	1.2	13.6	22	22	18	23	1.5	8.7
6.9	1.2	20.0	32	30	24	23	1.2	9.5

Table A.17: Flow property summary for 100% saltwater with carbon dioxide gas at a pressure of 0.79 MPa in a +2° inclined pipe at a superficial liquid velocity of 1.0 m/s.

V_{SG} (m/s)	V_t/V_m	Fr_f est.	F_{S1} (min^{-1})	F_{S2} (min^{-1})	F_V (min^{-1})	l_u (m)	F_{HW} (min^{-1})	F_{GS} (min^{-1})
0.9	2.1	3.1	0	0	0	---	22.0	21.7
3.3	1.2	5.2	40	42	38	8.1	17.2	20.0
5.9	1.2	13.9	54	50	44	11.5	2.7	21.1
7.4	1.2	18.3	60	58	50	12	2.3	22.9

Table A.18: Flow property summary for 100% saltwater with carbon dioxide gas at a pressure of 0.79 MPa in a +2° inclined pipe at a superficial liquid velocity of 1.5 m/s.

V_{SG} (m/s)	V_t/V_m	Fr_f est.	F_{S1} (min^{-1})	F_{S2} (min^{-1})	F_V (min^{-1})	l_u (m)	F_{HW} (min^{-1})	F_{GS} (min^{-1})
0.9	2.0	3.5	0	0	0	---	27.8	32.8
2.9	1.2	4.4	60	58	50	6.1	25.2	32.6
5.9	1.2	12.7	74	70	66	8.0	4.6	34.9
6.8	1.2	15.7	80	84	78	7.8	3.8	37.4

Table A.19: Flow property summary for 80% saltwater/20% light oil with carbon dioxide gas at a pressure of 0.27 MPa in a +2° inclined pipe at a superficial liquid velocity of 0.1 m/s.

V_{SG} (m/s)	V_t/V_m	Fr_f est.	F_{S1} (min^{-1})	F_{S2} (min^{-1})	F_V (min^{-1})	l_u (m)	F_{HW} (min^{-1})	F_{GS} (min^{-1})
1.4	1.3	2.0	12	12	2	60.	16.4	2.3
3.3	1.2	4.7	12	10	8	30.	20.8	1.4
6.3	1.2	17.5	10	8	4	112	1.0	1.3
8.5	1.2	29.1	2	4	2	300.	0.7	1.4

Table A.20: Flow property summary for 80% saltwater/20% light oil with carbon dioxide gas at a pressure of 0.27 MPa in a +2° inclined pipe at a superficial liquid velocity of 0.5 m/s.

V_{SG} (m/s)	V_t/V_m	Fr_f est.	F_{S1} (min^{-1})	F_{S2} (min^{-1})	F_V (min^{-1})	l_u (m)	F_{HW} (min^{-1})	F_{GS} (min^{-1})
1.4	1.9	3.3	8	8	0	---	20.8	9.8
3.3	1.2	5.0	22	20	16	17.6	23.3	8.9
6.3	1.2	14.0	24	20	18	27	3.1	9.0
8.4	1.2	21.2	26	24	22	29	2.1	10.3

Table A.21: Flow property summary for 80% saltwater/20% light oil with carbon dioxide gas at a pressure of 0.27 MPa in a +2° inclined pipe at a superficial liquid velocity of 1.0 m/s.

V_{SG} (m/s)	V_t/V_m	Fr_f est.	F_{S1} (min^{-1})	F_{S2} (min^{-1})	F_V (min^{-1})	l_u (m)	F_{HW} (min^{-1})	F_{GS} (min^{-1})
1.4	2.0	4.0	4	4	0	---	27.8	20.2
3.4	1.2	4.9	36	34	32	9.8	30.9	19.9
5.8	1.2	11.2	46	44	42	11.4	6.8	20.7
7.2	1.2	15.0	62	60	52	11.1	5.1	22.4

Table A.22: Flow property summary for 80% saltwater/20% light oil with carbon dioxide gas at a pressure of 0.27 MPa in a +2° inclined pipe at a superficial liquid velocity of 1.5 m/s.

V_{SG} (m/s)	V_t/V_m	Fr_f est.	F_{S1} (min^{-1})	F_{S2} (min^{-1})	F_V (min^{-1})	l_u (m)	F_{HW} (min^{-1})	F_{GS} (min^{-1})
1.4	1.9	4.1	0	0	0	---	35.6	32.1
3.3	1.2	4.7	62	58	52	6.6	38.5	32.1
6.1	1.2	11.4	70	68	62	8.6	9.6	35.1
7.4	1.2	14.8	80	82	72	8.8	7.6	38.3

Table A.23: Flow property summary for 80% saltwater/20% light oil with carbon dioxide gas at a pressure of 0.45 MPa in a +2° inclined pipe at a superficial liquid velocity of 0.1 m/s.

V_{SG} (m/s)	V_t/V_m	Fr_f est.	F_{S1} (min^{-1})	F_{S2} (min^{-1})	F_V (min^{-1})	l_u (m)	F_{HW} (min^{-1})	F_{GS} (min^{-1})
1.1	1.3	1.7	12	12	4	24	12.4	2.9
3.0	1.2	4.4	14	16	10	22	14.3	1.4
5.9	1.1	18.6	2	2	2	204	0.6	1.3
8.3	0.48	13.6	0	0	0	---	0.6	1.4

Table A.24: Flow property summary for 80% saltwater/20% light oil with carbon dioxide gas at a pressure of 0.45 MPa in a +2° inclined pipe at a superficial liquid velocity of 0.5 m/s.

V_{SG} (m/s)	V_t/V_m	Fr_f est.	F_{S1} (min^{-1})	F_{S2} (min^{-1})	F_V (min^{-1})	l_u (m)	F_{HW} (min^{-1})	F_{GS} (min^{-1})
0.9	2.1	2.6	0	0	0	---	16.2	11.2
3.0	1.2	4.4	26	24	16	15.4	17.4	9.3
6.1	1.2	14.9	20	20	12	40.	1.9	9.0
8.0	1.2	22.0	28	26	24	25	1.5	10.0

Table A.25: Flow property summary for 80% saltwater/20% light oil with carbon dioxide gas at a pressure of 0.45 MPa in a +2° inclined pipe at a superficial liquid velocity of 1.0 m/s.

V_{SG} (m/s)	V_t/V_m	Fr_f est.	F_{S1} (min^{-1})	F_{S2} (min^{-1})	F_V (min^{-1})	l_u (m)	F_{HW} (min^{-1})	F_{GS} (min^{-1})
1.2	2.0	3.6	0	0	0	---	24.1	20.8
3.0	1.2	4.4	38	36	34	8.3	22.9	20.4
5.9	1.2	12.8	52	50	44	11.3	4.0	21.0
7.7	1.2	17.8	62	58	52	11.8	2.9	23.2

Table A.26: Flow property summary for 80% saltwater/20% light oil with carbon dioxide gas at a pressure of 0.45 MPa in a +2° inclined pipe at a superficial liquid velocity of 1.5 m/s.

V_{SG} (m/s)	V_t/V_m	Fr_f est.	F_{S1} (min^{-1})	F_{S2} (min^{-1})	F_V (min^{-1})	l_u (m)	F_{HW} (min^{-1})	F_{GS} (min^{-1})
1.3	2.0	4.2	0	0	0	---	30.6	32.2
3.5	1.2	5.5	66	62	58	6.3	30.7	32.0
6.1	1.2	12.4	86	80	68	7.9	6.5	35.3
7.9	1.2	17.3	86	78	72	9.2	4.7	39.7

Table A.27: Flow property summary for 80% saltwater/20% light oil with carbon dioxide gas at a pressure of 0.79 MPa in a +2° inclined pipe at a superficial liquid velocity of 0.1 m/s.

V_{SG} (m/s)	V_t/V_m	Fr_f est.	F_{S1} (min^{-1})	F_{S2} (min^{-1})	F_V (min^{-1})	l_u (m)	F_{HW} (min^{-1})	F_{GS} (min^{-1})
1.0	1.5	1.6	4	4	2	48	10.0	2.9
4.0	1.2	6.8	4	4	2	144	7.7	1.3
5.1	1.2	15.8	2	2	2	180	0.6	1.2
5.6	1.1	18.8	2	2	0	---	0.5	1.2

Table A.28: Flow property summary for 80% saltwater/20% light oil with carbon dioxide gas at a pressure of 0.79 MPa in a +2° inclined pipe at a superficial liquid velocity of 0.5 m/s.

V_{SG} (m/s)	V_t/V_m	Fr_f est.	F_{S1} (min^{-1})	F_{S2} (min^{-1})	F_V (min^{-1})	l_u (m)	F_{HW} (min^{-1})	F_{GS} (min^{-1})
0.8	2.0	2.3	16	14	0	---	13.4	12.1
3.5	1.2	5.5	20	18	18	15.3	11.9	8.9
4.5	1.2	8.0	18	18	18	20.	10.1	8.6
5.9	1.2	15.3	28	26	20	22	1.3	8.8

Table A.29: Flow property summary for 80% saltwater/20% light oil with carbon dioxide gas at a pressure of 0.79 MPa in a +2° inclined pipe at a superficial liquid velocity of 1.0 m/s.

V_{SG} (m/s)	V_t/V_m	Fr_f est.	F_{S1} (min^{-1})	F_{S2} (min^{-1})	F_V (min^{-1})	l_u (m)	F_{HW} (min^{-1})	F_{GS} (min^{-1})
1.2	2.0	3.6	0	0	0	---	20.0	21.0
3.5	1.2	5.6	40	38	34	9.4	16.7	19.9
4.9	1.2	8.6	50	54	40	10.8	15.1	20.1
5.6	1.2	12.6	54	50	46	10.2	2.8	20.5

Table A.30: Flow property summary for 80% saltwater/20% light oil with carbon dioxide gas at a pressure of 0.79 MPa in a +2° inclined pipe at a superficial liquid velocity of 1.5 m/s.

V_{SG} (m/s)	V_t/V_m	Fr_f est.	F_{S1} (min^{-1})	F_{S2} (min^{-1})	F_V (min^{-1})	l_u (m)	F_{HW} (min^{-1})	F_{GS} (min^{-1})
1.0	2.1	3.9	0	0	0	---	27.4	32.4
3.8	1.2	5.9	68	64	54	6.8	22.8	32.0
5.1	1.2	10.5	78	76	72	6.5	5.2	33.4
6.1	1.2	13.3	82	78	78	6.9	4.4	35.3

Table A.31: Flow property summary for 40% saltwater/60% light oil with carbon dioxide gas at a pressure of 0.27 MPa in a +2° inclined pipe at a superficial liquid velocity of 0.1 m/s.

V_{SG} (m/s)	V_t/V_m	Fr_f est.	F_{S1} (min^{-1})	F_{S2} (min^{-1})	F_V (min^{-1})	l_u (m)	F_{HW} (min^{-1})	F_{GS} (min^{-1})
1.4	1.3	1.8	10	8	6	19.0	16.4	2.4
3.3	1.2	4.7	10	10	8	30.	20.8	1.4
5.8	1.2	14.8	6	6	4	108	1.5	1.3
7.9	1.1	27.0	2	2	2	273	0.7	1.4

Table A.32: Flow property summary for 40% saltwater/60% light oil with carbon dioxide gas at a pressure of 0.27 MPa in a +2° inclined pipe at a superficial liquid velocity of 0.5 m/s.

V_{SG} (m/s)	V_t/V_m	Fr_f est.	F_{S1} (min^{-1})	F_{S2} (min^{-1})	F_V (min^{-1})	l_u (m)	F_{HW} (min^{-1})	F_{GS} (min^{-1})
1.4	1.4	2.2	10	16	4	39	19.6	12.5
3.0	1.2	4.3	24	22	12	21	23.0	9.2
6.6	1.2	8.4	20	16	16	32	2.8	9.2
7.5	1.2	9.7	30	28	22	26	2.2	9.8

Table A.33: Flow property summary for 40% saltwater/60% light oil with carbon dioxide gas at a pressure of 0.27 MPa in a +2° inclined pipe at a superficial liquid velocity of 1.0 m/s.

V_{SG} (m/s)	V_t/V_m	Fr_f est.	F_{S1} (min^{-1})	F_{S2} (min^{-1})	F_V (min^{-1})	l_u (m)	F_{HW} (min^{-1})	F_{GS} (min^{-1})
1.3	2.0	3.7	8	6	0	---	26.7	20.5
2.9	1.2	4.4	42	46	36	8.0	29.3	20.3
5.7	1.2	11.0	46	44	40	11.7	6.2	20.5
6.8	1.2	14.1	58	56	48	11.5	4.9	21.9

Table A.34: Flow property summary for 40% saltwater/60% light oil with carbon dioxide gas at a pressure of 0.27 MPa in a +2° inclined pipe at a superficial liquid velocity of 1.5 m/s.

V_{SG} (m/s)	V_t/V_m	Fr_f est.	F_{S1} (min^{-1})	F_{S2} (min^{-1})	F_V (min^{-1})	l_u (m)	F_{HW} (min^{-1})	F_{GS} (min^{-1})
1.4	2.1	4.5	12	10	0	---	33.6	32.0
2.9	1.2	4.1	64	60	50	6.2	35.3	32.4
5.7	1.2	10.5	68	64	64	7.9	9.9	34.3
6.5	1.2	12.7	80	76	68	8.4	8.7	36.2

Table A.35: Flow property summary for 40% saltwater/60% light oil with carbon dioxide gas at a pressure of 0.45 MPa in a +2° inclined pipe at a superficial liquid velocity of 0.1 m/s.

V_{SG} (m/s)	V_t/V_m	Fr_f est.	F_{S1} (min^{-1})	F_{S2} (min^{-1})	F_V (min^{-1})	l_u (m)	F_{HW} (min^{-1})	F_{GS} (min^{-1})
1.2	1.3	1.7	10	8	6	17	12.6	2.7
3.4	1.2	5.1	12	10	6	41	14.0	1.4
6.1	1.1	19.8	2	2	2	210	0.6	1.3
7.1	0.51	11.6	0	0	0	---	0.6	1.4
8.1	0.46	13.5	0	0	0	---	0.5	1.4

Table A.36: Flow property summary for 40% saltwater/60% light oil with carbon dioxide gas at a pressure of 0.45 MPa in a +2° inclined pipe at a superficial liquid velocity of 0.5 m/s.

V_{SG} (m/s)	V_t/V_m	Fr_f est.	F_{S1} (min^{-1})	F_{S2} (min^{-1})	F_V (min^{-1})	l_u (m)	F_{HW} (min^{-1})	F_{GS} (min^{-1})
1.2	2.1	3.2	14	14	0	---	17.5	10.1
2.6	1.2	3.7	24	26	20	10.8	17.7	10.0
5.0	1.2	11.4	22	20	20	20.	2.5	8.6
7.6	1.2	20.6	34	30	30	19.2	1.5	9.7

Table A.37: Flow property summary for 40% saltwater/60% light oil with carbon dioxide gas at a pressure of 0.45 MPa in a +2° inclined pipe at a superficial liquid velocity of 1.0 m/s.

V_{SG} (m/s)	V_t/V_m	Fr_f est.	F_{S1} (min^{-1})	F_{S2} (min^{-1})	F_V (min^{-1})	l_u (m)	F_{HW} (min^{-1})	F_{GS} (min^{-1})
1.0	2.0	3.2	0	0	0	---	21.9	21.4
3.0	1.2	4.5	40	44	32	8.8	22.9	20.4
5.4	1.2	11.3	48	46	40	11.4	4.3	20.4
7.5	1.2	18.0	64	60	50	12.4	2.9	23.3

Table A.38: Flow property summary for 40% saltwater/60% light oil with carbon dioxide gas at a pressure of 0.45 MPa in a +2° inclined pipe at a superficial liquid velocity of 1.5 m/s.

V_{SG} (m/s)	V_t/V_m	Fr_f est.	F_{S1} (min^{-1})	F_{S2} (min^{-1})	F_V (min^{-1})	l_u (m)	F_{HW} (min^{-1})	F_{GS} (min^{-1})
1.2	2.0	4.2	0	0	0	---	29.5	32.2
3.2	1.2	5.0	68	62	60	5.7	28.8	32.1
5.3	1.2	10.5	70	66	64	7.6	6.8	33.8
7.5	1.2	16.8	84	80	70	9.3	4.8	39.2

Table A.39: Flow property summary for 40% saltwater/60% light oil with carbon dioxide gas at a pressure of 0.79 MPa in a +2° inclined pipe at a superficial liquid velocity of 0.1 m/s.

V_{SG} (m/s)	V_t/V_m	Fr_f est.	F_{S1} (min^{-1})	F_{S2} (min^{-1})	F_V (min^{-1})	l_u (m)	F_{HW} (min^{-1})	F_{GS} (min^{-1})
1.0	1.5	1.6	12	12	6	16.0	10.0	2.9
3.4	1.2	5.7	10	10	6	41	7.7	1.4
5.2	0.53	8.0	0	0	0	---	0.5	1.7
6.0	0.49	9.5	0	0	0	---	0.5	1.6
7.3	0.46	12.1	0	0	0	---	0.5	1.5

Table A.40: Flow property summary for 40% saltwater/60% light oil with carbon dioxide gas at a pressure of 0.79 MPa in a +2° inclined pipe at a superficial liquid velocity of 0.5 m/s.

V_{SG} (m/s)	V_t/V_m	Fr_f est.	F_{S1} (min^{-1})	F_{S2} (min^{-1})	F_V (min^{-1})	l_u (m)	F_{HW} (min^{-1})	F_{GS} (min^{-1})
0.9	2.1	2.6	10	8	0	---	13.6	11.5
2.9	1.2	4.6	26	26	24	10.0	12.6	9.4
5.2	1.2	13.1	22	20	22	18.5	1.4	8.7
8.1	1.2	25.2	40	36	34	18.4	1.1	10.2

Table A.41: Flow property summary for 40% saltwater/60% light oil with carbon dioxide gas at a pressure of 0.79 MPa in a +2° inclined pipe at a superficial liquid velocity of 1.0 m/s.

V_{SG} (m/s)	V_t/V_m	Fr_f est.	F_{S1} (min^{-1})	F_{S2} (min^{-1})	F_V (min^{-1})	l_u (m)	F_{HW} (min^{-1})	F_{GS} (min^{-1})
0.9	2.1	3.1	0	0	0	---	19.6	21.9
3.1	1.2	4.9	44	40	36	8.0	16.4	20.3
5.4	1.2	12.0	52	46	40	11.2	2.9	20.3
7.2	1.2	18.4	58	56	48	12.4	2.1	22.8

Table A.42: Flow property summary for 40% saltwater/60% light oil with carbon dioxide gas at a pressure of 0.79 MPa in a +2° inclined pipe at a superficial liquid velocity of 1.5 m/s.

V_{SG} (m/s)	V_t/V_m	Fr_f est.	F_{S1} (min^{-1})	F_{S2} (min^{-1})	F_V (min^{-1})	l_u (m)	F_{HW} (min^{-1})	F_{GS} (min^{-1})
0.9	2.0	3.4	0	0	0	---	26.3	33.0
3.4	1.2	5.3	66	66	52	6.6	21.1	32.1
5.4	1.2	12.0	72	78	70	7.3	4.7	34.4
6.3	1.2	14.6	90	84	82	7.0	3.9	36.4

Table A.43: Flow property summary for 100% saltwater with carbon dioxide gas at a pressure of 0.27 MPa in a +5° inclined pipe at a superficial liquid velocity of 0.1 m/s.

V_{SG} (m/s)	V_t/V_m	Fr_f est.	F_{S1} (min^{-1})	F_{S2} (min^{-1})	F_V (min^{-1})	l_u (m)	F_{HW} (min^{-1})	F_{GS} (min^{-1})
1.5	1.2	2.3	8	8	4	30	17.5	2.3
3.5	1.2	5.4	8	8	4	63	23.6	1.3
8.0	1.2	15.5	6	6	2	285	0.7	1.4
9.6	0.62	8.8	0	0	0	---	0.6	1.2

Table A.44: Flow property summary for 100% saltwater with carbon dioxide gas at a pressure of 0.27 MPa in a +5° inclined pipe at a superficial liquid velocity of 0.5 m/s.

V_{SG} (m/s)	V_t/V_m	Fr_f est.	F_{S1} (min^{-1})	F_{S2} (min^{-1})	F_V (min^{-1})	l_u (m)	F_{HW} (min^{-1})	F_{GS} (min^{-1})
1.5	1.3	2.6	28	22	12	13.0	20.6	12.5
4.0	1.2	6.4	28	26	20	15.9	25.7	8.7
8.0	1.2	16.5	36	30	26	23	2.3	10.0
9.5	1.2	19.9	34	32	28	25	1.8	11.1

Table A.45: Flow property summary for 100% saltwater with carbon dioxide gas at a pressure of 0.27 MPa in a +5° inclined pipe at a superficial liquid velocity of 1.0 m/s.

V_{SG} (m/s)	V_t/V_m	Fr_f est.	F_{S1} (min^{-1})	F_{S2} (min^{-1})	F_V (min^{-1})	l_u (m)	F_{HW} (min^{-1})	F_{GS} (min^{-1})
1.5	1.4	3	18	20	2	105	29.0	23.3
3.5	1.2	5.5	40	36	32	9.8	29.5	19.9
7.0	1.2	14.4	48	44	42	13.9	5.0	22.5
8.0	1.2	16.8	68	62	58	11.3	4.1	24.1

Table A.46: Flow property summary for 100% saltwater with carbon dioxide gas at a pressure of 0.27 MPa in a +5° inclined pipe at a superficial liquid velocity of 1.5 m/s.

V_{SG} (m/s)	V_t/V_m	Fr_f est.	F_{S1} (min^{-1})	F_{S2} (min^{-1})	F_V (min^{-1})	l_u (m)	F_{HW} (min^{-1})	F_{GS} (min^{-1})
1.5	1.9	5.0	20	12	0	---	36.8	32.1
3.0	1.2	4.8	50	46	42	7.6	38.5	32.3
5.5	1.2	10.7	64	60	56	9.1	11.2	34.4
7.0	1.2	13.9	76	74	72	8.4	7.3	37.4

Table A.47: Flow property summary for 100% saltwater with carbon dioxide gas at a pressure of 0.45 MPa in a +5° inclined pipe at a superficial liquid velocity of 0.1 m/s.

V_{SG} (m/s)	V_t/V_m	Fr_f est.	F_{S1} (min^{-1})	F_{S2} (min^{-1})	F_V (min^{-1})	l_u (m)	F_{HW} (min^{-1})	F_{GS} (min^{-1})
0.8	1.8	1.8	14	12	0	---	10.4	2.9
2.6	1.2	4.4	10	10	6	33	12.0	1.5
4.6	1.1	9.2	4	4	4	81	15.0	1.3
8.0	0.63	8.6	2	0	0	---	0.8	1.3
10.3	0.56	8.5	0	0	0	---	0.7	1.2

Table A.48: Flow property summary for 100% saltwater with carbon dioxide gas at a pressure of 0.45 MPa in a +5° inclined pipe at a superficial liquid velocity of 0.5 m/s.

V_{SG} (m/s)	V_t/V_m	Fr_f est.	F_{S1} (min^{-1})	F_{S2} (min^{-1})	F_V (min^{-1})	l_u (m)	F_{HW} (min^{-1})	F_{GS} (min^{-1})
1.2	1.2	1.9	22	18	10	12.6	18.6	15.1
2.9	1.2	4.7	28	24	22	10.9	19.4	9.4
5.0	1.2	10.1	22	22	20	19.5	2.7	8.6
7.0	1.2	14.9	20	20	18	30.	1.6	9.4
9.1	1.2	18.5	18	18	16	42	1.1	10.7

Table A.49: Flow property summary for 100% saltwater with carbon dioxide gas at a pressure of 0.45 MPa in a +5° inclined pipe at a superficial liquid velocity of 1.0 m/s.

V_{SG} (m/s)	V_t/V_m	Fr_f est.	F_{S1} (min^{-1})	F_{S2} (min^{-1})	F_V (min^{-1})	l_u (m)	F_{HW} (min^{-1})	F_{GS} (min^{-1})
1.2	1.9	3.7	14	12	0	---	24.1	21.4
2.7	1.2	4.7	42	38	36	7.7	24.3	20.5
4.1	1.2	7.4	46	42	40	9.0	12.1	19.7
8.0	1.2	16.8	62	62	62	10.5	2.6	24.0
8.8	1.2	18.4	68	66	64	11.1	1.7	25.4

Table A.50: Flow property summary for 100% saltwater with carbon dioxide gas at a pressure of 0.45 MPa in a +5° inclined pipe at a superficial liquid velocity of 1.5 m/s.

V_{SG} (m/s)	V_t/V_m	Fr_f est.	F_{S1} (min^{-1})	F_{S2} (min^{-1})	F_V (min^{-1})	l_u (m)	F_{HW} (min^{-1})	F_{GS} (min^{-1})
1.3	2.1	5.1	14	10	0	---	32.5	32.1
2.9	1.2	4.7	62	58	56	5.7	30.9	32.3
4.0	1.2	7.5	70	68	60	6.6	17.6	32.2
6.8	1.2	15.0	80	76	70	8.6	2.6	37.2
9.3	1.2	19.7	90	86	86	9.1	1.4	44.5

Table A.51: Flow property summary for 100% saltwater with carbon dioxide gas at a pressure of 0.79 MPa in a +5° inclined pipe at a superficial liquid velocity of 0.1 m/s.

V_{SG} (m/s)	V_t/V_m	Fr_f est.	F_{S1} (min^{-1})	F_{S2} (min^{-1})	F_V (min^{-1})	l_u (m)	F_{HW} (min^{-1})	F_{GS} (min^{-1})
1.0	1.4	1.7	14	10	2	45	10.0	3.1
2.1	1.1	3.2	10	10	6	25	12.6	1.9
3.7	1.2	6.7	12	10	6	46	8.3	1.3
4.9	1.1	9.5	2	2	2	165	6.3	1.2
7.3	0.08	0.8	0	0	0	---	0.5	8.7

Table A.52: Flow property summary for 100% saltwater with carbon dioxide gas at a pressure of 0.79 MPa in a +5° inclined pipe at a superficial liquid velocity of 0.5 m/s.

V_{SG} (m/s)	V_t/V_m	Fr_f est.	F_{S1} (min^{-1})	F_{S2} (min^{-1})	F_V (min^{-1})	l_u (m)	F_{HW} (min^{-1})	F_{GS} (min^{-1})
1.0	1.4	1.9	14	12	2	63	17.4	15.1
3.1	1.2	5.1	26	24	18	14.3	19.2	9.2
5.3	1.2	11.4	16	16	16	27	2.5	8.7
7.3	1.2	15.2	14	14	14	39	1.8	9.5

Table A.53: Flow property summary for 100% saltwater with carbon dioxide gas at a pressure of 0.79 MPa in a +5° inclined pipe at a superficial liquid velocity of 1.0 m/s.

V_{SG} (m/s)	V_t/V_m	Fr_f est.	F_{S1} (min^{-1})	F_{S2} (min^{-1})	F_V (min^{-1})	l_u (m)	F_{HW} (min^{-1})	F_{GS} (min^{-1})
0.9	2.1	3.6	0	0	0	---	22.0	21.7
2.0	1.2	3.1	38	36	32	7.5	22.5	22.9
3.0	1.2	5.0	44	42	40	7.2	18.5	20.3
5.2	1.2	10.6	48	48	46	9.7	3.1	20.2
6.7	1.2	14.4	64	60	56	9.9	3.0	21.9

Table A.54: Flow property summary for 100% saltwater with carbon dioxide gas at a pressure of 0.79 MPa in a +5° inclined pipe at a superficial liquid velocity of 1.5 m/s.

V_{SG} (m/s)	V_t/V_m	Fr_f est.	F_{S1} (min^{-1})	F_{S2} (min^{-1})	F_V (min^{-1})	l_u (m)	F_{HW} (min^{-1})	F_{GS} (min^{-1})
0.9	1.9	3.7	0	0	0	---	27.8	33.4
2.1	1.2	3.4	62	58	52	4.8	28.9	34.5
3.0	1.2	5.6	64	62	60	5.6	22.4	32.1
5.1	1.2	10.4	70	68	66	7.2	5.7	33.5
6.9	1.2	14.9	88	86	82	7.5	3.9	37.9

Table A.55: Flow property summary for 80% saltwater/20% light oil with carbon dioxide gas at a pressure of 0.27 MPa in a +5° inclined pipe at a superficial liquid velocity of 0.1 m/s.

V_{SG} (m/s)	V_t/V_m	Fr_f est.	F_{S1} (min^{-1})	F_{S2} (min^{-1})	F_V (min^{-1})	l_u (m)	F_{HW} (min^{-1})	F_{GS} (min^{-1})
1.4	1.5	2.0	10	10	2	66	20.5	2.1
3.9	1.2	5.1	14	12	10	28	32.1	1.3
7.8	1.1	18.6	4	4	2	270	2.0	1.4
9.2	1.0	28.7	4	2	2	273	0.7	1.4

Table A.56: Flow property summary for 80% saltwater/20% light oil with carbon dioxide gas at a pressure of 0.27 MPa in a +5° inclined pipe at a superficial liquid velocity of 0.5 m/s.

V_{SG} (m/s)	V_t/V_m	Fr_f est.	F_{S1} (min^{-1})	F_{S2} (min^{-1})	F_V (min^{-1})	l_u (m)	F_{HW} (min^{-1})	F_{GS} (min^{-1})
1.7	1.3	3.8	14	16	8	21	27.0	11.8
4.2	1.2	5.9	26	26	22	15.5	35.3	8.6
7.0	1.2	14.8	26	26	20	27	4.7	9.5
11.2	1.2	30.1	30	28	24	34	1.9	12.5

Table A.57: Flow property summary for 80% saltwater/20% light oil with carbon dioxide gas at a pressure of 0.27 MPa in a +5° inclined pipe at a superficial liquid velocity of 1.0 m/s.

V_{SG} (m/s)	V_t/V_m	Fr_f est.	F_{S1} (min^{-1})	F_{S2} (min^{-1})	F_V (min^{-1})	l_u (m)	F_{HW} (min^{-1})	F_{GS} (min^{-1})
1.3	2.0	3.6	12	12	0	---	31.5	20.4
3.9	1.2	5.4	48	42	38	9.2	41.9	19.7
5.6	1.2	10.0	50	52	46	10.2	10.6	20.5
7.8	1.2	15.9	66	62	56	11.1	6.4	23.4

Table A.58: Flow property summary for 80% saltwater/20% light oil with carbon dioxide gas at a pressure of 0.27 MPa in a +5° inclined pipe at a superficial liquid velocity of 1.5 m/s.

V_{SG} (m/s)	V_t/V_m	Fr_f est.	F_{S1} (min^{-1})	F_{S2} (min^{-1})	F_V (min^{-1})	l_u (m)	F_{HW} (min^{-1})	F_{GS} (min^{-1})
1.5	2.0	4.5	6	6	0	---	41.1	32.0
3.8	1.2	5.3	64	66	60	6.3	48.3	32.1
5.4	1.2	9.3	74	70	68	7.1	15.1	33.8
6.9	1.2	13.4	86	82	80	7.6	10.7	37.7

Table A.59: Flow property summary for 80% saltwater/20% light oil with carbon dioxide gas at a pressure of 0.45 MPa in a +5° inclined pipe at a superficial liquid velocity of 0.1 m/s.

V_{SG} (m/s)	V_t/V_m	Fr_f est.	F_{S1} (min^{-1})	F_{S2} (min^{-1})	F_V (min^{-1})	l_u (m)	F_{HW} (min^{-1})	F_{GS} (min^{-1})
1.3	1.4	1.9	12	12	4	28	17.2	2.4
4.8	1.2	7.2	10	10	8	44	24.3	1.2
6.4	1.1	13.4	8	8	2	222	3.0	1.3
8.4	0.48	12.9	0	0	0	---	0.7	1.4
11.1	0.46	19.6	0	0	0	---	0.7	1.3

Table A.60: Flow property summary for 80% saltwater/20% light oil with carbon dioxide gas at a pressure of 0.45 MPa in a +5° inclined pipe at a superficial liquid velocity of 0.5 m/s.

V_{SG} (m/s)	V_t/V_m	Fr_f est.	F_{S1} (min^{-1})	F_{S2} (min^{-1})	F_V (min^{-1})	l_u (m)	F_{HW} (min^{-1})	F_{GS} (min^{-1})
1.2	2.1	3.1	16	14	0	---	20.9	10.0
3.1	1.2	4.2	26	26	26	9.7	27.0	9.2
4.7	1.2	7.1	26	24	26	14.5	27.7	8.6
7.1	1.2	16.9	24	26	22	25	2.4	9.4
9.7	1.2	28.3	32	30	24	31	1.6	11.4

Table A.61: Flow property summary for 80% saltwater/20% light oil with carbon dioxide gas at a pressure of 0.45 MPa in a +5° inclined pipe at a superficial liquid velocity of 1.0 m/s.

V_{SG} (m/s)	V_t/V_m	Fr_f est.	F_{S1} (min^{-1})	F_{S2} (min^{-1})	F_V (min^{-1})	l_u (m)	F_{HW} (min^{-1})	F_{GS} (min^{-1})
1.1	2.0	3.1	0	0	0	---	27.2	21.2
2.8	1.2	4.1	42	38	38	7.4	32.5	20.4
4.9	1.2	7.3	50	46	44	9.5	31.5	20.0
8.0	1.2	18.1	72	70	64	9.9	3.3	23.7

Table A.62: Flow property summary for 80% saltwater/20% light oil with carbon dioxide gas at a pressure of 0.45 MPa in a +5° inclined pipe at a superficial liquid velocity of 1.5 m/s.

V_{SG} (m/s)	V_t/V_m	Fr_f est.	F_{S1} (min^{-1})	F_{S2} (min^{-1})	F_V (min^{-1})	l_u (m)	F_{HW} (min^{-1})	F_{GS} (min^{-1})
1.2	2.3	4.7	0	0	0	---	35.0	32.1
3.5	1.2	5.2	74	70	64	5.7	37.5	32.0
5.1	1.2	9.4	76	74	72	6.5	10.6	33.4
7.8	1.2	16.5	102	98	88	7.5	5.8	39.5

Table A.63: Flow property summary for 80% saltwater/20% light oil with carbon dioxide gas at a pressure of 0.79 MPa in a +5° inclined pipe at a superficial liquid velocity of 0.1 m/s.

V_{SG} (m/s)	V_t/V_m	Fr_f est.	F_{S1} (min^{-1})	F_{S2} (min^{-1})	F_V (min^{-1})	l_u (m)	F_{HW} (min^{-1})	F_{GS} (min^{-1})
0.9	1.6	1.5	14	10	8	12.0	12.3	2.9
3.6	1.2	5.5	14	12	12	22	18.4	1.3
5.2	1.2	13.1	4	4	4	94	1.2	1.2
6.4	0.48	9.0	0	2	0	---	0.6	1.6
7.9	0.46	12.9	0	0	0	---	0.5	1.4

Table A.64: Flow property summary for 80% saltwater/20% light oil with carbon dioxide gas at a pressure of 0.79 MPa in a +5° inclined pipe at a superficial liquid velocity of 0.5 m/s.

V_{SG} (m/s)	V_t/V_m	Fr_f est.	F_{S1} (min^{-1})	F_{S2} (min^{-1})	F_V (min^{-1})	l_u (m)	F_{HW} (min^{-1})	F_{GS} (min^{-1})
0.9	2.1	2.4	12	12	0	---	17.2	11.5
3.7	0.90	4.1	26	24	28	8.1	20.9	9.7
5.2	0.89	8.5	24	24	20	15.3	2.4	8.7
6.3	1.2	15.9	28	26	26	18.7	1.7	9.0
8.2	1.2	23.5	18	18	16	38	1.2	10.0

Table A.65: Flow property summary for 80% saltwater/20% light oil with carbon dioxide gas at a pressure of 0.79 MPa in a +5° inclined pipe at a superficial liquid velocity of 1.0 m/s.

V_{SG} (m/s)	V_t/V_m	Fr_f est.	F_{S1} (min^{-1})	F_{S2} (min^{-1})	F_V (min^{-1})	l_u (m)	F_{HW} (min^{-1})	F_{GS} (min^{-1})
1.2	2.0	3.6	4	4	0	---	24.1	20.7
2.1	1.2	2.9	44	38	38	5.7	24.9	22.9
3.6	1.2	5.7	44	40	40	8.6	24.5	19.7
5.5	1.2	12.0	60	58	56	8.5	3.8	20.6
6.7	1.2	15.8	64	66	60	9.3	2.8	22.0

Table A.66: Flow property summary for 80% saltwater/20% light oil with carbon dioxide gas at a pressure of 0.79 MPa in a +5° inclined pipe at a superficial liquid velocity of 1.5 m/s.

V_{SG} (m/s)	V_t/V_m	Fr_f est.	F_{S1} (min^{-1})	F_{S2} (min^{-1})	F_V (min^{-1})	l_u (m)	F_{HW} (min^{-1})	F_{GS} (min^{-1})
1.0	2.0	3.6	0	0	0	---	30.7	32.6
2.4	1.2	3.4	70	68	66	4.1	31.3	33.6
4.4	1.2	7.1	80	76	72	6.0	29.3	32.7
6.7	1.2	14.9	82	84	76	7.8	4.4	37.0

Table A.67: Flow property summary for 40% saltwater/60% light oil with carbon dioxide gas at a pressure of 0.27 MPa in a +5° inclined pipe at a superficial liquid velocity of 0.1 m/s.

V_{SG} (m/s)	V_t/V_m	Fr_f est.	F_{S1} (min^{-1})	F_{S2} (min^{-1})	F_V (min^{-1})	l_u (m)	F_{HW} (min^{-1})	F_{GS} (min^{-1})
1.3	1.4	1.7	12	12	6	19.0	19.2	2.4
3.5	1.2	4.6	10	10	8	32	30.8	1.3
7.0	1.2	15.2	10	8	8	63	3.3	1.3
8.1	1.1	20.1	4	4	4	141	1.8	1.4

Table A.68: Flow property summary for 40% saltwater/60% light oil with carbon dioxide gas at a pressure of 0.27 MPa in a +5° inclined pipe at a superficial liquid velocity of 0.5 m/s.

V_{SG} (m/s)	V_t/V_m	Fr_f est.	F_{S1} (min^{-1})	F_{S2} (min^{-1})	F_V (min^{-1})	l_u (m)	F_{HW} (min^{-1})	F_{GS} (min^{-1})
1.3	1.2	1.6	32	30	22	5.7	23.4	15.1
3.0	1.2	3.9	28	26	24	10.2	31.9	9.3
5.4	1.2	9.8	24	24	24	17.5	8.8	8.7
7.4	1.2	16.2	30	26	26	22	4.2	9.7

Table A.69: Flow property summary for 40% saltwater/60% light oil with carbon dioxide gas at a pressure of 0.27 MPa in a +5° inclined pipe at a superficial liquid velocity of 1.0 m/s.

V_{SG} (m/s)	V_t/V_m	Fr_f est.	F_{S1} (min^{-1})	F_{S2} (min^{-1})	F_V (min^{-1})	l_u (m)	F_{HW} (min^{-1})	F_{GS} (min^{-1})
1.8	1.2	2.4	44	38	32	6.2	32.5	24.1
4.3	1.2	6.3	48	40	36	10.8	39.8	19.8
5.6	1.2	10.1	36	44	38	12.3	10.6	20.5
7.4	1.2	16.2	50	52	48	12.8	6.7	23.2

Table A.70: Flow property summary for 40% saltwater/60% light oil with carbon dioxide gas at a pressure of 0.27 MPa in a +5° inclined pipe at a superficial liquid velocity of 1.5 m/s.

V_{SG} (m/s)	V_t/V_m	Fr_f est.	F_{S1} (min^{-1})	F_{S2} (min^{-1})	F_V (min^{-1})	l_u (m)	F_{HW} (min^{-1})	F_{GS} (min^{-1})
1.4	1.9	4.0	0	0	0	---	37.6	32.1
3.1	1.2	4.3	62	68	52	6.3	44.6	32.2
5.2	1.2	9.3	58	76	58	8.4	14.7	33.8
7.0	1.2	13.4	86	82	80	7.6	10.0	37.4

Table A.71: Flow property summary for 40% saltwater/60% light oil with carbon dioxide gas at a pressure of 0.45 MPa in a +5° inclined pipe at a superficial liquid velocity of 0.1 m/s.

V_{SG} (m/s)	V_t/V_m	Fr_f est.	F_{S1} (min^{-1})	F_{S2} (min^{-1})	F_V (min^{-1})	l_u (m)	F_{HW} (min^{-1})	F_{GS} (min^{-1})
1.1	1.4	1.6	16	14	8	12.8	15.6	2.7
2.8	1.2	3.7	8	8	6	34	23.2	1.5
5.9	1.2	13.2	8	8	6	71	2.4	1.3
8.8	1.2	34.5	2	2	2	309	0.7	1.5

Table A.72: Flow property summary for 40% saltwater/60% light oil with carbon dioxide gas at a pressure of 0.45 MPa in a +5° inclined pipe at a superficial liquid velocity of 0.5 m/s.

V_{SG} (m/s)	V_t/V_m	Fr_f est.	F_{S1} (min^{-1})	F_{S2} (min^{-1})	F_V (min^{-1})	l_u (m)	F_{HW} (min^{-1})	F_{GS} (min^{-1})
1.1	2.2	2.9	32	34	0	---	20.8	10.1
3.4	1.2	4.7	26	26	24	11.5	27.4	8.9
6.1	1.2	13.2	36	36	26	18.0	3.3	8.9
8.4	1.2	22.2	24	24	22	28	1.7	10.2

Table A.73: Flow property summary for 40% saltwater/60% light oil with carbon dioxide gas at a pressure of 0.45 MPa in a +5° inclined pipe at a superficial liquid velocity of 1.0 m/s.

V_{SG} (m/s)	V_t/V_m	Fr_f est.	F_{S1} (min^{-1})	F_{S2} (min^{-1})	F_V (min^{-1})	l_u (m)	F_{HW} (min^{-1})	F_{GS} (min^{-1})
1.1	2.1	3.3	38	36	0	---	27.2	20.8
3.6	1.2	5.4	42	38	34	9.9	30.2	19.8
6.0	1.2	12.3	48	42	40	12.6	5.5	21.1
8.5	1.2	19.9	76	72	68	9.9	3.2	24.5

Table A.74: Flow property summary for 40% saltwater/60% light oil with carbon dioxide gas at a pressure of 0.45 MPa in a +5° inclined pipe at a superficial liquid velocity of 1.5 m/s.

V_{SG} (m/s)	V_t/V_m	Fr_f est.	F_{S1} (min^{-1})	F_{S2} (min^{-1})	F_V (min^{-1})	l_u (m)	F_{HW} (min^{-1})	F_{GS} (min^{-1})
1.7	1.2	2.5	54	58	44	5.3	35.0	35.7
3.3	1.2	4.7	62	68	52	6.5	36.0	32.1
6.2	1.2	12.6	84	82	64	8.7	7.1	35.8
7.0	1.2	14.5	102	100	92	6.6	6.2	37.4

Table A.75: Flow property summary for 40% saltwater/60% light oil with carbon dioxide gas at a pressure of 0.79 MPa in a +5° inclined pipe at a superficial liquid velocity of 0.1 m/s.

V_{SG} (m/s)	V_t/V_m	Fr_f est.	F_{S1} (min^{-1})	F_{S2} (min^{-1})	F_V (min^{-1})	l_u (m)	F_{HW} (min^{-1})	F_{GS} (min^{-1})
1.1	1.3	1.5	14	14	6	16.0	13.9	2.9
2.9	1.2	4.1	12	12	8	26	18.4	1.5
5.1	1.2	12.5	4	4	4	94	1.6	1.2
6.7	1.2	25.2	0	0	0	---	0.6	1.3

Table A.76: Flow property summary for 40% saltwater/60% light oil with carbon dioxide gas at a pressure of 0.79 MPa in a +5° inclined pipe at a superficial liquid velocity of 0.5 m/s.

V_{SG} (m/s)	V_t/V_m	Fr_f est.	F_{S1} (min^{-1})	F_{S2} (min^{-1})	F_V (min^{-1})	l_u (m)	F_{HW} (min^{-1})	F_{GS} (min^{-1})
1.1	1.4	1.9	22	20	18	7.7	17.5	13.9
3.1	1.2	4.5	32	32	30	8.4	20.6	9.2
4.7	1.2	7.4	26	30	22	16.9	19.3	8.6
6.9	1.2	18.1	34	34	24	22	1.4	9.3

Table A.77: Flow property summary for 40% saltwater/60% light oil with carbon dioxide gas at a pressure of 0.79 MPa in a +5° inclined pipe at a superficial liquid velocity of 1.0 m/s.

V_{SG} (m/s)	V_t/V_m	Fr_f est.	F_{S1} (min^{-1})	F_{S2} (min^{-1})	F_V (min^{-1})	l_u (m)	F_{HW} (min^{-1})	F_{GS} (min^{-1})
0.9	1.8	2.5	0	0	0	---	23.3	23.3
3.0	1.2	4.5	50	42	40	7.2	24.5	20.3
5.0	1.2	10.3	52	48	46	9.3	4.4	20.0
6.6	1.2	15.7	72	56	54	10.2	2.8	21.9

Table A.78: Flow property summary for 40% saltwater/60% light oil with carbon dioxide gas at a pressure of 0.79 MPa in a +5° inclined pipe at a superficial liquid velocity of 1.5 m/s.

V_{SG} (m/s)	V_t/V_m	Fr_f est.	F_{S1} (min^{-1})	F_{S2} (min^{-1})	F_V (min^{-1})	l_u (m)	F_{HW} (min^{-1})	F_{GS} (min^{-1})
1.0	2.0	3.6	0	0	0	---	30.7	32.6
2.7	1.2	4.1	62	50	50	6.0	29.5	32.7
3.8	1.2	5.9	76	56	56	6.8	28.3	32.1
5.1	1.2	10.2	80	66	62	7.5	6.1	33.4
6.4	1.2	14.2	84	70	66	8.7	4.6	36.4

Table A.79: Flow property summary for 100% saltwater with carbon dioxide gas at a pressure of 0.27 MPa in a -2° inclined pipe at a superficial liquid velocity of 0.1 m/s.

V_{SG} (m/s)	Fr_f est.	F_A (min^{-1})	l_u (m)	F_{HW} (min^{-1})	F_{GS} (min^{-1})
1.4	---	0	---	0.1	---
3.6	---	0	---	0.3	---
7.9	---	0	---	0.6	---
9.4	---	0	---	0.7	---

Table A.80: Flow property summary for 100% saltwater with carbon dioxide gas at a pressure of 0.27 MPa in a -2° inclined pipe at a superficial liquid velocity of 0.5 m/s.

V_{SG} (m/s)	Fr_f est.	F_A (min^{-1})	l_u (m)	F_{HW} (min^{-1})	F_{GS} (min^{-1})
1.4	---	0	---	0.5	---
4.2	---	0	---	1.2	---
7.9	19.5	20	30.	1.6	8.9
9.2	23.6	22	32	1.6	8.6

Table A.81: Flow property summary for 100% saltwater with carbon dioxide gas at a pressure of 0.27 MPa in a -2° inclined pipe at a superficial liquid velocity of 1.0 m/s.

V_{SG} (m/s)	Fr_f est.	F_A (min^{-1})	l_u (m)	F_{HW} (min^{-1})	F_{GS} (min^{-1})
1.5	---	0	---	2.0	---
3.2	6.1	26	11.6	3.2	22.1
6.9	14.0	34	16.7	3.8	20.9
7.7	16.0	34	18.4	3.6	22.0

Table A.82: Flow property summary for 100% saltwater with carbon dioxide gas at a pressure of 0.27 MPa in a -2° inclined pipe at a superficial liquid velocity of 1.5 m/s.

V_{SG} (m/s)	Fr_f est.	F_A (min^{-1})	l_u (m)	F_{HW} (min^{-1})	F_{GS} (min^{-1})
1.4	---	0	---	6.4	---
2.9	4.9	40	7.9	8.4	32.4
5.5	9.6	44	11.5	9.0	37.0
7.0	13.0	58	10.6	7.2	43.4

Table A.83: Flow property summary for 100% saltwater with carbon dioxide gas at a pressure of 0.45 MPa in a -2° inclined pipe at a superficial liquid velocity of 0.1 m/s.

V_{SG} (m/s)	Fr_f est.	F_A (min^{-1})	l_u (m)	F_{HW} (min^{-1})	F_{GS} (min^{-1})
1.1	---	0	---	0.1	---
3.5	---	0	---	0.3	---
5.6	---	0	---	0.4	---
8.6	---	0	---	0.6	---

Table A.84: Flow property summary for 100% saltwater with carbon dioxide gas at a pressure of 0.45 MPa in a -2° inclined pipe at a superficial liquid velocity of 0.5 m/s.

V_{SG} (m/s)	Fr_f est.	F_A (min^{-1})	l_u (m)	F_{HW} (min^{-1})	F_{GS} (min^{-1})
1.1	---	0	---	0.4	---
3.3	---	0	---	1.0	---
5.3	12.4	20	21	1.4	10.8
8.6	22.3	22	29	1.4	8.7

Table A.85: Flow property summary for 100% saltwater with carbon dioxide gas at a pressure of 0.45 MPa in a -2° inclined pipe at a superficial liquid velocity of 1.0 m/s.

V_{SG} (m/s)	Fr_f est.	F_A (min^{-1})	l_u (m)	F_{HW} (min^{-1})	F_{GS} (min^{-1})
1.2	---	0	---	1.8	---
2.8	5.4	24	11.4	2.9	23.9
6.0	12.0	30	16.8	3.6	20.1
7.7	16.5	34	18.4	3.1	22.0

Table A.86: Flow property summary for 100% saltwater with carbon dioxide gas at a pressure of 0.45 MPa in a -2° inclined pipe at a superficial liquid velocity of 1.5 m/s.

V_{SG} (m/s)	Fr_f est.	F_A (min^{-1})	l_u (m)	F_{HW} (min^{-1})	F_{GS} (min^{-1})
1.2	---	0	---	6.0	---
3.1	5.3	48	6.9	8.0	32.1
6.2	11.4	48	11.6	6.9	39.8
7.5	14.6	60	10.8	5.6	45.8

Table A.87: Flow property summary for 100% saltwater with carbon dioxide gas at a pressure of 0.79 MPa in a -2° inclined pipe at a superficial liquid velocity of 0.1 m/s.

V_{SG} (m/s)	Fr_f est.	F_A (min^{-1})	l_u (m)	F_{HW} (min^{-1})	F_{GS} (min^{-1})
1.0	---	0	---	0.1	---
3.2	---	0	---	0.3	---
4.6	---	0	---	0.4	---
5.7	---	0	---	0.4	---
7.1	---	0	---	0.5	---

Table A.88: Flow property summary for 100% saltwater with carbon dioxide gas at a pressure of 0.79 MPa in a -2° inclined pipe at a superficial liquid velocity of 0.5 m/s.

V_{SG} (m/s)	Fr_f est.	F_A (min^{-1})	l_u (m)	F_{HW} (min^{-1})	F_{GS} (min^{-1})
0.8	---	0	---	0.3	---
3.1	---	0	---	0.9	---
5.4	12.9	20	21	1.3	10.6
6.9	17.4	28	19.0	1.3	9.3

Table A.89: Flow property summary for 100% saltwater with carbon dioxide gas at a pressure of 0.79 MPa in a -2° inclined pipe at a superficial liquid velocity of 1.0 m/s.

V_{SG} (m/s)	Fr_f est.	F_A (min^{-1})	l_u (m)	F_{HW} (min^{-1})	F_{GS} (min^{-1})
0.9	---	0	---	1.6	---
3.3	6.4	26	11.9	3.0	21.8
5.9	12.1	32	15.5	3.1	20.0
7.4	16.3	32	18.9	2.7	21.6

Table A.90: Flow property summary for 100% saltwater with carbon dioxide gas at a pressure of 0.79 MPa in a -2° inclined pipe at a superficial liquid velocity of 1.5 m/s.

V_{SG} (m/s)	Fr_f est.	F_A (min^{-1})	l_u (m)	F_{HW} (min^{-1})	F_{GS} (min^{-1})
0.9	---	0	---	5.4	---
2.9	5.1	46	6.9	7.1	32.4
5.9	11.1	56	9.5	6.0	38.6
6.8	13.4	56	10.7	5.0	42.5

Table A.91: Flow property summary for 80% saltwater/20% light oil with carbon dioxide gas at a pressure of 0.27 MPa in a -2° inclined pipe at a superficial liquid velocity of 0.1 m/s.

V_{SG} (m/s)	Fr_f est.	F_A (min^{-1})	l_u (m)	F_{HW} (min^{-1})	F_{GS} (min^{-1})
1.4	---	0	---	0.1	---
3.3	---	0	---	0.3	---
6.3	---	0	---	0.5	---
8.5	---	0	---	0.6	---

Table A.92: Flow property summary for 80% saltwater/20% light oil with carbon dioxide gas at a pressure of 0.27 MPa in a -2° inclined pipe at a superficial liquid velocity of 0.5 m/s.

V_{SG} (m/s)	Fr_f est.	F_A (min^{-1})	l_u (m)	F_{HW} (min^{-1})	F_{GS} (min^{-1})
1.4	---	0	---	0.5	---
3.3	---	0	---	1.0	---
6.3	14.8	18	27	1.5	9.7
8.4	20.9	18	36	1.6	8.7

Table A.93: Flow property summary for 80% saltwater/20% light oil with carbon dioxide gas at a pressure of 0.27 MPa in a -2° inclined pipe at a superficial liquid velocity of 1.0 m/s.

V_{SG} (m/s)	Fr_f est.	F_A (min^{-1})	l_u (m)	F_{HW} (min^{-1})	F_{GS} (min^{-1})
1.4	---	0	---	2.1	---
3.4	6.4	28	11.3	3.5	21.5
5.8	11.3	32	15.3	4.2	20.0
7.2	14.7	36	16.4	3.8	21.3

Table A.94: Flow property summary for 80% saltwater/20% light oil with carbon dioxide gas at a pressure of 0.27 MPa in a -2° inclined pipe at a superficial liquid velocity of 1.5 m/s.

V_{SG} (m/s)	Fr_f est.	F_A (min^{-1})	l_u (m)	F_{HW} (min^{-1})	F_{GS} (min^{-1})
1.4	---	0	---	6.9	---
3.3	5.6	32	10.8	9.2	32.0
6.1	10.9	44	12.4	8.4	39.4
7.4	13.9	54	11.9	6.9	45.3

Table A.95: Flow property summary for 80% saltwater/20% light oil with carbon dioxide gas at a pressure of 0.45 MPa in a -2° inclined pipe at a superficial liquid velocity of 0.1 m/s.

V_{SG} (m/s)	Fr_f est.	F_A (min^{-1})	l_u (m)	F_{HW} (min^{-1})	F_{GS} (min^{-1})
1.1	---	0	---	0.1	---
3.0	---	0	---	0.2	---
5.9	---	0	---	0.5	---
8.3	---	0	---	0.6	---

Table A.96: Flow property summary for 80% saltwater/20% light oil with carbon dioxide gas at a pressure of 0.45 MPa in a -2° inclined pipe at a superficial liquid velocity of 0.5 m/s.

V_{SG} (m/s)	Fr_f est.	F_A (min^{-1})	l_u (m)	F_{HW} (min^{-1})	F_{GS} (min^{-1})
0.9	---	0	---	0.4	---
3.0	---	0	---	0.9	---
6.1	14.5	14	34	1.4	9.9
8.0	20.3	24	26	1.4	8.8

Table A.97: Flow property summary for 80% saltwater/20% light oil with carbon dioxide gas at a pressure of 0.45 MPa in a -2° inclined pipe at a superficial liquid velocity of 1.0 m/s.

V_{SG} (m/s)	Fr_f est.	F_A (min^{-1})	l_u (m)	F_{HW} (min^{-1})	F_{GS} (min^{-1})
1.2	---	0	---	1.9	---
3.0	5.7	30	9.6	3.2	22.9
5.9	11.7	28	17.7	3.7	20.0
7.7	16.4	46	13.6	3.2	22.0

Table A.98: Flow property summary for 80% saltwater/20% light oil with carbon dioxide gas at a pressure of 0.45 MPa in a -2° inclined pipe at a superficial liquid velocity of 1.5 m/s.

V_{SG} (m/s)	Fr_f est.	F_A (min^{-1})	l_u (m)	F_{HW} (min^{-1})	F_{GS} (min^{-1})
1.3	---	0	---	3.2	---
3.5	6.0	42	8.6	6.5	32.1
6.1	11.2	56	9.8	8.6	39.4
7.9	15.6	52	13.0	7.1	47.8

Table A.99: Flow property summary for 80% saltwater/20% light oil with carbon dioxide gas at a pressure of 0.79 MPa in a -2° inclined pipe at a superficial liquid velocity of 0.1 m/s.

V_{SG} (m/s)	Fr_f est.	F_A (min^{-1})	l_u (m)	F_{HW} (min^{-1})	F_{GS} (min^{-1})
1.0	---	0	---	0.1	---
4.0	---	0	---	0.3	---
5.1	---	0	---	0.4	---
5.6	---	0	---	0.4	---

Table A.100: Flow property summary for 80% saltwater/20% light oil with carbon dioxide gas at a pressure of 0.79 MPa in a -2° inclined pipe at a superficial liquid velocity of 0.5 m/s.

V_{SG} (m/s)	Fr_f est.	F_A (min^{-1})	l_u (m)	F_{HW} (min^{-1})	F_{GS} (min^{-1})
0.8	---	0	---	0.4	---
3.5	---	0	---	1.0	---
4.5	---	0	---	1.2	---
5.9	14.3	26	17.7	1.3	10.1

Table A.101: Flow property summary for 80% saltwater/20% light oil with carbon dioxide gas at a pressure of 0.79 MPa in a -2° inclined pipe at a superficial liquid velocity of 1.0 m/s.

V_{SG} (m/s)	Fr_f est.	F_A (min^{-1})	l_u (m)	F_{HW} (min^{-1})	F_{GS} (min^{-1})
1.2	---	0	---	1.9	---
3.5	6.6	20	16.2	3.2	21.2
4.9	9.1	30	14.2	3.6	19.7
5.6	11.5	30	15.8	3.3	19.8

Table A.102: Flow property summary for 80% saltwater/20% light oil with carbon dioxide gas at a pressure of 0.79 MPa in a -2° inclined pipe at a superficial liquid velocity of 1.5 m/s.

V_{SG} (m/s)	Fr_f est.	F_A (min^{-1})	l_u (m)	F_{HW} (min^{-1})	F_{GS} (min^{-1})
1.0	---	0	---	5.9	---
3.8	6.6	46	8.3	7.6	32.4
5.1	9.1	54	8.8	7.6	35.6
6.1	11.5	66	8.3	5.8	39.4

Table A.103: Flow property summary for 40% saltwater/60% light oil with carbon dioxide gas at a pressure of 0.27 MPa in a -2° inclined pipe at a superficial liquid velocity of 0.1 m/s.

V_{SG} (m/s)	Fr_f est.	F_A (min^{-1})	l_u (m)	F_{HW} (min^{-1})	F_{GS} (min^{-1})
1.4	---	0	---	0.1	---
3.3	---	0	---	0.3	---
5.8	---	0	---	0.5	---
7.9	---	0	---	0.6	---

Table A.104: Flow property summary for 40% saltwater/60% light oil with carbon dioxide gas at a pressure of 0.27 MPa in a -2° inclined pipe at a superficial liquid velocity of 0.5 m/s.

V_{SG} (m/s)	Fr_f est.	F_A (min^{-1})	l_u (m)	F_{HW} (min^{-1})	F_{GS} (min^{-1})
1.4	---	0	---	1.5	---
3.0	---	0	---	1.0	---
6.6	15.5	12	43	1.6	9.5
7.5	18.1	18	32	1.6	9.0

Table A.105: Flow property summary for 40% saltwater/60% light oil with carbon dioxide gas at a pressure of 0.27 MPa in a -2° inclined pipe at a superficial liquid velocity of 1.0 m/s.

V_{SG} (m/s)	Fr_f est.	F_A (min^{-1})	l_u (m)	F_{HW} (min^{-1})	F_{GS} (min^{-1})
1.3	---	0	---	2.2	---
2.9	5.4	30	9.4	3.4	23.3
5.7	11.0	30	16.1	4.4	19.9
6.8	13.6	38	14.8	4.0	20.8

Table A.106: Flow property summary for 40% saltwater/60% light oil with carbon dioxide gas at a pressure of 0.27 MPa in a -2° inclined pipe at a superficial liquid velocity of 1.5 m/s.

V_{SG} (m/s)	Fr_f est.	F_A (min^{-1})	l_u (m)	F_{HW} (min^{-1})	F_{GS} (min^{-1})
1.4	---	0	---	7.7	---
2.9	4.8	38	8.3	9.6	32.4
5.7	9.9	52	10.0	9.3	37.8
6.5	11.7	56	10.3	8.0	41.1

Table A.107: Flow property summary for 40% saltwater/60% light oil with carbon dioxide gas at a pressure of 0.45 MPa in a -2° inclined pipe at a superficial liquid velocity of 0.1 m/s.

V_{SG} (m/s)	Fr_f est.	F_A (min^{-1})	l_u (m)	F_{HW} (min^{-1})	F_{GS} (min^{-1})
1.2	---	0	---	0.1	---
3.4	---	0	---	0.3	---
6.1	---	0	---	0.5	---
7.1	---	0	---	0.5	---
8.1	---	0	---	0.6	---

Table A.108: Flow property summary for 40% saltwater/60% light oil with carbon dioxide gas at a pressure of 0.45 MPa in a -2° inclined pipe at a superficial liquid velocity of 0.5 m/s.

V_{SG} (m/s)	Fr_f est.	F_A (min^{-1})	l_u (m)	F_{HW} (min^{-1})	F_{GS} (min^{-1})
1.2	---	0	---	0.5	---
2.6	---	0	---	0.9	---
5.0	11.4	10	40.	1.4	11.2
7.6	18.9	20	29	1.5	9.0

Table A.109: Flow property summary for 40% saltwater/60% light oil with carbon dioxide gas at a pressure of 0.45 MPa in a -2° inclined pipe at a superficial liquid velocity of 1.0 m/s.

V_{SG} (m/s)	Fr_f est.	F_A (min^{-1})	l_u (m)	F_{HW} (min^{-1})	F_{GS} (min^{-1})
1.0	---	0	---	1.9	---
3.0	5.7	24	12.0	3.4	22.9
5.4	10.4	34	13.6	4.1	19.8
7.5	15.8	36	17.0	3.3	21.7

Table A.110: Flow property summary for 40% saltwater/60% light oil with carbon dioxide gas at a pressure of 0.45 MPa in a -2° inclined pipe at a superficial liquid velocity of 1.5 m/s.

V_{SG} (m/s)	Fr_f est.	F_A (min^{-1})	l_u (m)	F_{HW} (min^{-1})	F_{GS} (min^{-1})
1.2	---	0	---	7.1	---
3.2	5.4	42	8.1	9.0	32.1
5.3	9.3	50	9.8	8.8	36.3
7.5	14.5	52	12.5	5.8	45.8

Table A.111: Flow property summary for 40% saltwater/60% light oil with carbon dioxide gas at a pressure of 0.79 MPa in a -2° inclined pipe at a superficial liquid velocity of 0.1 m/s.

V_{SG} (m/s)	Fr_f est.	F_A (min^{-1})	l_u (m)	F_{HW} (min^{-1})	F_{GS} (min^{-1})
1.0	---	0	---	0.1	---
3.4	---	0	---	0.3	---
5.2	---	0	---	0.4	---
6.0	---	0	---	0.5	---
7.3	---	0	---	0.5	---

Table A.112: Flow property summary for 40% saltwater/60% light oil with carbon dioxide gas at a pressure of 0.79 MPa in a -2° inclined pipe at a superficial liquid velocity of 0.5 m/s.

V_{SG} (m/s)	Fr_f est.	F_A (min^{-1})	l_u (m)	F_{HW} (min^{-1})	F_{GS} (min^{-1})
0.9	---	0	---	0.4	---
2.9	---	0	---	0.9	---
5.2	12.1	16	26	1.3	10.9
8.1	21.4	24	26	1.3	8.8

Table A.113: Flow property summary for 40% saltwater/60% light oil with carbon dioxide gas at a pressure of 0.79 MPa in a -2° inclined pipe at a superficial liquid velocity of 1.0 m/s.

V_{SG} (m/s)	Fr_f est.	F_A (min^{-1})	l_u (m)	F_{HW} (min^{-1})	F_{GS} (min^{-1})
0.9	---	0	---	1.8	---
3.1	5.9	36	8.2	3.2	22.5
5.4	10.7	34	13.6	3.6	19.8
7.2	15.6	38	15.5	2.8	21.3

Table A.114: Flow property summary for 40% saltwater/60% light oil with carbon dioxide gas at a pressure of 0.79 MPa in a -2° inclined pipe at a superficial liquid velocity of 1.5 m/s.

V_{SG} (m/s)	Fr_f est.	F_A (min^{-1})	l_u (m)	F_{HW} (min^{-1})	F_{GS} (min^{-1})
0.9	---	0	---	6.4	---
3.4	5.9	52	6.8	7.9	32.0
5.4	9.8	54	9.2	7.1	36.7
6.3	12.0	64	8.8	5.7	40.3

Table A.115: Flow property summary for 80% saltwater/20% light oil with carbon dioxide gas at a pressure of 0.27 MPa in a -5° inclined pipe at a superficial liquid velocity of 0.1 m/s.

V_{SG} (m/s)	Fr_f est.	F_A (min^{-1})	l_u (m)	F_{HW} (min^{-1})	F_{GS} (min^{-1})
1.4	---	0	---	0.1	---
3.9	---	0	---	0.3	---
7.8	---	0	---	0.5	---
10.2	---	0	---	0.7	---

Table A.116: Flow property summary for 80% saltwater/20% light oil with carbon dioxide gas at a pressure of 0.27 MPa in a -5° inclined pipe at a superficial liquid velocity of 0.5 m/s.

V_{SG} (m/s)	Fr_f est.	F_A (min^{-1})	l_u (m)	F_{HW} (min^{-1})	F_{GS} (min^{-1})
1.7	---	0	---	0.3	---
4.2	---	0	---	0.7	---
7.0	---	0	---	1.1	---
11.2	31.9	12	70.	1.4	8.6

Table A.117: Flow property summary for 80% saltwater/20% light oil with carbon dioxide gas at a pressure of 0.27 MPa in a -5° inclined pipe at a superficial liquid velocity of 1.0 m/s.

V_{SG} (m/s)	Fr_f est.	F_A (min^{-1})	l_u (m)	F_{HW} (min^{-1})	F_{GS} (min^{-1})
1.3	---	0	---	0.8	---
3.9	8.6	20	17.6	1.7	20.4
5.6	12.3	30	15.8	2.5	19.8
7.8	17.6	44	14.4	2.5	22.1

Table A.118: Flow property summary for 80% saltwater/20% light oil with carbon dioxide gas at a pressure of 0.45 MPa in a -5° inclined pipe at a superficial liquid velocity of 0.1 m/s.

V_{SG} (m/s)	Fr_f est.	F_A (min^{-1})	l_u (m)	F_{HW} (min^{-1})	F_{GS} (min^{-1})
1.3	---	0	---	0.1	---
3.2	---	0	---	0.2	---
4.8	---	0	---	0.3	---
6.4	---	0	---	0.4	---
8.4	---	0	---	0.5	---
11.1	---	0	---	0.7	---

Table A.119: Flow property summary for 80% saltwater/20% light oil with carbon dioxide gas at a pressure of 0.45 MPa in a -5° inclined pipe at a superficial liquid velocity of 0.5 m/s.

V_{SG} (m/s)	Fr_f est.	F_A (min^{-1})	l_u (m)	F_{HW} (min^{-1})	F_{GS} (min^{-1})
1.2	---	0	---	0.3	---
3.1	---	0	---	0.6	---
4.7	---	0	---	0.8	---
7.1	---	0	---	1.1	---
9.7	27.5	22	33.4	1.2	8.6

Table A.120: Flow property summary for 80% saltwater/20% light oil with carbon dioxide gas at a pressure of 0.45 MPa in a -5° inclined pipe at a superficial liquid velocity of 1.0 m/s.

V_{SG} (m/s)	Fr_f est.	F_A (min^{-1})	l_u (m)	F_{HW} (min^{-1})	F_{GS} (min^{-1})
1.1	---	0	---	0.7	---
2.8	---	0	---	1.3	---
4.9	---	0	---	2.0	---
8.0	18.4	40	16.2	2.3	22.4

Table A.121: Flow property summary for 80% saltwater/20% light oil with carbon dioxide gas at a pressure of 0.45 MPa in a -5° inclined pipe at a superficial liquid velocity of 1.5 m/s.

V_{SG} (m/s)	Fr_f est.	F_A (min^{-1})	l_u (m)	F_{HW} (min^{-1})	F_{GS} (min^{-1})
1.2	---	0	---	1.9	---
3.5	7.0	32	11.2	3.4	32.1
5.1	10.0	54	8.8	4.2	35.6
7.8	16.2	56	12.0	4.0	47.3

Table A.122: Flow property summary for 80% saltwater/20% light oil with carbon dioxide gas at a pressure of 0.79 MPa in a -5° inclined pipe at a superficial liquid velocity of 0.1 m/s.

V_{SG} (m/s)	Fr_f est.	F_A (min^{-1})	l_u (m)	F_{HW} (min^{-1})	F_{GS} (min^{-1})
0.9	---	0	---	0.1	---
3.6	---	0	---	0.3	---
5.2	---	0	---	0.4	---
6.4	---	0	---	0.4	---
7.9	---	0	---	0.5	---

Table A.123: Flow property summary for 80% saltwater/20% light oil with carbon dioxide gas at a pressure of 0.79 MPa in a -5° inclined pipe at a superficial liquid velocity of 0.5 m/s.

V_{SG} (m/s)	Fr_f est.	F_A (min^{-1})	l_u (m)	F_{HW} (min^{-1})	F_{GS} (min^{-1})
0.9	---	0	---	0.2	---
3.7	---	0	---	0.7	---
5.2	---	0	---	0.9	---
6.3	---	0	---	1.0	---
8.2	---	0	---	1.1	---

Table A.124: Flow property summary for 80% saltwater/20% light oil with carbon dioxide gas at a pressure of 0.79 MPa in a -5° inclined pipe at a superficial liquid velocity of 1.0 m/s.

V_{SG} (m/s)	Fr_f est.	F_A (min^{-1})	l_u (m)	F_{HW} (min^{-1})	F_{GS} (min^{-1})
1.2	---	0	---	0.8	---
2.1	---	0	---	1.1	---
3.6	---	0	---	1.6	---
5.5	12.2	32	14.6	2.0	19.8
6.7	15.3	46	12.1	2.1	20.7

Table A.125: Flow property summary for 80% saltwater/20% light oil with carbon dioxide gas at a pressure of 0.79 MPa in a -5° inclined pipe at a superficial liquid velocity of 1.5 m/s.

V_{SG} (m/s)	Fr_f est.	F_A (min^{-1})	l_u (m)	F_{HW} (min^{-1})	F_{GS} (min^{-1})
1.0	---	0	---	1.8	---
2.4	---	0	---	2.7	---
4.4	8.7	50	8.5	3.7	33.5
6.7	13.9	56	10.5	3.7	42.0

Table A.126: Flow property summary for 40% saltwater/60% light oil with carbon dioxide gas at a pressure of 0.27 MPa in a -5° inclined pipe at a superficial liquid velocity of 0.1 m/s.

V_{SG} (m/s)	Fr_f est.	F_A (min^{-1})	l_u (m)	F_{HW} (min^{-1})	F_{GS} (min^{-1})
1.3	---	0	---	0.1	---
3.5	---	0	---	0.2	---
7.0	---	0	---	0.5	---
8.1	---	0	---	0.5	---

Table A.127: Flow property summary for 40% saltwater/60% light oil with carbon dioxide gas at a pressure of 0.27 MPa in a -5° inclined pipe at a superficial liquid velocity of 0.5 m/s.

V_{SG} (m/s)	Fr_f est.	F_A (min^{-1})	l_u (m)	F_{HW} (min^{-1})	F_{GS} (min^{-1})
1.3	---	0	---	0.3	---
3.0	---	0	---	0.6	---
5.4	---	0	---	0.9	---
7.4	19.6	22	26	1.2	9.0

Table A.128: Flow property summary for 40% saltwater/60% light oil with carbon dioxide gas at a pressure of 0.27 MPa in a -5° inclined pipe at a superficial liquid velocity of 1.0 m/s.

V_{SG} (m/s)	Fr_f est.	F_A (min^{-1})	l_u (m)	F_{HW} (min^{-1})	F_{GS} (min^{-1})
1.8	---	0	---	1.0	---
3.1	---	0	---	1.5	---
4.3	9.3	22	17.3	1.9	20.0
5.6	12.1	30	15.8	2.3	19.8
7.4	16.4	30	20.	2.5	21.6

Table A.129: Flow property summary for 40% saltwater/60% light oil with carbon dioxide gas at a pressure of 0.27 MPa in a -5° inclined pipe at a superficial liquid velocity of 1.5 m/s.

V_{SG} (m/s)	Fr_f est.	F_A (min^{-1})	l_u (m)	F_{HW} (min^{-1})	F_{GS} (min^{-1})
1.4	---	0	---	2.2	---
3.1	---	0	---	3.4	---
5.2	10.1	28	17.2	4.7	35.9
7.0	13.9	56	10.9	4.7	43.4

Table A.130: Flow property summary for 40% saltwater/60% light oil with carbon dioxide gas at a pressure of 0.45 MPa in a -5° inclined pipe at a superficial liquid velocity of 0.1 m/s.

V_{SG} (m/s)	Fr_f est.	F_A (min^{-1})	l_u (m)	F_{HW} (min^{-1})	F_{GS} (min^{-1})
1.1	---	0	---	0.1	---
2.8	---	0	---	0.2	---
5.9	---	0	---	0.4	---
8.8	---	0	---	0.6	--

Table A.131: Flow property summary for 40% saltwater/60% light oil with carbon dioxide gas at a pressure of 0.45 MPa in a -5° inclined pipe at a superficial liquid velocity of 0.5 m/s.

V_{SG} (m/s)	Fr_f est.	F_A (min^{-1})	l_u (m)	F_{HW} (min^{-1})	F_{GS} (min^{-1})
1.1	---	0	---	0.3	---
3.4	---	0	---	0.6	---
6.1	16.0	14	34	1.0	9.9
8.4	23.0	28	23	1.2	8.7

Table A.132: Flow property summary for 40% saltwater/60% light oil with carbon dioxide gas at a pressure of 0.45 MPa in a -5° inclined pipe at a superficial liquid velocity of 1.0 m/s.

V_{SG} (m/s)	Fr_f est.	F_A (min^{-1})	l_u (m)	F_{HW} (min^{-1})	F_{GS} (min^{-1})
1.1	---	0	---	0.8	---
3.6	---	0	---	1.7	---
6.0	13.2	28	18.0	2.3	20.1
8.5	19.7	40	17.1	2.3	23.2

Table A.133: Flow property summary for 40% saltwater/60% light oil with carbon dioxide gas at a pressure of 0.45 MPa in a -5° inclined pipe at a superficial liquid velocity of 1.5 m/s.

V_{SG} (m/s)	Fr_f est.	F_A (min^{-1})	l_u (m)	F_{HW} (min^{-1})	F_{GS} (min^{-1})
1.7	---	0	---	2.4	---
3.3	---	0	---	3.5	---
6.2	12.3	46	12.1	4.4	39.8
7.0	14.2	64	9.6	4.3	43.4

Table A.134: Flow property summary for 40% saltwater/60% light oil with carbon dioxide gas at a pressure of 0.79 MPa in a -5° inclined pipe at a superficial liquid velocity of 0.1 m/s.

V_{SG} (m/s)	Fr_f est.	F_A (min^{-1})	l_u (m)	F_{HW} (min^{-1})	F_{GS} (min^{-1})
1.1	---	0	---	0.1	---
2.9	---	0	---	0.2	---
5.1	---	0	---	0.4	---
6.7	---	0	---	0.4	---

Table A.135: Flow property summary for 40% saltwater/60% light oil with carbon dioxide gas at a pressure of 0.79 MPa in a -5° inclined pipe at a superficial liquid velocity of 0.5 m/s.

V_{SG} (m/s)	Fr_f est.	F_A (min^{-1})	l_u (m)	F_{HW} (min^{-1})	F_{GS} (min^{-1})
1.1	---	0	---	0.3	---
3.1	---	0	---	0.6	---
4.7	---	0	---	0.8	---
6.9	18.7	24	22	1.0	9.3

Table A.136: Flow property summary for 40% saltwater/60% light oil with carbon dioxide gas at a pressure of 0.79 MPa in a -5° inclined pipe at a superficial liquid velocity of 1.0 m/s.

V_{SG} (m/s)	Fr_f est.	F_A (min^{-1})	l_u (m)	F_{HW} (min^{-1})	F_{GS} (min^{-1})
0.9	---	0	---	0.7	---
3.0	---	0	---	1.5	---
5.0	10.9	44	9.8	2.1	19.7
6.6	14.9	38	14.4	2.1	20.6

Table A.137: Flow property summary for 40% saltwater/60% light oil with carbon dioxide gas at a pressure of 0.79 MPa in a -5° inclined pipe at a superficial liquid velocity of 1.5 m/s.

V_{SG} (m/s)	Fr_f est.	F_A (min^{-1})	l_u (m)	F_{HW} (min^{-1})	F_{GS} (min^{-1})
1.0	---	0	---	1.9	---
2.7	---	0	---	3.1	---
3.8	7.5	40	9.5	3.7	32.4
5.1	10.0	50	9.5	4.2	35.6
6.4	13.1	48	11.8	3.9	40.7

CHAPTER 12

APPENDIX B

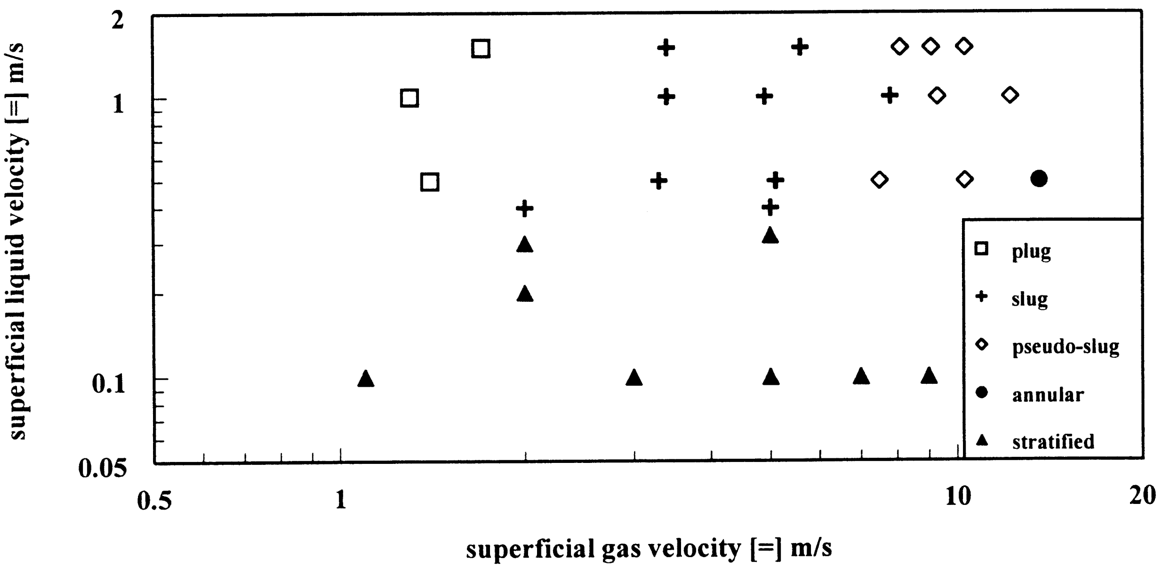

Figure B1: Flow regime map for 100% saltwater at 0.45 MPa and 0° inclination.

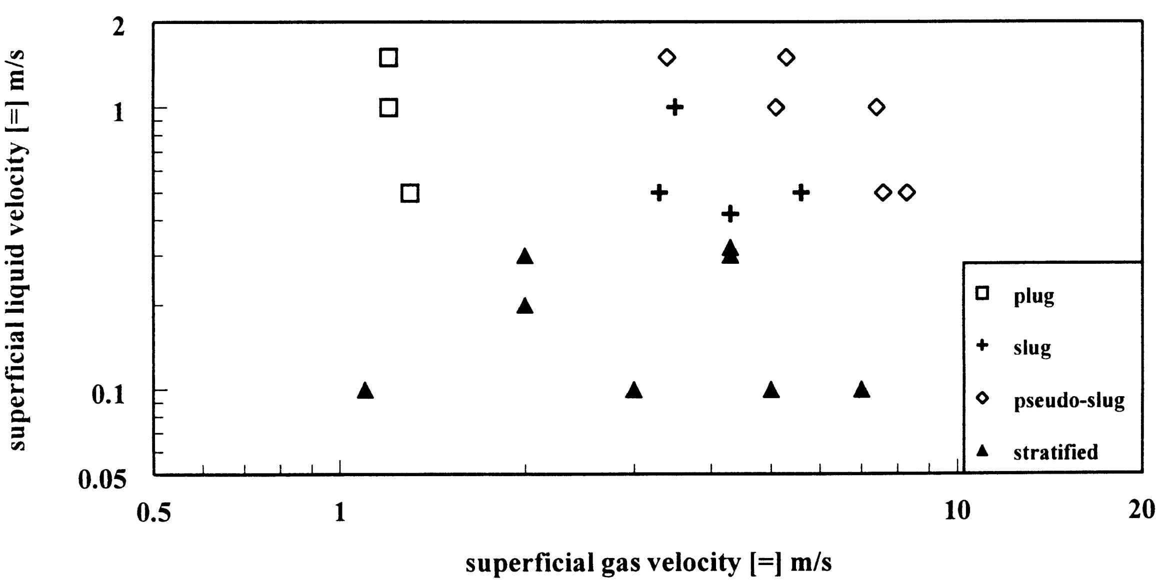

Figure B2: Flow regime map for 100% saltwater at 0.79 MPa and 0° inclination.

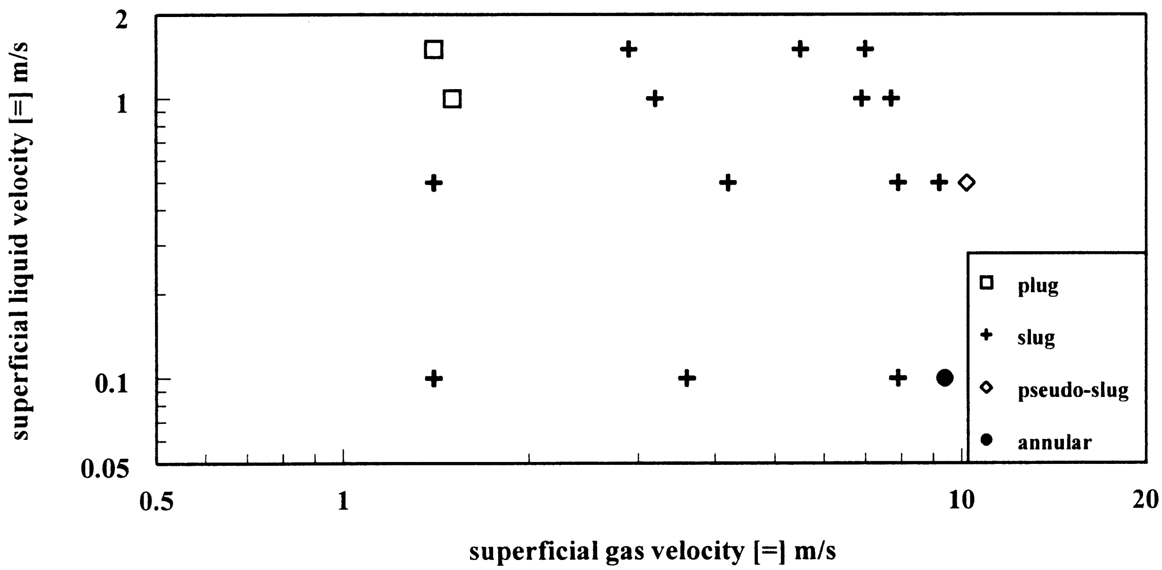

Figure B3: Flow regime map for 100% saltwater at 0.27 MPa and +2° inclination.

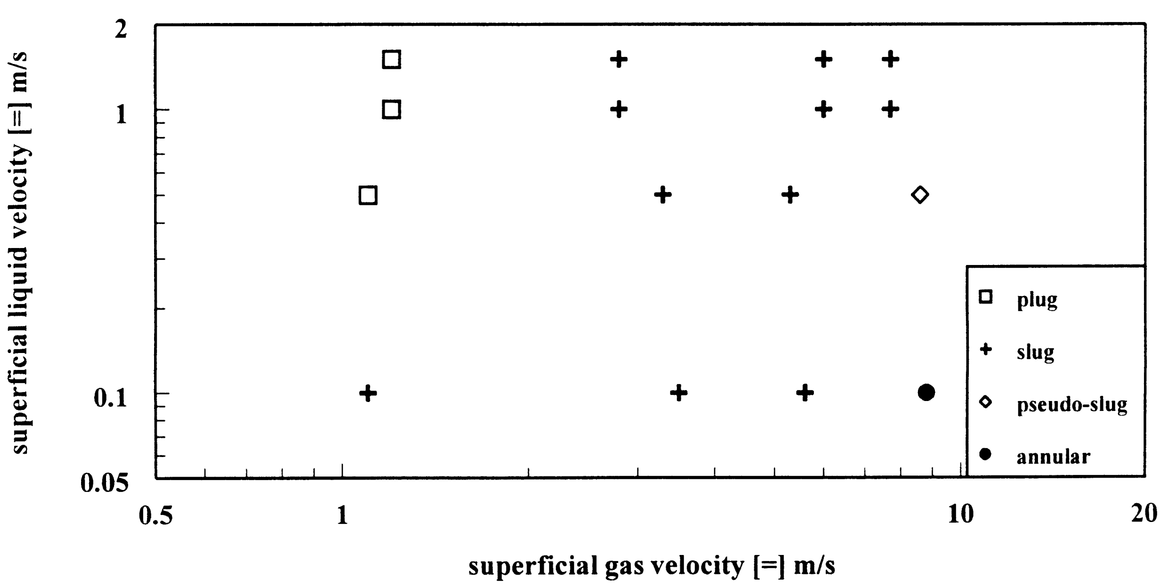

Figure B4: Flow regime map for 100% saltwater at 0.45 MPa and +2° inclination.

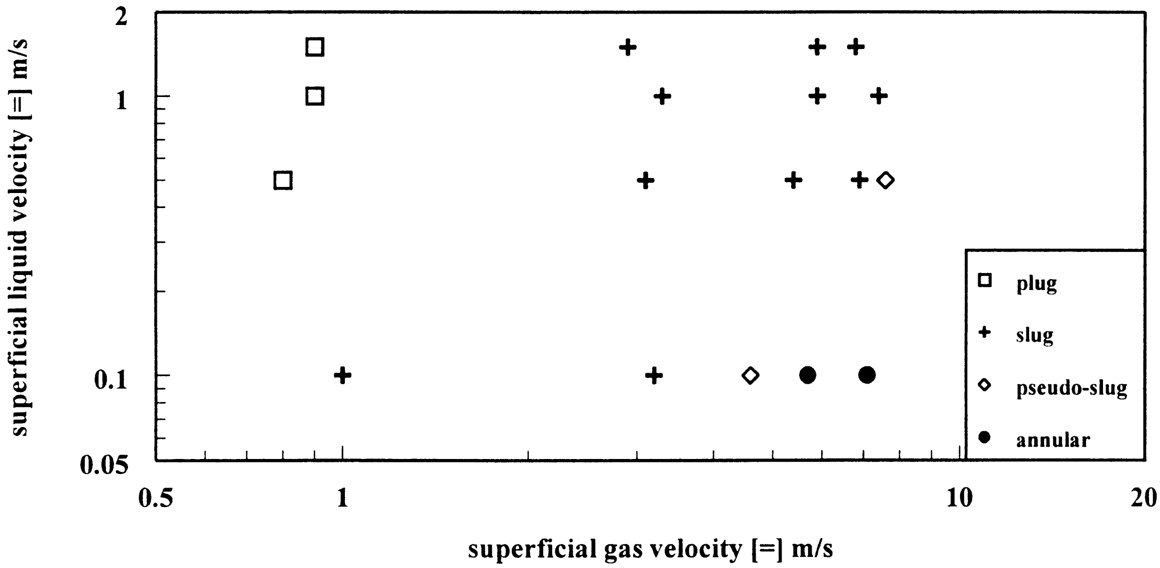

Figure B5: Flow regime map for 100% saltwater at 0.79 MPa and +2° inclination.

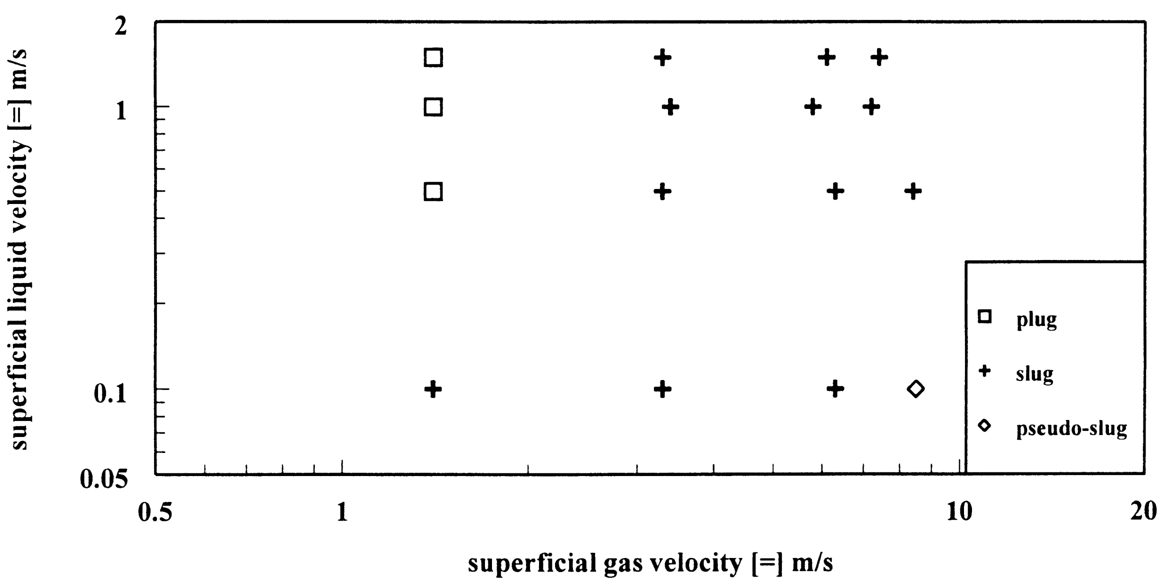

Figure B6: Flow regime map for 80% saltwater/20% light oil at 0.27 MPa and +2° inclination.

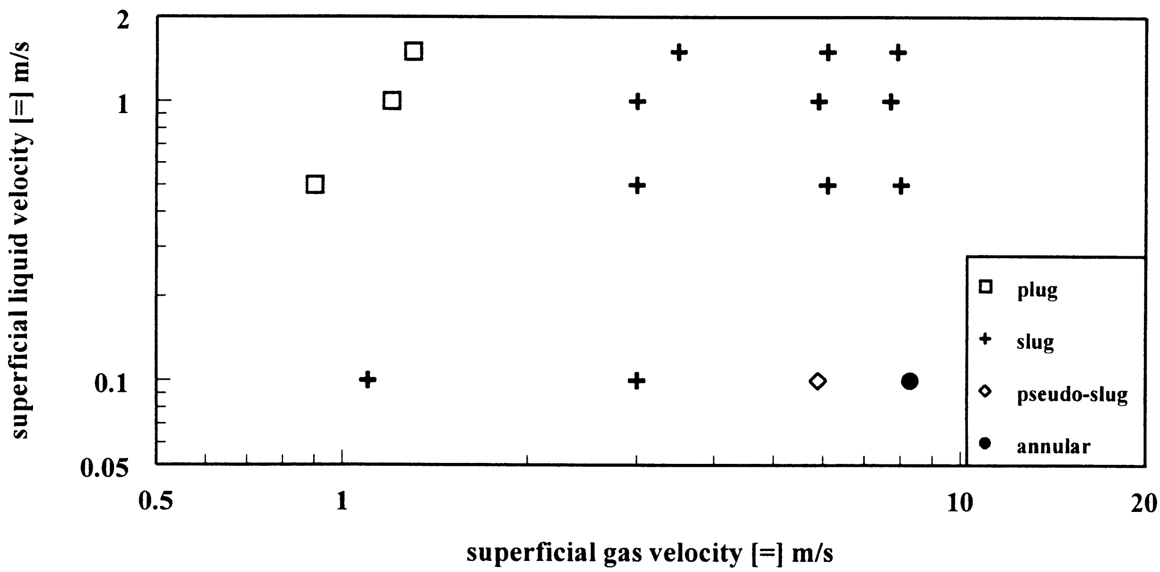

Figure B7: Flow regime map for 80% saltwater/20% light oil at 0.45 MPa and +2° inclination.

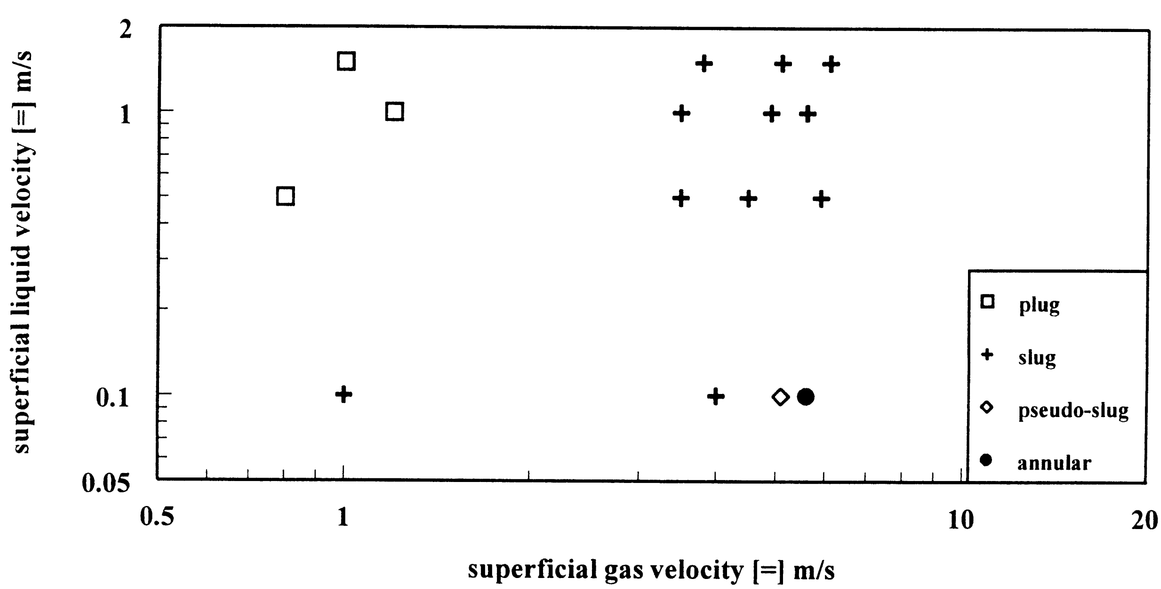

Figure B8: Flow regime map for 80% saltwater/20% light oil at 0.79 MPa and +2° inclination.

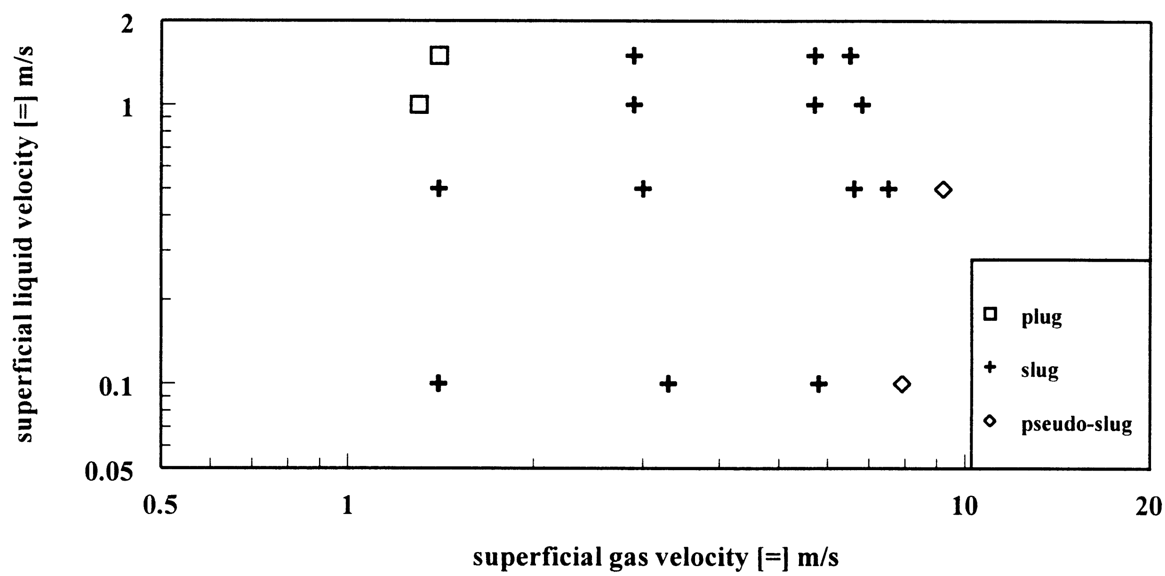

Figure B9: Flow regime map for 40% saltwater/60% light oil at 0.27 MPa and +2° inclination.

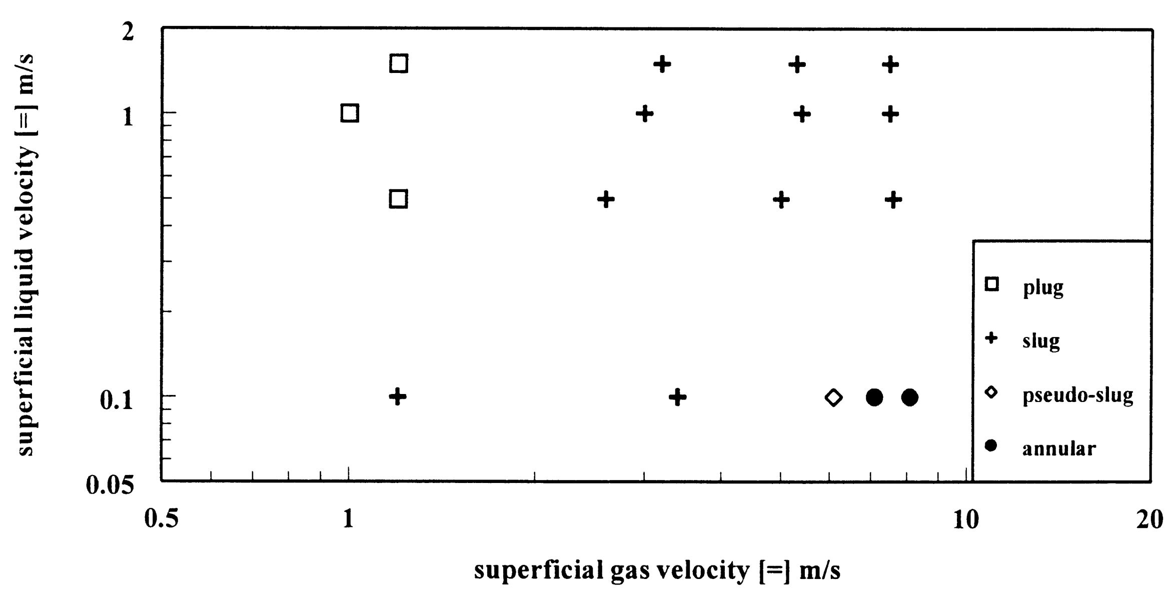

Figure B10: Flow regime map for 40% saltwater/60% light oil at 0.45 MPa and +2° inclination.

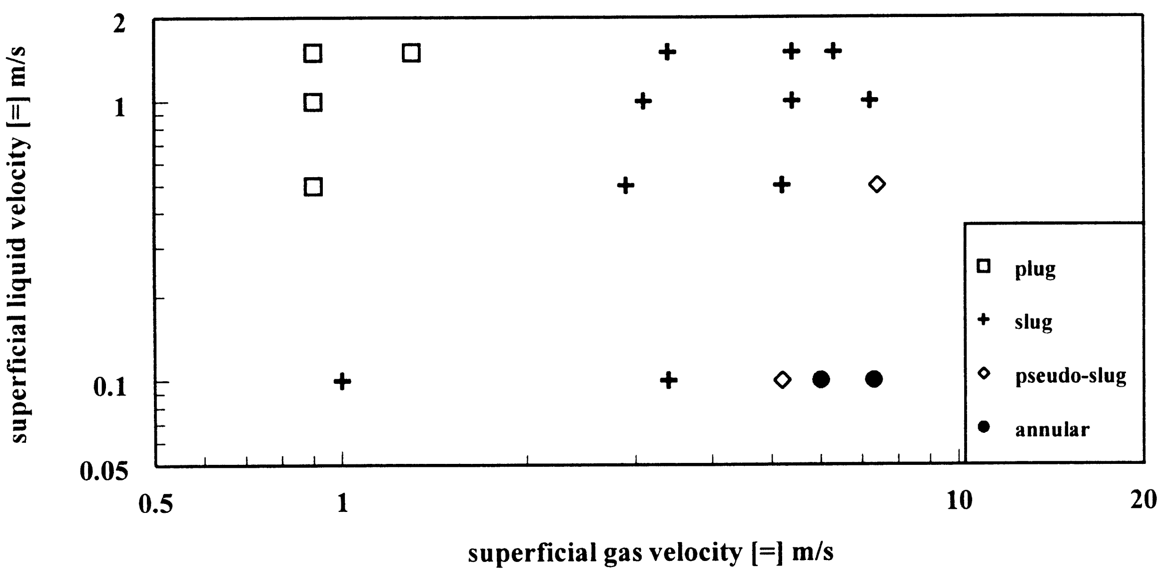

Figure B11: Flow regime map for 40% saltwater/60% light oil at 0.79 MPa and +2° inclination.

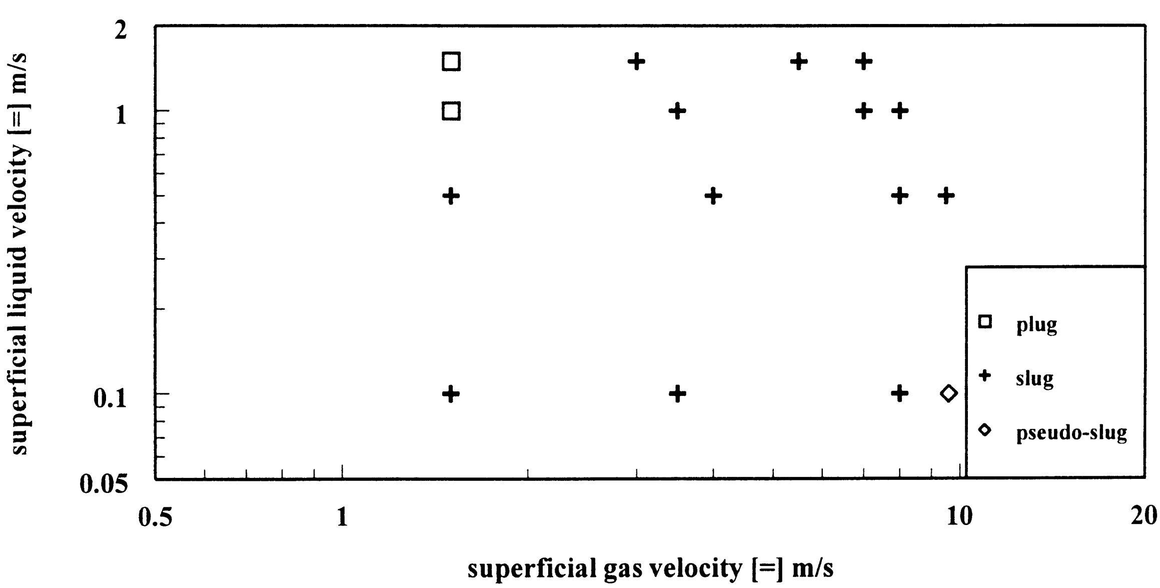

Figure B12: Flow regime map for 100% saltwater at 0.27 MPa and +5° inclination.

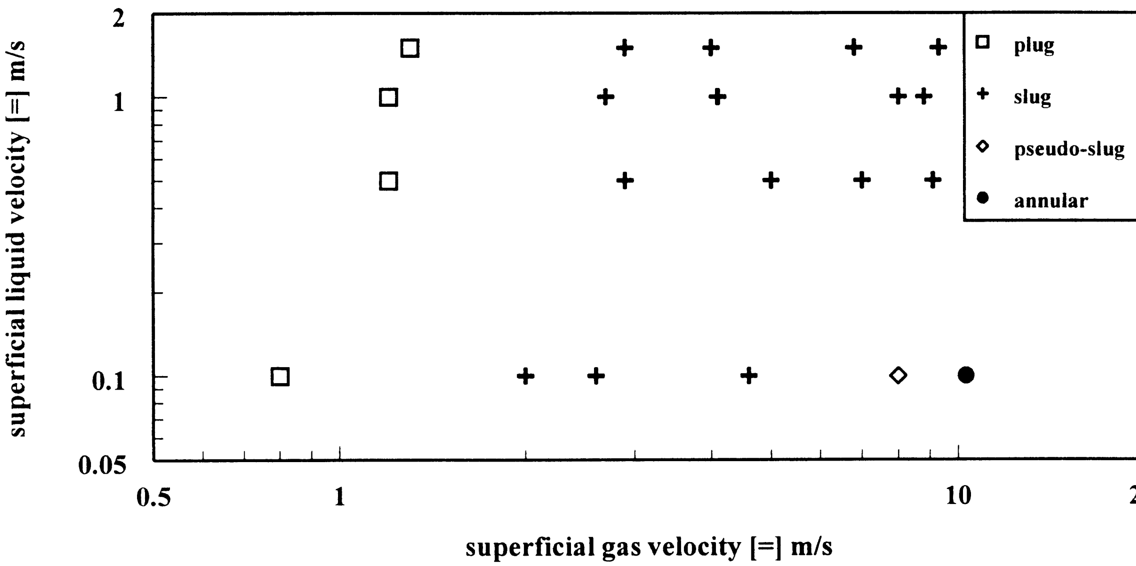

Figure B13: Flow regime map for 100% saltwater at 0.45 MPa and +5° inclination.

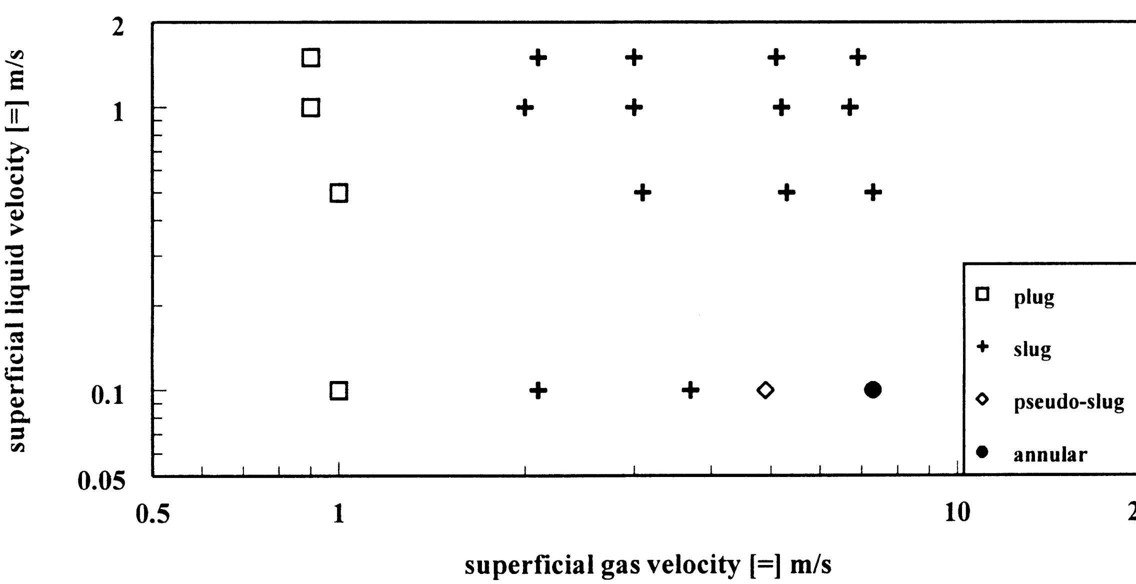

Figure B14: Flow regime map for 100% saltwater at 0.79 MPa and +5° inclination.

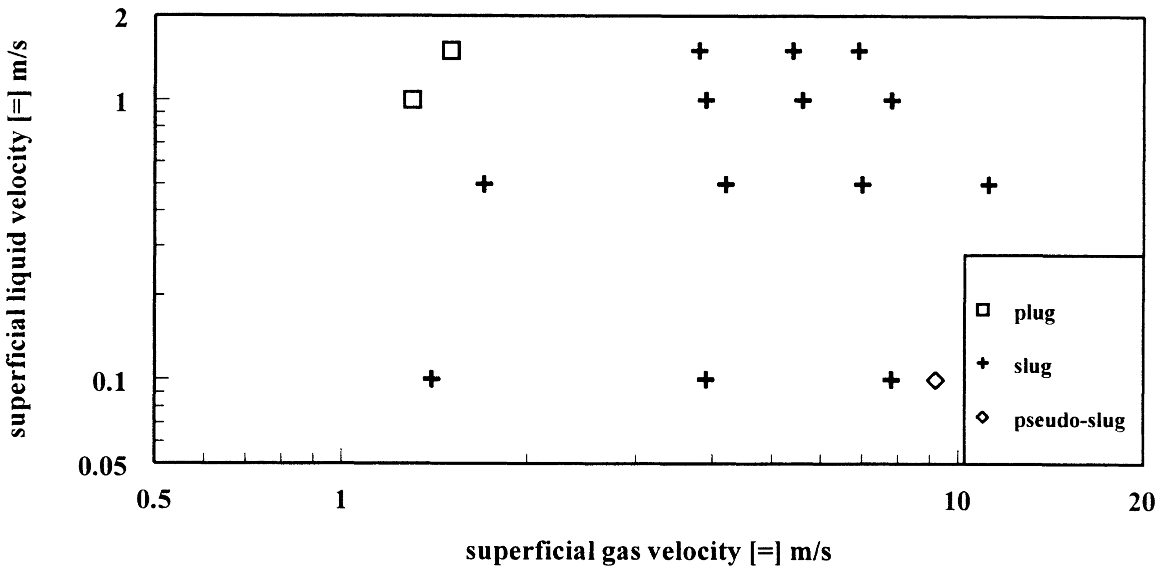

Figure B15: Flow regime map for 80% saltwater/20% light oil at 0.27 MPa and +5° inclination.

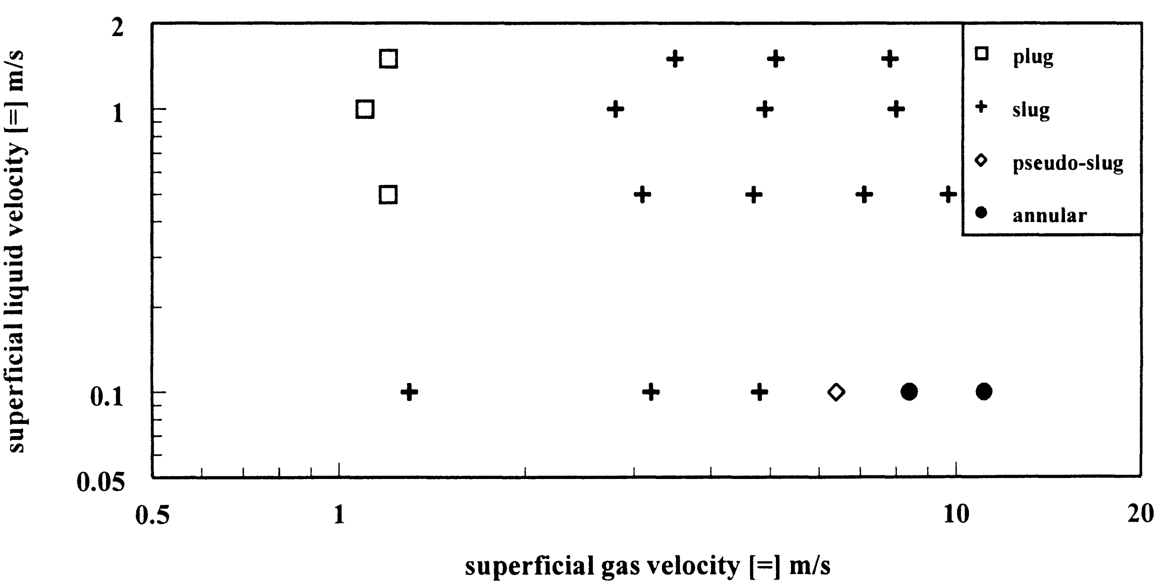

Figure B16: Flow regime map for 80% saltwater/20% light oil at 0.45 MPa and +5° inclination.

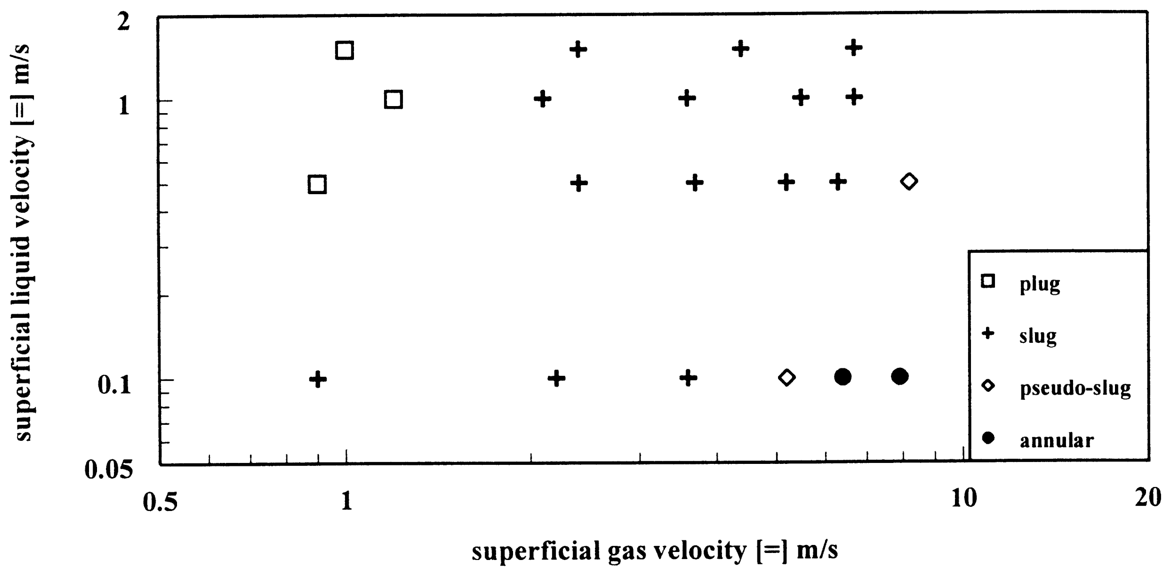

Figure B17: Flow regime map for 80% saltwater/20% light oil at 0.79 MPa and +5° inclination.

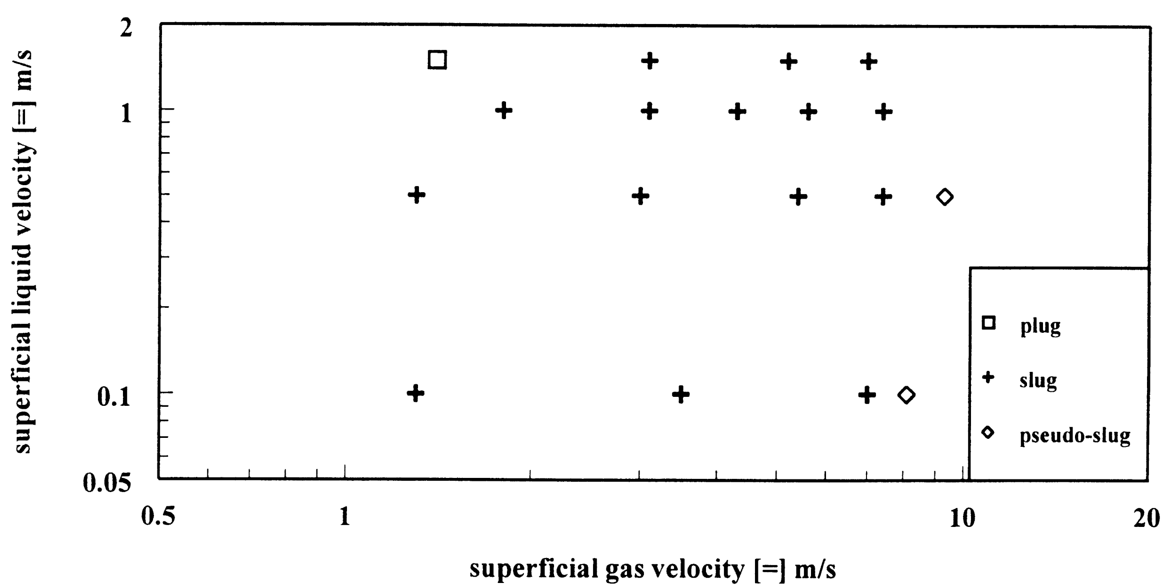

Figure B18: Flow regime map for 40% saltwater/60% light oil at 0.27 MPa and +5° inclination.

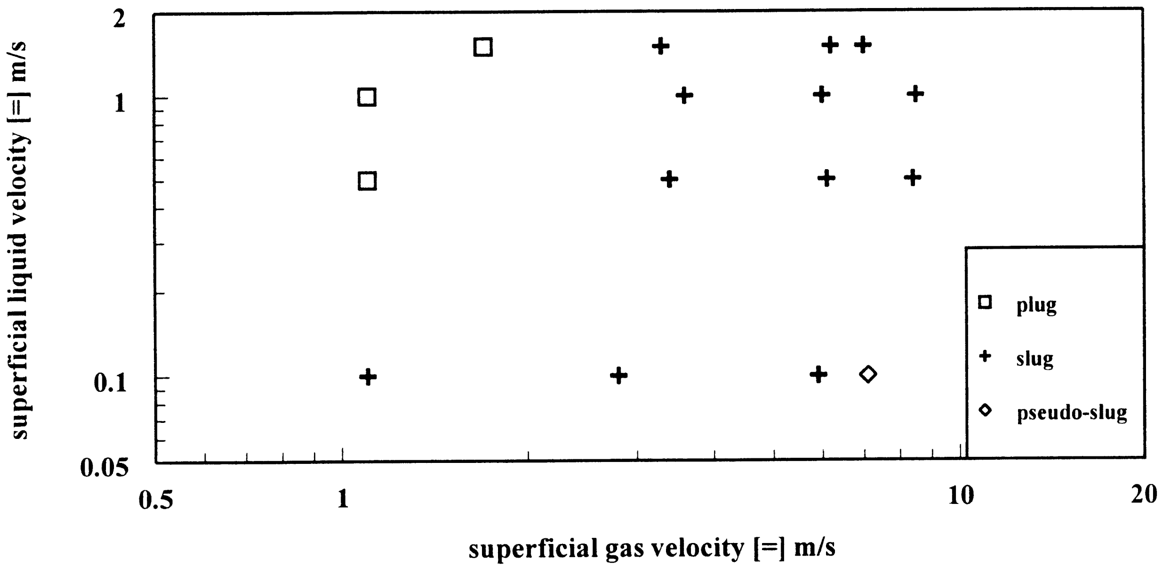

Figure B19: Flow regime map for 40% saltwater/60% light oil at 0.45 MPa and +5° inclination.

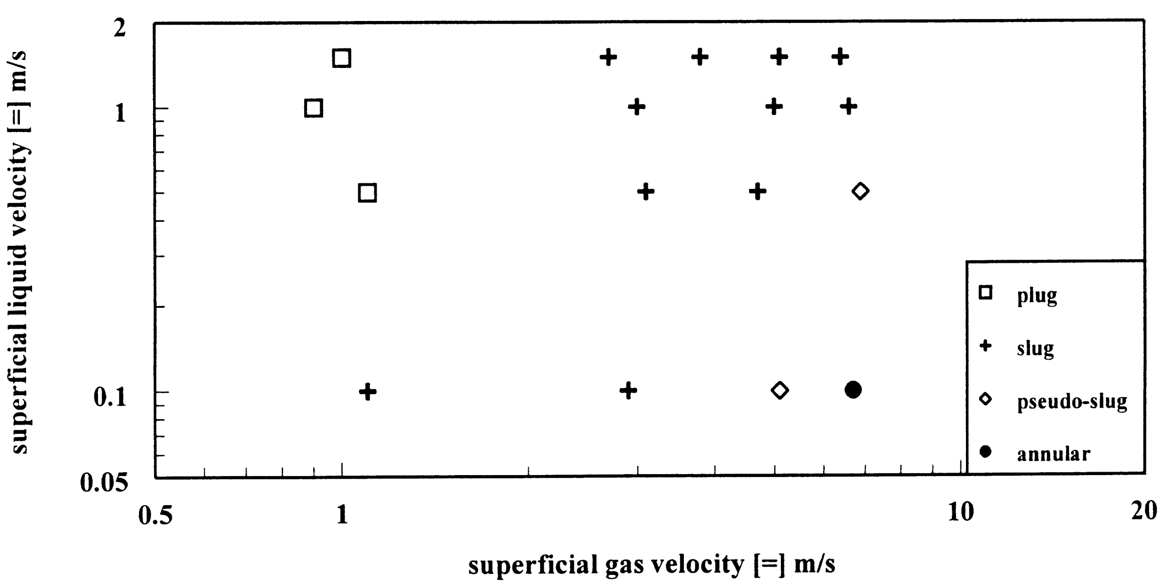

Figure B20: Flow regime map for 40% saltwater/60% light oil at 0.79 MPa and +5° inclination.

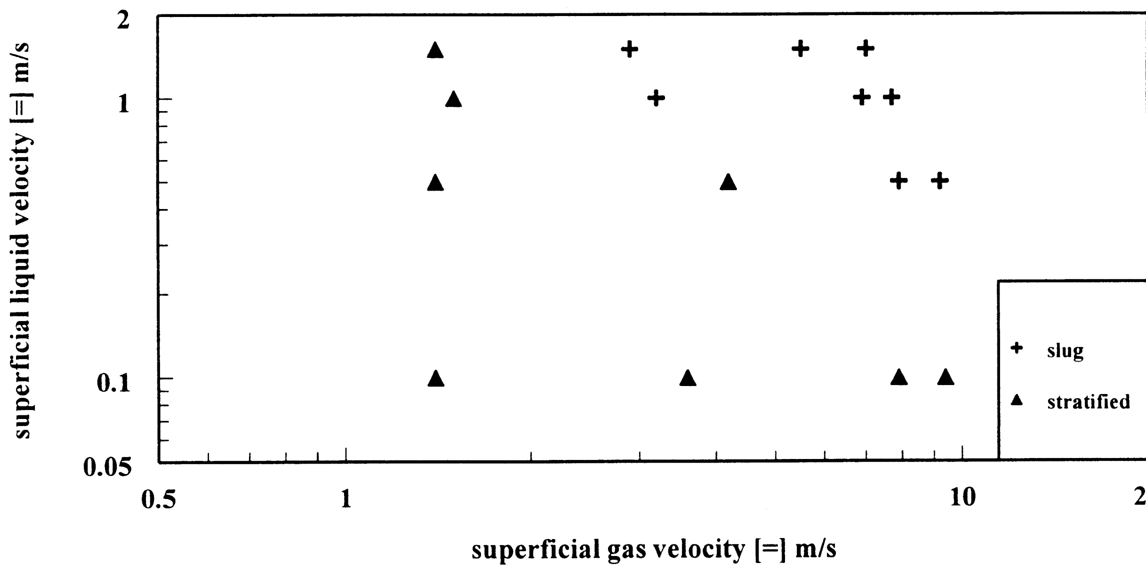

Figure B21: Flow regime map for 100% saltwater at 0.27 MPa and -2° inclination.

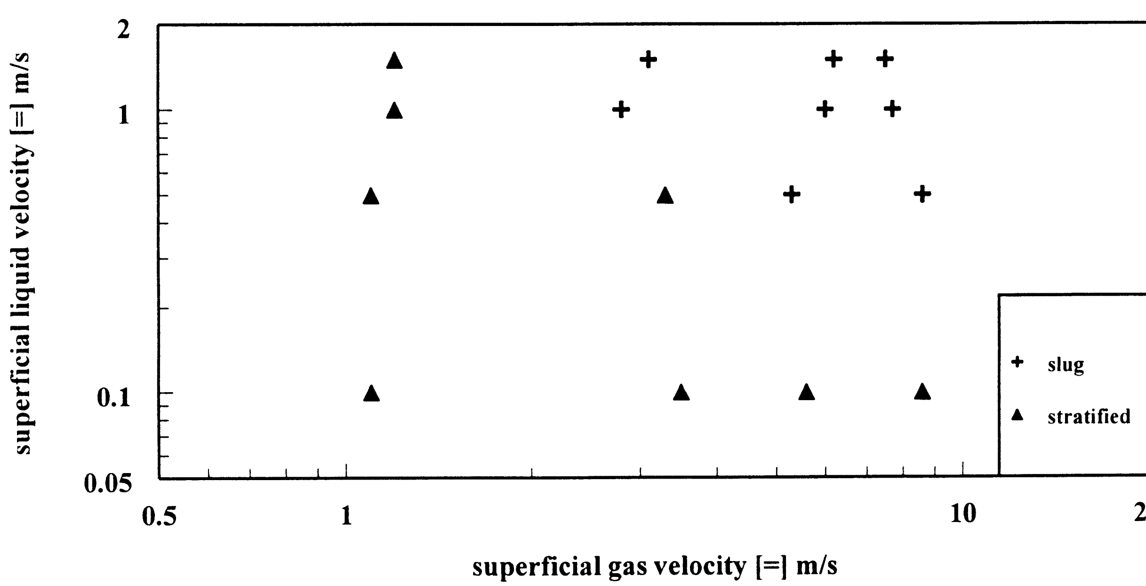

Figure B22 Flow regime map for 100% saltwater at 0.45 MPa and -2° inclination.

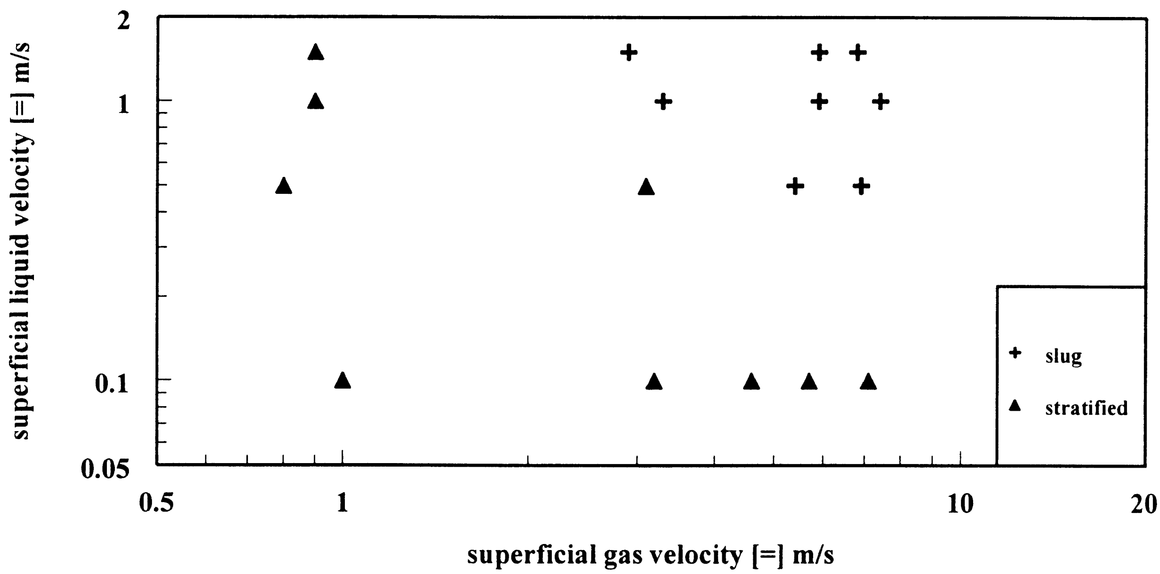

Figure B23: Flow regime map for 100% saltwater at 0.79 MPa and -2° inclination.

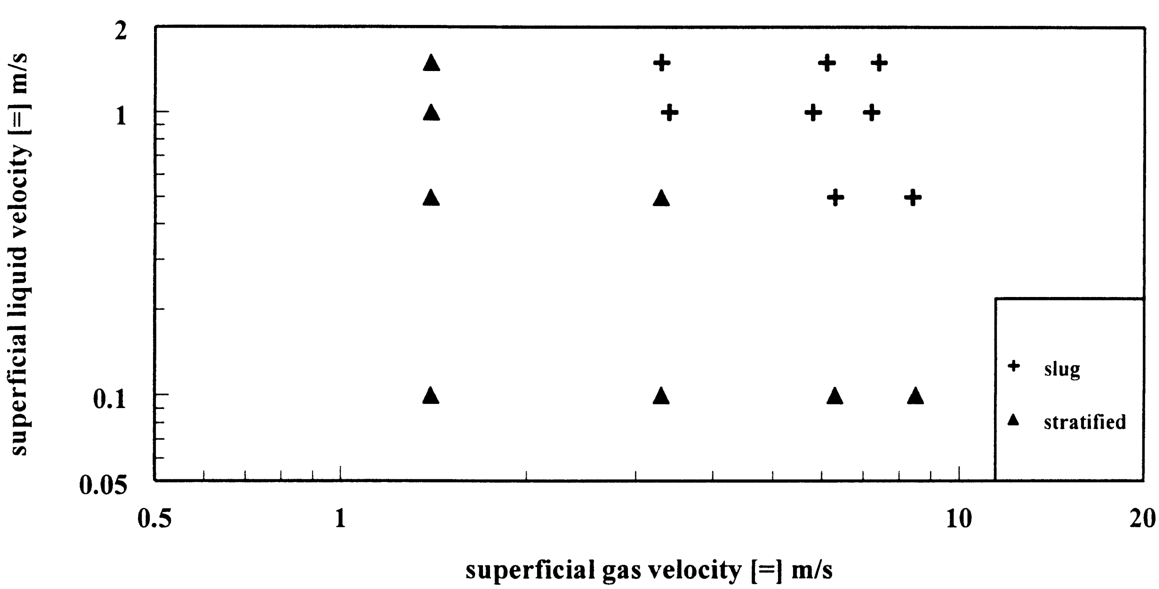

Figure B24: Flow regime map for 80% saltwater/20% light oil at 0.27 MPa and -2° inclination.

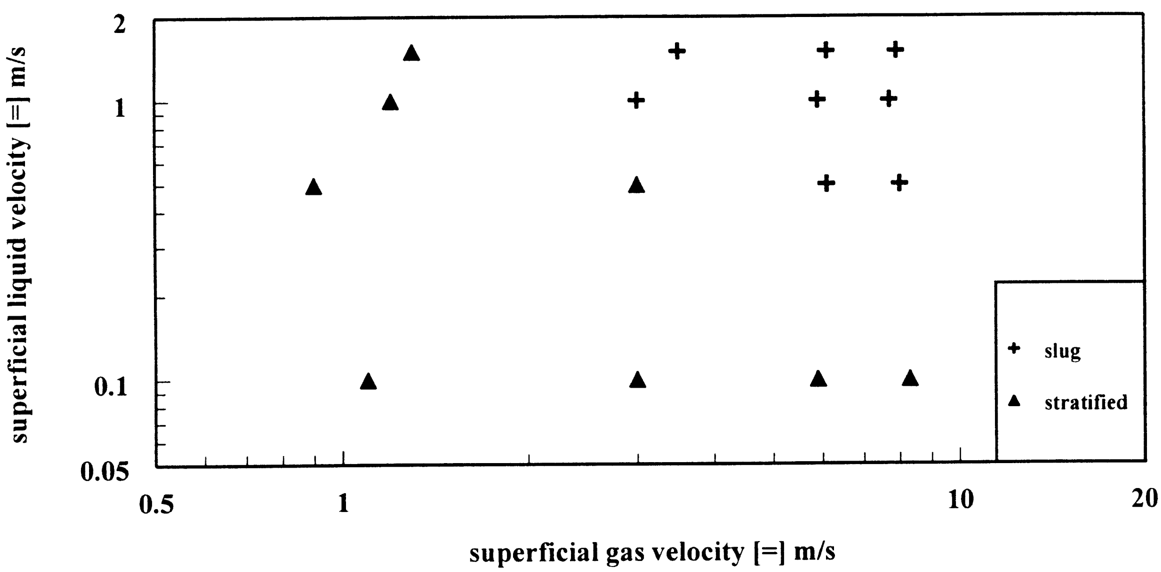

Figure B25: Flow regime map for 80% saltwater/20% light oil at 0.45 MPa and -2° inclination.

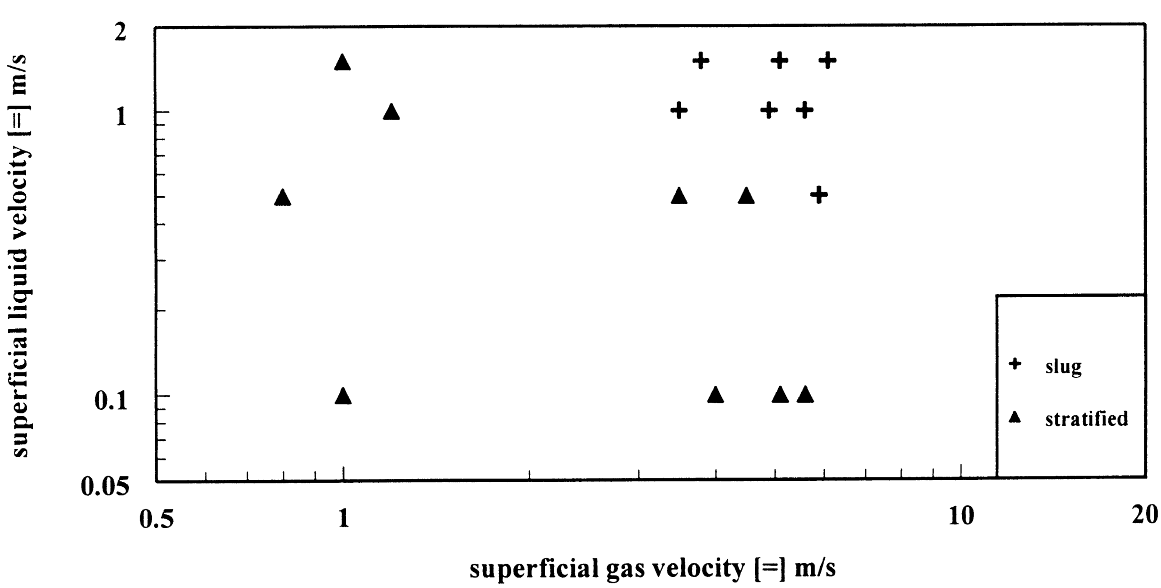

Figure B26: Flow regime map for 80% saltwater/20% light oil at 0.79 MPa and -2° inclination.

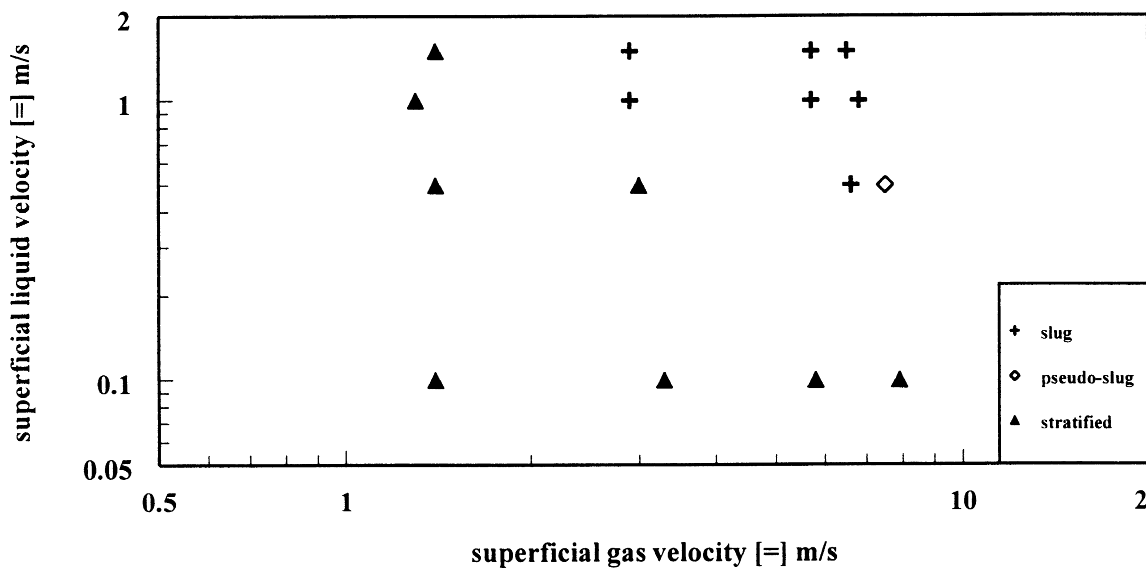

Figure B27: Flow regime map for 40% saltwater/60% light oil at 0.27 MPa and -2° inclination.

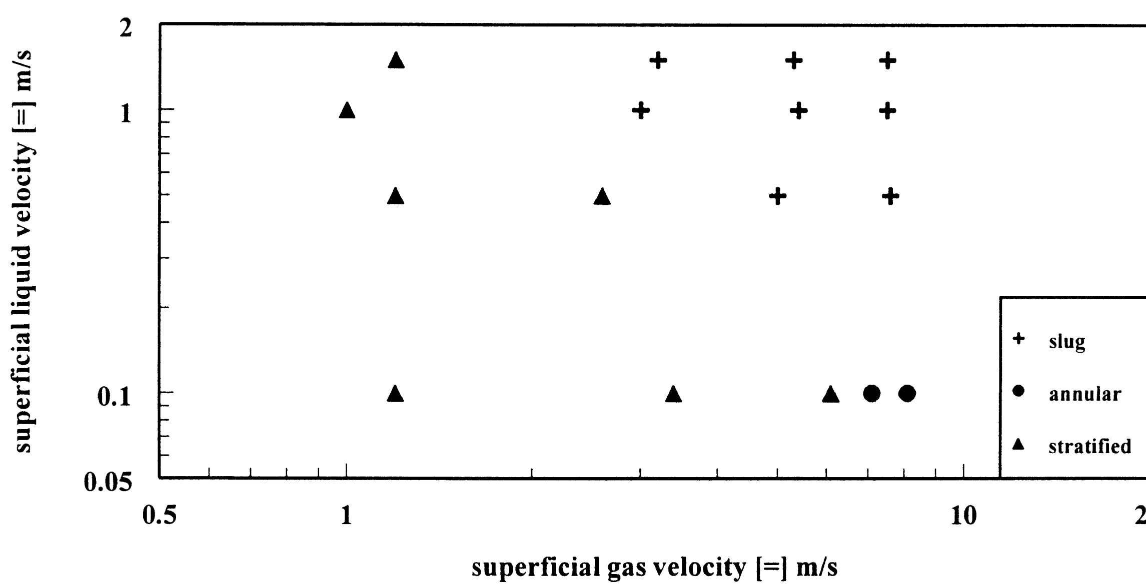

Figure B28: Flow regime map for 40% saltwater/60% light oil at 0.45 MPa and -2° inclination.

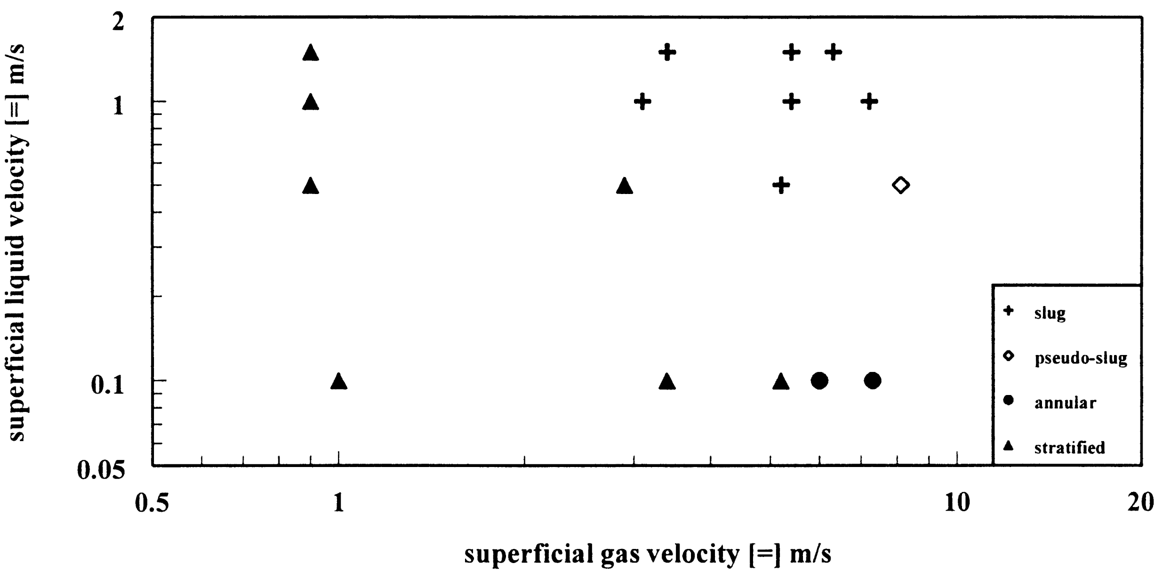

Figure B29: Flow regime map for 40% saltwater/60% light oil at 0.79 MPa and -2° inclination.

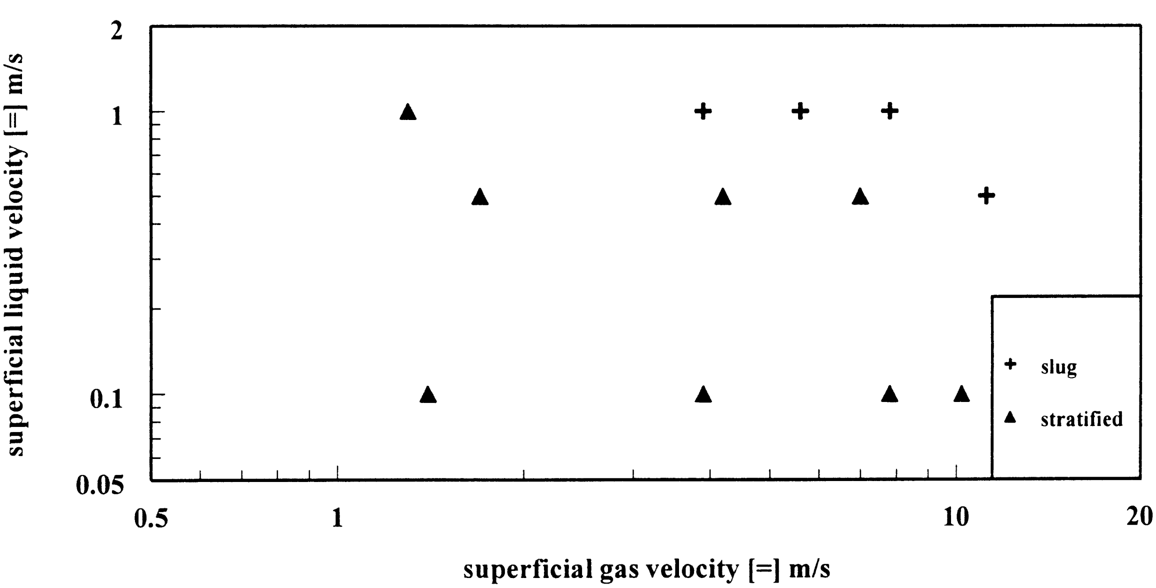

Figure B30: Flow regime map for 80% saltwater/20% light oil at 0.27 MPa and -5° inclination.

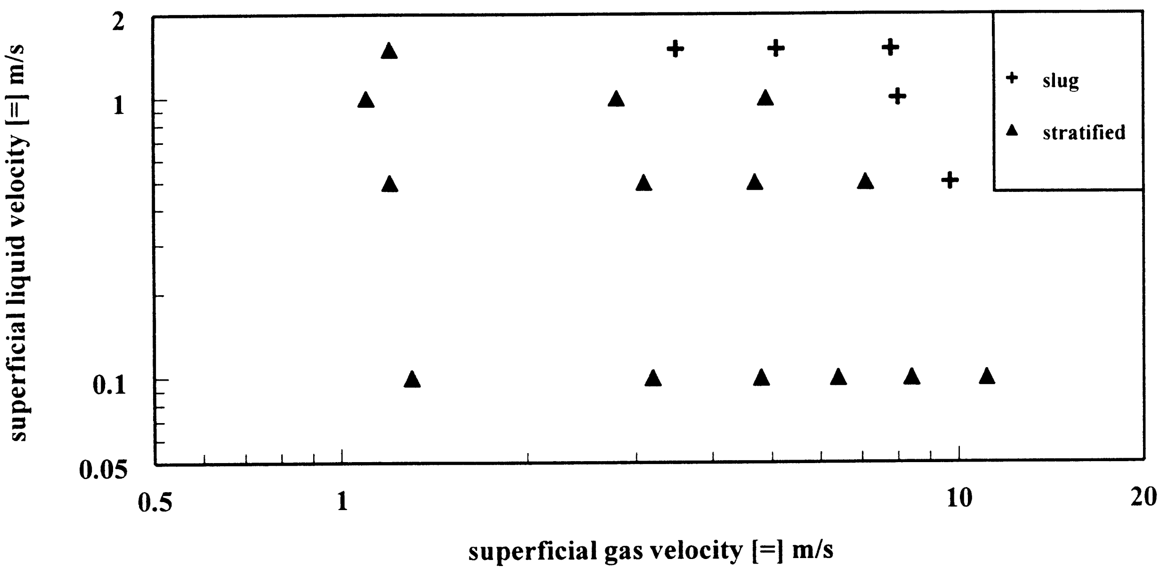

Figure B31: Flow regime map for 80% saltwater/20% light oil at 0.45 MPa and -5° inclination.

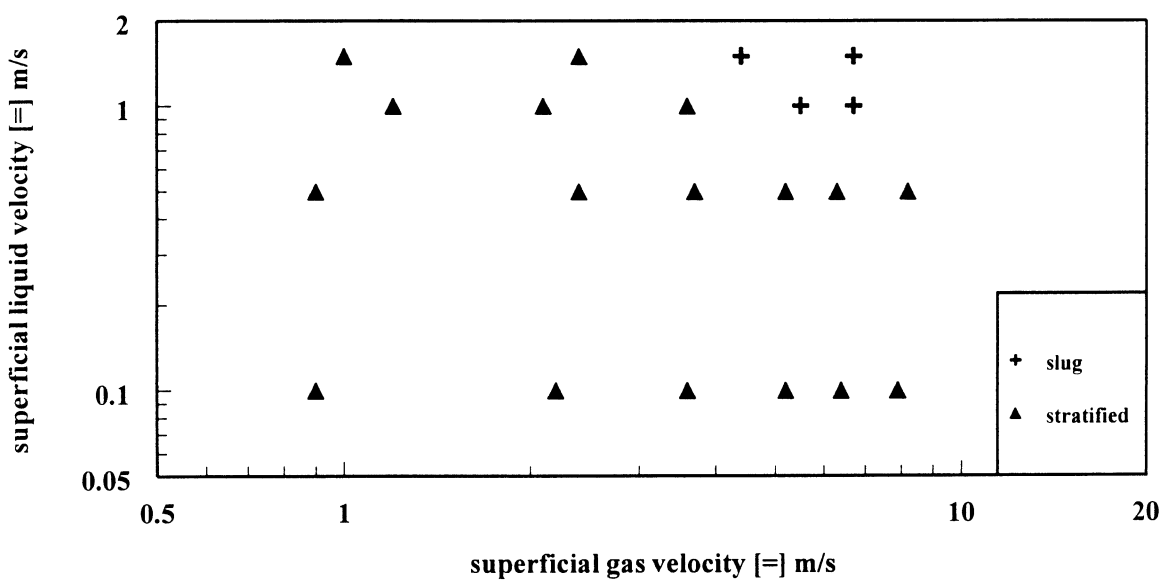

Figure B32: Flow regime map for 80% saltwater/20% light oil at 0.79 MPa and -5° inclination.

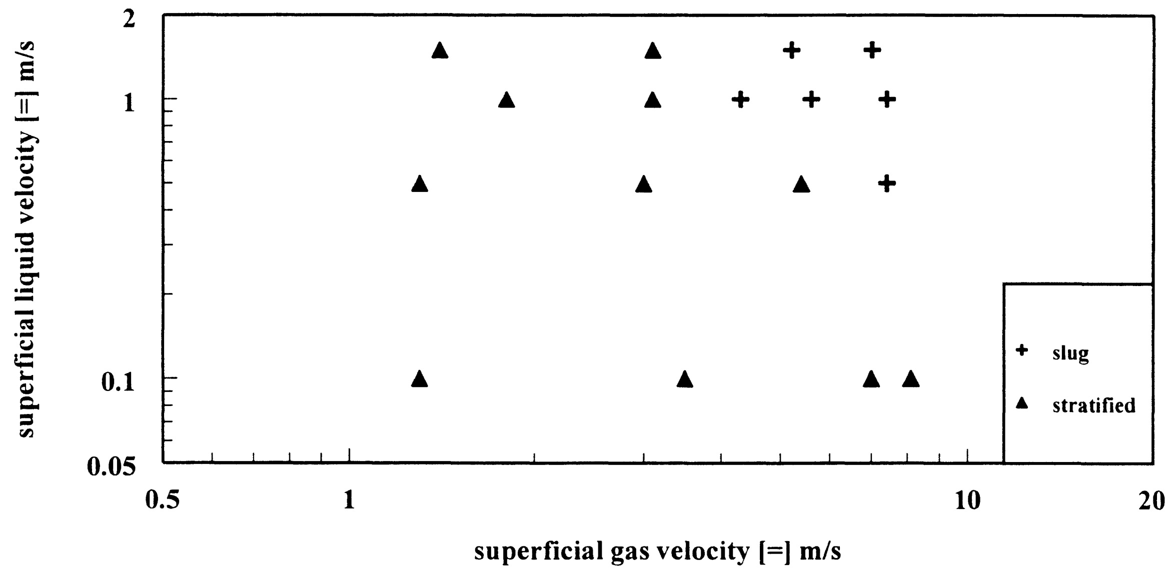

Figure B33: Flow regime map for 40% saltwater/60% light oil at 0.27 MPa and -5° inclination.

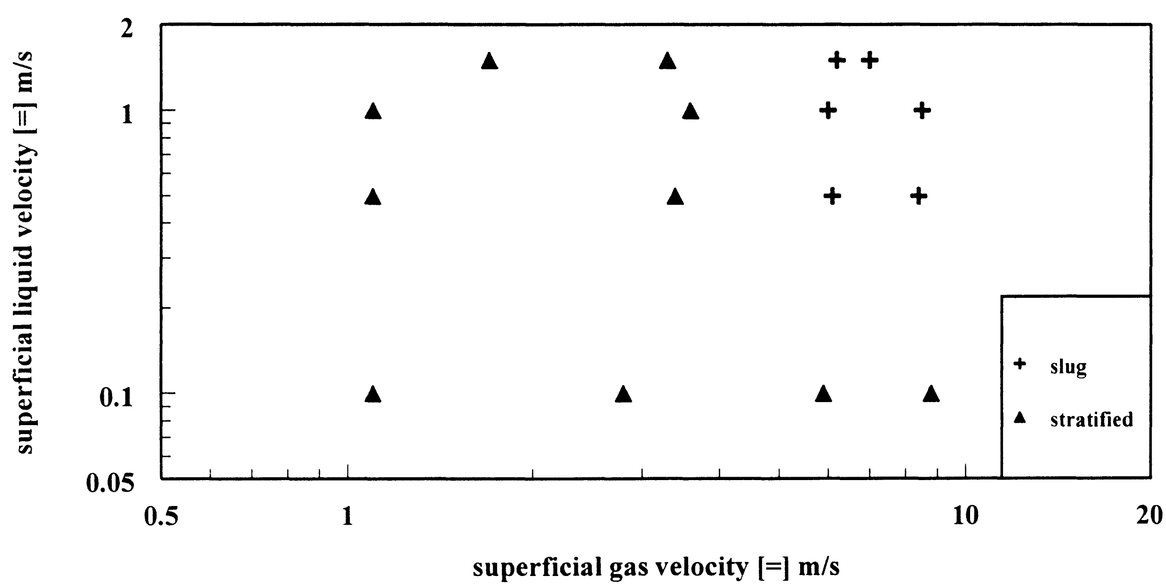

Figure B34: Flow regime map for 40% saltwater/60% light oil at 0.45 MPa and -5° inclination.

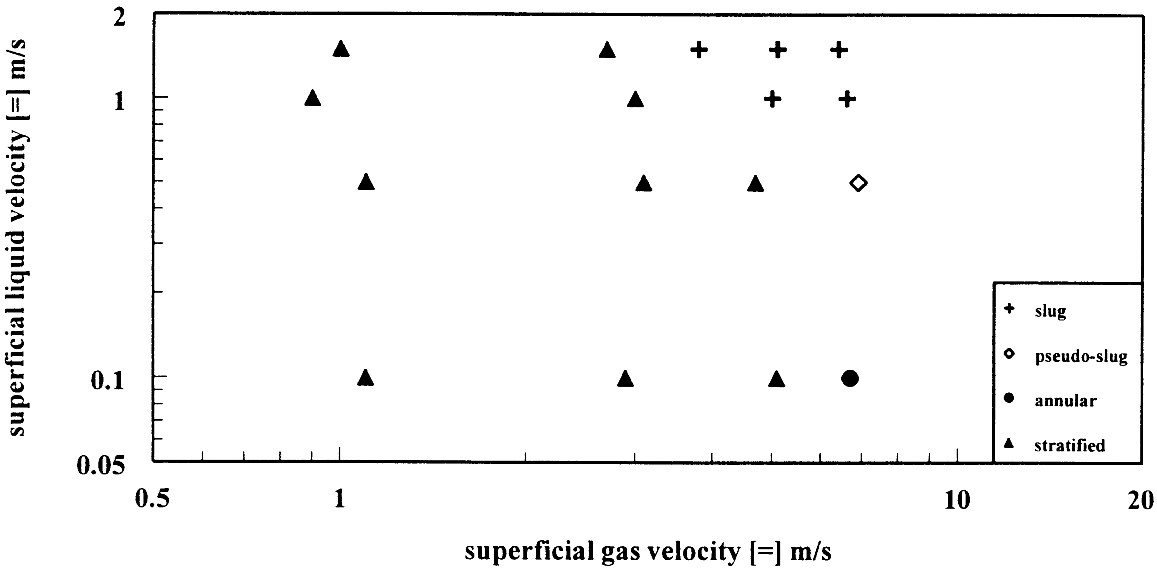

Figure B35: Flow regime map for 40% saltwater/60% light oil at 0.79 MPa and -5° inclination.

CHAPTER 13

APPENDIX C

```
C***********************************************************************
C
C   THIS PROGRAM DETERMINES THE TRANSITION BETWEEN STRATIFIED AND SLUG
C   FLOW FOR LIQUID-GAS SYSTEMS.
C
C   THE PROGRAM SIMULTANEOUSLY SOLVES THE CONSERVATION OF MASS, THE
C   CONSERVATION OF MOMENTUM, AND A MODEL FOR THE SLUG VOID FRACTION.
C
C   'STRAT_SL.FOR'
C   WRITTEN BY BOB WILKENS 4/97 USING MICROSOFT FORTRAN POWERSTATION V1.0
C
C***********************************************************************

C
C    DECLARE VARIABLES AND FUNCTIONS
C

      IMPLICIT NONE
      INTRINSIC DACOS, DABS, DSQRT, DMAX1, DSIN, DEXP, DMIN1
      DOUBLE PRECISION G, PI, C01
      DOUBLE PRECISION PI2, PI3, XLDM, XLDB, XLGM, XLGB
      DOUBLE PRECISION D, THETA, RHOL, RHOG, MUL, MUG, TOL
      DOUBLE PRECISION VSLIG, VSLINITPWR, AL02, AG02, DUMMY1
      DOUBLE PRECISION A, DAL, LHU, DLTAIL, DAG
      DOUBLE PRECISION VSL, VSG, VSLPWR, H, HOLD
      DOUBLE PRECISION CL, CG, N, M, REL, REG, lhu2
      DOUBLE PRECISION SI, SG, SL, DG, DL
      DOUBLE PRECISION VG, V0, VT, VS, ROML, ROMG
      DOUBLE PRECISION SI2, D2, FPRIME, MOMENTUMPART4, F
      DOUBLE PRECISION DALOLDER, DALOLD, LHUNEW
      DOUBLE PRECISION VSLOLDER, VSLOLD, VTEMP, FR, FRMIN
      DOUBLE PRECISION FIFG, VSGT, VSGTA, RHOGA, DBASIS

      INTEGER IPRINTSWITCH, IFILESWITCH, ITAILVOIDSWITCH, IMAXITER
      INTEGER ICOUNT, IVSLSIGN, I, IRUNAGAIN, IMODEL, ILOOP

      CHARACTER OUTPUTFILE*11

      COMMON /MOST_SUBS/ D, A, PI, PI2, PI3, DAL
      COMMON /LEAD_LAG/ XLGM, XLGB, XLDM, XLDB
      COMMON /FLUID_PROPERTIES/ RHOL, RHOG, MUL, MUG
      COMMON /REYNOLDS/ CL, CG, N, M, REL, REG
      COMMON /LENGTHS/ SI, SG, SL, DG, DL
      COMMON /VELOCITIES/ VSL, VSG, VG, V0, VT, VS
      COMMON /OTHER/ AL02, AG02, DUMMY1

      IRUNAGAIN=1
      DO WHILE(IRUNAGAIN .EQ. 1)
       IMODEL=2
```

```
C
C     INPUT THE BASIC CONFIGURATION PARAMETERS FROM THE INPUT FILE
C

      OPEN(UNIT=1, FILE='STRAT_SL.CFG', ERR=99, MODE='READ',
     +          STATUS='OLD')
       DO I=1,17
         READ(1,*)
       ENDDO
       READ(1,*) G
       READ(1,*) PI
       READ(1,*) DLTAIL
       READ(1,*) TOL
       READ(1,*) IMAXITER
       READ(1,*) VSLIG
       READ(1,*) VSLINITPWR
       READ(1,*) ITAILVOIDSWITCH
       READ(1,*) VSGTA
      CLOSE(UNIT=1, ERR=99)

C
C     PRINT TITLES FOR PROGRAM
C

      WRITE(*,*)"****************************************************"
      WRITE(*,*)
      WRITE(*,*)"NATIONAL SCIENCE FOUNDATION INDUSTRY/UNIVERSITY"
      WRITE(*,*)"COOPERATIVE RESEARCH CENTER"
      WRITE(*,*)
      WRITE(*,*)"CORROSION IN MULTIPHASE SYSTEMS CENTER"
      WRITE(*,*)
      WRITE(*,*)"OHIO UNIVERSITY, ATHENS AND"
      WRITE(*,*)"UNIVERSITY OF ILLINOIS, URBANA-CHAMPAIGN"
      WRITE(*,*)
      WRITE(*,*)"THIS PROGRAM MODELS THE TRANSITION FROM STRATIFIED"
      WRITE(*,*)"TO SLUG FLOW FOR GAS-LIQUID SYSTEMS IN HORIZONTAL"
      WRITE(*,*)"AND SLIGHTLY INCLINED PIPELINES."
      WRITE(*,*)
      WRITE(*,*)"****************************************************"
      WRITE(*,*)
      WRITE(*,*)"ENTER A '0' FOR THE DEFAULT VALUES"

C
C     ALLOW THE USER TO INPUT THE SYSTEM PARAMETERS
C

      WRITE(*,*)"What is the inner diameter of the pipe [=] m (default =
     +0.0972)?"
      READ(*,*)D
      IF (D .EQ. 0.D0) THEN
       D=.0972D0
      ENDIF
      WRITE(*,*)"What is the pipe inclination (positive for upflow, defa
     +ult = 0) [=] degrees?"
      READ(*,*)THETA
      WRITE(*,*)"What is the in-situ gas density [=] kg/m^3 (default =
     +8.25)?"
```

```
 READ(*,*)RHOG
 IF (RHOG .EQ. 0.D0) THEN
  RHOG=8.25D0
 ENDIF
 WRITE(*,*)"What is the gas density at atmospheric pressure [=] kg
+/m^3 (default = 1.84)?"
 READ(*,*)RHOGA
 IF (RHOGA .EQ. 0.D0) THEN
  RHOGA=1.84D0
 ENDIF
 WRITE(*,*)"What is the gas viscosity [=] Pa·s (default = 1.6E-5)?"
 READ(*,*)MUG
 IF (MUG .EQ. 0.D0) THEN
  MUG=1.6D-5
 ENDIF
 WRITE(*,*)"What is the liquid density [=] kg/m^3 (default = 1025)
+?"
 READ(*,*)RHOL
 IF (RHOL .EQ. 0.D0) THEN
  RHOL=1025
 ENDIF
 WRITE(*,*)"What is the liquid viscosity [=] Pa·s (default = 1E-3)?
+"
 READ(*,*)MUL
 IF (MUL .EQ. 0.D0) THEN
  MUL=1.D-3
 ENDIF
 WRITE(*,*)"What are the lag distance coefficients for the lead-lag
+ model (defaults are for water-carbon dioxide:  0.16, -0.63)?"
 READ(*,*)XLGM, XLGB
 IF (XLGM .EQ. 0.D0) THEN
  XLGM=0.16D0
 ENDIF
 IF (XLGB .EQ. 0.D0) THEN
  XLGB=-0.63D0
 ENDIF
 WRITE(*,*)"What are the lead distance coefficients for the lead-la
+g model (defaults are"
 WRITE(*,*)"for water-carbon dioxide:  0.057, -0.25)?"
 READ(*,*)XLDM, XLDB
 IF (XLDM .EQ. 0.D0) THEN
  XLDM=0.057D0
 ENDIF
 IF (XLDB .EQ. 0.D0) THEN
  XLDB=-0.25D0
 ENDIF
 WRITE(*,*)"If you would like a copy of the solution sent to the pr
+inter, enter a '1'."
 WRITE(*,*)"Otherwise enter a '0'."
 READ(*,*)IPRINTSWITCH
 IF (IPRINTSWITCH .EQ. 1) THEN
  OPEN(UNIT=3,FILE='LPT1',ERR=199)
 ENDIF
 WRITE(*,*)"If you would like a copy of the results sent to a file,
+enter a '1'."
 WRITE(*,*)"Otherwise enter a '0'."
 READ(*,*)IFILESWITCH
```

```
      IF (IFILESWITCH .EQ. 1) THEN
       WRITE(*,*)"What is the filename (include the extension)?"
       READ(*,9)OUTPUTFILE
       OPEN(UNIT=5, FILE=OUTPUTFILE, ERR=299, MODE='WRITE', STATUS=
     +             'NEW')
      ENDIF

C
C     CALCULATE OTHER CONSTANTS
C

      PI2=1.D0/PI
      PI3=PI**.5
      THETA=THETA*PI/180.D0
      MOMENTUMPART4=-(RHOL-RHOG)*G*DSIN(THETA)
      D2=1.D0/D
      A=.25D0*PI*D**2
      C01=2.D0*DLTAIL*(.25D0*G*D*PI)**.5/3.D0
      ROML=RHOL/MUL
      ROMG=RHOG/MUG
      VSGT=VSGTA*DSQRT(RHOGA/RHOG)
      DBASIS=.1D0

C
C     PREVENT BAD SOLUTIONS BY ESTABLISHING A MINIMUM FROUDE NUMBER
C

      FRMIN=DMAX1((-XLGB/XLGM), 6.D0)

C
C     CONTINUE WITH THE OUPUT
C

      WRITE(*,*)
      WRITE(*,*)"THESE ARE THE INPUT PROPERTIES OF THE SYSTEM:"
      WRITE(*,*)
      WRITE(*,1) G
      WRITE(*,2) THETA
      WRITE(*,3) D
      WRITE(*,*)
      WRITE(*,4) RHOG
      WRITE(*,5) MUG
      WRITE(*,6) RHOL
      WRITE(*,7) MUL
      WRITE(*,12) RHOGA
      WRITE(*,*)
      WRITE(*,*)"TAIL VOID = VOID AT END OF MIXING ZONE"
      WRITE(*,*)
      WRITE(*,*) "THIS IS THE STRATIFIED TO SLUG TRANSITION USING"
      WRITE(*,*) "TAITEL AND DUKLER, MALEY, AND THE BREAKING DAM"
      WRITE(*,*) "ANALOGY (NOTE:  Vsl = 0 MEANS NO TRANSITION AT"
      WRITE(*,*) "THE GIVEN Vsg):"
      WRITE(*,*)
      WRITE(*,*) "   Vsl   Vsg    h/d  AL0/A  αslug  Vt/Vm  Fr,f"

C
C     SEND OUTPUT HEADERS TO THE PRINTER IF NECESSARY
```

```
C

      IF (IPRINTSWITCH .EQ. 1) THEN
       WRITE(3,*)"****************************************************"
       WRITE(3,*)
       WRITE(3,*)"NATIONAL SCIENCE FOUNDATION INDUSTRY/UNIVERSITY"
       WRITE(3,*)"COOPERATIVE RESEARCH CENTER"
       WRITE(3,*)
       WRITE(3,*)"CORROSION IN MULTIPHASE SYSTEMS CENTER"
       WRITE(3,*)
       WRITE(3,*)"OHIO UNIVERSITY, ATHENS AND"
       WRITE(3,*)"UNIVERSITY OF ILLINOIS, URBANA-CHAMPAIGN"
       WRITE(3,*)
       WRITE(3,*)"THIS PROGRAM MODELS THE TRANSITION FROM STRATIFIED"
       WRITE(3,*)"TO SLUG FLOW FOR GAS-LIQUID SYSTEMS IN HORIZONTAL"
       WRITE(3,*)"AND SLIGHTLY INCLINED PIPELINES."
       WRITE(3,*)
       WRITE(3,*)"****************************************************"
       WRITE(3,*)
       WRITE(3,*)"THESE ARE THE INPUT PROPERTIES OF THE SYSTEM:"
       WRITE(3,*)
       WRITE(3,1) G
       WRITE(3,2) THETA
       WRITE(3,3) D
       WRITE(3,*)
       WRITE(3,4) RHOG
       WRITE(3,5) MUG
       WRITE(3,6) RHOL
       WRITE(3,7) MUL
       WRITE(3,12) RHOGA
       WRITE(3,*)
       WRITE(3,*)"TAIL VOID = VOID AT END OF MIXING ZONE"
       WRITE(3,*)
       WRITE(3,*) "THIS IS THE STRATIFIED TO SLUG TRANSITION USING"
       WRITE(3,*) "TAITEL AND DUKLER, MALEY, AND THE BREAKING DAM"
       WRITE(3,*) "ANALOGY (NOTE:  Vsl = 0 MEANS NO TRANSITION AT"
       WRITE(3,*) "THE GIVEN Vsg):"
       WRITE(3,*)
       WRITE(3,*)"   Vsl   Vsg    h/d  AL0/A  αslug  Vt/Vm  Fr,f"
      ENDIF

C
C     BEGIN THE OUTER SOLUTION LOOP WHICH INCREMENTS THROUGH THE VSG
C

      VSL=VSLIG
      DO ILOOP=1,14,1
       IF (ILOOP .LE. 6) THEN
         VSG=.8d0+.2d0*ILOOP
       ELSE
         VSG=ILOOP-4.D0
       ENDIF

       VSLPWR=VSLINITPWR
       VSLOLD=0.D0
       IF ((VSL .GT. 8.D0) .OR. (VSL .LE. 0.D0)) THEN
         VSL=VSLIG
```

```
      ENDIF
      ICOUNT=0

C
C     BEGIN THE VSL SOLUTION WHICH APPLIES THE BREAKING DAM & MALEY RELATIONS
C

      DO WHILE (DABS(VSL-VSLOLD)/VSL .GE. TOL)
        H=.5D0*D
        HOLD=H+2.D0*TOL

C
C     BEGIN THE H/D SOLUTION WHICH APPLIES THE TAITEL & DUKLER RELATION
C

        DO WHILE (DABS(H-HOLD)/H .GE. TOL)
          CALL GEOMETRY(H, D2, SI2, DAG)
          CALL PARAMETERS
          CALL COEFFICIENTS(ROML, ROMG)
          CALL DIFF(DAG, ROML, ROMG, FPRIME, SI2, D2)
          CALL MOMENTUM(MOMENTUMPART4, F, FIFG, vsgt, h, imodel)
          HOLD=H
          H=H-F/FPRIME

          ICOUNT=ICOUNT+1
          IF (H .GT. D) THEN
            H=.9999D0*D
          ELSE IF (H .LT. 0.D0) THEN
            H=.0001D0*D
          ENDIF
        END DO

        IF (IMODEL .EQ. 1) THEN
          write(*,*)"This shouldn't happen!"

        ELSE

C
C     SOLVE THE BREAKING DAM MASS CONSERVATION
C

          CALL BREAKINGDAM(C01, LHU, lhu2)

          DALOLDER=DALOLD
          DALOLD=DAL

C
C     DETERMINE THE SLUG VOID USING THE PROPER RELATION
C

          CALL HOLDUP(G, SI2, LHUNEW, DBASIS, FR, imodel, lhu2)

          IF (LHU .GT. LHUNEW) THEN
            IVSLSIGN=-1
          ELSE
            IVSLSIGN=1
          ENDIF
```

```
          VSLOLDER=VSLOLD
          VSLOLD=VSL

          VSL=VSL+IVSLSIGN*VSLPWR

          IF (VSLOLDER .EQ. VSL) THEN
            VSLPWR=VSLPWR*.2D0
          ENDIF
        ENDIF

C
C     PREVENT NON-SOLUTIONS
C

        IF ((ICOUNT .GT. IMAXITER).OR.(VSL .LT. -2.D0*VSLINITPWR)
     +             .OR. (VSL .GT. 15.D0)) THEN
          WRITE(*,*)"SOLUTION CONVERSION ERROR"
          WRITE(*,*)ICOUNT
          VSL=9.D0
          VSLOLD=9.D0
        ENDIF

      CALL OTHERVALUES(G, SI2, FR)

      END DO
      IF (VSL .LT. 0.D0) THEN
        VSL=9.D0
      ENDIF

C
C     UPDATE THE APPROPRIATE VALUES
C

      CALL OTHERVALUES(G, SI2, FR)

C
C     OUTPUT THE SOLUTION
C

      VTEMP=VSL
      IF ((VSL .GE. 8.D0).OR.(FR.LE.1.D0)) THEN
        VSL=0.D0
        H=0.D0
        FR=0.D0
        VT=0.D0
        LHU=1.D0
        DAL=0.D0
      ENDIF
      WRITE(*,8) VSL, VSG, (H/D), DAL, (1.D0-LHU), VT/(VSL+VSG), FR
      IF (IPRINTSWITCH .EQ. 1) THEN
        WRITE(3,8) VSL, VSG, (H/D), DAL, (1.D0-LHU), VT/(VSL+VSG), FR
      ENDIF
      IF (IFILESWITCH .EQ. 1) THEN
        WRITE(5,10) VSG, VSL
      ENDIF
      VSL=VTEMP
      IF (FR .GT. 9.D0) THEN
```

```
          IMODEL=3
        ELSEIF (FR .GT. 5.D0) THEN
          IMODEL=2
        ENDIF
       END DO
       IF (IPRINTSWITCH .EQ. 1) THEN
        WRITE(3,*) "\f"C
        CLOSE(UNIT=3, ERR=199)
       ENDIF
       IF (IFILESWITCH .EQ. 1) THEN
        CLOSE(UNIT=5, ERR=299)
       ENDIF
       WRITE(*,*)"RUN AGAIN (1 = YES, 0 = NO)?"
       READ(*,*)IRUNAGAIN
       END DO
       STOP

C
C      FORMATTED INPUT/OUTPUT LISTING
C

     1 FORMAT(' GRAVITY ='F6.2' kg·m/s²')
     2 FORMAT(' INCLINATION ='F8.4' radians (+ for upflow)')
     3 FORMAT(' PIPE INNER DIAMETER ='F6.4' m')
     4 FORMAT(' GAS DENSITY ='F8.3' kg/m^3')
     5 FORMAT(' GAS VISCOSITY ='D9.3' Pa·S')
     6 FORMAT(' LIQUID DENSITY ='F5.0' kg/m^3')
     7 FORMAT(' LIQUID VISCOSITY ='D9.3' Pa·S')
     8 FORMAT(' 'F6.4'  'F4.1'  'F5.3'  'F5.3'  'F5.3'  'F5.3'  'F4.1)
     9 FORMAT(A11)
    10 FORMAT(F7.4'   'F7.5)
    12 FORMAT(' GAS DENSITY AT ATMOSPHERIC PRESSURE ='F6.3' kg/m^3')
       STOP

C
C      ERROR TRAPPING OUTPUT LINES
C

    99 WRITE(*,*) "CONFIGURATION FILE ERROR!  ENSURE THAT IT IS IN THE"
       WRITE(*,*) "SAME DIRECTORY AS THE EXECUTABLE FILE AND THAT THE"
       WRITE(*,*) "VALUES ARE APPROPRIATE (SEE README.TXT)."
       STOP

   199 WRITE(*,*) "PRINTER ERROR."
       STOP

   299 WRITE(*,*) "ERROR CREATING THE OUPUT FILE."
       STOP

       END

C
C      PROGRAM SUBROUTINES
C

       SUBROUTINE BREAKINGDAM(C01, LHU, lhu2)
        IMPLICIT NONE
```

```
      COMMON /MOST_SUBS/ D, A, PI, PI2, PI3, DAL
      COMMON /VELOCITIES/ VSL, VSG, VG, V0, VT, VS
      DOUBLE PRECISION C01, LHU
      DOUBLE PRECISION D, A, PI, PI2, PI3, DAL
      DOUBLE PRECISION VSL, VSG, VG, V0, VT, VS
      DOUBLE PRECISION AA, BB, CC, lhu2

      VS=VSL+VSG

      LHU=DMIN1(LHU, 0.99D0)
      LHU=DMAX1(LHU, 0.01D0)

      VT=DMIN1((VS*LHU-VSL)/(LHU-DAL),9.D0*VS)
      VT=DMAX1(VT, 0.5D0*VS)
      AA=VS*DAL-VSL
      BB=C01*lhu2-C01*lhu2*DAL+DAL*VSL-VS*DAL**2
      CC=2.D0*(VS*DAL**3-VSL*DAL**2-VS*DAL**2+VSL*DAL)+C01*lhu2
     &        *DAL**2-C01*lhu2*DAL

      LHU=(-BB+DSQRT(BB**2-4.D0*AA*CC))/(2.D0*AA)

      LHU=DMIN1(LHU,.99D0)
      LHU=DMAX1(LHU,0.01D0)

     RETURN
     END

     SUBROUTINE COEFFICIENTS(ROML,ROMG)
      IMPLICIT NONE
      COMMON /REYNOLDS/ CL, CG, N, M, REL, REG
      COMMON /LENGTHS/ SI, SG, SL, DG, DL
      COMMON /VELOCITIES/ VSL, VSG, VG, V0, VT, VS
      DOUBLE PRECISION CL, CG, N, M, REL, REG, SI, SG, SL, DG, DL
      DOUBLE PRECISION VSL, VSG, VG, V0, VT, VS, ROML, ROMG

      REL=DL*V0*ROML
      REG=DG*VG*ROMG
      IF (REL .GT. 1500.D0) THEN
        N=.2D0
        CL=.046D0
      ELSE
        N=1.D0
        CL=16.D0
      ENDIF
      IF (REG .GT. 1500.D0) THEN
        M=.2D0
        CG=.046D0
      ELSE
        M=1.D0
        CG=16.D0
      ENDIF
     RETURN
     END

     SUBROUTINE DIFF(DAG, ROML, ROMG, FPRIME, SI2, D2)
      IMPLICIT NONE
      COMMON /MOST_SUBS/ D, A, PI, PI2, PI3, DAL
```

```
      COMMON /FLUID_PROPERTIES/ RHOL, RHOG, MUL, MUG
      COMMON /REYNOLDS/ CL, CG, N, M, REL, REG
      COMMON /LENGTHS/ SI, SG, SL, DG, DL
      COMMON /VELOCITIES/ VSL, VSG, VG, V0, VT, VS
      COMMON /OTHER/ AL02, AG02, DUMMY1
      DOUBLE PRECISION DAG, ROML, ROMG, FPRIME, SI2, D2
      DOUBLE PRECISION D, A, PI, PI2, PI3, DAL
      DOUBLE PRECISION RHOL, RHOG, MUL, MUG
      DOUBLE PRECISION CL, CG, N, M, REL, REG
      DOUBLE PRECISION SI, SG, SL, DG, DL
      DOUBLE PRECISION VSL, VSG, VG, V0, VT, VS
      DOUBLE PRECISION AL02, AG02, DUMMY1
      DOUBLE PRECISION PART1, PART2
      DOUBLE PRECISION DERIV1, DERIV2, DERIV3, DERIV4, DERIV5, DERIV6
      DOUBLE PRECISION DERIV7, DERIV8, DERIV9, DERIV10, DERIV11

      DERIV1=-2.D0*D*DUMMY1*SI2
      DERIV2=2.D0*D*SI2
      DERIV3=2.D0*A*(SI*D2**2+(1-DUMMY1**2)*SI2)*PI2
      DERIV4=4.D0*(SL*DERIV3-DAL*A*DERIV2)/SL**2
      DERIV5=-4.D0*((SG+SI)*DERIV3+DAG*A*(DERIV1-DERIV2))/(SG+SI)**2
      DERIV6=-VSL*AL02/DAL
      DERIV7=VSG*AG02/DAG
      DERIV8=(DAL*A*DERIV2-SL*DERIV3)*AL02**2
      DERIV9=-N*ROML*REL**(-N-1.D0)*(DL*DERIV6+V0*DERIV4)
      DERIV10=(DAG*A*(DERIV1-DERIV2)+(SI+SG)*DERIV3)*AG02**2+(DAL*A*
     &              DERIV1-SI*DERIV3)*AL02**2
      DERIV11=-M*ROMG*REG**(-M-1.D0)*(DG*DERIV7+VG*DERIV5)

      PART1=RHOL*CL*(SL*AL02*REL**(-N)*2.D0*V0*DERIV6+V0**2*(REL**(-N)
     &             *DERIV8+SL*AL02*DERIV9))
      PART2=-RHOG*CG*(((SG+SI)*AG02+SI*AL02)*REG**(-M)*2.D0*VG*DERIV7+
     &             VG**2*(REG**(-M)*DERIV10+((SG+SI)*AG02+SI*AL02*DERIV11)))

      FPRIME=PART1+PART2
     RETURN
     END

     SUBROUTINE GEOMETRY(H, D2, SI2, DAG)
      COMMON /MOST_SUBS/ D, A, PI, PI2, PI3, DAL
      COMMON /LENGTHS/ SI, SG, SL, DG, DL
      COMMON /OTHER/ AL02, AG02, DUMMY1
      DOUBLE PRECISION H, D2, SI2, ARCCOS, DAG
      DOUBLE PRECISION D, A, PI, PI2, PI3, DAL
      DOUBLE PRECISION SI, SG, SL, DG, DL
      DOUBLE PRECISION AL02, AG02, DUMMY1

      DUMMY1=2.D0*H*D2-1.D0
      ARCCOS=DACOS(DUMMY1)
      SG=D*ARCCOS
      SL=PI*D-SG
      SI=D*DSQRT(1.D0-DUMMY1**2)
      DAG=(ARCCOS-DUMMY1*SI/D)*PI2
      DAL=1.D0-DAG
      DL=4.D0*A*DAL/SL
      DG=4.D0*A*DAG/(SI+SG)
      SI2=1.D0/SI
```

```
 AL02=1.D0/(A*DAL)
 AG02=1.D0/(A*DAG)
RETURN
END

SUBROUTINE HOLDUP(G, SI2, LHUNEW, DBASIS, FR, imodel, lhu2)
 IMPLICIT NONE
 COMMON /LEAD_LAG/ XLGM, XLGB, XLDM, XLDB
 COMMON /MOST_SUBS/ D, A, PI, PI2, PI3, DAL
 COMMON /VELOCITIES/ VSL, VSG, VG, V0, VT, VS
 DOUBLE PRECISION G, SI2, LHUNEW, HEFF, FR, XLD, XLG
 DOUBLE PRECISION D, A, PI, PI2, PI3, DAL
 DOUBLE PRECISION VSL, VSG, VG, V0, VT, VS
 DOUBLE PRECISION LMZ, DBASIS, lhu2
 DOUBLE PRECISION XLGM, XLGB, XLDM, XLDB, ls
 INTEGER imodel

 ls=15*d

 HEFF=A*DAL*SI2
 FR=(VT-V0)/DSQRT(G*HEFF)

 LMZ=(0.061D0*FR+0.067D0)*D/DBASIS
 XLD=(XLDM*FR+XLDB)*D/DBASIS
 XLG=(XLGM*FR+XLGB)*D/DBASIS

 IF (IMODEL .EQ. 2) THEN
   LHUNEW=1.D0/(1.D0+((VSL+VSG)/8.66D0)**(1.39))
   if (fr .gt. 60.d0) then
     lhu2=1.D0+(XLD-XLG)/XLG*DEXP(-LMZ/XLG)
     lhu2=dmax1(lhu2, lhunew)
   else
     lhu2=1.d0
   endif
 ELSE
   lhu2=1.D0+(XLD-XLG)/XLG*DEXP(-LMZ/XLG)
   if (ls.gt.lmz)then
     lhu2=1.D0+(XLD-XLG)/XLG*DEXP(-LMZ/XLG)
     LHUNEW=1.d0-(xld-xlg)/lmz*(dexp(-lmz/xlg)-1.d0)
     lhunew=lmz*(lhunew-lhu2)/ls+lhu2
   else
     lhu2=1.D0+(XLD-XLG)/XLG*DEXP(-ls/XLG)
     LHUNEW=1.d0-(xld-xlg)/ls*(dexp(-ls/xlg)-1.d0)
   endif
 ENDIF

 lhunew=dmin1(lhunew, 0.98d0)
 lhunew=dmax1(lhunew, 0.02d0)

RETURN
END

SUBROUTINE MOMENTUM(MOMENTUMPART4, F, FIFG, vsgt, h, imodel)
 IMPLICIT NONE
 COMMON /MOST_SUBS/ D, A, PI, PI2, PI3, DAL
 COMMON /FLUID_PROPERTIES/ RHOL, RHOG, MUL, MUG
 COMMON /REYNOLDS/ CL, CG, N, M, REL, REG
```

```
 COMMON /LENGTHS/ SI, SG, SL, DG, DL
 COMMON /VELOCITIES/ VSL, VSG, VG, V0, VT, VS
 COMMON /OTHER/ AL02, AG02, DUMMY1
 DOUBLE PRECISION MOMENTUMPART4, F, h
 DOUBLE PRECISION D, A, PI, PI2, PI3, DAL
 DOUBLE PRECISION RHOL, RHOG, MUL, MUG
 DOUBLE PRECISION CL, CG, N, M, REL, REG
 DOUBLE PRECISION SI, SG, SL, DG, DL, vsgt
 DOUBLE PRECISION VSL, VSG, VG, V0, VT, VS
 DOUBLE PRECISION AL02, AG02, DUMMY1
 DOUBLE PRECISION PART1, PART2, PART3, PART4
 DOUBLE PRECISION TAUG, TAUL, TAUI, FIFG
 INTEGER imodel

 IF ((IMODEL .EQ. 3) .AND. (VSG .GT. VSGT)) THEN
   FIFG=DMIN1(1.D0+15.D0*DSQRT(H/D)*(VSG/VSGT-1.D0),15.D0)
 ELSE
   FIFG=1.D0
 ENDIF

 TAUL=CL*REL**(-N)*RHOL*V0**2/2.D0
 TAUG=CG*REG**(-M)*RHOG*VG**2/2.D0
 TAUI=TAUG*FIFG
 PART1=TAUG*SG*AG02
 PART2=-TAUL*SL*AL02
 PART3=TAUI*SI*(AL02+AG02)
 PART4=MOMENTUMPART4
 F=-(PART1+PART2+PART3+PART4)
RETURN
END

SUBROUTINE OTHERVALUES(G, SI2, FR)
 IMPLICIT NONE
 COMMON /MOST_SUBS/ D, A, PI, PI2, PI3, DAL
 COMMON /VELOCITIES/ VSL, VSG, VG, V0, VT, VS
 DOUBLE PRECISION G, SI2, FR, HEFF
 DOUBLE PRECISION D, A, PI, PI2, PI3, DAL
 DOUBLE PRECISION VSL, VSG, VG, V0, VT, VS

 HEFF=A*DAL*SI2
 FR=(VT-V0)/DSQRT(G*HEFF)
RETURN
END

SUBROUTINE PARAMETERS
 IMPLICIT NONE
 COMMON /MOST_SUBS/ D, A, PI, PI2, PI3, DAL
 COMMON /VELOCITIES/ VSL, VSG, VG, V0, VT, VS
 DOUBLE PRECISION D, A, PI, PI2, PI3, DAL
 DOUBLE PRECISION VSL, VSG, VG, V0, VT, VS

 V0=VSL/DAL
 VG=VSG/(1.D0-DAL)
RETURN
END
```

CHAPTER 14

APPENDIX D

```
C**************************************************************************
C   THIS PROGRAM DETERMINES THE TRANSITION BETWEEN ANNULAR AND SLUG FLOW
C   FOR LIQUID-GAS SYSTEMS.
C
C   THE PROGRAM SIMULTANEOUSLY SOLVES A MINIMIZATION OF PRESSURE DROP
C   FROM THE CONSERVATION OF MOMENTUM ALONG WITH A MAXIMUM SLUG VOID.
C
C   'SL_AN.FOR'
C   WRITTEN BY BOB WILKENS 4/97 USING MICROSOFT FORTRAN POWERSTATION V1.0
C
C**************************************************************************
C
C  VARIABLE LISTING:
C
C  VARIABLE      UNITS            DEFINITION
C
C  A             m²               pipe cross-sectional area
C  AG/AL         m²               gas and liquid areas in film region
C  CG/CL         ---              gas and liquid friction factor coefficients
C  D             m                pipe inner diameter
C  DAL           ---              dimensionless liquid area in film region
C  DAL2          ---              dummy comparison variable
C  DBASIS        m                diameter basis for void fraction
C  FCN1          kg/(m·s²)        minimization of pressure drop equation
C  FCNOLD1       kg/(m·s²)        dummy comparison variable
C  FR            ---              film Froude number
C  G             m/s²             gravity
C  H             m                film height
C  HFCN          ---              dummy variable for computation speed
C  ICHANGE       ---              switch for increment change
C  ICOUNT        ---              counter variable
C  IFILEYN       ---              switch for file output
C  INCREMENT     ---              dummy loop variable
C  ISKIP         ---              loop step size
C  ISTART/ISTOP ---               loop starting and stopping points
C  IPRINTYN      ---              switch for printer output
C  IRUNAGAIN     ---              switch to run the program again
C  LHU           ---              liquid holdup in the slug body
C  M/N/NN        ---              gas and liquid friction factor exponents
C  MALEYB/MALEYM   m              coefficients for the lag distance
C  MUG/MUL       Pa·s             gas and liquid viscosities
C  PARTA         ---              dummy variable for computation speed
C  PI            ---              ratio of circle circumference to diameter
C  RHOG/RHOL     kg/m^3           gas and liquid densities
C  TAUG/TAUL     kg/(m·s²)        gas and liquid-wall shear stresses
C  TOL           ---              conversion tolerance
C  THETA         rad              inclination (positive for upflow)
C  UG/UL         m/s              gas and liquid velocities in film region
C  VSG/VSL       m/s              superficial gas and liquid velocities
C  VSGIG/VSLIG  m/s               initial guess
C  VSGIP         m/s              initial conversion increment
```

```
C  VSGPWR       m/s              conversion increment
C  XLD          m                lead distance
C  XLDM/XLDB    ---              lead distance correlation coefficients
C  XLG          m                lag distance
C  XLGM/XLGB    ---              lag distance correltation coefficients
C

C
C   DECLARE VARIABLES AND FUNCTIONS
C

      IMPLICIT NONE
      INTRINSIC DABS, DACOS, DEXP, DSQRT, DSIN

      DOUBLE PRECISION A, AG, AL, D, PI
      DOUBLE PRECISION DAL, DAL2, dg, dl, si, reg, rel
      DOUBLE PRECISION MUG, MUL, RHOG, RHOL
      DOUBLE PRECISION G, TAUG, TAUL, THETA
      DOUBLE PRECISION VSGIG, VSLIG, VSGIP, VSGPWR
      DOUBLE PRECISION CL, CG, NN
      DOUBLE PRECISION FCN1, FCNOLD1
      DOUBLE PRECISION PARTA
      DOUBLE PRECISION TOL
      DOUBLE PRECISION DBASIS, FR, Ls, XLD, XLG
      DOUBLE PRECISION LHU, XLDM, XLDB, XLGM, XLGB
      DOUBLE PRECISION UG, UL, VSG, VSL

      REAL M, N

      INTEGER INCREMENT, ISKIP, ISTART, ISTOP
      INTEGER IFILEYN, IPRINTYN, IRUNAGAIN, ICOUNT, ICHANGE

      CHARACTER OUTPUTFILE*11

C
C   DECLARE CONSTANTS
C

      G = 9.8D0
      PI = 3.141592653589793D0
      TOL = 1.D-7
      VSGIG=10.D0
      VSLIG=5.D-8
      VSGIP=2.D0
      ISTART=50
      ISTOP=950
      ISKIP=50
      N=.2
      NN=.2D0
      M=.2
      CL=.046D0
      CG=.046D0
      IRUNAGAIN=1

      DO WHILE(IRUNAGAIN .EQ. 1)

C
```

```
C   PRINT TITLES FOR PROGRAM
C

      WRITE(*,*)"*****************************************************"
      WRITE(*,*)
      WRITE(*,*)"NATIONAL SCIENCE FOUNDATION INDUSTRY/UNIVERSITY"
      WRITE(*,*)"COOPERATIVE RESEARCH CENTER"
      WRITE(*,*)
      WRITE(*,*)"CORROSION IN MULTIPHASE SYSTEMS CENTER"
      WRITE(*,*)
      WRITE(*,*)"OHIO UNIVERSITY, ATHENS AND"
      WRITE(*,*)"UNIVERSITY OF ILLINOIS, URBANA-CHAMPAIGN"
      WRITE(*,*)
      WRITE(*,*)"THIS PROGRAM MODELS THE TRANSITION FROM ANNULAR"
      WRITE(*,*)"TO SLUG FLOW FOR GAS-LIQUID SYSTEMS IN HORIZONTAL"
      WRITE(*,*)"AND SLIGHTLY INCLINED PIPELINES"
      WRITE(*,*)
      WRITE(*,*)"*****************************************************"
      WRITE(*,*)
      WRITE(*,*)"ENTER A '0' FOR THE DEFAULT VALUES"

C
C   ALLOW THE USER TO INPUT THE SYSTEM PARAMETERS
C

      WRITE(*,*)"What is the inner diameter of the pipe [=] m (default =
     + 0.0972)?"
      READ(*,*)D
      IF (D .EQ. 0.D0) THEN
        D=.0972D0
      ENDIF
      WRITE(*,*)"What is the maximum film Froude number (default = 35)?"
      READ(*,*)fr
      IF (fr .EQ. 0.D0) THEN
        fr=35.d0
      ENDIF
      WRITE(*,*)"What is the pipe inclination [=] degrees (positive for
     +upflow, default = 0)?"
      READ(*,*)THETA
      theta=0
      WRITE(*,*)"What is the in-situ gas density [=] kg/m^3 (default = 5
     +.02)?"
      READ(*,*)RHOG
      IF (RHOG .EQ. 0.D0) THEN
        RHOG=5.02D0
      ENDIF
      WRITE(*,*)"What is the gas viscosity [=] Pa·s (default = 1.6E-5)?"
      READ(*,*)MUG
      IF (MUG .EQ. 0.D0) THEN
        MUG=1.6D-5
      ENDIF
      WRITE(*,*)"What is the liquid density [=] kg/m^3 (default = 1025)?
     +"
      READ(*,*)RHOL
      IF (RHOL .EQ. 0.D0) THEN
        RHOL=1025.D0
      ENDIF
```

```
      WRITE(*,*)"What is the liquid viscosity [=] Pa·s (default = 1E-3)?
     +"
      READ(*,*)MUL
      IF (MUL .EQ. 0.D0) THEN
        MUL=1.D-3
      ENDIF
      WRITE(*,*)"What are the lag distance coefficients for the lead-lag
     + model (defaults are for water-carbon dioxide:  0.16, -0.63)?"
      READ(*,*)XLGM, XLGB
      IF (XLGM .EQ. 0.D0) THEN
        XLGM=0.16D0
      ENDIF
      IF (XLGB .EQ. 0.D0) THEN
        XLGB=-0.63D0
      ENDIF
      WRITE(*,*)"What are the lead distance coefficients for the lead-la
     +g model (defaults are"
      WRITE(*,*) "for water-carbon dioxide:  0.057, -0.25)?"
      READ(*,*)XLDM, XLDB
      IF (XLDM .EQ. 0.D0) THEN
        XLDM=0.057D0
      ENDIF
      IF (XLDB .EQ. 0.D0) THEN
        XLDB=-0.25D0
      ENDIF
      WRITE(*,*)"If you would like a copy of the solution sent to the pr
     +inter, enter a '1'."
      WRITE(*,*)"If not, enter a '0'."
      READ(*,*)IPRINTYN
      IF (IPRINTYN .EQ. 1) THEN
        OPEN(UNIT=3,FILE='LPT1',ERR=199)
      ENDIF
      WRITE(*,*)"If you would like a copy of the results sent to a file,
     + enter a '1'."
      WRITE(*,*)"If not, enter a '0'."
      READ(*,*)IFILEYN
      IF (IFILEYN .EQ. 1) THEN
        WRITE(*,*)"What is the filename (include the extension)?"
        READ(*,9)OUTPUTFILE
        OPEN(UNIT=5,FILE=OUTPUTFILE,ERR=299,MODE='WRITE',STATUS='NEW')
      ENDIF

C
C   CALCULATE OTHER CONSTANTS
C

      A=.25D0*PI*D**2
      DBASIS=0.1D0

C
C     CONTINUE WITH THE OUPUT
C

      WRITE(*,*)
      WRITE(*,*)"THESE ARE THE INPUT PROPERTIES OF THE SYSTEM:"
      WRITE(*,*)
      WRITE(*,1) G
```

```
      WRITE(*,2) THETA
      WRITE(*,3) D
      WRITE(*,*)
      WRITE(*,4) RHOG
      WRITE(*,5) MUG
      WRITE(*,6) RHOL
      WRITE(*,7) MUL
      WRITE(*,*)
      WRITE(*,*) "THIS IS THE ANNULAR TO SLUG TRANSITION USING"
      WRITE(*,*) "MINIMIZATION OF PRESSURE DROP IN THE MOMENTUM"
      WRITE(*,*) "CONSERVATION EQUATION AND A MAXIMUM SLUG VOID."
      WRITE(*,*) "(NOTE:  Vsl = 0 MEANS NO TRANSITION AT THE"
      WRITE(*,*) "GIVEN Vsg)"
      WRITE(*,*)

C
C     SEND OUTPUT HEADERS TO THE PRINTER IF NECESSARY
C

      IF (IPRINTYN .EQ. 1) THEN
        WRITE(3,*)"****************************************************"
        WRITE(3,*)
        WRITE(3,*)"NATIONAL SCIENCE FOUNDATION INDUSTRY/UNIVERSITY"
        WRITE(3,*)"COOPERATIVE RESEARCH CENTER"
        WRITE(3,*)
        WRITE(3,*)"CORROSION IN MULTIPHASE SYSTEMS CENTER"
        WRITE(3,*)
        WRITE(3,*)"OHIO UNIVERSITY, ATHENS AND"
        WRITE(3,*)"UNIVERSITY OF ILLINOIS, URBANA-CHAMPAIGN"
        WRITE(3,*)
        WRITE(3,*)"THIS PROGRAM MODELS THE TRANSITION FROM STRATIFIED"
        WRITE(3,*)"TO SLUG FLOW FOR GAS-LIQUID SYSTEMS IN HORIZONTAL"
        WRITE(3,*)"AND SLIGHTLY INCLINED PIPELINES."
        WRITE(3,*)
        WRITE(3,*)"****************************************************"
        WRITE(3,*)
        WRITE(3,*)"THESE ARE THE INPUT PROPERTIES OF THE SYSTEM:"
        WRITE(3,*)
        WRITE(3,1) G
        WRITE(3,2) THETA
        WRITE(3,3) D
        WRITE(3,*)
        WRITE(3,4) RHOG
        WRITE(3,5) MUG
        WRITE(3,6) RHOL
        WRITE(3,7) MUL
        WRITE(3,*)
        WRITE(*,*) "THIS IS THE ANNULAR TO SLUG TRANSITION USING"
        WRITE(*,*) "MINIMIZATION OF PRESSURE OF TAITEL AND DUKLER"
        WRITE(*,*) "AND MAXIMUM SLUG VOID WITH MALEY (NOTE:"
        WRITE(*,*) "Vsl = 0 MEANS NO TRANSITION AT THE GIVEN Vsg):"
        WRITE(3,*)
        WRITE(3,*)"   Vsl    Vsg     AL/A  αslug  Vt/Vm  Fr,f"
      ENDIF

      WRITE(*,*) "   Vsl    Vsg     AL/A  αslug  Vt/Vm  Fr,f"
```

```
      VSL=0.D0
      DO INCREMENT=ISTART,ISTOP,ISKIP
        ICOUNT=0
        AL=.001D0*INCREMENT*A
        AG=A-AL
        DAL=AL/A
        LHU=1.D0
        XLG=(XLGM*FR+XLGB)*D/DBASIS
        XLD=(XLDM*FR+XLDB)*D/DBASIS
        LS= 15.d0 * d
        LHU=1.D0-(XLD-XLG)/Ls*(DEXP(-Ls/XLG)-1.D0)

        IF ( (VSL .LT. 2.D0)) THEN
          VSG=VSGIG
          VSGPWR=VSGIP
          DAL2=0.D0
          FCN1=2.D0*TOL
          FCNOLD1=4.D0*TOL
          DO WHILE (DABS(FCN1) .GT. TOL)
            ICOUNT=ICOUNT+1
            VSL=(FR*DSQRT(G*AL*.5D0/DSQRT(PI*AG))-1.2D0*VSG)/(1.2D0-A/
     &           AL)
            IF ( VSL .LT. 0.D0) THEN
             VSL=VSLIG
            ENDIF
            UG=VSG*A/AG
            UL=VSL*A/AL
            si=2*dsqrt(pi*ag)
            dg=4*ag/si
            dl= 4*al/(pi*d)
            reg=rhog*dg*ug/mug
            rel=rhol*dl*ul/mul

            taug=0.5d0*rhog*ug**2*cg*reg**(-m)
            taul=0.5d0*rhol*ul**2*cl*rel**(-n)
            parta=(1.d0+si*d/al+nn)

            FCNOLD1=FCN1
            fcn1=taug-taul*parta+(rhol-rhog)*g*dsin(thetaa*pi/180.d0)
     &           *dsqrt(ag/pi)

            IF(FCNOLD1*FCN1 .LT. 0.D0) THEN
             VSGPWR=-.1D0*VSGPWR
             VSG=VSG+VSGPWR
            ELSE
             VSG=VSG+VSGPWR
            ENDIF
            IF (VSG .LT. 0.D0) THEN
             VSG=VSGIG
            ENDIF
            IF (ICOUNT .GT. 5000) THEN
             FCN1=0.D0
             VSG=0.D0
            ENDIF
          END DO

C
```

```
C   OUTPUT THE SOLUTION
C
          IF(VSG .GT. 0.D0) THEN
            WRITE(*,8)VSL, VSG, DAL, (1.D0-LHU), 1.2, FR
            IF (IPRINTYN .EQ. 1) THEN
             WRITE(3,8)VSL, VSG, DAL, (1.D0-LHU), 1.2, FR
            ENDIF
          ENDIF
          IF (IFILEYN .EQ. 1) THEN
            WRITE(5,10) VSG, VSL
          ENDIF
        ENDIF
      END DO
      IF (IPRINTYN .EQ. 1) THEN
        WRITE(3,*)"\f"C
        CLOSE(UNIT=3, ERR=199)
      ENDIF
      IF (IFILEYN .EQ. 1) THEN
        CLOSE(UNIT=5, ERR=299)
      ENDIF
      WRITE(*,*)"RUN AGAIN (1 = YES, 0 = NO)?"
      READ(*,*)IRUNAGAIN
      IF (IRUNAGAIN .EQ. 1) THEN
        WRITE(*,*) "CHANGE 'AL/A' START OR INCREMENT (1 = YES, 0 = NO)?"
        READ(*,*) ICHANGE
        IF(ICHANGE .EQ.1) THEN
          WRITE(*,*)"ENTER THE STARTING 'AL/A' IN THOUSANDTHS (E.G. 500
     +FOR 'AL/A' OF 0.5)?"
          READ(*,*) ISTART
          WRITE(*,*)"ENTER THE INCREMENT FOR 'AL/A' IN THOUSANDTHS (E.G.
     + 50 FOR 0.05)?"
          READ(*,*) ISKIP
        ENDIF
      ENDIF
     END DO
     STOP

C
C   FORMATTED INPUT/OUTPUT LISTING
C

    1 FORMAT(' GRAVITY ='F6.2' kg·m/s²')
    2 FORMAT(' INCLINATION ='F8.4' degrees (+ for upflow)')
    3 FORMAT(' PIPE INNER DIAMETER ='F6.4' m')
    4 FORMAT(' GAS DENSITY ='F8.3' kg/m^3')
    5 FORMAT(' GAS VISCOSITY ='D9.3' Pa·s')
    6 FORMAT(' LIQUID DENSITY ='F5.0' kg/m^3')
    7 FORMAT(' LIQUID VISCOSITY ='D9.3' Pa·s')
    8 FORMAT(' 'F7.4'  'F5.1'  'F5.3'  'F5.3'  'F5.3'  'F10.1)
    9 FORMAT(A11)
   10 FORMAT(F7.4'   'F7.5)
      STOP

C
C   ERROR TRAPPING OUTPUT LINES
C
```

```
199 WRITE(*,*) "PRINTER ERROR"
    STOP

299 WRITE(*,*) "ERROR CREATING THE OUTPUT FILE."
    STOP

    END
```

ABSTRACT

WILKENS, ROBERT, JOSEPH. Ph.D. June 1997

Chemical Engineering

Prediction of the Flow Regime Transitions in High Pressure, Large Diameter, Inclined Multiphase Pipelines

Director of Dissertation: W. Paul Jepson

In multiphase flows, flow regime determination has many design applications such as boiler tubes and oil and gas pipelines. This study focuses on the oil production from older wells in which brine and carbon dioxide gas are commonly present in the pipelines. Often these oil, water, and gas mixtures create a highly corrosive environment for typical carbon steel pipelines. Since the highest corrosion rate occurs in slug flow, the ability to predict this flow regime becomes of great importance.

The transitions from stratified to slug and from slug to annular flow are not well understood. Further, little data is available for flows in large diameter, multiphase pipes which include the effects of pressure and inclination.

For this purpose, oil/water/gas tests were conducted in a 9.72-cm diameter, 18-m long pipe at inclinations of 0, ±2, and ±5° and pressures of 0.27, 0.45, and 0.79 MPa. The ratio of the translational velocity to the superficial mixture velocity was found to be about 2.0 for plug flow, 1.2 for slug flow, and 0.5 - 1.2 for pseudo-slug flow. The film Froude number in slug flow was found to increase with increasing gas flow rate to a value of about 18. The value then dropped as pseudo-slug flow was achieved. It again increased with gas flow rate until it reached a value of about 16, then annular flow ensued.